UNIVERSITY OF CALIFORNIA, SAN DIEGO

Regulation of Excitation/Inhibition balance in the motor neuron circuit of *C. elegans*

A dissertation submitted in partial satisfaction of the requirements for the degree
Doctor of Philosophy

in

Biology

by

Seika Takayanagi

Committee in Charge:

Professor Yishi Jin, Chair
Professor Sreekanth Chalasani
Professor Don Cleveland
Professor Emily Troemel
Professor Jing Wang

2016

The Dissertation of Seika Takayanagi is approved, and it is acceptable in quality and form for publication on microfilm and electronically:

Chair

University of California, San Diego

2016

DEDICATION

This dissertation is dedicated to my husband Taketoshi Kiya, who continuously supported and encouraged me through my entire Ph.D. process.

TABLE OF CONTENTS

LIST OF FIGURES

LIST OF TABLES

ACKNOWLEDGEMENTS

Foremost, I would like to thank my Ph.D. advisor Dr. Yishi Jin, for accepting me in her lab and providing me with the great opportunity to persue my Ph.D. research. I am very greatful for her guidance and mentorship over the past years. I would also like to express my greatest gratitude to the committee members, Professor Sreekanth Chalasani, Professor Don Cleveland, Professor Emily Troemel and Professor Jing Wang for serving as my committee members and kindly providing advice and helpful discussions on my research.

I wish to thank the past and present Jin and Chisholm lab members, for their assistance and friendship. Special thanks to Naina Kurup, Panid Sharifnia and Marian Chuang.

My deep appreciation goes to all my friends I met in San Diego. Special thanks to Fred and Gretchen Schnitzer, who kindly welcomed me as my host paernts when I first arrived at San Diego, and truly made me feel at home.

I would like to thank all of my family members, especially my parents Etsuo and Hiroko Takayanagi, for their continuous support through my Ph.D. They were always supportive and helped me persue my interest in science.

I greatfully acknowledge the graduate student fellowship I received for five years from Nakajima Foundtation, Japan.

Finally, I would like to express my gratest gratitutde and love to my husband Taketoshi Kiya, who always helped me when I needed it.

Chapter 1, in full, is a reprint of Takayanagi-Kiya S. and Jin Y. Nematodes: Genetic Dissection of Pathways Regulating Seizure and Epileptic-like Behaviors. In A. Pitkänen, S. Moshe, A. S. Galanopoulou & P. Buckmaster (Eds.), *Models of Seizure and Epilepsy* (2nd ed.): Elsevier Academic Press (in preparation) with permission of all authors. The dissertation author was the primary author of the chapter.

Chapter 2, in full, is a reprint of Takayanagi-Kiya, S., Zhou, K., and Jin, Y. A ligand-gated anion channel LGC-46 regulates release-dependent presynaptic inhibition and

excitation-inhibition balance (in preparation) with permission of all authors.

Chapter 3, in full, is a reprint of Stawicki, T.M., Takayanagi-Kiya, S., Zhou, K., and Jin, Y. Neuropeptides Function in a Homeostatic Manner to Modulate Excitation-Inhibition Imbalance in *C. elegans*. PloS Genet. with permission of all authors. The dissertation author was one of the two co-first authors of this paper.

Chapter 4, in full, is a reprint of Takayanagi-Kiya, S. and Jin, Y. Altered function of the DnaJ family co-chaperone DNJ-17 modulates locomotor circuit activity in a *C. elegans* seizure model (in press) with permission of all authors.

VITA

2007-2008	Research Assistant for Dr. Yoshiomi Kato, International Christian University, Tokyo
2008	Bachelor of Arts, International Christian University, Tokyo
2008-2010	Research Assistant for Dr. Takeo Kubo, University of Tokyo
2010	Master of Science, University of Tokyo
2010-2016	Ph.D. Student, University of California, San Diego
2011-2016	Research Assistant for Dr. Yishi Jin, University of California, San Diego
2016	Doctor of Philosophy, University of California, San Diego

FELLOWSHIP

2010-2015 Recipient of The Nakajima Foundation Predoctoral Fellowship

PUBLICATIONS

Stawicki TM, Takayanagi-Kiya S, Zhou K, Jin Y. Neuropeptides Function in a Homeostatic Manner to Modulate Excitation-Inhibition Imbalance in *C. elegans*. PLoS Genet. 2013 May;9(5):e1003472.

Takayanagi-Kiya S, Misawa-Hojo K, Kiya T, Kunieda T, Kubo T. Splicing variants of NOL4 differentially regulate the transcription activity of Mlr1 and Mlr2 in cultured cells. Zoolog. Sci. 2014 Nov; 31(11): 735-40.

Takayanagi-Kiya, S. and Jin, Y. Altered function of the DnaJ family co-chaperone DNJ-17 modulates locomotor circuit activity in a *C. elegans* seizure model (Accepted for publication in G3)

ABSTRACTS

Takayanagi-Kiya S, Stawicki TM, Zhou K, Jin Y. "Neuropeptides Function in a Homeostatic Manner to Modulate Excitation-Inhibition Imbalance in *C. elegans*." *C.elegans* International Meeting, 2013. Poster

Takayanagi-Kiya S, Cherra S, Qi YB, Jin Y. "Pathways that modulate excitation-inhibition imbalance in *C. elegans* locomotor circuit." *C. elegans* Developmental Cell Biology and Gene Expression Meeting in association with Asia-Pacific *C. elegans* meeting, 2014. Talk

Takayanagi-Kiya S, Cherra S, Qi YB, Jin Y. "A novel mutation in the ligand-gated ion channel *lgc-46* affects excitation-inhibition imbalance in the *C. elegans* locomotor circuit." *C.elegans* International Meeting, 2016. Poster

ABSTRACT OF THE DISSERTATION

Regulation of Excitation/Inhibition balance in the motor neuron circuit of *C. elegans*

by

Seika Takayanagi

Doctor of Philosophy

University of California, San Diego, 2016

Professor Yishi Jin, Chair

Behaviors of animals require the coordinated activity of excitatory and inhibitory transmission within neural circuits. Imbalanced neuronal circuit activity is an underlying cause of many neuronal disorders such as epilepsy. Thus, understanding the mechanisms of how the balanced neural activity is maintained and what occurs when this E/I balance is disrupted will provide insights for developing effective treatment of disease conditions. In my dissertation, I addressed these questions using the relatively simple locomotory motor neuron circuit of *C. elegans*. It was previously reported that an activating mutation *acr-2(gf)* in an acetylcholine (ACh) receptor subunit ACR-2 expressed in neruons causes muscle hyper-contraction, which leads to the animal's spontaneous shrinking behavior termed convulsion. The mutant exhibits overexcitation of cholinergic motor neuron activity accompanied by suppression of GABAergic motor neuron activity, resulting in E/I imbalance in the motor neuron circuit. Through studies of a genetic suppressor of *acr-2(gf)*, I characterized a ligand-gated ion channel which localizes to the presynaptic terminals and functions to suppress cholinergic motor neuron activity. Next, I

identified the neuropeptide pathway that is suppresses the E/I imbalance, and using the *acr-2(gf)* convulsion as the model of E/I imbalance, we found that animals express specific neuropeptides upon overexcitation of neurons to suppress the imbalance. Third, I identified a mutation in a putative co-chaprone protein that exacerbates the convulsion phenotype of *acr-2(gf)*. Finally, I identified a single amino acid substitution mutation in a highly conserved eukaryotic translation initiation factor which can suppress E/I imbalance. Overall, my dissertation characterizes multiple pathways that regulate the E/I balance within a neural circuit.

Chapter 1

Introduction: Genetic Dissection of Pathways Regulating Seizure and Epileptic-like Behaviors in *C. elegans*

Abstract

The past decade has seen increasing reports on genetic variants associated with human diseases. Determining the causality of such variants requires better understanding of the functions of disease-associated genes. Researches conducted using the nematode *Caenorhabditis elegans* have had tremendous impact in the discovery of fundamental mechanisms underlying the development and function of the nervous system. This chapter focuses on studies relevant to the overarching goals in the investigation of causes and cures in seizure and epilepsy. Many genes implicated in seizure or epilepsy in humans are conserved in *C. elegans.* Genetic dissection of seizure or epilepsy-like phenotypes in *C. elegans* has revealed molecular and physiological similarities to those implicated in human epileptogenesis. Here, we review the studies using *C. elegans* locomotor circuit to model seizure/epilepsy, and further discuss how the findings can contribute to the mechanistic understanding of genetic factors in the treatment of seizure and epilepsy.

Introduction

The nematode *Caenorhabditis elegans* was established by Sydney Brenner about half a century ago as a model organism to study development and the nervous system using genetics (Brenner, 1974; Corsi, Wightman, & Chalfie, 2015). Today, *C. elegans* is used to study a huge variety of biological problems in more than one thousand laboratories over the world. *C. elegans* has a number of traits well suited for laboratory research. First, they have a rapid life cycle of 3-4 days under laboratory culture conditions at 20-25°C. They primarily reproduce as

self-fertilizing hermaphrodites, which allows easy maintenance of genetic mutations as isogenic strains. Males emerge at low frequency in the wild, and can be obtained at desirable rate in the lab under conditions that favor chromosomal non-disjunction, enabling transfer of genetic information (J. Sulston & Hodgkin., 1988). Moreover, cryopreservation of *C. elegans* allows long-term storage of strains, greatly reducing efforts and costs in animal husbandry. Second, *C. elegans* is made up of a small number of cells (959 somatic cells in an adult hermaphrodite). Its development proceeds in a stereotypical pattern with invariant cell lineages (Kimble & Hirsh, 1979; J. E. Sulston, 1983; J. E. Sulston & Horvitz, 1977; J. E. Sulston, Schierenberg, White, & Thomson, 1983), facilitating precise identification of developmental and behavioral defects with single-cell resolution. Third, genome-wide mutagenesis allows isolation of desirable mutants based on functional disruption. Genetic mapping in combination with whole-genome sequencing greatly speeds up the process from mutants to gene identification. Fourth, the entire connectivity of *C. elegans* nervous system has been reconstructed at the ultrastrutural level, providing an unprecedented knowledge to interrogate the logic of information processing in a living organism (Howell, White, & Hobert, 2015; Ward, Thomson, White, & Brenner, 1975; White, Southgate, Thomson, & Brenner, 1976, 1986). Fifth, transgenesis is simple, and manipulation of gene expression can be achieved through high-copy extrachromosomal arrays or single-copy integration in the genome. The transparent body, with the aid of transgenic labeling, enables direct observation of cells from anatomic position to cellular dynamics, and of neuronal activity by calcium imaging and optogenetics (Kerr et al., 2000). Finally, *C. elegans* uses classical neurotransmitters and receptors as those in human to transmit information between neurons and their targets. Together, using powerful molecular, genetic, pharmacological, and cellular manipulations, research findings using *C. elegans* have provided profound insights into many areas of neuroscience. In this chapter, we focus on how *C. elegans* has been used to examine fundamental mechanisms relevant to our understanding of epileptic conditions.

Conservation of genes and pathways in *C. elegans* to those implicated in human epilepsy

Despite the behavioral complexities and anatomical differences among animals, many genes are evolutionarily conserved. It is estimated that at least 38% of the genes in *C. elegans* are orthologs of those in humans, and >60% of the human genes have orthologs in *C. elegans* (Shaye & Greenwald, 2011). Also, approximately 40% of the genes associated with human diseases have *C. elegans* orthologs (Culetto & Sattelle, 2000; Kaletta & Hengartner, 2006). Importantly, the proteins that function in neurons are highly conserved between human and *C. elegans*. *C. elegans* genome encodes the most known families of ion channels, classical neurotransmitter pathway-related genes and G-protein coupled receptors (GPCRs) (Hobert, 2013). The high degree of genetic conservation makes *C. elegans* a valuable experimental model to study biological mechanisms relevant to human diseases (Kaletta & Hengartner, 2006).

Epilepsy is associated with a broad spectrum of neurological disorders (Lossin, Wang, Rhodes, Vanoye, & George, 2002). Recent surveys have revealed >500 genes with tentative links to suscepbility or risk to epilepsy in humans or mouse models, although only a portion of them has been established to have causality (Meisler, Kearney, Ottman, & Escayg, 2001; Nicita et al., 2012; Noebels, 2015). Table1.1 lists the *C. elegans* homologs of human genes of which mutations have been shown to be causative for epilepsy.

Ligand- and voltage-gated ion channels are two large groups of genes associated with epileptogenesis in human, consistent with the disruption of neural circuit activities being a major mechanistic pathway that can lead to epilepsy. The cannonical ligand-gated nicotinic acetylcholine receptors (nAChRs) and GABA receptors in *C. elegans* are highly conserved with humans (Hobert, 2013). Voltage-gated calcium channels and potassium channels are also found in *C. elegans* and are shown to have similar functional properties as their mammalian counterparts (Caylor, Jin, & Ackley, 2013; Salkoff et al., 2005; Steger, Shtonda, Thacker, Snutch, & Avery, 2005). One notable absence of ion channels in *C. elegans* is the voltage-gated sodium

channels, reflecting the fact that *C. elegans* neurons use graded potential and calcium-mediated spiking to propagate information (Gao & Zhen, 2011; Hobert, 2013; Q. Liu, Hollopeter, & Jorgensen, 2009).

Multiple genes involved in synaptic vesicle exocytosis and endocytosis are also associated with epilepsy (Consortium, Project, & Consortium, 2014; Saitsu et al., 2008). Studies of *C. elegans* mutants were instrumental for the discovery and functional dissection of many genes essential for synaptic transmission, such as *unc-18,* a homolog of STXBP1 also known as Munc18 (McEwen & Kaplan, 2008; Saitsu, et al., 2008; Weimer et al., 2003), and dynamin, a GTPase required for endocytosis (Clark, Shurland, Meyerowitz, Bargmann, & van der Bliek, 1997).

It is becoming increasingly clear that mutations of more than one gene are often associated with development of epilepsy symptoms within individuals (Allen et al., 2013; Noebels, 2015). With its short life cycle and powerful genetics, *C. elegans* is particularly suited for examining interaction of multiple genes. As discussed later in this chapter, several *C. elegans* genes (*unc-49, lis-1, acr-2* in Table 1.1) have already been linked to seizure-like phenotypes, and genetic interaction studies will reveal their functional networks.

C. elegans **motor circuit as a model for seizure**

C. elegans nervous system consists of 302 neurons, which form about 7,000 synaptic connections (White, et al., 1986). One hundred and thirteen neurons directly synapse onto body muscles and control locomotion, foraging and reproductive behavior (Reviewed in (Von Stetina, Treinin, & Miller, 2006)). Sinusoidal locomotion of *C. elegans* is controlled by acetylcholine (ACh)-releasing excitatory and GABA-releasing inhibitory motor neurons in the ventral cord. Abnormal activities in the motor circuit can cause aberrant muscle contraction, which can be detected visually under dissecting microscopes. Decades of studies have revealed multi-level

regulation of this circuit, which has provided an excellent model to dissect genetic mechanisms related to physiological processes of seizure and epilepsy. Below, we summarize the general knowledge of *C. elegans* motor circuit to provide background for interpreting the behavioral phenotypes of the animals.

The ventral cord motor neurons form *en passant* synapses, namely neuromuscular junctions (NMJs), to body wall muscles (Q. Liu, Chen, Hall, & Wang, 2007; White, et al., 1976, 1986). These motor neurons are divided into 8 different classes based on morphology, neurotransmitter specificity and innervating muscle partners (White, et al., 1976, 1986). A- and B- type motor neurons are cholinergic and excitatory, whereas D-type motor neurons are GABAergic and inhibitory to body muscle contraction. Each type is further divided into ventrally- and dorsally- innervating subtypes (Figure 1.1A). The operational logic of the locomotor circuit was deduced based on anatomical connections and behavioral studies of animals after laser ablation of neurons (Chalfie et al., 1985; McIntire, Jorgensen, Kaplan, & Horvitz, 1993). A-type cholinergic motor neurons control backward locomotion, whereas B-type motor neurons control forward locomotion. D-type GABAergic motor neurons receive synaptic inputs from both A- and B-motor neurons and are involved in both forward and backward locomotion. When ventrally innervating cholinergic neurons (VA and VB) are activated, synaptic transmission at NMJs causes ventral muscle contraction and also excitation of the GABAergic Dorsal type D (DD) neurons. DD neurons then release GABA to cause relaxation of the dorsal muscle, creating the body curvature of the animal by ventral contraction and dorsal relaxation (Figure 1.1A). Conversely, when dorsally innervating cholinergic neurons (DA and DB) are activated, dorsal muscles contract and the ventral muscles relax.

Pharmacological assays, which can be easily performed in the lab, have been widely used for characterization of motor neuron activities in the locomotor circuit. Animals are exposed to chemicals that act as agonists or antagonists for neurotransmitter receptors (e.g.

levamisole, pentylenetetrazole/PTZ), or those that affect the uptake or turnover of neurotransmitters at the neuromuscular junction (e.g. aldicarb); and the effects on animals' movement and viability are quantified. A number of genetic screens using drug selection led to the identification of genes functioning in synaptic transmission. An example is the screen for aldicarb resistant (Ric: resistant to inhibitors of cholinesterase) mutants (Miller et al., 1996). Acetylcholine esterase inhibitor aldicarb blocks breakdown of acetylcholine and causes accumulation of acetylcholine and prolonged synaptic action at the neuromuscular junction leading to paralysis and death of wild type animals (Mahoney, Luo, & Nonet, 2006). In contrast, Ric mutants can arise due to defective cholinergic transmission, and can be easily isolated.

Production of acetylcholine depends on choline acetyltransferase ChAT/CHA-1, homologous to the vertebrate ChAT enzymes (Rand & Russell, 1985). Acetylcholine is transported into synaptic vesicles by UNC-17, the vesicular acetylcholine transporter VAChT, cloning of which helped to identify its mammalian orthologs (Alfonso, Grundahl, Duerr, Han, & Rand, 1993; Erickson et al., 1994). Null mutations in these two genes cause lethality (Alfonso, et al., 1993; Rand, 1989), but hypomorphic mutants of *cha-1* or *unc-17* are viable, resistant to aldicarb, and show slow locomotion (Alfonso, et al., 1993; Brenner, 1974; Rand, 1989). The plasma membrane choline transporter CHO-1/ChT, function to uptake choline (Matthies, Fleming, Wilkes, & Blakely, 2006). *cho-1* mutants have milder phenotypes compared to *cha-1* or *unc-17*, possibly because of baseline low-affinity choline uptake effect in the nerve terminals.

C. elegans genome has a large number of AChR-encoding genes (Mongan et al., 1998). Functional characterization of muscle nAChR subunit proteins came from mutants resistant to levamisole, an agonist for nAChR (Fleming et al., 1997; Lewis, Wu, Levine, & Berg, 1980). Studies of the levamisole-sensitive ionotropic AChR reveal a pentameric subunit composition, including α subunit UNC-38 and UNC-63, and non-α subunit UNC-29 and LEV-1(Culetto et al., 2004; Fleming, et al., 1997; Richmond & Jorgensen, 1999), similar to those in vertebrate

cholinergic NMJs. A transmembrane protein RIC-3 was first identified from aldicarb resistant screen (Nguyen, Alfonso, Johnson, & Rand, 1995), and later found to have conserved roles for folding and trafficking of nAChRs from *C. elegans* to mammals (Millar, 2008; Miller, et al., 1996).Channel reconstitution analyses in heterologous systems such as *Xenopus* oocytes or HEK cells have provided channel properties of the AChRs. In addition to the levamisole-sensitive AChRs, body wall muscles also express another AChR that is sensitive to nicotine but not to levamisole, and forms homomeric channels with an α subunit ACR-16 (Touroutine et al., 2005).

Immunostaining against GABA revealed 26 GABAergic neurons in *C. elegans*, including the two classes (DD, VD) of ventral cord motor neurons (McIntire, Jorgensen, & Horvitz, 1993; McIntire, Jorgensen, Kaplan, et al., 1993; McIntire, Reimer, Schuske, Edwards, & Jorgensen, 1997; Schuske, Beg, & Jorgensen, 2004). Laser ablation of these neurons resulted in a hypercontraction behavior, nicknamed "Shrinker". Studies of genetic mutants that show similar shrinker phenotype led to the identification of *C. elegans* GABA synthesis and neurotransmission pathway. *unc-25* encodes the GABA biosynthetic enzyme glutamic acid decarboxylase GAD (Y. Jin, Jorgensen, Hartwieg, & Horvitz, 1999) (Figure 1.1B). The vesicular GABA transporter VGAT protein is encoded by *unc-47* (McIntire, et al., 1997). An additional "Shrinker" gene *unc-46* is required for UNC-47 trafficking and indirectly helps vesicular transport of GABA(Schuske, Palfreyman, Watanabe, & Jorgensen, 2007). Ionotropic $GABA_A$ Receptor ($GABA_AR$) subunits are encoded by *unc-49* (Bamber, Twyman, & Jorgensen, 2003) (Figure 1.1C). The mutants with defects in GABAergic transmission exhibit seizure-like phenotype as further discussed in the next section.

While pharmacological assays provide fast results and are very powerful for genetic screening purposes, they may not reveal precise effects on neurotransmission. Electrophysiological analysis at the neuromuscular junction is a valuable technique to examine the motor neuron activity (Goodman, Lindsay, Lockery, & Richmond, 2012). Patch-clamp

electrophysiology from muscles and neurons provide temporally precise information of neural activity. More recently, imaging of genetically encoded calcium indicator GCaMP has been applied to motor neurons and measurement of calcium transients during locomotion provides another aspect of neural activity in the locomotor circuit (Kawano et al., 2011; Qi et al., 2013). These techniques allow researchers to examine the phenotype of mutants from multiple aspects.

Epilepsy in humans involves aberrant activity of neurons in a region, or the entirety, of the brain (Fisher et al., 2005). With human patients or mammalian models, currently it is technically challenging to examine the precise effect of abnormal neuron activity caused by genetic mutations. *C. elegans* motor circuit is composed of a small number of neurons, yet still contains both excitatory and inhibitory neurons as seen in the mammalian brain. By genetic and molecular techniques one can examine the roles of genes in cell type-specific manner. Thus, *C. elegans* provides a minimal circuit to model the regulation of neuronal activity with functional output.

C. elegans **seizure 1: genes involved in GABAergic neuron fate and transmission**

It is widely acknowledged that seizure is caused by imbalance of excitatory and inhibitory (E/I) neurotransmission within neural circuits (Avanzini, Franceschetti, & Mantegazza, 2007; Briggs & Galanopoulou, 2011; Mantegazza, Rusconi, Scalmani, Avanzini, & Franceschetti, 2010). Defects in GABAergic transmission are often associated with epileptogenesis in humans and mouse models (Allen, et al., 2013; DeLorey et al., 1998; Meisler, et al., 2001). In *C. elegans*, when GABAergic motor neurons are ablated, the animals can still move forward and backward, with reduced sinusoidal amplitude. However, when these animals are stimulated by mechanical touch, they show aberrant muscle contraction where both dorsal and ventral body wall muscles contract simultaneously (“shrink”) (McIntire, Jorgensen, Kaplan, et al., 1993). This observation indicates that the inhibitory effects of GABAergic motor neurons are necessary for the

coordinated locomotion upon stimulus. Consistently, loss-of-function in the genes required for GABA synthesis and synaptic transmission recapitulates the shrinking behavior (Y. Jin, Hoskins, & Horvitz, 1994; Y. Jin, et al., 1999; McIntire, Jorgensen, & Horvitz, 1993; McIntire, Jorgensen, Kaplan, et al., 1993). However, it is worth noting that none of these mutants show spontaneous convulsion.

Studies of other "Shrinker" mutants led to the identification of *unc-30,* encoding a homeodomain transcription factor that controls GABAergic motor neuron identity (Eastman, Horvitz, & Jin, 1999; Y. Jin, et al., 1994; McIntire, Jorgensen, & Horvitz, 1993) (Figure 1.1C). UNC-30 is homologous to mammalian Pitx2 protein, which is also involved in GABAergic neuron differentiation (Westmoreland, McEwen, Moore, Jin, & Condie, 2001). Transcriptional targets of UNC-30 include *unc-25/GAD, unc-47/VGAT* and *unc-46,* as well as nAChR subunits, secreted proteins and neuropeptide genes (Cinar, Keles, & Jin, 2005). Several other transcription factors including UNC-55 and ALR-1 are involved in determining GABAergic motor neuron subtypes in *C. elegan*s (Melkman & Sengupta, 2005; Tucker, Sieber, Morphew, & Han, 2005). Consistently, single mutants of *unc-55* or *alr-1* do not show the shrinker phenotype. ALR-1 is related to human homeodomain protein ARX, and UNC-55 is related to human COUP family. In mouse embryonic nervous system development, ARX and COUP have important roles in GABA neuron specification (Kitamura et al., 2002; Lodato et al., 2011). Both loss- and gain-of-function mutations in human ARX is associated with epilepsy and known to affect neuronal proliferation and differentiation during development (Nicita, et al., 2012). These findings implicate mechanistic conservation for transcriptional regulation of GABAergic neuron fate by UNC-30, ALR-1 and UNC-55 with their human homologs.

Defects in GABAergic transmission have also been extensively studied using pharmacological analyses. Earlier experiments using acetylcholine esterase inhibitor aldicarb revealed that mutants with GABAergic transmission defects are hypersensitive to aldicarb (Loria,

Hodgkin, & Hobert, 2004). An RNAi screen looking for aldicarb hypersensitivity phenotype identified 90 genes (Vashlishan et al., 2008). This includes genes required for GABAergic motor neuron development and modulation of GABAergic transmission. For example, it was shown that genes involved in Wnt signaling affect GABAergic motor neuron development, whereas neuropeptide receptor, MAPK kinase and TGFβ-pathway related genes are required for proper levels of GABAergic transmission. Importantly, 51 of the 90 genes identified have mammalian orthologs, and 21 of these genes are implicated in seizure phenotype or GABA transmission. The study provides a list of targets, further investigation of which may reveal therapeutic options for seizure or epilepsy.

C. elegans seizure 2: *lis-1* pathway mutants with PTZ treatment

"Epileptic-like seizure" in *C. elegans* was first mentioned in a study examining the effect of pentylenetetrazole (PTZ) on *lis-1* mutant (Williams, Locke, Braden, Caldwell, & Caldwell, 2004). PTZ acts as a competitive inhibitor of ionotropic GABA receptors (R. Q. Huang et al., 2001) and is used as respiratory and circulatory stimulant, which is also known to cause seizure in high doses in humans in rodents (Olsen, 1981; Psarropoulou, Matsokis, Angelatou, & Kostopoulos, 1994). LIS1 is one of the proteins mutated in Type I lissencephaly in humans, a childhood birth defect which is characterized by neuronal cell migration defects, brain malformation and epilepsy (O. Reiner & Sapir, 2013). LIS1 is known to interact with and regulate the microtubule motor protein dynein (J. Huang, Roberts, Leschziner, & Reck-Peterson, 2012). *C. elegans lis-1* shares 60% amino acid identity to the human ortholog, and is expressed widely and functions in many aspects of development (Dawe, Caldwell, Harris, Morris, & Caldwell, 2001). An hypomorphic *lis-1* allele causes embryonic cell division defects and embryonic lethality (Williams, et al., 2004). However, approximately 30% of the homozygous mutants reach adulthood, allowing researchers to investigate the roles of *lis-1* in mature nervous

system (Gönczy et al., 1999; Williams, et al., 2004).

Since most human patients with lissencephaly show epilepsy (Kerjan & Gleeson, 2007), whether *C. elegans lis-1* mutants also have epilepsy-like phenotype was an interesting question to ask. Williams et al. examined the response of wild-type and *lis-1* mutants to PTZ by placing the animals onto agar plates containing the drug (Williams, et al., 2004). While wild type animals did not show seizure or convulsions within the 30 min observation period, *lis-1* mutants displayed convulsions upon PTZ treatment in a concentration-dependent manner (Williams, et al., 2004). This phenotype was described as "head-bobbing" convulsions, where the animals show muscle contraction in their anterior parts of the body (Figure 1.2A). Moreover, mutations in other genes that encode LIS1 pathway proteins (NUD-1, NUD-2, DHC-1, CDK-5 and CDKA-1) in *C. elegans* cause the similar PTZ-induced convulsion phenotype (Locke, Williams, Schwarz, Caldwell, & Caldwell, 2006) (Figure 1.2B). These studies therefore support that the observed convulsion phenotype in these *C. elegans* mutants share similar molecular pathways with those associated with epilepsy in humans.

Further genetic and pharmacological analyses demonstrated that defects in synaptic transmission are associated with the PTZ-induced convulsion phenotype. Mutants of genes that affect GABAergic transmission (GABA synthetic enzyme *unc-25*/GAD, vesicular GABA transporters *unc-46* and *unc-47*/VGAT, $GABA_A$ receptor *unc-49*) all exhibit the PTZ-induced convulsion phenotype, similar to the *lis-1* mutants (Williams, et al., 2004). In addition, hypomorphic mutation in synaptobrevin, a synaptic-vesicle associated protein required for fusion of synaptic vesicles, causes animals to show PTZ-induced convulsion. In *lis-1* mutant animals, the GABAergic motor neurons develop normal axonal morphology but show abnormal distribution of synaptic vesicles (Williams, et al., 2004). Moreover, disruption of cytoskeletal motor protein functions also causes the PTZ-induced convulsion. Microtubule minus-end directed motor protein dynein has important roles in retrograde transport and also interacts with

LIS-1 (J. Huang, et al., 2012), and a plus-end directed motor KIF1A is required for proper synaptic vesicle transport from *C. elegans* to mammals (Bloom, 2001). Genetic mutations or RNAi treatment disrupting either of the two motor proteins causes mislocalization of synaptic vesicles, as well as PTZ-induced convulsion (Williams, et al., 2004). Taken together, synaptic vesicle trafficking and localization defects coincide with the PTZ-induced convulsions.

In human lissencephaly, it is widely known that cell migration defects occur and results in abnormal cortical morphology in the brain. This mis-positioning of neurons can disrupt the network neurons and contribute to epileptogenesis (J. S. Liu, 2011). However, it is also possible that the migration defect itself is not the whole cause of epilepsy exhibited by the patients, and there can be neuronal cell intrinsic mechanisms that underlie epilepsy(Ross, 2002). The *lis-1* study in *C. elegans* may shed light on the cell-intrinsic mechanisms that occur in patients with lissencephaly and provide genetic tool for further analyses.

C. elegans seizure 3: *acr-2(gf)* shows E/I imbalance and spontaneous convulsions

(1) A missense mutation acetylcholine receptor *acr-2(gf)* causes convulsion phenotype

As described earlier, *C. elegans* with GABAergic motor neurons ablated or mutants with defects in GABAergic transmission shrink when stimulated by gentle touch (McIntire, Jorgensen, & Horvitz, 1993; McIntire, Jorgensen, Kaplan, et al., 1993). Following these studies, in a forward genetic screen aimed to search for additional mutants with the “shrink-upon-touch” phenotype, a novel mutant *acr-2(gf)* was isolated. The mutant is unique in that in addition to the “shrink-upon-touch”, the animals show spontaneous muscle hypercontraction behavior without touch stimulus, referred to as “convulsion” (Jospin et al., 2009) (Figure 1.3A).

The *acr-2(gf)* mutant possesses a missense mutation in an ionotropic non-alpha acetylcholine receptor subunit protein ACR-2, resulting in substitution of a highly conserved valine to methionine in the pore-lining transmembrane domain (TM2) (Figure 1.3B, C).

Importantly, missense mutations in human acetylcholine receptor β2 subunit CHRNB2, which is expressed in the brain, have been linked to familial nocturnal frontal lobe epilepsy (De Fusco et al., 2000; Phillips et al., 2001). In addition, a patient with myasthenia gravis has an valine to methionine mutation at an identical position of TM2 in the β subunit expressed in the muscle (Engel et al., 1996). Forward genetic screening for suppressor mutations of the *acr-2(gf)* convulsion phenotype identified other AChR subunit proteins, UNC-38, UNC-63 and ACR-12 that form a functional channel with ACR-2 (Jospin, et al., 2009) (Figure 1.3B). Channel reconstitution analyses showed that the missense ACR-2 mutation make the channel overactive, similar to the mutant human proteins (Jospin, et al., 2009; Phillips, et al., 2001). These observations imply that *C. elegans acr-2(gf)* convulsion phenotype can be caused by mechanisms similar to human epilepsy.

ACR-2 is expressed in the nervous system including cholinergic motor neurons, and expression of mutant ACR-2 specifically in B-type cholinergic motor neurons can cause the convulsion phenotype (Qi, et al., 2013). The ACR-2 protein localizes to the dendrites and soma, and is excluded from axons, suggesting that it functions mainly postsynaptically (Qi, et al., 2013). Ablation of the command interneurons that control the activity of B-type cholinergic motor neurons can suppress the convulsion phenotype in *acr-2(gf)* animals, further supporting that abnormal activity in the B-type motor neurons causes generation of convulsions (Qi, Garren, Shu, Tsien, & Jin, 2012; Qi, et al., 2013).

Seizure in humans is characterized by abnormal excessive and/or synchronous neural activity in the brain, and epilepsy is defined by recurring unprovoked seizure. Studies using patch clamp electrophysiological recordings from *C. elegans* muscles reveal that *acr-2(gf)* animals show an increase in spontaneous cholinergic transmission accompanied by a decrease in GABAergic transmission, indicating that E/I imbalance in the locomotor circuit underlies the convulsion of *acr-2(gf)* animals (Jospin, et al., 2009; Stawicki, Zhou, Yochem, Chen, & Jin,

2011). Examination of neurons during locomotion by calcium imaging revealed that there is aberrant synchrony in the motor neuron activities in the *acr-2(gf)* animals (Qi, et al., 2013). In wild type animals, different classes of cholinergic motor neurons innervating the muscles show off-phase activation pattern to generate sinusoidal body posture and locomotion (Kawano, et al., 2011). In contrast, in *acr-2(gf)* animals, neurons responsible for forward and reverse locomotion show synchronous activity, as well as the neurons innervating dorsal and ventral body wall muscles (Qi, et al., 2013) (Figure 1.3D). Thus, *acr-2(gf)* disrupts the off-phase activity pattern of these motor neurons and causes aberrant synchrony that lead to convulsion phenotype.

As *acr-2(gf)* animals exhibit spontaneous convulsion behavior, E/I imbalance in the motor neuron circuit, as well as aberrant synchrony of the motor neurons, we can consider the *acr-2(gf)* convulsions as a model of "epileptic-like seizure" in *C. elegans.* Analyses of genetic modifiers of *acr-2(gf)* convulsions can characterize molecular pathways underlying the regulation of E/I balance and the neuron circuit activity, which can potentially be conserved to higher animals. Below, we describe four mechanisms modifying this seizure model: synaptic transmission, ion homeostasis, neuropeptide pathway and inter-cellular signaling between neuron and epidermis.

(2) Roles of fast synaptic transmission in E/I imbalance

Synaptic transmission occurs at millisecond scale, and depends on fast action of synaptic fusion machinery at the presynaptic release site. The key components at the presynaptic active zone include voltage-gated calcium channels and multi-domain scaffolding proteins, such as UNC-13/Munc13, to ensure synaptic vesicle docking and priming (Augustin, Rosenmund, Südhof, & Brose, 1999; Betz et al., 2001; Richmond, Davis, & Jorgensen, 1999). A genetic suppressor of *acr-2(gf)* convulsion identified a mutation in the conserved presynaptic active zone protein UNC-13/Munc13 (Zhou, Stawicki, Goncharov, & Jin, 2013). These proteins contain a

non-calcium binding C2A domain at the N-terminus, and interact with SV fusion process through the MUN and other calcium-binding and protein-binding domains (Figure 1.4Ai). The convulsion-suppressing effect of *unc-13* mutation is caused by selective removal of C2A domain. In this mutant the number of docked synaptic vesicles at the presynaptic active zone is reduced. Electrophysiology studies show slow SV release kinetics (Zhou, et al., 2013) (Figure 1.4Aii). Thus, reduction of excess cholinergic activity by the *unc-13* mutation explains the suppression on *acr-2(gf)* convulsions in the double mutant. The study has not only revealed the function of a specific domain of the conserved UNC-13/Munc13 protein in synaptic transmission, and also points to potential venues to prevent or control seizure through selective regulation of synaptic activity.

(3) Ion homeostasis affects E/I balance

Concentrations of certain ions have been shown to affect seizure (Bitanihirwe & Cunningham, 2009; Sharma, Babu, Singh, Singh, & Singh, 2007). For example, Zn^{2+} affects epileptic symptoms in humans (Bitanihirwe & Cunningham, 2009). Forward genetic screen for suppressors of *acr-2(gf)* convulsions identified multiple genes that directly or indirectly affect the motor neuron circuit. One of such genes is *gtl-2,* which encodes one of the four TRPM channel proteins in *C. elegans* (Stawicki, et al., 2011). TRPM channels are nonselective cation channels, and GTL-2 was previously known to play roles in regulating ion homeostasis of Mg^{2+} and Ca^{2+} (Teramoto et al., 2010; Venkatachalam & Montell, 2007). *gtl-2(lf)* by itself does not have significant effects on motor neuron activities but strongly suppresses *acr-2(gf)* convulsions.

Electrophysiological recordings demonstrated that *gtl-2(lf)* restores the E/I balance in *acr-2(gf)* animals at the neuromuscular junctions. In wild type animals, frequency of cholinergic and GABAergic transmission correlates with the extracellular calcium level (Stawicki, et al., 2011). In contrast, *acr-2(gf)* animals show decreases in GABAergic transmission when the

calcium concentration gets higher, though the cholinergic transmission keeps increasing. The *gtl-2(lf)* mutation restores the calcium-dependent increase of GABAergic motor neuron activity, thereby restoring the E/I balance in the circuit. Interestingly, *gtl-2(lf)* does not have a significant effect on cholinergic transmission of *acr-2(gf)* animals (Stawicki, et al., 2011).

gtl-2 is expressed in the epidermis and excretory cells that are connected by gap junctions, and expression of *gtl-2* in either of the tissues induces convulsion in the *gtl-2(lf); acr-2(gf)* double mutant background. On the other hand, *gtl-2* expression in neurons or muscle cells does not affect convulsions, suggesting that *gtl-2* affects E/I balance by non-neuronal pathways. To further understand which ions *gtl-2* was regulating, effects of application of multiple cation chelators were examined. Interestingly, cation chelator ethylenediaminetetraacetic acid (EDTA), heavy metal specific chelator DTPA and TPEN all suppress *acr-2(gf)* convulsions whereas a more calcium-selective chelator EGTA does not have an effect on convulsions. These results suggest that heavy metal ion homeostasis, but not necessarily Ca^{2+}, can act to regulate the motor neuron circuit activity. Whether this effect comes from local composition of ions at the epidermis located near the axon of motor neurons, or the systemic ion composition of the entire body, or both, remains to be elucidated. The study of *gtl-2* highlights the importance of ion homeostasis in regulation of epileptic-like convulsions and E/I balance in neuronal circuit and also uncovers novel function of non-neuronal tissues in regulating neural circuit activity (Stawicki, et al., 2011).

(4) Homeostatic expression of neuropeptides affects GABAergic transmission

Neuropeptides have important roles in modulating seizures end epilepsy in humans and mammalian models (Kovac & Walker, 2013). Peptide processing mechanisms in *C. elegans* is similar to those in mammals, where the neuropeptide precursor properties are processed by a series of enzymes including proprotein convertases and carboxypeptidases (Jacob & Kaplan,

2003; Li & Kim, 2008; Steiner, 1998). When neuropeptide processing is blocked in *acr-2(gf)* animals by removing proprotein convertase EGL-3, the convulsion frequency significantly increases, suggesting that there are neuropeptides that reduce convulsions (Stawicki, Takayanagi-Kiya, Zhou, & Jin, 2013). Further genetic analyses identified two neuropeptide encoding genes *flp-1* and *flp-18* that have inhibitory functions. In triple mutant animals that lack *flp-1, flp-18* in *acr-2(gf)* background, the convulsion frequency is increased and E/I imbalance is exacerbated, where GABAergic transmission is further reduced compared to the *acr-2(gf)* single mutant (Stawicki, et al., 2013). Overexpression of either of the two genes in neurons can suppress convulsions, consistent with their role as inhibitory neuropeptides. *flp* neuropeptides in *C. elegans* have homology to mammalian neuropeptide Y, which is known to have anticonvulsant roles (Wu et al., 2011). *flp-18* neuropeptides can activate three G-protein coupled receptors NPR-1, NPR-4 and NPR-5, which are homologous to mammalian neuropeptide Y receptors (Cohen et al., 2009; de Bono & Bargmann, 1998; Rogers et al., 2003). These neuropeptide receptors appear to function in multiple tissues including muscles to suppress convulsion (Stawicki, et al., 2013) (Figure 1.4B).

Importantly, the expression level of *flp-18* is increased specifically in cholinergic motor neurons in the *acr-2(gf)* background, and a similar increase can be observed in the wild type background by pharmacological aldicarb treatment to induce increase in cholinergic motor neuron activity. This suggests that *flp-18* is increased in response to elevated neuronal activity. In contrast, reduction of cholinergic motor neuron activity by blocking the activity of AChR channels with mecamylamine, a non-competitive channel blocker, causes reduction in *flp-18* expression. These observations suggest that expression of inhibitory neuropeptides including *flp-18* is regulated in a homeostatic manner, where the expression level correlates with the level of neural activity.

Homeostatic regulations of neuropeptides have been reported from mammalian seizure

models (Christiansen & Woldbye, 2010; Fetissov et al., 2003; Lerner, Sankar, & Mazarati, 2008). The observations from *C. elegans* suggest that there can be evolutionarily conserved mechanisms to induce inhibitory neuropeptides in the hyperactive neurons to modulate the neural circuit activity.

(5) Inter-cellular signaling affects E/I imbalance through control of synaptic density

Synapse density is a critical factor that determines the overall strength of neuronal connections within neural circuits, and is dynamically maintained throughout life time of an animal. Multiple mechanisms function in synapse maintenance, including interactions between neurons and non-neuronal cells such as glia (Eroglu & Barres, 2010). Aberrant synaptic density in the hippocampus has been previously reported from human epilepsy patients (Alonso-Nanclares, Kastanauskaite, Rodriguez, Gonzalez-Soriano, & Defelipe, 2011). *C. elegans* motor neurons and epidermal tissue are in close proximity at the neuromuscular junction, raising a possibility that epidermis affects the motor neuron functions (White, et al., 1986). From an RNAi screen targeting cell-surface molecules expressed in the epidermis, a novel transmembrane protein ZIG-10 was identified to affect excitation and inhibition imbalance (Jin & Cherra, 2016). *zig-10(0); acr-2(gf)* double mutants showed increase in convulsion frequency. The ZIG-10 protein has two extracellular immunoglobulin domains, and is similar in topology to junction adhesion molecules (JAM) in mammals (Rougon & Hobert, 2003). In *zig-10* null mutant, there is an increase in the density of cholinergic motor neuron synapses, with no detectable changes in the morphology of each synapse. Notably, there is also an increase in the postsynaptic ACh receptors in the muscles, indicating that *zig-10* affects both presynaptic and postsynaptic cells. The increase in number of synapses is correlated with the increase in *acr-2(gf)* convulsion, suggesting that the increased cholinergic transmission further exacerbates the E/I imbalance in *acr-2(gf)* animals, leading to increased convulsion.

ZIG-10 is expressed in both neurons and the non-neuronal epidermis, similar to its mammalian homologs (Rougon & Hobert, 2003). Importantly, expression of ZIG-10 in both cholinergic motor neurons and in epidermis is required to rescue the increased *acr-2(gf)* convulsion and synapse number (Jin & Cherra, 2016). Expression in one tissue only, or expression in the muscle and cholinergic motor neurons, does not have rescuing effects. These observations suggest that ZIG-10 acts as a homophilic molecule. Consistently, ZIG-10 shows hemophilic interactions when expressed in mammalian cell culture system. In addition, analysis of ZIG-10 expression under developmental stage-specific promoter suggests that the ZIG-10 functions throughout development to maintain proper synaptic density. Interestingly, ectopic expression of ZIG-10 in GABAergic motor neurons in the wild type background causes reduction of GABAergic synapses, further supporting the role of ZIG-10 in regulating the number of synapses, and also suggesting that GABAergic motor neurons also have the ability to respond to the ZIG-10-mediated regulation of synapses.

ZIG-10 can bind a Src family kinase SRC-2, and this interaction regulates the activity of the phagocytic receptor CED-1 in the epidermis (Jin & Cherra, 2016). Other phagocytosis pathway-related genes *ced-2, ced-5* and *ced-10* exhibit similar genetic interaction with *acr-2(gf)* as *ced-1*. Overall, the results support a model where ZIG-10 activating the phagocytosis pathway to constrain the number of synapses (Figure 1.4C). Elimination of synapses by phagocytosis has also been reported from mammals (Chung et al., 2013; Schafer et al., 2012), but the molecular mechanisms of the specificity of synapse targeting remain elusive. Results from ZIG-10 analysis provide a novel perspective that cell type-specific expression of immunoglobulin superfamily (IgSF) protein may contribute to the specificity of synapse elimination by non-neuronal cells. Studies of the cell-cell interaction pathways may lead to further understanding of the mechanisms of synapse formation and maintenance in epilepsy and in other neurological diseases.

C. elegans seizure 4: CamKII pathway regulates seizure in male-specific muscles

Calcium/calmodulin-dependent kinase II (CaMKII) is a multifunctional serine/threonine kinase that plays many roles in synaptic plasticity and neuronal activity. Studies from rodent models show that seizure induction leads to prolonged decrease of CaMKII activity levels (Churn et al., 2000; Dong & Rosenberg, 2004), whereas decreased level of CaMKII is associated with hyperexcitabily (Churn, et al., 2000). Loss-of-function mutants of *C. elegans* CamKII ortholog *unc-43* show behavioral defects including rapid defecation cycle and uncoordinated muscle contraction (D. J. Reiner, Newton, Tian, & Thomas, 1999). In addition, *unc-43* mutant males show spontaneous contraction of sex muscles without mating cues (LeBoeuf, Gruninger, & Garcia, 2007). Contraction of male sex muscles is regulated by acetylcholine, and an acetylcholine agonist arecoline activates the receptors responsible for the contraction (Garcia, Mehta, & Sternberg, 2001). Thus, examining the sex muscle contraction upon exposure to arecoline provides readout of muscle excitability. Gain-of-function mutant of *unc-43* shows resistance to arecoline, consistent with *unc-43* acting to suppress the sex muscle contraction. Spontaneous sex-muscle seizure is also seen in mutants of UNC-103 ether-a-go-go–related gene (ERG)–like K+ channel (Garcia & Sternberg, 2003; LeBoeuf, et al., 2007). The gain-of-function effect of *unc-43* was partially dependent on *unc-103,* suggesting that UNC-43 acts both upstream of, and in parallel with UNC-103 to suppress muscle contraction (Figure 1.5).

Studies from Drosophila show that CamKII can phosphorylate and activate another group of potassium channel proteins, ether-a-go-go (EAG) K+ channels (Griffith, Wang, Zhong, Wu, & Greenspan, 1994; Sun, Hodge, Zhou, Nguyen, & Griffith, 2004). Mutants of the *C. elegans EAG egl-2* do not show spontaneous sex muscle contraction. However, loss of *egl-2* enhances the seizure phenotype of *unc-103* mutants, suggesting that the two genes act redundantly to suppress muscle contraction (LeBoeuf, Guo, & García, 2011) (Figure 1.5). Also, the arecoline resistance of *unc-43(gf)* allele is partially suppressed by loss of functional *egl-3*,

suggesting that *egl-3* acts downstream of *unc-43* (LeBoeuf, et al., 2007) (Figure 1.5). Loss of both *unc-103* and *egl-2* do not completely suppress the arecoline resistance of *unc-43(gf)*, implying that there are downstream targets of UNC-43 yet to be identified which act in parallel with UNC-103 and EGL-2.

Interestingly, food deprivation attenuates the sex-muscle seizure in *unc-103* mutants (LeBoeuf, et al., 2007). This attenuation is not seen in *unc-43* mutants, suggesting that UNC-43 is required to suppress sex-muscle seizure upon starvation conditions. Food deprivation has weaker suppression effect on *unc-103(0); egl-2(0)* double mutant, suggesting that EGL-2 is partially required for this pathway (LeBoeuf, et al., 2011). Transcriptional reporter assay showed that starvation induces increased expression of *egl-2.* Also, analysis of protein interaction suggested that UNC-43 directly interacts with and modifies EGL-103 at its C-terminus in response to starvation. In addition, mutating a possible UNC-43 interacting site in EGL-2 interferes with the effect of the protein to suppress muscle excitability. These observations raise a model where upon starvation UNC-43 interacts with EGL-2 and modifies the protein to activate the channel functions (Figure 1.5). Also, the expression of EGL-2 can be regulated by UNC-43-related pathway or a parallel pathway in response to food deprivation. Thus, CaMKII/UNC-43 and EAG K+ channel/EGL-2 act together to suppress cell excitability upon starvation in lack of ERG K+ channel/UNC-103.

Human ERG proteins contribute to the electrical activities of heart cells and are associated with cardiac disorders (Mustroph, Maier, & Wagner, 2014). The *C. elegans* studies will contribute to understanding of the CaMKII-K+ channel pathways that regulate neuron and muscle excitability, that are potentially conserved up to higher animals.

Conclusion/perspectives

Genes and proteins regulating neural functions have been of interest of researchers ever

since *C. elegans* was introduced to the field. The accumulated knowledge of neural circuits and proteins in *C. elegans* can serve as a basis for building models and test hypothesis for managing seizure or epilepsy in human. Indeed, as discussed above, recent efforts to address such questions have shown great promise. There are certain limitations in using *C. elegans* to model human diseases, as the small neural circuit may not be equivalent to the neural ensembles in human brain and some molecular pathways in human are also not present in the animal. Nonetheless, the ease of genetic manipulations, *in vivo* protein analyses, high-throughput drug screening and precise examination of neural and muscle activities in *C. elegans* will allow researchers to examine certain aspects of epilepsy in a time-efficient manner.

Acknowledgements

This chapter is a reprint in full of Takayanagi-Kiya, S., & Jin, Y. (In Preparation). Nematodes: Genetic Dissection of Pathways Regulating Seizure and Epileptic-like Behaviors. In A. Pitkänen, S. Moshe, A. S. Galanopoulou & P. Buckmaster (Eds.), *Models of Seizure and Epilepsy* (2nd ed.): Elsevier Academic Press, with permission of both authors. The dissertation author was the primary author.

Figure 1.1. *C. elegans* motor neuron circuit. (A) Cholinergic motor neurons (solid circle) synapse onto the muscles as well as GABAergic motor neurons (open circle). GABAergic motor neurons synapse onto the muscles at opposite side of the body. Top panel shows B-type cholinergic motor neurons, bottom panel shows A-type cholinergic motor neurons. The ventral VA/VB and dorsal DA/DB cholinergic neurons show out-of-phase changes in activity measured by intracellular calcium levels (when VA/VB neurons are more active, DA/DB neurons are less active and vice versa. Also see Figure 3D), consistent with their roles in creating body curvature efficiently for locomotion. (B) Response of *C. elegans* to gentle touch to the head. White line indicates the position of head; black arrow indicates the position of posterior end of animals when the touch stimulus was applied. Left panel: A wild type animal shows reversal upon gentle touch. Right panel: An unc-25(0) animal with defects in GABA biosynthesis shows uncoordinated muscle contraction upon touch stimulus, called "shrinker" phenotype. Note that the head is retracted while the tail is not moving. (C) Proteins required for GABAergic transmission in *C. elegans*. Homeodomain transcription factor UNC-30 regulates transcription of unc-25 and unc-47. UNC-25 is the sole *C. elegans* glutamic acid decarboxylase required for synthesizes of GABA. UNC-47 is the vesicular GABA transporter, and UNC-46 likely functions as an accessory protein for GABA transport. UNC-49 acts as ionotropic GABA receptor on muscles.

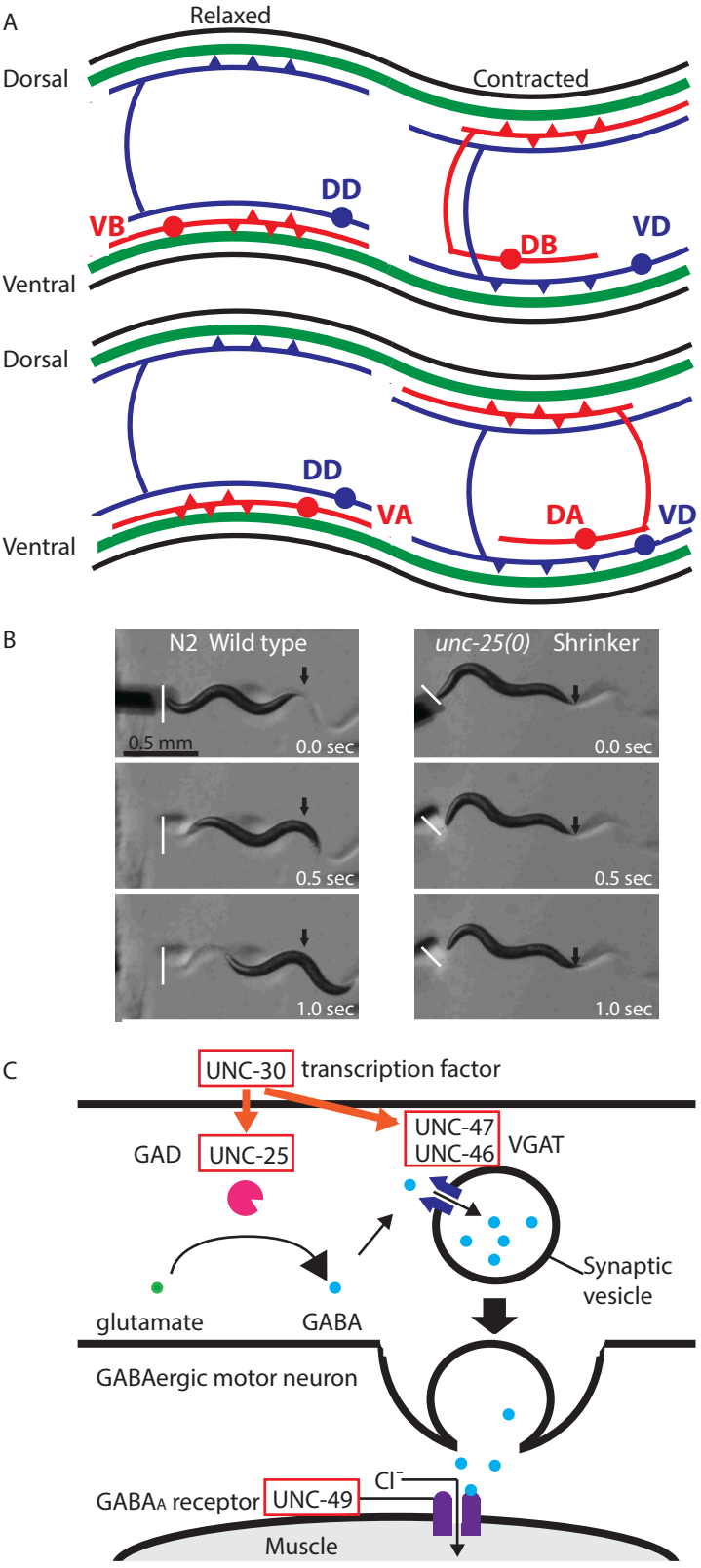
A
Relaxed
Dorsal
Contracted
DD
VB
DB
VD
Ventral
Dorsal
DD
VA
DA
VD
Ventral
B
N2 Wild type
unc-25(0) Shrinker
0.5 mm
0.0 sec
0.0 sec
0.5 sec
0.5 sec
1.0 sec
1.0 sec
C
UNC-30 transcription factor
GAD
UNC-25
UNC-47
UNC-46
VGAT
Synaptic vesicle
glutamate
GABA
GABAergic motor neuron
GABAA receptor
UNC-49
Cl-
Muscle

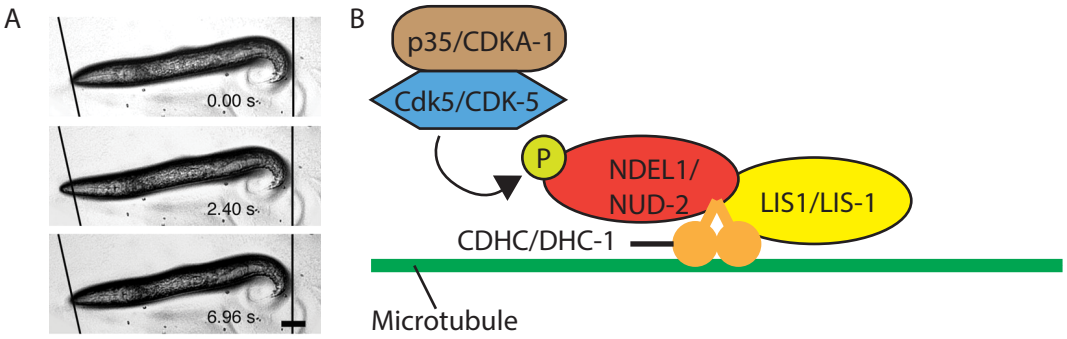

Figure 1.2. Disruption of C. elegans LIS-1 pathway causes epileptic-like seizures upon exposure to PTZ. (A) A lis-1 hypormorphic mutant showing head-bobbing convulsion upon application of GABA receptor antagonist PTZ. Note that anterior body is showing muscle contraction. Adopted from (Williams, et al., 2004) with modifications. (B) LIS-1 and its known interacting proteins that affect dynein. Current model predicts that defects in these proteins disrupt synaptic morphology and functions by affecting dynein-mediated transport, and thus makes the animal susceptible to PTZ-induced seizure. Created based on (Locke, et al., 2006).

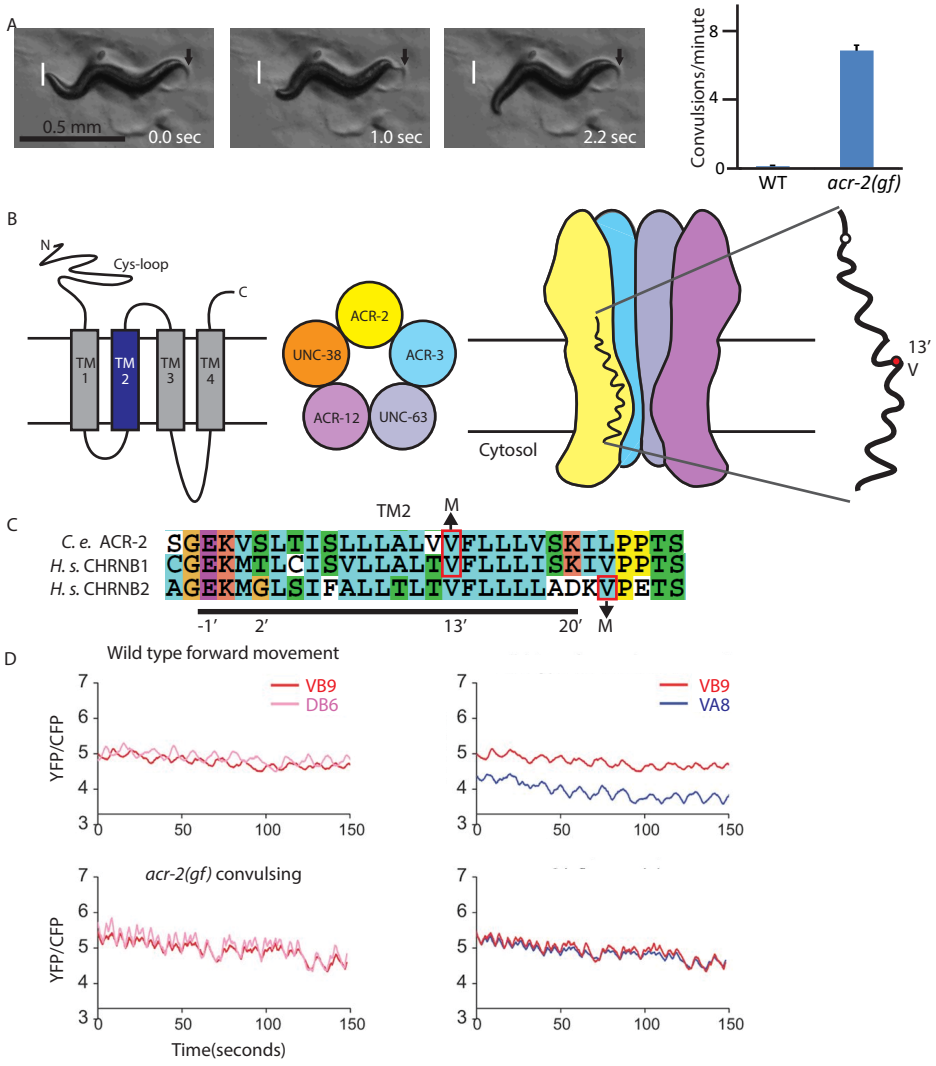

Figure 1.3. A Gain-of-function mutation in an acetylcholine receptor causes convulsion phenotype in *C. elegans*. (A) Left panel: An *acr-2(gf)* animal showing convulsion. Note that both anterior and posterior sides of the body show muscle contraction. Right panel: Frequency of the convulsion evement of *acr-2(gf)* animals, scored visually by observation under dissection scope. (B) Structuer of an nAChR. Left panel: Ligand-gated ion channel subunits have four transmembrane domains, with transmembrane domain 2 (TM2) facing the ion channel pore. A ligand-gated ion channel forms a pentamer as a functional channel. Middle panel: A possible toplogy of nAChR channelincluding the ACR-2 subunit. Right panel: Schematic diagram of an nAChR. TM2 is aligned to the pore. Circle represents the location of the amino acid residue mutated in *acr-2(gf)*. The diagram of receptor is based on (Unwin, 1995). (C) Alignment of amino acid sequences of TM2 from *C. elegans* and human nAChRs. (D) *acr-2(gf)* causes aberrant synchronized activation of motor neurons. Calcium imaging traces from motor neurons in animals showing forward locomotion from wild type and in *acr-2(gf)* animals. Left panel: In wild type, a neuron innvervating the ventral muscle (VB9) and dorsal muscle (DB9) show off-phase activation pattern. The neurons show syncronous activity in *acr-2(gf)*. Right pannel: VB neuron shows higher calcium levels over the VA neuron during forward locomotion in wild type. The calcium levels are similar in acr-2(gf) animals. Adopted with modification from (Qi, et al., 2013).

Figure 1.4. Multiple pathways modulate the *acr-2(gf)* convulsion phenotype. (A) UNC-13 C2A domain affects synaptic release kinetics by modulating the localization of synaptic vesicles around the active zone. Top panel: Structure of UNC-13 protein. A non calcium-binding C2A domain is located at the N-terminus. It also contains conserved motifs including calmodulin binding (CaM) site and MUN domain with the Munc13 homology domain. Bottom panel: In wild type animals, UNC-13 bound to synaptic vesicle (SV)-associated protein interacts with the zinc finger (ZF) domain of RIM/UNC-10 at the C2A domain and promotes the localization of SV at or close to the active zone. In animals lacking the C2A domain, there is reduction in the number of docked SVs at the precise synaptic localization and more SVs are located distal to the active zones, which affects the kinetics of evoked release. (B) Homeostatic expression of neuropeptides suppresses *acr-2(gf)* convulsions. In neurons, neuropeptide precursor propeptides are packaged into dense core vesicles (DCVs) and processed by enzymes such as a protein convertase EGL-3. Mature neuropeptides are released from synaptic regions and act on downstream GPCRs. FLP-1 and FLP-18 act inhibitory on *acr-2(gf)* convulsions and ameliorate the E/I imbalance by modulating GABAergic transmission and acting on the muscles. The expression level of FLP-18, and likely FLP-1, in cholinergic motor neurons are increased in cholinergic motor neurons of *acr-2(gf)* animals. Also, pharmacologically manipulating neuronal activities can induce changes in the expression levels of neuropeptides, suggesting that their expression levels are regulated in a homeostatic manner to suppress hyperactivity of the neurons. At least three GPCRs, NPR-1, NPR-4 and NPR-5 are involved in this pathway. NPR-5 functions in the muscles to suppress convulsions, whereas NPR-1 and NPR-4 likely act in other tissues including neurons. (C) ZIG-10 regulates inter-cellular signaling and phagocytosis pathway which is required for constraining the number of synapses in cholinergic motor neurons. The figure describes a cross section near a neuromuscular junction where cholinergic motor neuron, epidermis and muscle are in close proximity. ZIG-10 is expressed in both the epidermis and cholinergic motor neurons. Cell-cell interaction by ZIG-10 activates the downstream pathway in the epidermis including phosphorylation of CED-1 by SRC-2. CED-1, with other proteins involved in the phagocytosis pathway, functions to reduce synaptic density at the neuromuscular junction by preventing the formation of synapses and/or eliminating the existing synapses.

A

(i) UNC-13/Munc13 protein structure illustration

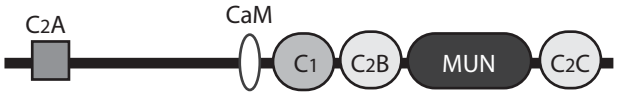

(ii) Illustration of presynaptic terminal

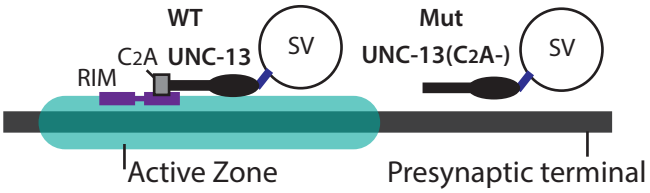

B

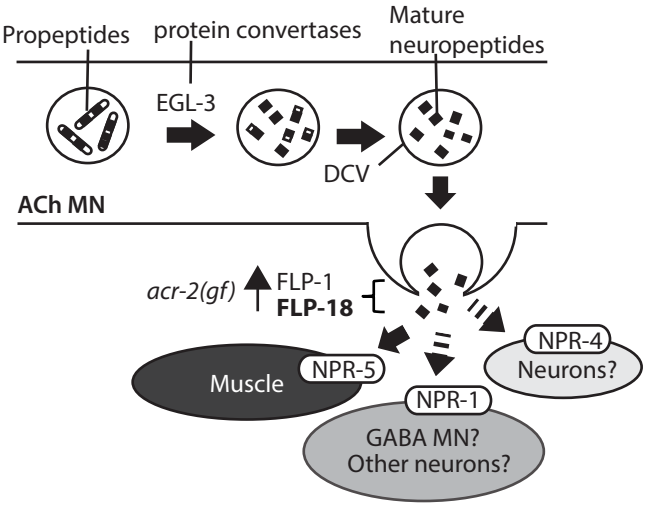

C

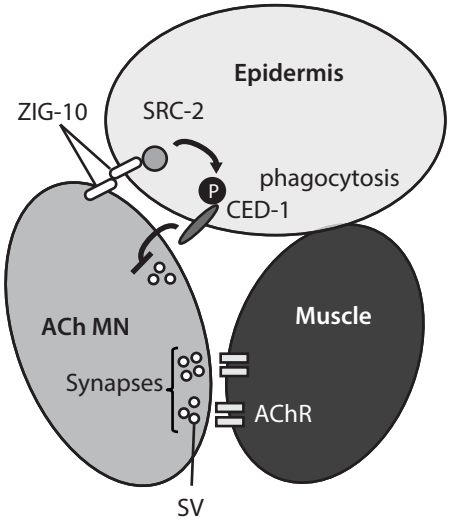

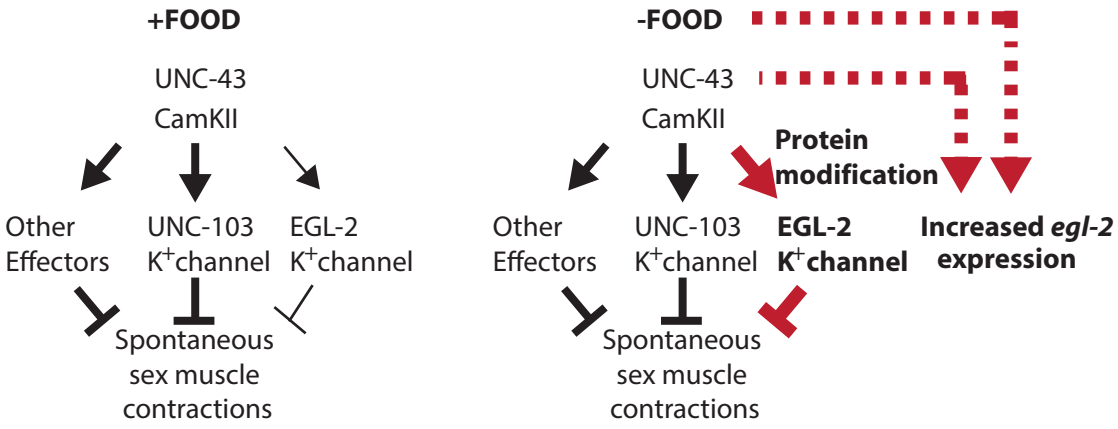

Figure 1.5. CamKII, ERG- and EAG- potassium channels modulate sex muscle seizure. ERG K+ channel/UNC-103 and EAG K+ channel/EGL-2 can act downstream of UNC-43 to suppress sex muscle contractions. UNC-43 also acts on other effectors for suppression of contractions. Left panel: Under fed condition, EGL-2 has minor effects as the expression level is low and loss of *egl-2* does not have a severe effect. Right panel: Upon food deprivation, UNC-43 interacts with and modifies EGL-2 which likely promotes the channel activity that is required for the suppression of sex muscle contraction in lack of UNC-103. Expression of *egl-2* is upregulated, which can be a downstream effect of UNC-43 or through other pathways induced by starvation. Created based on (LeBoeuf, et al., 2007) and (LeBoeuf, et al., 2011).

Table 1.1. *C. elegans* homologs of human genes associated with epilepsy. References: [1](Noebels, 2015), [2](Salkoff et al., 2005), [3](Meisler, Kearney, Ottman, & Escayg, 2001), [4](Fawcett et al., 2006), [5](Nicita, et al., 2012), [6](Aridon et al., 2006), [7](Culetto et al., 2004), [8](Fleming et al., 1997), [9](Jospin et al., 2009), [10](Allen, et al., 2013), [11](DeLorey et al., 1998), [12](Richmond & Jorgensen, 1999), [13](Bamber, et al., 2003), [14](Feng, et al., 2002), [15](Hobert, 2013), [16](Liang, et al., 2006), [17](Liang, et al., 2007), [18](Caylor, et al., 2013) [19](Steger, et al., 2005), [20](Saitsu, et al., 2008), [21](Weimer, et al., 2003), [22](McEwen, et al. 2011) [23](Graham, et al., 2008), [24](Thierry-Mieg and Thierry-Mieg, 2006), [25](Claes, et al., 2001), [26](Veeramah, et al., 2012), [27](Kamiya, et al., 2004), [28](Consortium, et al., 2014), [29](Clark, et al., 1997), [30](Hitomi, et al., 2013), [31](Jose, et al., 2012), [32](Raich, et al., 2003), [33](Novarino, et al., 2013), [34](Timal, et al., 2012), [35](Zhang, et al., 2002), [36](Hao, et al., 2001), [37](Feng, et al., 2013), [38](Kitaoka, et al., 2013), [39](Li, et al., 2006), [40](Hill, et al., 2001), [41](Steimel, et al., 2010), [42](Melkman, et al., 2005), [43](Tucker, et al., 2005), [44](Pujol, et al., 2000), [45](Van Buskirk, et al., 2010), [46](Yuan, et al., 2000), [47](Zhang, et al., 2004), [48](Ashrafi, et al., 2003), [49](Wynshaw-Boris, et al., 2010), [50](Huang, et al., 2012), [51](Reiner, 2013), [52](Reiner and Sapier, 2013), [53](Dawe, et al., 2001), [54](Williams, et al., 2004), [55](Locke, et al., 2006)

Description	Human gene	*C. elegans* homologs
KCNQ Potassium channel	*KCNQ1*[1] *KCNQ2*[3] *KCNQ3*[3]	*kqt-1, kqt-2, kqt-3*[2]
KCNA Potassium channel	*KCNA1*[1]	*shk-1*[4]
Nicotinic ACh receptor, α subunit	*CHRNA2*[5, 6] *CHRNA4*[3]	*unc-63* [7], *unc-38* [8, 9]
Nicotinic ACh receptor, non-α subunit	*CHRNB2*[3]	*acr-2*[9], *acr-3*[9], *unc-29*, *lev-1*[7, 8]
Ionotropic GABA receptor	*GABRB3*[10] [11] *GABRG2*[3]	*unc-49*[12, 13], *gab-1*[14] *lgc-36*, *lgc-37*, *lgc-38*[15]
Voltage-gated calcium channel	*Cav3.2*[16, 17]	*cca-1*[18, 19]
Syntaxin binding protein	*STXBP1*[10, 20]	*unc-18*[21-23], *T07A9.10*[24]
Voltage-gated sodium channel	*SCN1A*[10, 25] *SCN8A*[10, 26] *SCN2A*[10] [27] *SCN1B*[3]	**C. elegans* lacks voltage-gated sodium channels
Dynamin GTPase	*DNM1*[10, 28]	*dyn-1*[29]
Tyrosine kinase	*TNK2*[30]	*sid-3*[31]
Cyclin-dependent kinase	*CDKL5*[10]	*mbk-1*[32]
Bipartite UDP-N-acetylglucosamine transferase	*ALG13*[33, 34]	*mtd-1*[24, 35]
Leucine-rich neuronal secreted protein	*LGI1*[5]	*slt-1*[36]
Solute carrier family 2	*SLC2A1*[1, 5]	*fgt-1*[37, 38], *R09B5.11*[24]
EF-hand-containing calcium binding protein	*EFHC1*[5]	*Y49A10A.1*[39]
Protocadherin	*PCDH19*[5]	*cdh-1*[40], *cdh-6/fmi-1*[40, 41]
Homeobox protein	*ARX*[5]	*alr-1*[42, 43], *ceh-17*[44, 45]
Sodium-activated potassium channel	*KCNT1*[1]	*slo-2*[46]
SUMO protease	*SENP2*[1]	*ulp-1*[47]
Mitochondrial glutamate carrier	*SLC25A22*[5]	*F20D1.9*[24, 39, 48], *F55G1.5*[24]
Dynein binding protein	*LIS1*[49-52]	*lis-1*[53-55]

References

Alfonso, A., Grundahl, K., Duerr, J. S., Han, H. P., & Rand, J. B. (1993). The *Caenorhabditis elegans unc-17* gene: a putative vesicular acetylcholine transporter. *Science, 261*(5121), 617-619.

Allen, A. S., Berkovic, S. F., Cossette, P., Delanty, N., Dlugos, D., Eichler, E. E., Epstein, M. P., Glauser, T., Goldstein, D. B., Han, Y., Heinzen, E. L., Hitomi, Y., Howell, K. B., Johnson, M. R., Kuzniecky, R., Lowenstein, D. H., Lu, Y. F., Madou, M. R., Marson, A. G., Mefford, H. C., Esmaeeli Nieh, S., O'Brien, T. J., Ottman, R., Petrovski, S., Poduri, A., Ruzzo, E. K., Scheffer, I. E., Sherr, E. H., Yuskaitis, C. J., Abou-Khalil, B., Alldredge, B. K., Bautista, J. F., Berkovic, S. F., Boro, A., Cascino, G. D., Consalvo, D., Crumrine, P., Devinsky, O., Dlugos, D., Epstein, M. P., Fiol, M., Fountain, N. B., French, J., Friedman, D., Geller, E. B., Glauser, T., Glynn, S., Haut, S. R., Hayward, J., Helmers, S. L., Joshi, S., Kanner, A., Kirsch, H. E., Knowlton, R. C., Kossoff, E. H., Kuperman, R., Kuzniecky, R., Lowenstein, D. H., McGuire, S. M., Motika, P. V., Novotny, E. J., Ottman, R., Paolicchi, J. M., Parent, J. M., Park, K., Poduri, A., Scheffer, I. E., Shellhaas, R. A., Sherr, E. H., Shih, J. J., Singh, R., Sirven, J., Smith, M. C., Sullivan, J., Lin Thio, L., Venkat, A., Vining, E. P., Von Allmen, G. K., Weisenberg, J. L., Widdess-Walsh, P., & Winawer, M. R. (2013). De novo mutations in epileptic encephalopathies. *Nature, 501*(7466), 217-221.

Alonso-Nanclares, L., Kastanauskaite, A., Rodriguez, J. R., Gonzalez-Soriano, J., & Defelipe, J. (2011). A stereological study of synapse number in the epileptic human hippocampus. *Front Neuroanat, 5*, 8.

Augustin, I., Rosenmund, C., Südhof, T. C., & Brose, N. (1999). Munc13-1 is essential for fusion competence of glutamatergic synaptic vesicles. *Nature, 400*(6743), 457-461.

Avanzini, G., Franceschetti, S., & Mantegazza, M. (2007). Epileptogenic channelopathies: experimental models of human pathologies. *Epilepsia, 48 Suppl 2*, 51-64.

Bamber, B. A., Twyman, R. E., & Jorgensen, E. M. (2003). Pharmacological characterization of the homomeric and heteromeric UNC-49 GABA receptors in *C. elegans*. *Br J Pharmacol, 138*(5), 883-893.

Betz, A., Thakur, P., Junge, H. J., Ashery, U., Rhee, J. S., Scheuss, V., Rosenmund, C., Rettig, J., & Brose, N. (2001). Functional interaction of the active zone proteins Munc13-1 and RIM1 in synaptic vesicle priming. *Neuron, 30*(1), 183-196.

Bitanihirwe, B. K., & Cunningham, M. G. (2009). Zinc: the brain's dark horse. *Synapse, 63*(11), 1029-1049.

Bloom, G. S. (2001). The UNC-104/KIF1 family of kinesins. *Curr Opin Cell Biol, 13*(1), 36-40.

Brenner, S. (1974). The genetics of *Caenorhabditis elegans*. *Genetics, 77*(1), 71-94.

Briggs, S. W., & Galanopoulou, A. S. (2011). Altered GABA signaling in early life epilepsies. *Neural Plast, 2011*, 527605.

Caylor, R. C., Jin, Y., & Ackley, B. D. (2013). The *Caenorhabditis elegans* voltage-gated

calcium channel subunits UNC-2 and UNC-36 and the calcium-dependent kinase UNC-43/CaMKII regulate neuromuscular junction morphology. *Neural Dev, 8*, 10.

Chalfie, M., Sulston, J. E., White, J. G., Southgate, E., Thomson, J. N., & Brenner, S. (1985). The neural circuit for touch sensitivity in *Caenorhabditis elegans*. *J Neurosci, 5*(4), 956-964.

Christiansen, S. H., & Woldbye, D. P. (2010). Regulation of the galanin system by repeated electroconvulsive seizures in mice. *J Neurosci Res, 88*(16), 3635-3643.

Chung, W. S., Clarke, L. E., Wang, G. X., Stafford, B. K., Sher, A., Chakraborty, C., Joung, J., Foo, L. C., Thompson, A., Chen, C., Smith, S. J., & Barres, B. A. (2013). Astrocytes mediate synapse elimination through MEGF10 and MERTK pathways. *Nature, 504*(7480), 394-400.

Churn, S. B., Sombati, S., Jakoi, E. R., Severt, L., DeLorenzo, R. J., & Sievert, L. (2000). Inhibition of calcium/calmodulin kinase II alpha subunit expression results in epileptiform activity in cultured hippocampal neurons. *Proc Natl Acad Sci U S A, 97*(10), 5604-5609.

Cinar, H., Keles, S., & Jin, Y. (2005). Expression profiling of GABAergic motor neurons in *Caenorhabditis elegans*. *Curr Biol, 15*(4), 340-346.

Clark, S. G., Shurland, D. L., Meyerowitz, E. M., Bargmann, C. I., & van der Bliek, A. M. (1997). A dynamin GTPase mutation causes a rapid and reversible temperature-inducible locomotion defect in *C. elegans*. *Proc Natl Acad Sci U S A, 94*(19), 10438-10443.

Cohen, M., Reale, V., Olofsson, B., Knights, A., Evans, P., & de Bono, M. (2009). Coordinated regulation of foraging and metabolism in *C. elegans* by RFamide neuropeptide signaling. *Cell Metab, 9*(4), 375-385.

Consortium, E.-R., Project, E. P. G., & Consortium, E. K. (2014). De novo mutations in synaptic transmission genes including DNM1 cause epileptic encephalopathies. *Am J Hum Genet, 95*(4), 360-370.

Corsi, A. K., Wightman, B., & Chalfie, M. (2015). A Transparent Window into Biology: A Primer on *Caenorhabditis elegans*. *Genetics, 200*(2), 387-407.

Culetto, E., Baylis, H. A., Richmond, J. E., Jones, A. K., Fleming, J. T., Squire, M. D., Lewis, J. A., & Sattelle, D. B. (2004). The *Caenorhabditis elegans unc-63* gene encodes a levamisole-sensitive nicotinic acetylcholine receptor alpha subunit. *J Biol Chem, 279*(41), 42476-42483.

Culetto, E., & Sattelle, D. B. (2000). A role for Caenorhabditis elegans in understanding the function and interactions of human disease genes. *Hum Mol Genet, 9*(6), 869-877.

Dawe, A. L., Caldwell, K. A., Harris, P. M., Morris, N. R., & Caldwell, G. A. (2001). Evolutionarily conserved nuclear migration genes required for early embryonic development in *Caenorhabditis elegans*. *Dev Genes Evol, 211*(8-9), 434-441.

de Bono, M., & Bargmann, C. I. (1998). Natural variation in a neuropeptide Y receptor homolog

modifies social behavior and food response in *C. elegans*. *Cell, 94*(5), 679-689.

De Fusco, M., Becchetti, A., Patrignani, A., Annesi, G., Gambardella, A., Quattrone, A., Ballabio, A., Wanke, E., & Casari, G. (2000). The nicotinic receptor beta 2 subunit is mutant in nocturnal frontal lobe epilepsy. *Nat Genet, 26*(3), 275-276.

DeLorey, T. M., Handforth, A., Anagnostaras, S. G., Homanics, G. E., Minassian, B. A., Asatourian, A., Fanselow, M. S., Delgado-Escueta, A., Ellison, G. D., & Olsen, R. W. (1998). Mice lacking the beta3 subunit of the GABAA receptor have the epilepsy phenotype and many of the behavioral characteristics of Angelman syndrome. *J Neurosci, 18*(20), 8505-8514.

Dong, Y., & Rosenberg, H. C. (2004). Prolonged changes in Ca2+/calmodulin-dependent protein kinase II after a brief pentylenetetrazol seizure; potential role in kindling. *Epilepsy Res, 58*(2-3), 107-117.

Eastman, C., Horvitz, H. R., & Jin, Y. (1999). Coordinated transcriptional regulation of the unc-25 glutamic acid decarboxylase and the unc-47 GABA vesicular transporter by the *Caenorhabditis elegans* UNC-30 homeodomain protein. *J Neurosci, 19*(15), 6225-6234.

Engel, A. G., Ohno, K., Milone, M., Wang, H. L., Nakano, S., Bouzat, C., Pruitt, J. N. II, Hutchinson, D. O., Brengman, J. M., Bren, N., Sieb, J. P., Sine, S. M. (1996). New mutations in acetylcholine receptor subunit genes reveal heterogeneity in the slow-channel congenital myasthenic syndrome. *Hum Mol Genet, 5*(9), 1217-1227.

Erickson, J. D., Varoqui, H., Schäfer, M. K., Modi, W., Diebler, M. F., Weihe, E., Rand, J., Eiden, L. E., Bonner, T. I., & Usdin, T. B. (1994). Functional identification of a vesicular acetylcholine transporter and its expression from a "cholinergic" gene locus. *J Biol Chem, 269*(35), 21929-21932.

Eroglu, C., & Barres, B. A. (2010). Regulation of synaptic connectivity by glia. *Nature, 468*(7321), 223-231.

Fetissov, S. O., Jacoby, A. S., Brumovsky, P. R., Shine, J., Iismaa, T. P., & Hökfelt, T. (2003). Altered hippocampal expression of neuropeptides in seizure-prone GALR1 knockout mice. *Epilepsia, 44*(8), 1022-1033.

Fisher, R. S., van Emde Boas, W., Blume, W., Elger, C., Genton, P., Lee, P., & Engel J. Jr. (2005). Epileptic seizures and epilepsy: definitions proposed by the International League Against Epilepsy (ILAE) and the International Bureau for Epilepsy (IBE). *Epilepsia, 46*(4), 470-472.

Fleming, J. T., Squire, M. D., Barnes, T. M., Tornoe, C., Matsuda, K., Ahnn, J.,Fire, A., Sulston, J. E., Barnard, E. A., Sattelle D. B., & Lewis J. A. (1997). *Caenorhabditis elegans* levamisole resistance genes *lev-1*, *unc-29*, and *unc-38* encode functional nicotinic acetylcholine receptor subunits. *J Neurosci, 17*(15), 5843-5857.

Gönczy, P., Schnabel, H., Kaletta, T., Amores, A. D., Hyman, T., & Schnabel, R. (1999). Dissection of cell division processes in the one cell stage *Caenorhabditis elegans* embryo by mutational analysis. *J Cell Biol, 144*(5), 927-946.

Gao, S., & Zhen, M. (2011). Action potentials drive body wall muscle contractions in *Caenorhabditis elegans*. *Proc Natl Acad Sci U S A, 108*(6), 2557-2562.

Garcia, L. R., Mehta, P., & Sternberg, P. W. (2001). Regulation of distinct muscle behaviors controls the *C. elegans* male's copulatory spicules during mating. *Cell, 107*(6), 777-788.

Garcia, L. R., & Sternberg, P. W. (2003). *Caenorhabditis elegans* UNC-103 ERG-like potassium channel regulates contractile behaviors of sex muscles in males before and during mating. *J Neurosci, 23*(7), 2696-2705.

Goodman, M. B., Lindsay, T. H., Lockery, S. R., & Richmond, J. E. (2012). Electrophysiological methods for *Caenorhabditis elegans* neurobiology. *Methods Cell Biol, 107*, 409-436.

Griffith, L. C., Wang, J., Zhong, Y., Wu, C. F., & Greenspan, R. J. (1994). Calcium/calmodulin-dependent protein kinase II and potassium channel subunit eag similarly affect plasticity in Drosophila. *Proc Natl Acad Sci U S A, 91*(21), 10044-10048.

Hobert, O. (2013). The neuronal genome of *Caenorhabditis elegans*. *WormBook*, 1-106.

Howell, K., White, J. G., & Hobert, O. (2015). Spatiotemporal control of a novel synaptic organizer molecule. *Nature, 523*(7558), 83-87.

Huang, J., Roberts, A. J., Leschziner, A. E., & Reck-Peterson, S. L. (2012). Lis1 acts as a "clutch" between the ATPase and microtubule-binding domains of the dynein motor. *Cell, 150*(5), 975-986.

Huang, R. Q., Bell-Horner, C. L., Dibas, M. I., Covey, D. F., Drewe, J. A., & Dillon, G. H. (2001). Pentylenetetrazole-induced inhibition of recombinant gamma-aminobutyric acid type A (GABA(A)) receptors: mechanism and site of action. *J Pharmacol Exp Ther, 298*(3), 986-995.

Jacob, T. C., & Kaplan, J. M. (2003). The EGL-21 carboxypeptidase E facilitates acetylcholine release at *Caenorhabditis elegans* neuromuscular junctions. *J Neurosci, 23*(6), 2122-2130.

Jin, Y., & Cherra, S. (2016). A two-immunoglobulin-domain transmembrane protein mediates an epidermal-neuronal interaction to maintain synapse density. *Neuron*. *89*(2), 325-336.

Jin, Y., Hoskins, R., & Horvitz, H. R. (1994). Control of type-D GABAergic neuron differentiation by *C. elegans* UNC-30 homeodomain protein. *Nature, 372*(6508), 780-783.

Jin, Y., Jorgensen, E., Hartwieg, E., & Horvitz, H. R. (1999). The *Caenorhabditis elegans* gene unc-25 encodes glutamic acid decarboxylase and is required for synaptic transmission but not synaptic development. *J Neurosci, 19*(2), 539-548.

Jospin, M., Qi, Y. B., Stawicki, T. M., Boulin, T., Schuske, K. R., Horvitz, H. R., Bessereau, J. L, Jorgensen, E. M., & Jin, Y. (2009). A neuronal acetylcholine receptor regulates the balance of muscle excitation and inhibition in *Caenorhabditis elegans*. *PLoS Biol, 7*(12), e1000265.

Kaletta, T., & Hengartner, M. O. (2006). Finding function in novel targets: *C. elegans* as a model organism. *Nat Rev Drug Discov, 5*(5), 387-398.

Kawano, T., Po, M. D., Gao, S., Leung, G., Ryu, W. S., & Zhen, M. (2011). An imbalancing act: gap junctions reduce the backward motor circuit activity to bias *C. elegans* for forward locomotion. *Neuron, 72*(4), 572-586.

Kerjan, G., & Gleeson, J. G. (2007). Genetic mechanisms underlying abnormal neuronal migration in classical lissencephaly. *Trends Genet, 23*(12), 623-630.

Kerr, R., Lev-Ram, V., Baird, G., Vincent, P., Tsien, R. Y., & Schafer, W. R. (2000). Optical imaging of calcium transients in neurons and pharyngeal muscle of *C. elegans*. *Neuron, 26*(3), 583-594.

Kimble, J., & Hirsh, D. (1979). The postembryonic cell lineages of the hermaphrodite and male gonads in *Caenorhabditis elegans*. *Dev Biol, 70*(2), 396-417.

Kitamura, K., Yanazawa, M., Sugiyama, N., Miura, H., Iizuka-Kogo, A., Kusaka, M., Omichi, K., Suzuki, R., Kato-Fukui, Y., Kamiirisa, K., Matsuo, M., Kamijo, S., Kasahara, M., Yoshioka, H., Ogata, T., Fukuda, T., Kondo, I., Kato, M., Dobyns, W. B., Yokoyama, M., & Morohashi, K. (2002). Mutation of ARX causes abnormal development of forebrain and testes in mice and X-linked lissencephaly with abnormal genitalia in humans. *Nat Genet, 32*(3), 359-369.

Kovac, S., & Walker, M. C. (2013). Neuropeptides in epilepsy. *Neuropeptides, 47*(6), 467-475.

LeBoeuf, B., Gruninger, T. R., & Garcia, L. R. (2007). Food deprivation attenuates seizures through CaMKII and EAG K+ channels. *PLoS Genet, 3*(9), 1622-1632.

LeBoeuf, B., Guo, X., & García, L. R. (2011). The effects of transient starvation persist through direct interactions between CaMKII and ether-a-go-go K+ channels in *C. elegans* males. *Neuroscience, 175*, 1-17.

Lerner, J. T., Sankar, R., & Mazarati, A. M. (2008). Galanin and epilepsy. *Cell Mol Life Sci, 65*(12), 1864-1871.

Lewis, J. A., Wu, C. H., Levine, J. H., & Berg, H. (1980). Levamisole-resistant mutants of the nematode *Caenorhabditis elegans* appear to lack pharmacological acetylcholine receptors. *Neuroscience, 5*(6), 967-989.

Li, C., & Kim, K. (2008). Neuropeptides. *WormBook*, 1-36.

Liu, J. S. (2011). Molecular genetics of neuronal migration disorders. *Curr Neurol Neurosci Rep, 11*(2), 171-178.

Liu, Q., Chen, B., Hall, D. H., & Wang, Z. W. (2007). A quantum of neurotransmitter causes minis in multiple postsynaptic cells at the *Caenorhabditis elegans* neuromuscular junction. *Dev Neurobiol, 67*(2), 123-128.

Liu, Q., Hollopeter, G., & Jorgensen, E. M. (2009). Graded synaptic transmission at the

Caenorhabditis elegans neuromuscular junction. *Proc Natl Acad Sci U S A, 106*(26), 10823-10828.

Locke, C. J., Williams, S. N., Schwarz, E. M., Caldwell, G. A., & Caldwell, K. A. (2006). Genetic interactions among cortical malformation genes that influence susceptibility to convulsions in *C. elegans*. *Brain Res, 1120*(1), 23-34.

Lodato, S., Tomassy, G. S., De Leonibus, E., Uzcategui, Y. G., Andolfi, G., Armentano, M., Touzot, A., Gaztelu, J. M., Arlotta, P., Menendez de la Prida, L., & Studer, M.. (2011). Loss of COUP-TFI alters the balance between caudal ganglionic eminence- and medial ganglionic eminence-derived cortical interneurons and results in resistance to epilepsy. *J Neurosci, 31*(12), 4650-4662.

Loria, P. M., Hodgkin, J., & Hobert, O. (2004). A conserved postsynaptic transmembrane protein affecting neuromuscular signaling in *Caenorhabditis elegans*. *J Neurosci, 24*(9), 2191-2201.

Lossin, C., Wang, D. W., Rhodes, T. H., Vanoye, C. G., & George, A. L. (2002). Molecular basis of an inherited epilepsy. *Neuron, 34*(6), 877-884.

Mahoney, T. R., Luo, S., & Nonet, M. L. (2006). Analysis of synaptic transmission in *Caenorhabditis elegans* using an aldicarb-sensitivity assay. *Nat Protoc, 1*(4), 1772-1777.

Mantegazza, M., Rusconi, R., Scalmani, P., Avanzini, G., & Franceschetti, S. (2010). Epileptogenic ion channel mutations: from bedside to bench and, hopefully, back again. *Epilepsy Res, 92*(1), 1-29.

Matthies, D. S., Fleming, P. A., Wilkes, D. M., & Blakely, R. D. (2006). The *Caenorhabditis elegans* choline transporter CHO-1 sustains acetylcholine synthesis and motor function in an activity-dependent manner. *J Neurosci, 26*(23), 6200-6212.

McEwen, J. M., & Kaplan, J. M. (2008). UNC-18 promotes both the anterograde trafficking and synaptic function of syntaxin. *Mol Biol Cell, 19*(9), 3836-3846.

McIntire, S. L., Jorgensen, E., & Horvitz, H. R. (1993). Genes required for GABA function in *Caenorhabditis elegans*. *Nature, 364*(6435), 334-337.

McIntire, S. L., Jorgensen, E., Kaplan, J., & Horvitz, H. R. (1993). The GABAergic nervous system of *Caenorhabditis elegans*. *Nature, 364*(6435), 337-341.

McIntire, S. L., Reimer, R. J., Schuske, K., Edwards, R. H., & Jorgensen, E. M. (1997). Identification and characterization of the vesicular GABA transporter. *Nature, 389*(6653), 870-876.

Meisler, M. H., Kearney, J., Ottman, R., & Escayg, A. (2001). Identification of epilepsy genes in human and mouse. *Annu Rev Genet, 35*, 567-588.

Melkman, T., & Sengupta, P. (2005). Regulation of chemosensory and GABAergic motor neuron development by the *C. elegans* Aristaless/Arx homolog alr-1. *Development, 132*(8), 1935-1949.

Millar, N. S. (2008). RIC-3: a nicotinic acetylcholine receptor chaperone. *Br J Pharmacol, 153 Suppl 1*, S177-183.

Miller, K. G., Alfonso, A., Nguyen, M., Crowell, J. A., Johnson, C. D., & Rand, J. B. (1996). A genetic selection for *Caenorhabditis elegans* synaptic transmission mutants. *Proc Natl Acad Sci U S A, 93*(22), 12593-12598.

Mongan, N. P., Baylis, H. A., Adcock, C., Smith, G. R., Sansom, M. S., & Sattelle, D. B. (1998). An extensive and diverse gene family of nicotinic acetylcholine receptor alpha subunits in *Caenorhabditis elegans*. *Receptors Channels, 6*(3), 213-228.

Mustroph, J., Maier, L. S., & Wagner, S. (2014). CaMKII regulation of cardiac K channels. *Front Pharmacol, 5*, 20.

Nguyen, M., Alfonso, A., Johnson, C. D., & Rand, J. B. (1995). *Caenorhabditis elegans* mutants resistant to inhibitors of acetylcholinesterase. *Genetics, 140*(2), 527-535.

Nicita, F., De Liso, P., Danti, F. R., Papetti, L., Ursitti, F., Castronovo, A., Allemand, F., Gennaro, E., Zara, F., Striano, P., & Spalice, A. (2012). The genetics of monogenic idiopathic epilepsies and epileptic encephalopathies. *Seizure, 21*(1), 3-11.

Noebels, J. (2015). Pathway-driven discovery of epilepsy genes. *Nat Neurosci, 18*(3), 344-350.

Olsen, R. W. (1981). The GABA postsynaptic membrane receptor-ionophore complex. Site of action of convulsant and anticonvulsant drugs. *Mol Cell Biochem, 39*, 261-279.

Phillips, H. A., Favre, I., Kirkpatrick, M., Zuberi, S. M., Goudie, D., Heron, S. E., Scheffer, I. E., Sutherland, G. R., Berkovic, S. F., Bertrand, D., & Mulley, J. C. (2001). CHRNB2 is the second acetylcholine receptor subunit associated with autosomal dominant nocturnal frontal lobe epilepsy. *Am J Hum Genet, 68*(1), 225-231.

Psarropoulou, C., Matsokis, N., Angelatou, F., & Kostopoulos, G. (1994). Pentylenetetrazol-induced seizures decrease gamma-aminobutyric acid-mediated recurrent inhibition and enhance adenosine-mediated depression. *Epilepsia, 35*(1), 12-19.

Qi, Y. B., Garren, E. J., Shu, X., Tsien, R. Y., & Jin, Y. (2012). Photo-inducible cell ablation in *Caenorhabditis elegans* using the genetically encoded singlet oxygen generating protein miniSOG. *Proc Natl Acad Sci U S A, 109*(19), 7499-7504.

Qi, Y. B., Po, M. D., Mac, P., Kawano, T., Jorgensen, E. M., Zhen, M., & Jin, Y. (2013). Hyperactivation of B-type motor neurons results in aberrant synchrony of the *Caenorhabditis elegans* motor circuit. *J Neurosci, 33*(12), 5319-5325.

Rand, J. B. (1989). Genetic analysis of the cha-1-unc-17 gene complex in Caenorhabditis. *Genetics, 122*(1), 73-80.

Rand, J. B., & Russell, R. L. (1985). Properties and partial purification of choline acetyltransferase from the nematode *Caenorhabditis elegans*. *J Neurochem, 44*(1), 189-200.

Reiner, D. J., Newton, E. M., Tian, H., & Thomas, J. H. (1999). Diverse behavioural defects caused by mutations in *Caenorhabditis elegans* unc-43 CaM kinase II. *Nature, 402*(6758), 199-203.

Reiner, O., & Sapir, T. (2013). LIS1 functions in normal development and disease. *Curr Opin Neurobiol, 23*(6), 951-956.

Richmond, J. E., Davis, W. S., & Jorgensen, E. M. (1999). UNC-13 is required for synaptic vesicle fusion in *C. elegans*. *Nat Neurosci, 2*(11), 959-964.

Richmond, J. E., & Jorgensen, E. M. (1999). One GABA and two acetylcholine receptors function at the *C. elegans* neuromuscular junction. *Nat Neurosci, 2*(9), 791-797.

Rogers, C., Reale, V., Kim, K., Chatwin, H., Li, C., Evans, P., & de Bono, M. (2003). Inhibition of *Caenorhabditis elegans* social feeding by FMRFamide-related peptide activation of NPR-1. *Nat Neurosci, 6*(11), 1178-1185.

Ross, M. E. (2002). Brain malformations, epilepsy, and infantile spasms. *Int Rev Neurobiol, 49*, 333-352.

Rougon, G., & Hobert, O. (2003). New insights into the diversity and function of neuronal immunoglobulin superfamily molecules. *Annu Rev Neurosci, 26*, 207-238.

Saitsu, H., Kato, M., Mizuguchi, T., Hamada, K., Osaka, H., Tohyama, J., Uruno, K., Kumada, S., Nishiyama, K., Nishimura, A., Okada, I., Yoshimura, Y., Hirai, S., Kumada, T., Hayasaka, K., Fukuda, A., Ogata, K., & Matsumoto, N. (2008). De novo mutations in the gene encoding STXBP1 (MUNC18-1) cause early infantile epileptic encephalopathy. *Nat Genet, 40*(6), 782-788.

Salkoff, L., Wei, A. D., Baban, B., Butler, A., Fawcett, G., Ferreira, G., & Santi, C. M. (2005). Potassium channels in *C. elegans*. *WormBook*, 1-15.

Schafer, D. P., Lehrman, E. K., Kautzman, A. G., Koyama, R., Mardinly, A. R., Yamasaki, R., Ransohoff, R. M., Greenberg, M. E., Barres, B. A., & Stevens, B. (2012). Microglia sculpt postnatal neural circuits in an activity and complement-dependent manner. *Neuron, 74*(4), 691-705.

Schuske, K., Beg, A. A., & Jorgensen, E. M. (2004). The GABA nervous system in *C. elegans*. *Trends Neurosci, 27*(7), 407-414.

Schuske, K., Palfreyman, M. T., Watanabe, S., & Jorgensen, E. M. (2007). UNC-46 is required for trafficking of the vesicular GABA transporter. *Nat Neurosci, 10*(7), 846-853.

Sharma, V., Babu, P. P., Singh, A., Singh, S., & Singh, R. (2007). Iron-induced experimental cortical seizures: electroencephalographic mapping of seizure spread in the subcortical brain areas. *Seizure, 16*(8), 680-690.

Shaye, D. D., & Greenwald, I. (2011). OrthoList: a compendium of *C. elegans* genes with human orthologs. *PLoS One, 6*(5), e20085.

Stawicki, T. M., Takayanagi-Kiya, S., Zhou, K., & Jin, Y. (2013). Neuropeptides function in a

homeostatic manner to modulate excitation-inhibition imbalance in *C. elegans*. *PLoS Genet, 9*(5), e1003472.

Stawicki, T. M., Zhou, K., Yochem, J., Chen, L., & Jin, Y. (2011). TRPM channels modulate epileptic-like convulsions via systemic ion homeostasis. *Curr Biol, 21*(10), 883-888.

Steger, K. A., Shtonda, B. B., Thacker, C., Snutch, T. P., & Avery, L. (2005). The *C. elegans* T-type calcium channel CCA-1 boosts neuromuscular transmission. *J Exp Biol, 208*(Pt 11), 2191-2203.

Steiner, D. F. (1998). The proprotein convertases. *Curr Opin Chem Biol, 2*(1), 31-39.

Sulston, J., & Hodgkin., J. (1988). Methods. In W. B. Wood (Ed.), *The Nematode Caenorhabditis elegans* (pp. 587-606). Cold Spring Harbor, NY: Cold Spring Harbor Laboratory Press.

Sulston, J. E. (1983). Neuronal cell lineages in the nematode *Caenorhabditis elegans*. *Cold Spring Harb Symp Quant Biol, 48 Pt 2*, 443-452.

Sulston, J. E., & Horvitz, H. R. (1977). Post-embryonic cell lineages of the nematode, *Caenorhabditis elegans*. *Dev Biol, 56*(1), 110-156.

Sulston, J. E., Schierenberg, E., White, J. G., & Thomson, J. N. (1983). The embryonic cell lineage of the nematode *Caenorhabditis elegans*. *Dev Biol, 100*(1), 64-119.

Sun, X. X., Hodge, J. J., Zhou, Y., Nguyen, M., & Griffith, L. C. (2004). The eag potassium channel binds and locally activates calcium/calmodulin-dependent protein kinase II. *J Biol Chem, 279*(11), 10206-10214.

Teramoto, T., Sternick, L. A., Kage-Nakadai, E., Sajjadi, S., Siembida, J., Mitani, S., Iwasaki, K. & Lambie, E. J. (2010). Magnesium excretion in *C. elegans* requires the activity of the GTL-2 TRPM channel. *PLoS One, 5*(3), e9589.

Touroutine, D., Fox, R. M., Von Stetina, S. E., Burdina, A., Miller, D. M., & Richmond, J. E. (2005). acr-16 encodes an essential subunit of the levamisole-resistant nicotinic receptor at the *Caenorhabditis elegans* neuromuscular junction. *J Biol Chem, 280*(29), 27013-27021.

Tucker, M., Sieber, M., Morphew, M., & Han, M. (2005). The *Caenorhabditis elegans* aristaless orthologue, alr-1, is required for maintaining the functional and structural integrity of the amphid sensory organs. *Mol Biol Cell, 16*(10), 4695-4704.

Unwin, N. (1995). Acetylcholine receptor channel imaged in the open state. *Nature, 373*(6509), 37-43.

Vashlishan, A. B., Madison, J. M., Dybbs, M., Bai, J., Sieburth, D., Ch'ng, Q., Tavazoie, M., Kaplan, J. M. (2008). An RNAi screen identifies genes that regulate GABA synapses. *Neuron, 58*(3), 346-361.

Venkatachalam, K., & Montell, C. (2007). TRP channels. *Annu Rev Biochem, 76*, 387-417.

Von Stetina, S. E., Treinin, M., & Miller, D. M. (2006). The motor circuit. *Int Rev Neurobiol, 69*, 125-167.

Ward, S., Thomson, N., White, J. G., & Brenner, S. (1975). Electron microscopical reconstruction of the anterior sensory anatomy of the nematode *Caenorhabditis elegans*.?2UU. *J Comp Neurol, 160*(3), 313-337.

Weimer, R. M., Richmond, J. E., Davis, W. S., Hadwiger, G., Nonet, M. L., & Jorgensen, E. M. (2003). Defects in synaptic vesicle docking in unc-18 mutants. *Nat Neurosci, 6*(10), 1023-1030.

Westmoreland, J. J., McEwen, J., Moore, B. A., Jin, Y., & Condie, B. G. (2001). Conserved function of *Caenorhabditis elegans* UNC-30 and mouse Pitx2 in controlling GABAergic neuron differentiation. *J Neurosci, 21*(17), 6810-6819.

White, J. G., Southgate, E., Thomson, J. N., & Brenner, S. (1976). The structure of the ventral nerve cord of *Caenorhabditis elegans*. *Philos Trans R Soc Lond B Biol Sci, 275*(938), 327-348.

White, J. G., Southgate, E., Thomson, J. N., & Brenner, S. (1986). The structure of the nervous system of the nematode *Caenorhabditis elegans*. *Philos Trans R Soc Lond B Biol Sci, 314*(1165), 1-340.

Williams, S. N., Locke, C. J., Braden, A. L., Caldwell, K. A., & Caldwell, G. A. (2004). Epileptic-like convulsions associated with LIS-1 in the cytoskeletal control of neurotransmitter signaling in *Caenorhabditis elegans*. *Hum Mol Genet, 13*(18), 2043-2059.

Wu, G., Feder, A., Wegener, G., Bailey, C., Saxena, S., Charney, D., & Mathé, A. A. (2011). Central functions of neuropeptide Y in mood and anxiety disorders. *Expert Opin Ther Targets, 15*(11), 1317-1331.

Zhou, K., Stawicki, T. M., Goncharov, A., & Jin, Y. (2013). Position of UNC-13 in the active zone regulates synaptic vesicle release probability and release kinetics. *Elife, 2*, e01180.

Chapter 2

A ligand-gated anion channel LGC-46 regulates release-dependent presynaptic inhibition and excitation-inhibition balance

Abstract

Presynaptic ligand-gated ion channels (LGICs) regulate neurotransmitter release and play significant roles in tuning neural circuit activity (Eccles, Schmidt, & Willis, 1963; Engelman & MacDermott, 2004; Kullmann et al., 2005; Schicker, Dorostkar, & Boehm, 2008). While many studies have revealed mechanisms involving presynaptic metabotropic receptors in synaptic modulation (Atwood, Lovinger, & Mathur, 2014; Chalifoux & Carter, 2011), the *in vivo* action of presynaptic LGICs in neurotransmission remains mostly unknown. Here we report that *C. elegans* LGC-46, a member of the Cys-loop family of acetylcholine (ACh)-gated chloride (ACC) channels (Putrenko, Zakikhani, & Dent, 2005), localizes to presynaptic terminals and inhibits cholinergic transmission upon evoked release of ACh. In cholinergic motor neurons, loss of *lgc-46* alters synaptic vesicle (SV) release kinetics to cause slow decay in postsynaptic currents, without altering the spontaneous activity of cholinergic neurons. Conversely, a gain-of-function mutation in LGC-46, caused by a Met to Ile change in the pore-lining transmembrane domain 2, accelerates the decay and causes inhibition of SV release. Further, we show *lgc-46(gf)* ameliorates over-excitation in a *C. elegans* seizure model that displays excitation and inhibition imbalance (Jospin et al., 2009), a common physiological feature in epilepsy and other neurological disorders. The inhibition on presynaptic release by LGC-46 depends on its anion selectivity and on another ACC channel subunit, ACC-4. These data demonstrate a novel mechanism of presynaptic feedback control by which an anion LGIC acts as an autoreceptor to inhibit SV release upon neuronal activation. Our findings suggest ionotropic anion channels should be considered potential targets for modulating neuronal circuit function

and in treatments for neurological disorders.

Main

lgc-46 is a member of the acetylcholine gated chloride (ACC) channel subfamily in *C. elegans* (Putrenko, et al., 2005*)* (Figure 2.1A, B, 2.2 A-C). The pore-lining transmembrane region of this family has extensive homology to GABA- and glycine-gated chloride channels (Putrenko, et al., 2005; Ringstad, Abe, & Horvitz, 2009) (Figure 2.1B). To dissect the function of *lgc-46*, we first determined its cellular expression using a transcriptional reporter (Extended data Figure 2.1A, D), and observed broad expression in the nervous system, including motor neurons. Co-expression of *Plgc-46-GFP* with markers for cholinergic (P*unc-17-mCherry*) and GABAergic (P*ttr-39-mCherry*) neurons revealed that *lgc-46* was strongly expressed in cholinergic motor neurons, and weakly expressed in GABAergic motor neurons (Figure 2.2E). We next examined the subcellular localization of LGC-46 in cholinergic motor neurons using functional LGC-46::GFP, in which GFP was inserted in-frame in the cytoplasmic loop between TM3 and TM4 (Figure 2.2B). In L1 animals, LGC-46::GFP was only seen in the dorsal nerve cords (Figure 2.1C), where cholinergic motor neurons form synapses onto dorsal body wall muscles (Sulston, 1976; White, Albertson, & Anness, 1978). We also expressed LGC-46::GFP in a single cholinergic neuron DA9, which synapses onto dorsal body wall muscles, and found LGC-46::GFP was detected only in the dorsal side of L4 and adult animals (Figure 2.1D). These results indicate that the LGC-46 primarily localizes to the axonal compartment throughout development.

To determine if the punctate pattern of LGC-46::GFP corresponded to presynaptic terminals, we co-immunostained LGC-46::GFP expressed from a single-copy insertion line together with endogenous active zone protein RIM/UNC-10 (Figure 2.1E). LGC-46::GFP displayed high degree of overlap with UNC-10, suggesting that LGC-46 localizes at, or in close proximity to, the release sites of synaptic vesicles (SVs). We observed similar colocalization of

punctate LGC-46::GFP relative to a synaptic vesicle marker RAB-3::mCherry in cholinergic motor neurons (Figure 2.1F). To our knowledge LGC-46 is the first presynaptically localized LGIC in *C. elegans.*

To analyze the function of *lgc-46*, we examined two genetic deletion alleles *ok2900* and *ok2949*, both predicted to result in non-functional proteins (Figure 2.2A, B), designated as *lgc-46(0).* Cholinergic synapse morphology and density in *lgc-46(0)* mutants were comparable to those in wild type (Figure 2.3), and *lgc-46(0)* animals displayed normal growth, reproduction and locomotion. We performed pharmacological analyses to assess cholinergic transmission at the neuromuscular junction (Mahoney, Luo, & Nonet, 2006). *lgc-46(0)* were hypersensitive to aldicarb, an inhibitor of acetylcholine esterase, which was rescued by cholinergic motor neuron-specific expression of LGC-46 (Figure 2.4A). On the other hand, *lgc-46(0)* showed normal sensitivity to the acetylcholine receptor agonist levamisole (Figure 2.4B). These observations implied that LGC-46 likely represses cholinergic motor neuron activities.

We next investigated how LGC-46 regulates synaptic vesicle release by performing electrophysiological recordings on muscle cells (Figure 2.5). Evoked excitatory post-synaptic currents (eEPSCs) represent depolarization triggered SV release. The amplitude of eEPSCs in *lgc-46(0)* animals was comparable to that in wild type (Figure 2.5 A, C). However, analysis of release kinetics revealed that eEPSCs in *lgc-46(0)* were prolonged, reflecting a significantly slower decay than that of wild type, while the rise phase of eEPSCs was similar to wild type (Figure 2.5B, D). The slower decay of eEPSCs in *lgc-46(0)* mutants led to a significant increase in cumulative charge transfer, indicating more release of SVs than that in wild type (Figure 2.5E). The charge transfer during evoked release of SVs shows a burst in the early phase and a slower sustained increase afterwards. *lgc-46(0)* mutants displayed a normal early phase of SV release, but exhibited a large increase in the late phase, compared to wild type. These observations show that LGC-46 has a specific role in modulation of late phase SV release, possibly as the synaptic membrane repolarizes. Both the slow decay of eEPSCs and the increased late phase of SV

release were rescued by expression of LGC-46 in cholinergic motor neurons (Figure 2.5D, E).

We also recorded endogenous excitatory post-synaptic currents triggered by random SV release from cholinergic motor neurons. The amplitude and kinetics of endogenous EPSCs were normal in *lgc-46(0)* mutants (Figure 2.6), confirming that the specific increase in late phase of evoked response in *lgc-46(0)* mutants was not due to altered kinetics of postsynaptic receptor response on muscles. The frequency of endogenous EPSCs in *lgc-46(0)* mutants was also comparable to that in wild type (Figure 2.5F), indicating that cholinergic transmission was not affected in the resting condition. These data support a conclusion that LGC-46 acts as an auto-receptor to inhibit presynaptic activity upon synaptic vesicle release.

We previously characterized an ionotropic ACh-gated cation channel ACR-2 that localizes to the dendrites and soma of cholinergic motor neurons and regulates their excitability (Jospin, et al., 2009). An *acr-2(gf)* mutation causes increased channel activity and hyperactivity of cholinergic motor neurons. *acr-2(gf)* animals show distinctive repetitive convulsions, due to excitation and inhibition imbalance in the locomotor circuit(Jospin, et al., 2009; Qi et al., 2013; Stawicki, Takayanagi-Kiya, Zhou, & Jin, 2013). By screening for suppressors of the *acr-2(gf)* convulsion behavior (see methods), we isolated a *lgc-46(ju825)* mutation that strongly suppressed the convulsion of *acr-2(gf)* (Figure 2.7A). *acr-2(gf)* shows hypersensitivity to both aldicarb and levamisole (Jospin, et al., 2009). *lgc-46(ju825)* partially suppressed the aldicarb hypersensitivity, but not the levamisole sensitivity of *acr-2(gf)*, suggesting that *lgc-46(ju825)* likely affects presynaptic activity of cholinergic neurons (Extended Data Fig. 3 c, d). We determined that the *lgc-46(ju825)* mutation causes a substitution of methionine to isoleucine (M314I) in the pore-lining transmembrane TM2 domain (Figure 2.1B). *lgc-46(0)* did not show significant effects on *acr-2(gf)* convulsion (Figure 2.7A). In addition, transgenic overexpression of LGC-46(M314I), but not LGC-46(WT), driven by *lgc-46* promoter strongly suppressed *acr-2(gf)* convulsion. By expressing *lgc-46* in a cell-type specific manner, we found that pan-neuronal and cholinergic LGC-46(M314I) expression suppressed *acr-2(gf)* convulsions

whereas its expression in muscles or GABAergic motor neurons had no effect (Figure 2.7B). Expression of LGC-46(M314I) in cholinergic motor neurons also fully suppressed the aldicarb hypersensitivity of *lgc-46(0)* (Figure 2.4A). These data indicate that *lgc-46(ju825)* is a gain-of-function mutation, and acts cell-autonomously to suppress cholinergic neuron activity.

The localization of GFP-tagged LGC-46(M314I) resembled that of wild type LGC-46 (Figure 2.8 A-D), indicating that it functions at presynaptic release sites. We wanted to address if anion selectivity of LGC-46(M314I) is required for its activity. In anion channels, the PAR motif preceding TM2 is crucial for ion selectivity (Galzi et al., 1992; Jensen, Pedersen, Timmermann, Schousboe, & Ahring, 2005; Jensen, Schousboe, & Ahring, 2005; Keramidas, Moorhouse, French, Schofield, & Barry, 2000). We generated mutations in the PAR motif by deleting P301 and replacing A302 with glutamate (Extended Data Fig. 6). When expressed in cholinergic motor neurons, PAR-mutant LGC-46(M314I) did not suppress *acr-2(gf)* convulsions (Figure 2.9), consistent with LGC-46 acting as an anion-selective channel.

We next investigated how LGC-46(M314I) alters presynaptic release by electrophysiological recordings. The time constant of the rise phase was not affected in *lgc-46(ju825)*, however, these mutants showed significantly reduced amplitudes of eEPSCs and release kinetics with much shorter decay phase, compared to wild type (Figure 2.10A-D). Consequently, the charge transfer during eEPSCs was significantly reduced in *lgc-46(ju825)* mutants, indicating inhibition of SV release (Figure 2.10E). Similar to *lgc-46(0)*, the amplitude and kinetics of endogenous EPSC were not affected in *lgc-46(ju825)* mutants (Figure 2.11). However, *lgc-46(ju825)* significantly reduced endogenous EPSC frequency, suggesting lower excitability in cholinergic motor neurons compared to wild type (Figure 2.10F). Expression of LGC-46(M314I) in *lgc-46(0)* mutant background mimicked the defects observed from the *lgc-46(ju825)* strain (Figure 2.10, 2.11), confirming that the LGC-46(M314I) mutation resulted in an overactive anion channel.

ACC-1 and ACC-2 can form homomeric channels and respond to acetylcholine when

expressed in Xenopus oocytes(Putrenko, et al., 2005). However, similar studies of LGC-46 have not revealed ACh-gated channel activity (Joseph Dent, personal communication), or responsiveness to other neurotransmitters (Ringstad, et al., 2009), suggesting that LGC-46 may require additional subunits or accessory factors to form a functional channel. *lgc-46(ju825)* animals display curly body posture and slow locomotion speed (Fig. 3c). Expression of LGC-46(M314I) under its own promoter in *lgc-46(0)* background mimicked the locomotion phenotypes, indicating that LGC-46(M314I) is responsible for the phenotype. We took advantage of the slow locomotion and curly body posture phenotype of *lgc-46(ju825)* to identify potential partners of LGC-46. We systematically examined null mutations in seven other ACC genes (*acc-1* to *acc-4* and *lgc-47* to *lgc-49*) (Figure 2.12A). All showed grossly normal movement. We then made double mutants with *lgc-46(ju825),* and found that *acc-4(0)* showed a specific suppression of the *lgc-46(ju825)* phenotype such that double mutant animals regained normal locomotion. *acc-4* was also required for the suppression of *acr-2(gf)* convulsion by *lgc-46(ju825)* (Figure 2.12B, C). ACC-4 is expressed in all cholinergic motor neurons(Pereira et al., 2015). Transgenic expression of *acc-4,* driven by its own promoter, or of an *acc-4* cDNA in cholinergic motor neurons fully rescued the effects of *acc-4(0)* in *acr-2(gf); lgc-46(ju825); acc-4(0)* background. *acc-4(0)* did not affect the punctate localization of LGC-46 (Figure 2.12D), suggesting that ACC-4 is not required for LGC-46 trafficking and clustering. These results suggest that both ACC-4 and LGC-46 function in the cholinergic motor neurons and may likely co-assemble into one channel.

Anion-selective LGICs have been studied extensively, but deciphering the functions of postsynaptic and presynaptic channels is often challenging. Direct evidence for presynaptic localization of LGICs remains lacking(Belenky, Sagiv, Fritschy, & Yarom, 2003; Cattaert & El Manira, 1999; Hruskova et al., 2012; Kullmann, et al., 2005) . Acetylcholine is an excitatory neurotransmitter in many organisms, but classical electrophysiological studies from *Aplysia* suggested the presence of ACh-gated ionotropic anion channels (Kehoe, 1972a, 1972b; Kehoe &

McIntosh, 1998). Studies of *C. elegans* ACC proteins have shown that they are ACh-gated chloride channels (Putrenko, et al., 2005), although the *in vivo* functions of the ACC channels remain largely unknown, with the exception of ACC-2 in regulation of reversal behavior (Li, Liu, Zheng, & Xu, 2014). Here we have provided multiple lines of data to demonstrate that LGC-46 acts as a presynaptic auto-receptor to mediate an SV release-dependent feedback inhibition in cholinergic motor neurons. The effects of LGC-46 on presynaptic release kinetics differ from those recently described for the presynaptic active zone protein UNC-13/Munc13. UNC-13/Munc13 variants affect both rise and decay phases of eEPSCs via positional proximity to the presynaptic active zone, resulting in a general kinetic effect on SV release in both early and late phases(Hu, Tong, & Kaplan, 2013; Zhou, Stawicki, Goncharov, & Jin, 2013) (K. Z. and Y. J. unpublished data). In contrast, *lgc-46* mutants specifically affect the decay phase, but not the rise phase, of eEPSC. Upon a burst of ACh release, opening of wild type LGC-46 channels can limit further SV release in the sustained late phase. This rapid feedback inhibition ensures tight control of neurotransmitter release. The observation that *lgc-46(gf)* dampens excitation and inhibition imbalance displayed by the *acr-2(gf)* seizure model offers novel insights for treatment of neuropsychiatric disorders.

Methods

C. elegans genetics and strains

C. elegans strains were grown at 22.5°C following standard procedures. The *acr-2(gf)* suppressor screen was conducted essentially as previously described[8] (Y. B. Qi and Y. J., unpublished data). Whole-genome sequence analysis of CZ21292 *lgc-46(ju825); acr-2(gf)* was performed using Galaxy platform(Giardine et al., 2005) on data obtained by Beijing Genomics Institute (Shenzhen, China). Subsequent mapping using outcrossed strains led to the identification of the *ju825* missense mutation in *lgc-46.* Double and triple mutants were constructed following standard procedures. Extended Data Table 1 lists all the strains with allele

and transgene information.

Molecular biology, RNA analyses and transgenes

Molecular biology was performed following standard methods. Gateway recombination technology (Invitrogen, CA) was used for generating expression constructs. Extended Data Table 2 describes the details of constructs generated in this study. High-copy transgenic arrays were generated following standard protocols. Single-copy insertion lines of *Punc-17β-LGC-46(WT)::GFP* and *Punc-17β-LGC-46(M314I)::GFP* were made at Chromosome IV site cxTi10882 (pCFJ201) by microinjection using modified vectors (Z. Wang and Y. J., unpublished data). Briefly, N2 animals were injected with following three constructs: a construct carrying the *Punc-17β-LGC-46(WT)::GFP* sequence with cxTi10882 homology arms and a copy of hygromycin resistance gene; a construct which drives expression in the germline of Cas9 and sgRNA targeted for the cxTi10882 region, and a fluorescent coinjection marker. F2 animals resistant to hygromycin were selected. Insertion of single copy in the genomic locus was confirmed by PCR using primers outside of the homology arms. Loss of the fluorescent coinjection marker indicated the loss of extrachromosomal array. The single copy insertion strains were outcrossed twice before use in further experiments.

To verify *lgc-46* transcripts in wild type and mutants, we isolated mRNA from animals of mixed stages using Trizol (ThermoFisher Scientific), and generated cDNAs using SuperScript III (ThermoFisher Scientific), following the manufacturer's protocol. *lgc-46* cDNA was amplified using primers YJ11741: 5'ATGCAATATCTGCAATTCCT3' and YJ11742: 5'TTATATTTATTATCATTCGTTGACTAG3'. Sequence analyses of cDNAs from *ok2949* and *ok2900* showed neither allele would produce any functional protein. *lgc-46* cDNAs from N2 and *lgc-46(ju825); acr-2(n2420)* were cloned into Topo PCR8 vector (Invitrogen). *acc-4* cDNA from N2 was amplified using following primers : YJ11811: 5'ATGCGACTAATCATATTAGTAATCTCCATTC3' and YJ11812:

5’CTTAGATAGTTCTAACCAATAGTTTTCCGAG3’, then cloned into Topo PCR8 vector.

Locomotion analysis and quantification of convulsion behavior

L4 larvae were transferred to NGM plates seeded with OP50. On the next day, young adults were transferred to fresh plates without OP50, allowed to crawl away from bacteria, and were then transferred to assay plates without OP50. For each strain tested, 10 adult animals were placed on one assay plate. Videos of the animals were captured for 5 min at 3 fps using Pixelink camera. The videos were analyzed using a multi-worm tracking custom software, and the average velocities of 10 animals were obtained. The experiment was repeated three times per strain on three different days.

Quantification of convulsion was performed as previously described[13] with several modifications. L4 larvae were transferred to NGM plates seeded with OP50 one day before the experiment. Young adults were transferred to fresh plates on the following day and their behaviors were visually scored under a dissecting scope by an observer blind to the genotype. One convulsion event was defined as a shortening of the animals body length. The assay was repeated at least twice per genotype on different days. At least two independent transgenic lines were used for each experiment.

Pharmacological assays

L4 animals were transferred to fresh plates seeded with OP50. On the next day, 15 animals were transferred to a NGM plate containing the drug (500 μM aldicarb for Figure 2.4A, 150 μM aldicarb for Figure 2.4C, 500 μM levamisole for Figure 2.4B, D). Animal behavior was scored at 30 min intervals. Animals were scored paralyzed when they did not move in response to touch for three times.

Fluorescent imaging of GFP reporters and immunocytochemistry

Zeiss LSM 710 confocal microscope (63x objective) was used for all images. Whole-mount immunostaining followed procedures described previously (Van Epps, Dai, Qi, Goncharov, & Jin, 2010). Antibodies used were as follows. Primary antibodies: polyclonal rabbit anti-GFP (A-11122, ThermoFisher Scientific) at 1:500, mouse anti-RIM2/UNC-10 (DSHB) at 1:50. Secondary antibodies: Alexa Fluor488 goat anti-rabbit IgG (Invitrogen) at 1:1000, Alexa Fluor594 goat anti-mouse IgG (Invitrogen) at 1:1000. Maximum-intensity Z stack images of dorsal nerve cords were obtained from 3 sections at 0.5 µm intervals. Images were processed using ImageJ software.

For Figure 2.1F, Figure 2.3A, Figure 2.8C, D and Figure 2.12B, L4 animals were picked the day before experiment and imaged on the following day as day 1 adults. Animals were immobilized using 0.05 µm polystyrene beads (Polysciences) and placed on 10% agarose pads with dorsal side facing the coverslip. Maximum-intensity Z stack images were obtained from 3 sections at 0.5 µm intervals. For Figure 2.1D, Figure 2.2D, E and Figure 2.12B, L4 animals with transgene were picked on the day of experiment. Animals were anesthetized using 1 mM levamisole and placed on 4% agarose pads. Z-stack images of lateral side at 0.5 µm intervals were obtained. For Figure 2.1C and Figure 2.8A, adult animals were transferred to a fresh plate1 day before experiment and allowed to lay eggs. On the following day, hatched L1 animals were collected and subjected to imaging. Animals were anesthetized using 1 mM levamisole and placed on 4% agarose pads. Z-stack images from 3 sections at 0.5 µm intervals were obtained. Images were processed using ImageJ software. Linescan analyses were performed using MetaMorph (Molecular Devices Corp.).

For fluorescent puncta analysis (Figure 2.3B), signal intensities obtained from linescan analyses were imported to IGOR Pro (WaveMetrics, Lake Oswego, OR) and processed using a custom made program. Linescans from dorsal nerve cords (20 µm per animal) from six animals per genotype were analyzed.

Electrophysiology

Neuromuscular dissection methods were adapted from previous studies (Richmond, Davis, & Jorgensen, 1999; Zhou, et al., 2013). Adult worms were immobilized on Sylgard-coated cover slips with cyanoacrylate glue. A dorsolateral incision was made with a sharp glass pipette and the cuticle flap was folded back and glued down to expose the ventral medial body wall muscles. The preparation was then treated by collagenase type IV (Sigma-Aldrich) for ~ 30 s at a concentration of 0.4 mg/ml at room temperature.

The bath solution contains (in mM): 127 NaCl, 5 KCl, 26 $NaHCO_3$, 1.25 NaH_2PO_4, 1.2 $CaCl_2$, 4 $MgCl_2$, 10 glucose and sucrose to 340 mOsm, bubbled with 5% CO_2, 95% O_2 at 20ºC. The pipette solution contains (in mM): 120 CH_3O_3SCs, 4 CsCl, 15 CsF, 4 $MgCl_2$, 5 EGTA, 0.25 $CaCl_2$, 10 HEPES and 4 Na_2ATP, adjusted to pH 7.2 with CsOH. Conventional whole-cell recordings from muscle cells were performed at 20°C with 2-3 MΩ pipettes. An EPC-10 patch-clamp amplifier was used together with the Patchmaster software package (HEKA Electronics, Lambrecht, Germany). Endogenous EPSCs were recorded at -60 mV. For recording evoked EPSCs, a second glass pipet filled with bath solutions was put on the ventral nerve cord as stimulating electrode. The stimulating electrode gently touched the anterior region of ventral nerve cord to form loose patch configuration, which is around 1 muscle distance from recording pipets. A 0.5 ms, 85 μA square current pulse was generated by the isolated stimulator (WPI A320RC) as stimulus to obtain the maximal responses. All current traces were imported to IGOR Pro (WaveMetrics, Lake Oswego, OR) for further analysis. A single exponential equation was used to fit the rise phase or decay phase of eEPSCs. The traces for cumulative transferred charge were obtained by integration of eEPSCs.

Acknowledgements

This chapter is a reprint in full of Takayanagi-Kiya, S., Zhou, K., and Jin, Y. A ligand-gated anion channel LGC-46 regulates release-dependent presynaptic inhibition and excitation-inhibition balance (in preparation) with permission of all authors.

We are grateful for N. Pokala, C. Bargmann, S. Chalasani, A. Calhoun for sharing the multi-worm tracking analyses software prior to publication, J. Dent for sharing unpublished data on ACC channels. We thank Y. B. Qi for isolating *ju825,* and Z. Wang for CasCi protocol, and A. D. Chisholm, J. Wang and our lab members for comments. Some strains were obtained from the Japan National BioResource Project (NBRP) and the *Caenorhabditis* Genetics Center (CGC). T-K. S. was a recipient of Nakajima Foundation Predoctoral Fellowship. Y. J. is an investigator of, and K. Z., an associate of, the Howard Hughes Medical Institute.

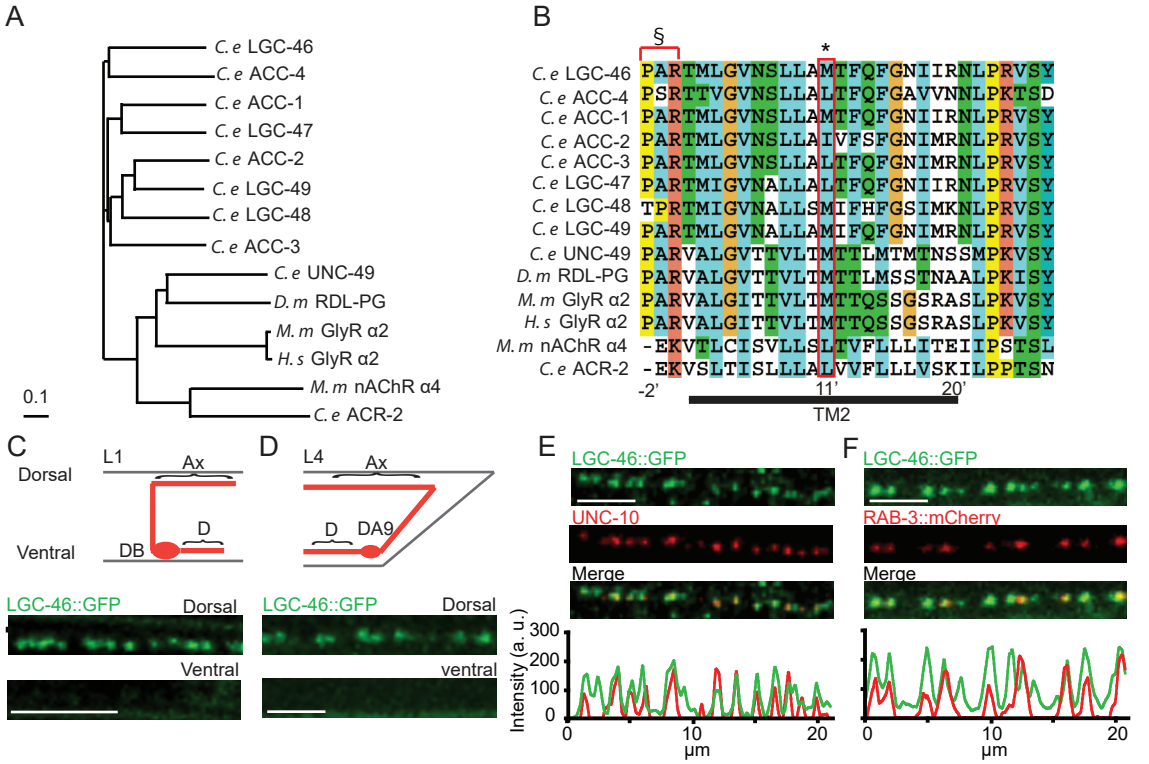

Figure 2.1. LGIC LGC-46 localizes to presynaptic terminals. (A) Phylogenetic tree of LGICs shows that LGC-46 is a member of the ACC family of proteins from *C. elegans* (ACC-1 to ACC-4, LGC-46 to LGC-49). Generated by ClustalX2 using the neighbor-joining method (Larkin et al., 2007). (B) Alignment of TM2 of LGC-46 with other anion channels. * marks Met314, which is mutated to Ile in LGC-46(*ju825*). § marks PAR motif, a signature of ionotropic anion channels. (C-F) LGC-46::GFP localizes to presynaptic terminals of cholinergic motor neurons. (C) Upper panel shows a schematic of a cholinergic motor neuron in L1 animals. Lower panel shows a confocal image of LGC-46::GFP from P*unc-17β-LGC-46(WT)::GFP(juSi295)IV* showing punctate localization in the dorsal nerve cord. (D) Upper panel shows a schematic of DA9 cholinergic motor neuron in the tail of L4 animals. Lower panel shows LGC-46::GFP expressed in DA9 neuron, from P*itr-1-LGC-46(WT)::GFP(juEx6843),* showing punctate localization in the dorsal axon. (C-D): Ax: Axon. D: Dendrite. (E, F) LGC-46::GFP colocalizes with active zone protein UNC-10/Rim and synaptic vesicles in cholinergic motor neurons. Images of dorsal nerve cord are shown above, linescan analyses of fluorescent signal intensities below. (E) Conformal images of anti-GFP for LGC-46 (green) and anti-UNC-10 (red) from an animal carrying P*unc-17β-LGC-46(WT)::GFP(juSi295)IV*. (F) Presynaptic protein RAB-3::mCherry expressed in cholinergic motor neurons overlapped with LGC-46::GFP signals. Images are from P*unc-17β-LGC-46(WT)::GFP(juSi295)IV*; P*acr-2-RAB-3::mCherry(juEx7053).* Scale bar: 5μm.

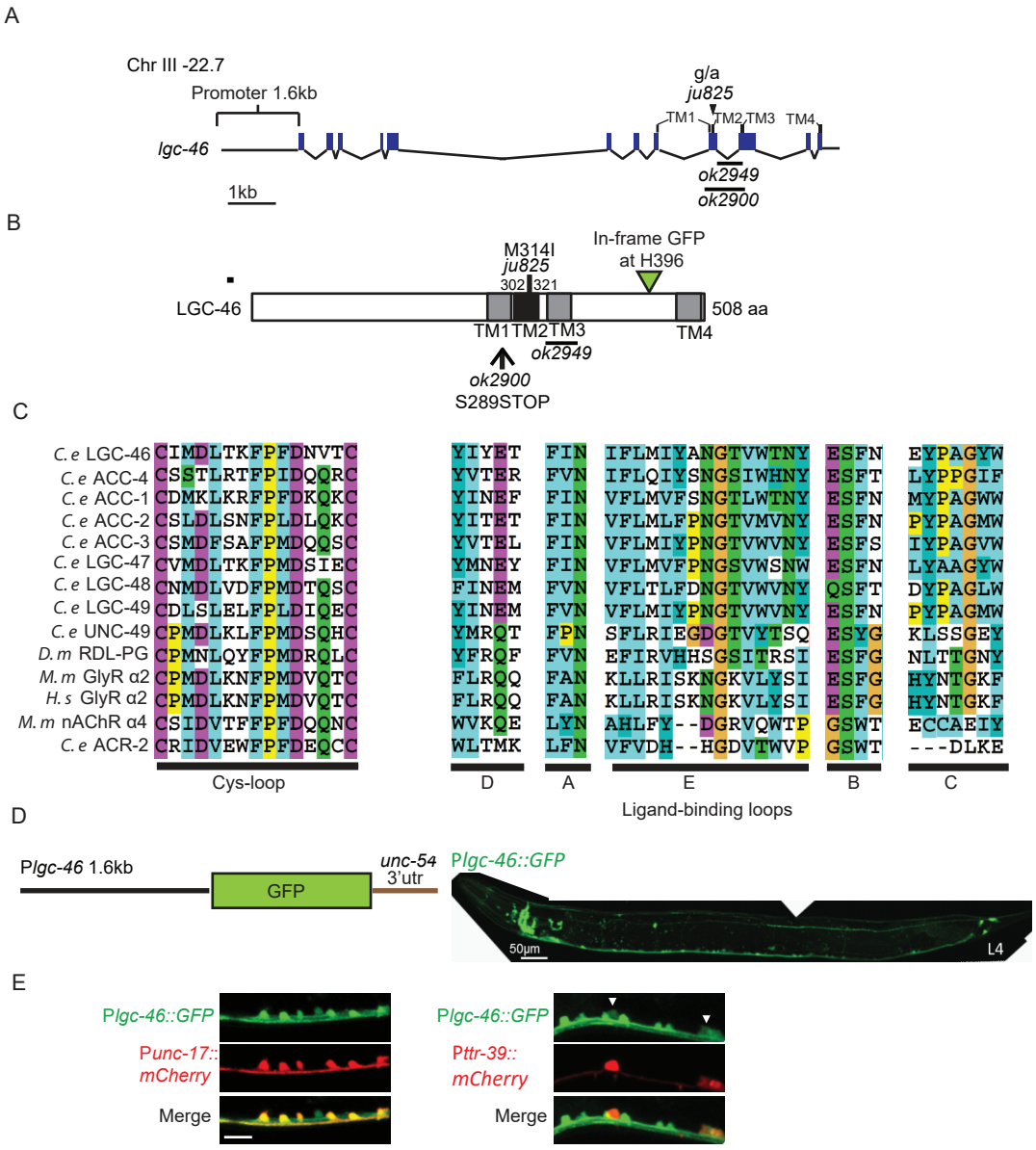

Figure 2.2. *lgc-46* is expressed in the nervous system including cholinergic motor neurons. (A) Gene structure of *lgc-46.* Positions of the deletion alleles and the M314I mutation are noted. *ok2900* removes TM2 and TM3 and generates a premature stop codon, and *ok2949* generates an in-frame deletion which removes TM3. (B) Protein structure of LGC-46. Four transmembrane domains and the sites of mutations are noted. For protein localization analysis, GFP was inserted at the cytoplasmic loop between TM3 and TM4. (C) Amino acid sequence alignment of the Cys-loop region, and regions corresponding to the ligand-binding loops of nAChR. (D) The construct illustration (left) and expression (right) of *lgc-46* transcriptional reporter. Note GFP expression is present in the nervous system including the ventral nerve cord. (E) Expression of *Plgc-46*-GFP overlaps with cholinergic motor neuron-specific (*Punc-17-mCherry*) and GABAergic motor neuron-specific (*Pttr-39-mCherry*) markers. Scale bar: 10µm.

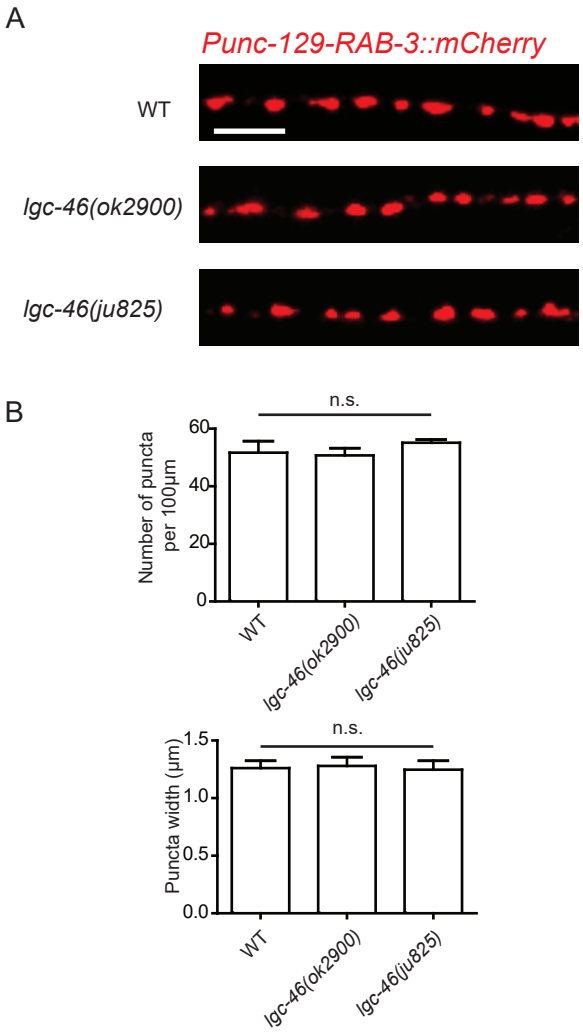

Figure 2.3. Morphology of cholinergic synapses is not affected by *lgc-46* mutations. (A) Representative images of RAB-3::mCherry puncta in the dorsal nerve cord from each genotype. Scale. (B) Quantification of the puncta density and width show no significant differences among the wild type, *lgc-46(ok2900)* and *lgc-46(ju825)* backgrounds. Data shown as mean ± SEM, n= 6 animals each (20 µm per animal) per genotype. Scale bar: 5µm.

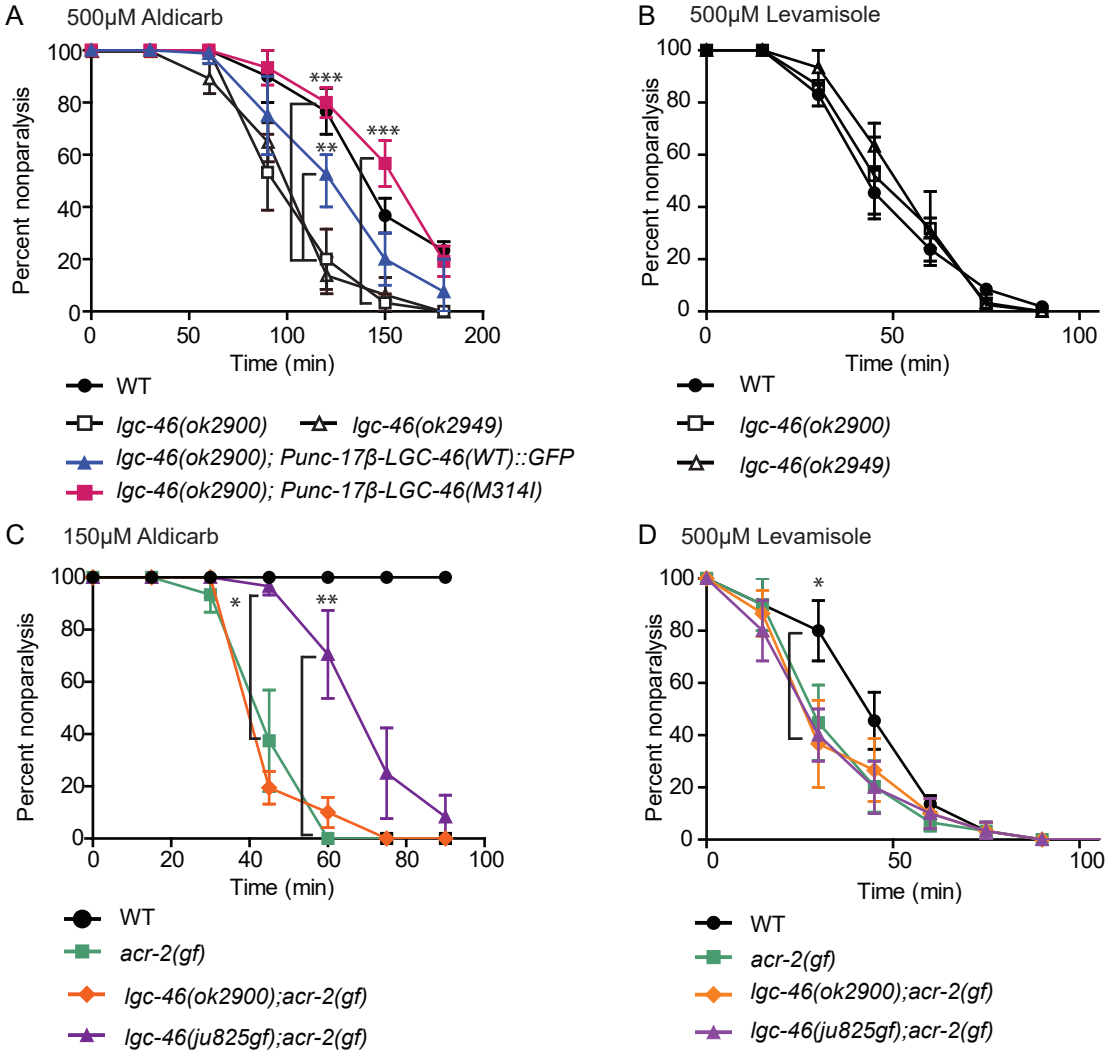

Figure 2.4. *lgc-46* affects aldicarb sensitivity but not levamisole sensitivity. (A) Aldicarb hypersensitivity in *lgc-46(ok2900)* is suppressed by cholinergic motor neuron-specific expression of LGC-46 tagged with GFP. (B) *lgc-46(0)* alleles do not affect levamisole sensitivity. (C,D) *lgc-46(M314I)* partially suppresses the aldicarb hypersensitivity (C) but not levamisole hypersensitivity (D) of *acr-2(gf)*. Results are from three independent trials. n = 15 for one group per trial. Mean rate of paralysis at each time point is shown. Error bars indicate SEM. Statistics: **: $p<0.01$, *: $p<0.05$ by two-way ANOVA and Bonferroni post-hoc test.

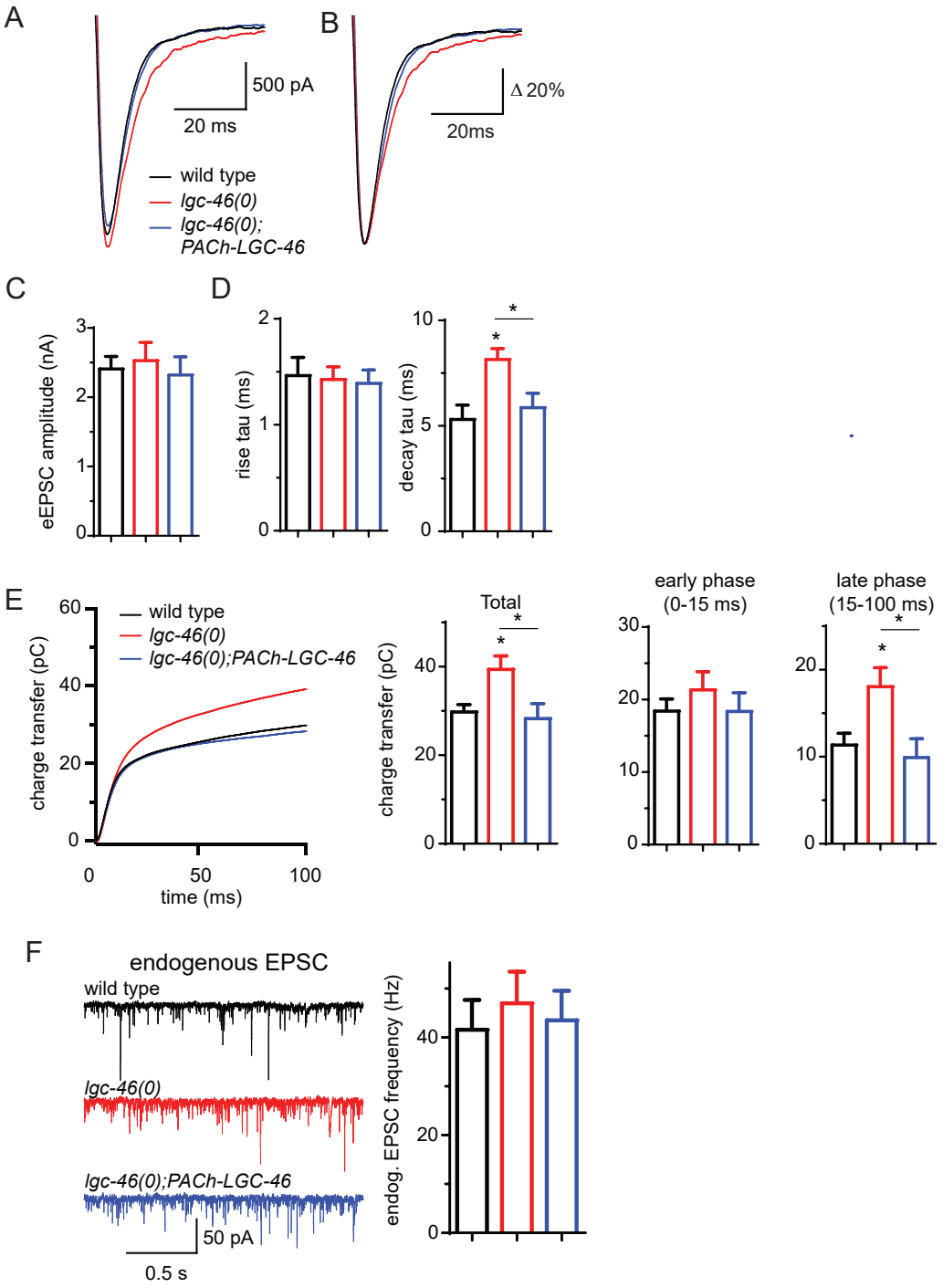

Figure 2.5. LGC-46 regulates the decay phase of eEPSCs to modulate late phase of SV release. (A,B) Average traces (A) and normalized average traces (B) of eEPSCs. (C) Mean amplitude of eEPSCs. (D) Rise tau and decay tau of eEPSCs. (E) Average traces of cumulative charges of eEPSCs, and charge transfers after stimulation. (F) Representative traces and mean frequency of endogenous EPSCs. wild type (n=11), *lgc-46(ok2900)* (n=10), and *lgc-46(ok2900); PACh-LGC-46* (n=11). Statistics, one-way ANOVA, Bonferroni's post hoc test. * $p < 0.05$. Error bars indicate SEM.

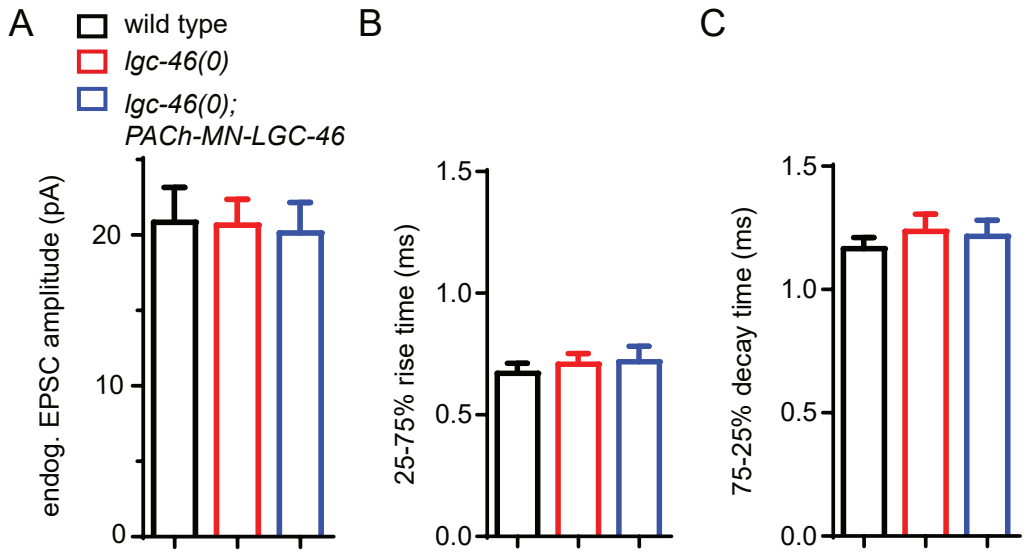

Figure 2.6. Amplitude and kinetics of endogenous EPSCs are normal in *lgc-46(0)*. (A-C) Amplitude (A), 25-75% rise time (B) and 75-25% decay time (C) of endogenous EPSCs. wild type (n=11), *lgc-46(ok2900)* (n=10), and *lgc-46(ok2900); PACh-LGC-46* (n=11). Statistics, one-way ANOVA, Bonferroni's post hoc test. Error bars indicate SEM.

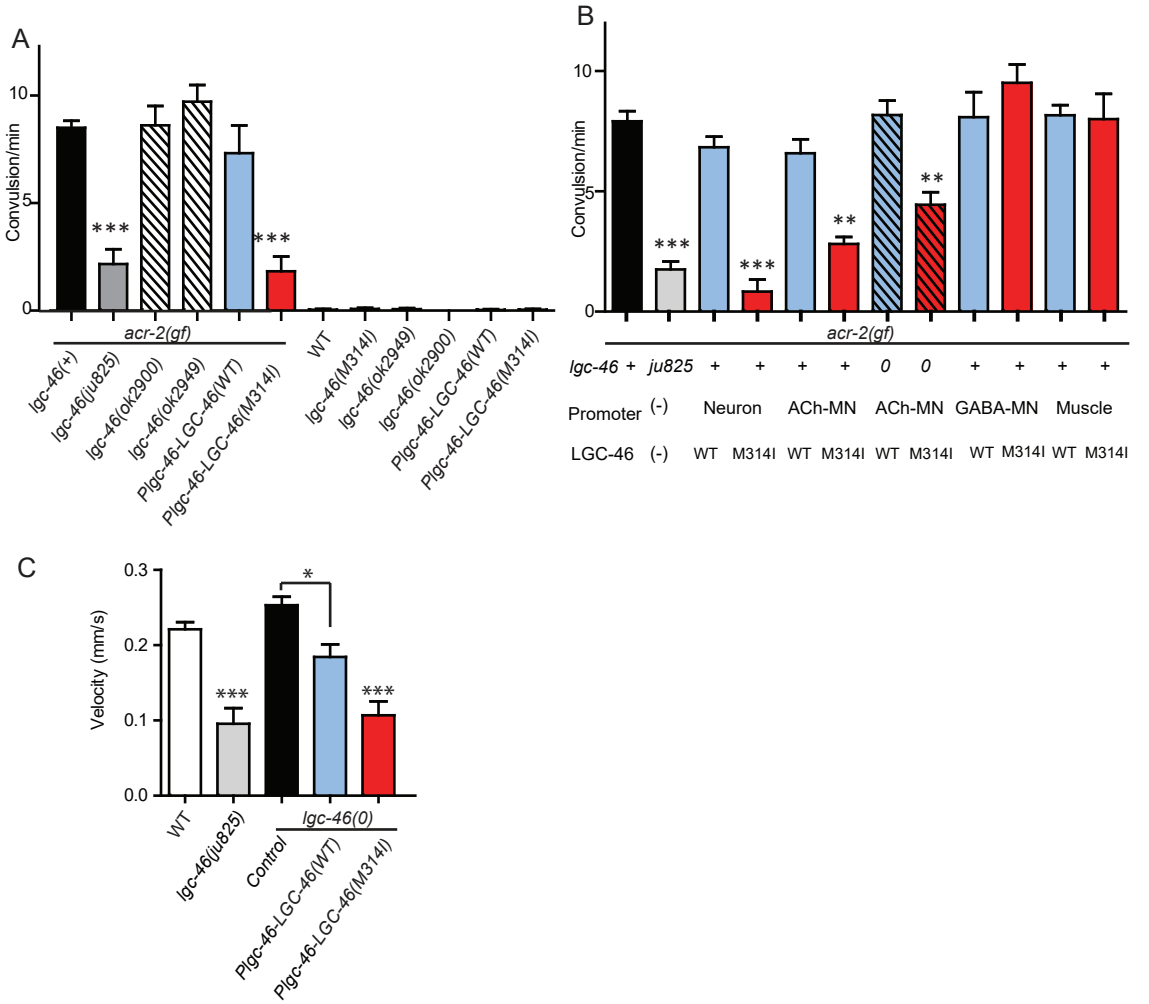

Figure 2.7. A gain-of-function mutation LGC-46(M314I) affects excitation and inhibition imbalance in locomotor circuit. (A) Quantification of convulsion frequencies. *lgc-46(ju825,* but not *lgc-46(0),* suppresses *acr-2(gf)* convulsions. Overexpression of LGC-46(M314I) under its own promoter also strongly suppresses convulsion. Data shown as mean ± SEM; n≥16. (B) Overexpression of LGC-46(M314I) in cholinergic motor neurons can suppress *acr-2(gf)* convulsions. Data shown as mean ± SEM; n≥16. Promoters used to drive expression are, *Prgef-1* for neurons, *Punc-17β*for cholinergic motor neurons, *Punc-25* for GABAergic motor neurons, *Pmyo-3* for muscles (See Extended Data Table 1, Extended Data Table 2). (A,B) Statistics: one-way ANOVA followed by Dunnett's post-hoc test. **: p<0.01, ***: p<0.001. (C) Off-food velocities for each genotype. Statistics: one-way ANOVA followed by Bonferroni's post-hoc test. Data shown as mean ± SEM. **: p<0.01, ***: p<0.001.

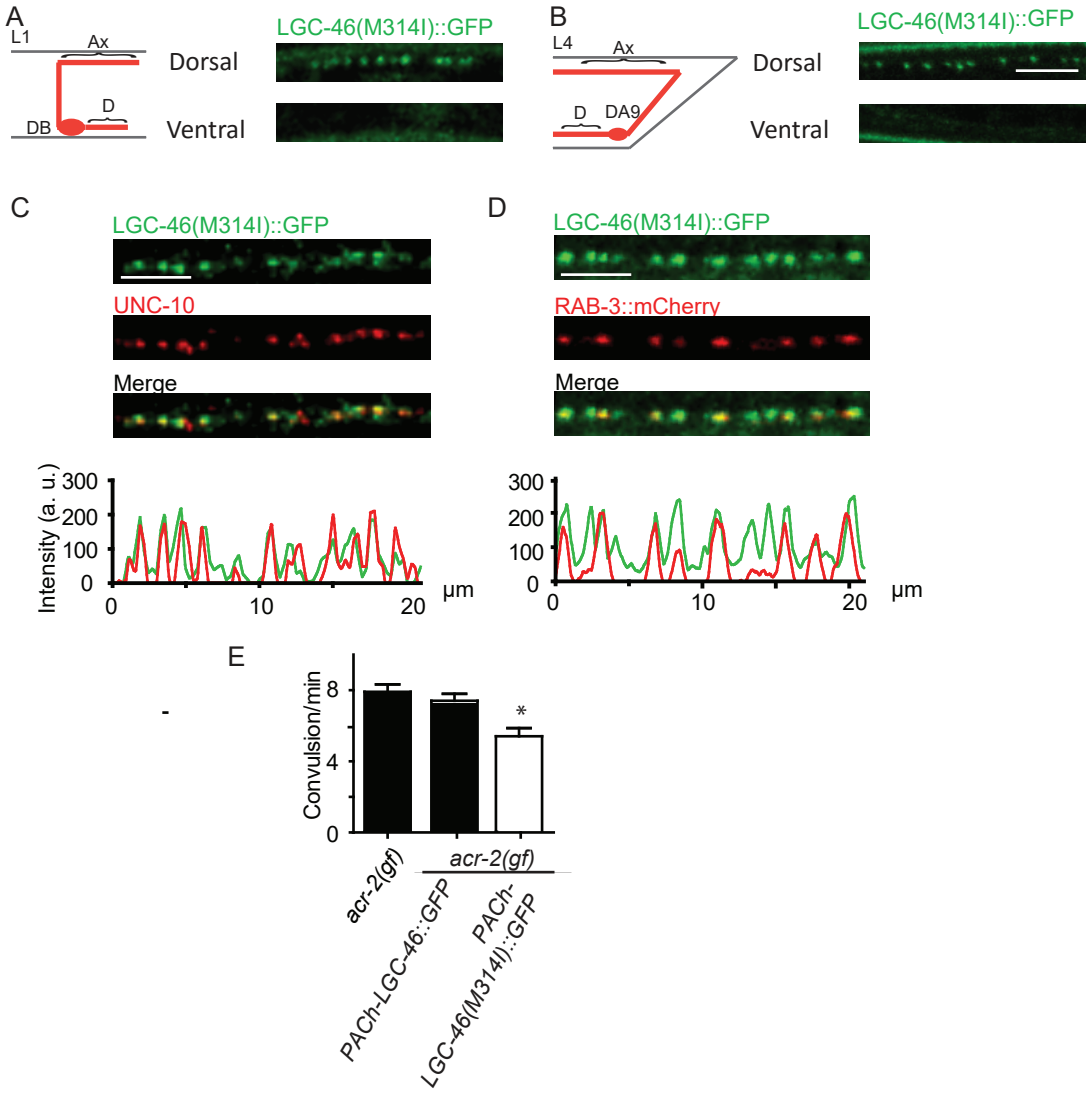

Figure 2.8. LGC-46(M314I) shows similar presynaptic punctate localization pattern as LGC-46(WT). (A-D) Confocal images of animals expressing LGC-46::GFP in cholinergic motor neurons. (A) (Left panel) Schematic of a cholinergic motor neuron in L1 animals. (Right panel) LGC-46(M314I)::GFP shows puncta-like localization on the dorsal side in cholinergic motor neurons of L1 animals. Images are from P*unc-17β-LGC-46(M314I)::GFP(juSi282)IV*. (D) (Left panel) Schematic of a cholinergic motor neuron DA9 in L4 animals. (Right panel) LGC-46::GFP expressed in DA9 neuron shows punctate signals in the dorsal side of L4 animals indicating their axonal localization. Images are from P*itr-1-LGC-46(M314I)::GFP(juEx6845).* (C,D) Presynaptic proteins colocalize with LGC-46::GFP in cholinergic motor neurons. Images taken from dorsal nerve cord are shown. Lower panels show the linescan of fluorescent signal intensities. (C) Anti-GFP and anti-UNC-10 signals from an animal carrying P*unc-17β-LGC-46(M314I)::GFP(juSi282)IV*. (D) Presynaptic protein RAB-3::mCherry expressed in cholinergic motor neurons overlapped with LGC-46(M314I)::GFP signals. Images are from P*unc-17β-LGC-46(M314I)::GFP(juSi282)IV*; P*acr-2-RAB-3::mCherry(juEx7053).* (E) Single copy insertion allele P*unc-17β-LGC-46(M314I)::GFP(juSi282)IV* can significantly suppress the *acr-2(gf)* convulsion frequency. Mean ± SEM.; n=20, 16, 16, respectively. Statistics: one-way ANOVA followed by Dunnett's post-hoc test. *: $p<0.05$. Scale bar: 5μm.

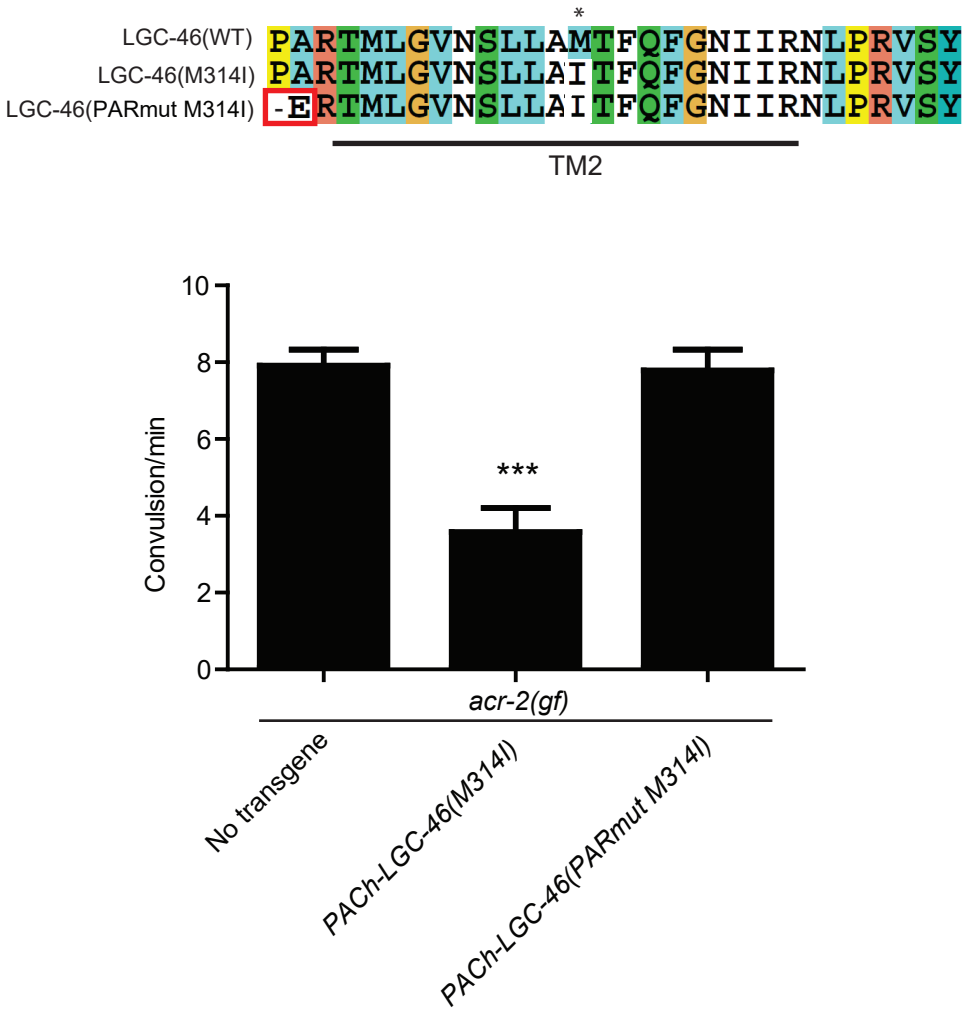

Figure 2.9. PAR motif is required for suppression of *acr-2(gf)* convulsion by LGC-46(M314I). (Top) Amino acid sequences of the wild type, M314I, and M314I with mutations added to the PAR motif. (Bottom) Convulsion frequencies of each genotype are shown. Cholinergic motor neuron-specific expression of LGC-46(M314I) suppresses *acr-2(gf)* convulsions, whereas the PAR motif mutated LGC-46(P301Δ A302E M314I) does not. Mean ± SEM.; n=24, 16, 16, respectively. Statistics: one-way ANOVA followed by Dunnett's post-hoc test. ***: $p<0.001$.

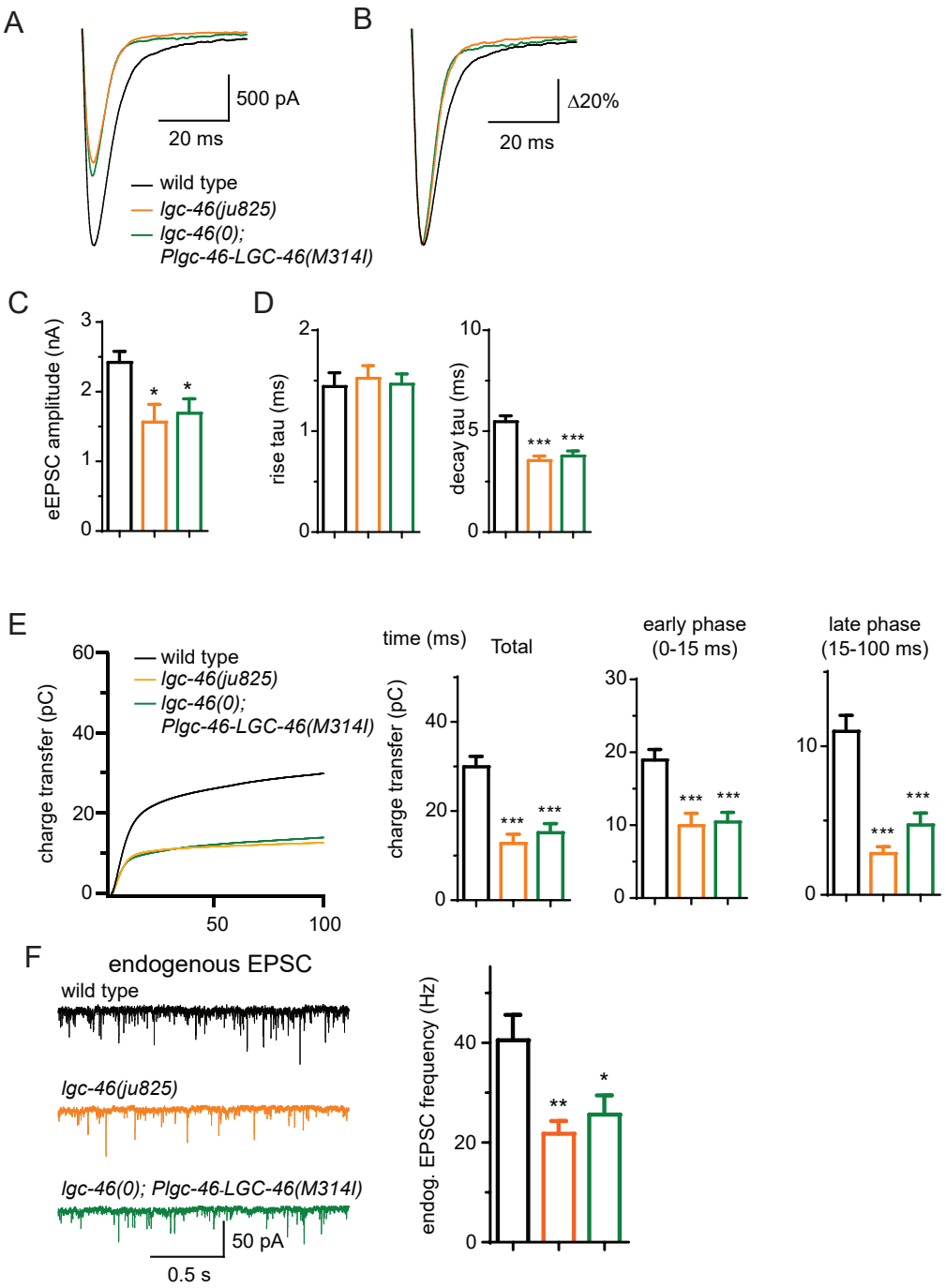

Figure 2.10. LGC-46(M314I) limits synaptic transmission by shortening the decay phase of evoked release. (A,B) Average traces (A) and normalized average traces (B) of eEPSCs. (C) Mean amplitude of eEPSCs. (D) Rise tau and decay tau of eEPSCs. (E) Average traces of cumulative charges of eEPSCs, and charge transfers after stimulation. (F) Representative traces and mean frequency of endogenous EPSCs. wild type (n=12), *lgc-46(ju825)* (n=10), and *lgc-46(0);Plgc-46-LGC-46(M314I)* (n=12). Statistics, one-way ANOVA, Bonferroni's post hoc test. *** $p < 0.001$, ** $p < 0.01$, * $p < 0.05$. Error bars indicate SEM.

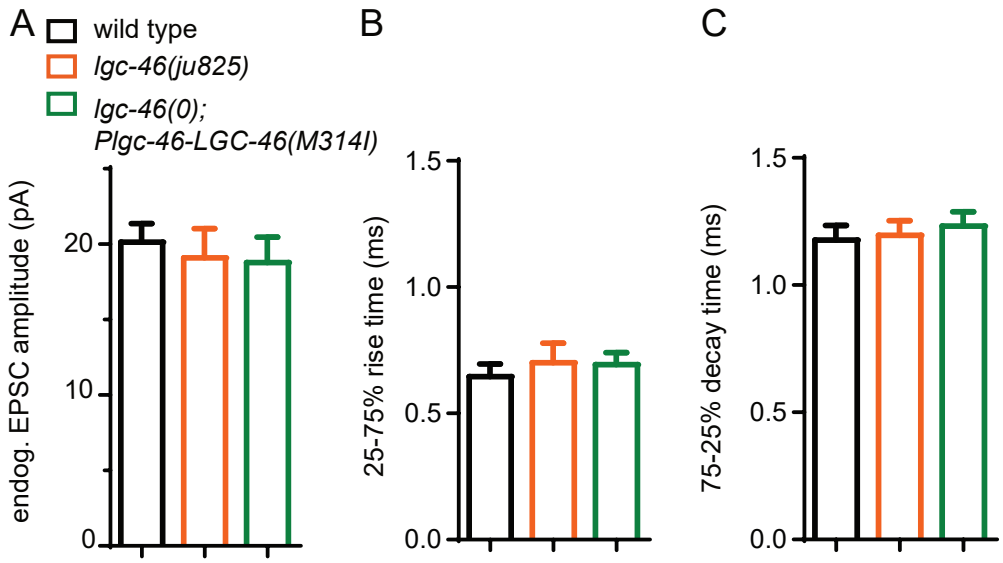

Figure 2.11. Amplitude and kinetics of endogenous EPSCs are unaltered in *lgc-46(gf)*. (A-C) Amplitude (A), 25-75% rise time (B) and 75-25% decay time (C) of endogenous EPSCs. wild type (n=12), *lgc-46(ju825)* (n=10), and *lgc-46(ok2900);Plgc-46-LGC-46(M314I)* (n=12). Statistics, one-way ANOVA, Bonferroni's post hoc test. Error bars indicate SEM.

A

Genotype	Body posture & locomotion
lgc-46(ju825)III	Curly, Slow
lgc-46(ju825)III; acc-1(tm3268)IV	Curly, Slow
lgc-46(ju825)III; acc-2(ok2216)IV	Curly, Slow
lgc-46(ju825)III; acc-3(tm3174)IV	Curly, Slow
lgc-46(ju825)III acc-4(ok2371)III	**Superfically wild type**
lgc-46(ju825)III; lgc-47(ok2963)X	Curly, Slow
lgc-46(ju825)III; lgc-48(gk961621)V	Curly, Slow
lgc-46(ju825)III; lgc-49(tm6556)V	Curly, Slow

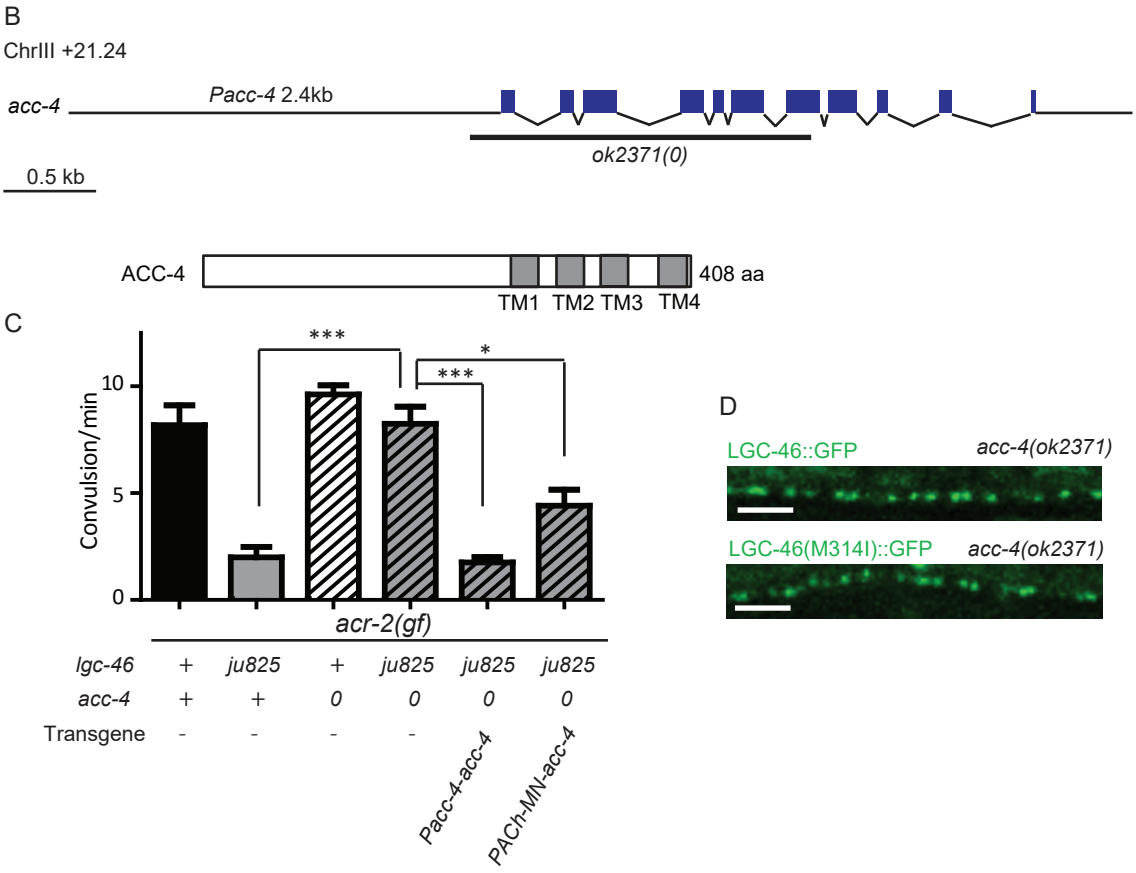

Figure 2.12. LGC-46(M314I) requires ACC-4 for its function. (A) Locomotion observed in double mutants of *lgc-46(ju825)* and *acc* family genes. (B) Gene and protein structure of *acc-4.* Arrows indicate the position of primers designed to amplify cDNA. (C) Frequency of convulsion in animals of indicated genotypes. Loss of functional *acc-4* reverses the suppression of *acr-2(gf)* by *lgc-46(ju825)*. Expression of *acc-4* under the endogenous promoter or cholinergic motor neuron-specific promoter can rescue the effect. Mean ± SEM.; n≥16. Statistics: one-way ANOVA followed by Dunnett's post-hoc test. **: $p<0.01$, ***: $p<0.001$. (D) The punctate localization of LGC-46 is maintained in the *acc-4(ok2371)* background. Scale bar: 10µm.

Table 2.1. List of strains and transgenes used in the study.

Strain number	Genotype	Allele or transgene information
N2	Wild type	
MT6242	*acr-2(n2420) X*	*n2420*: g925a V309M
CZ21292	*lgc-46(ju825) III ; acr-2(n2420) X*	*ju825*: g942a M314I
CZ21630	*lgc-46(ju825) III*	
CZ23071	*lgc-46(ok2900) III*	*ok2900*: 709 bp deletion
CZ21932	*lgc-46(ok2949) III*	*ok2949*: 492 bp deletion and 18 bp insertion
CZ22518	*lgc-46(ok2900)III; acr-2(n2420)X*	
CZ22048	*lgc-46(ok2949)III; acr-2(n2420)X*	
CZ22521	*acr-2(n2420) X ; Plgc-46::lgc-46(wt)(juEx6858)*	*juEx6858*: *Plgc-46-LGC-46(WT) (pCZGY2814)* 5ng/µl, *Pmyo-2-mCherry* 1ng/µl
CZ22522	*acr-2(n2420) X ; Plgc-46::lgc-46(M314I)(juEx6859)*	*juEx6859*: *Plgc-46-LGC-46(M314I)(pCZGY2815)* 5ng/µl, *Pmyo-2-mCherry* 1ng/µl
CZ19768	*Plgc-46-GFP(juEx6783)*	*juEx6859*: *Plgc-46-GFP(pCZGY2810)* 20ng/µl, *Pmyo-2-mCherry* 1ng/µl
CZ22745	*Plgc-46-LGC-46(WT)(juEx6858)*	
CZ23607	*Plgc-46-LGC-46(M314I)(juEx6859)*	
CZ22372	*Pttr-39-mCherry(juIs223); Plgc-46-GFP(juEx6783)*	
CZ22373	*Punc-17-mCherry(nuIs321); Plgc-46-GFP(juEx6783)*	
CZ21820	*acr-2(n2420) X ; Prgef-1-LGC-46(WT)(juEx6612)*	*juEx6612*: *Prgef-1-LGC-46(WT)(pCZGY2816)* 20ng/µl, *Punc-122-RFP* 20ng/µl
CZ21823	*acr-2(n2420) X ; Prgef-1-LGC-46(M314I)(juEx6615)*	*juEx6615*: *Prgef-1-LGC-46(WT)(pCZGY2817)* 20ng/µl, *Punc-122-RFP* 20ng/µl
CZ21826	*acr-2(n2420) X ; Pmyo-3-LGC-46(WT)(juEx6618)*	*juEx6618*: *Pmyo-3-LGC-46(WT)(pCZGY2822)* 20ng/µl, *Punc-122-RFP* 20ng/µl
CZ21829	*acr-2(n2420) X ; Pmyo-3-LGC-46(M314I)(juEx6621)*	*juEx6621*: *Pmyo-3-LGC-46(M314I)(pCZGY2823)* 20ng/µl, *Punc-122-RFP* 20ng/µl
CZ21942	*acr-2(n2420) X ; Punc-25-LGC-46(wt)(juEx6637)*	*juEx6637*: *Punc-25-LGC-46(WT)(pCZGY2820)* 20ng/µl, *Punc-122-RFP* 20ng/µl
CZ21944	*acr-2(n2420) X ; Punc-25-LGC-46(M314I)(juEx6638)*	*juEx6638*: *Punc-25-LGC-46(M314I)(pCZGY2821)* 20ng/µl, *Punc-122-RFP* 20ng/µl
CZ21947	*acr-2(n2420) X ; Punc-17β-LGC-46(wt)(juEx6641)*	*juEx6641*: *Punc-17β-LGC-46(WT)(pCZGY2818)* 20ng/µl, *Punc-122-RFP* 20ng/µl
CZ21949	*acr-2(n2420) X ; Punc-17β-LGC-46(M314I)(juEx6643)*	*juEx6643*: *Punc-17β-LGC-46(M314I)(pCZGY2819)* 20ng/µl, *Punc-122-RFP* 20ng/µl
CZ23870	*acr-2(n2420) X ; Punc-17β-LGC-46(PAR motif edited, M314I)(juEx7274)*	*juEx7274*: *Punc-17β-LGC-46(P301Δ A302E M314I)* (pCZGY3005) 20ng/µl , *Pmyo-2-mCherry* 1ng/µl
CZ23482	*Punc-17β-LGC-46(WT)::GFP(juSi295) IV*	*juSi295*: *Punc-17β-LGC-46(WT)::GFP* single copy inserted at ChrIV site cxTi10882
CZ21485	*Punc-17β-LGC-46(M314I)::GFP(juSi282)IV*	*juSi282*: *Punc-17β-LGC-46(M314I)::GFP* single copy inserted at ChrIV site cxTi10882
CZ23969	*lgc-46(ok2900)III; Punc-17β-LGC-46(WT)::GFP(juEx7333)*	*juEx7333*: *Punc-17β-LGC-46(WT)::GFP(pCZGY2828)* 5ng/µl, *Pmyo-2-mCherry* 1ng/µl
CZ23492	*lgc-46(ok2900)III; Punc-17β::LGC-46(M314I)(juEx6945)*	*juEx6945*: : *Punc-17β-LGC-46(M314I)(pCZGY2819)* 5ng/µl, *Pmyo-2-mCherry* 1ng/µl
CZ23503	*lgc-46(ok2900)III; Plgc-46-LGC-46(WT)(juEx6858)*	
CZ23504	*lgc-46(ok2900)III; Plgc-46-LGC-46(M314I)(juEx6859)*	
CZ22616	*lgc-46(ju825) III ; acc-1(tm3268) IV*	*tm3268*: 241 bp deletion and 4 bp insertion
CZ22617	*lgc-46(ju825) III ; acc-2(ok2216) IV*	*ok2216*: 1749 bp deletion and 14 bp insertion
CZ22809	*lgc-46(ju825) III ; acc-3(tm3174) X*	*tm3174*: 283 bp deletion
CZ23751	*lgc-46(ju825) III acc-4(ok2371)III*	*ok2371*: 1981 bp deletion
CZ20425	*lgc-46(ju825)III; lgc-47(ok2963)X*	*ok2963*: 521 bp deletion
CZ23703	*lgc-46(ju825)III; lgc-49(tm6556)V*	*tm6556*: 725 bp deletion
CZ23809	*lgc-46(ju825)III; lgc-48(gk961621)V*	*gk961621*: 212 bp deletion
CZ23752	*lgc-46(ju825) acc-4(ok2371)III; acr-2(n2420)X*	
CZ23180	*acc-4(ok2371)III; acr-2(n2420)*	
CZ23179	*lgc-46(ok2900)III acc-4(ok2371)III; acr-2(n2420)*	
CZ23790	*lgc-46(ju825) acc-4(ok2371)III; acr-2(n2420)X; Pacc-4-acc-4(genomic)(juEx7251)*	*juEx7251*: *Pacc-4-acc-4(genomic)(pCZGY2866)* 5ng/µl, *Pmyo-2::mCherry* 1ng/µl
CZ23788	*lgc-46(ju825) acc-4(ok2371)III; acr-2(n2420)X; Punc-17β-acc-4cDNA(juEx7249)*	*juEx7249*: *Punc-17β-acc-4cDNA(pCZGY2865)* 5ng/µl, *Pmyo-2-mCherry* 1ng/µl
CZ19997	*Punc-129-RAB-3::mCherry(tauIs46)*	
CZ23973	*lgc-46(ok2900)III; Punc-129-RAB-3::mCherry(tauIs46)*	
CZ23974	*lgc-46(ju825)III; Punc-129-RAB-3::mCherry(tauIs46)*	
CZ24071	*acc-4(ok2371)III; Punc-17b-LGC-*	
CZ24073	*acc-4(ok2371)III; Punc-17b-LGC-*	
CZ22502	*Pitr-1-LGC-46(WT)::GFP(juEx6843)*	*juEx6843*: *Pitr-1-LGC-46(WT)::GFP(pCZGY2830)* 5ng/µl, *Pmyo-2-mCherry* 1ng/µl
CZ22504	*Pitr-1-LGC-46(M314I)::GFP(juEx6845)*	*juEx6845*: *Pitr-1-LGC-46(M314I)::GFP(pCZGY2831)* 5ng/µl, *Pmyo-2-mCherry 1ng/µl*
CZ23594	*Punc-17β-LGC-46(WT)::GFP(juSi295)IV; acr-2(n2420)X*	
CZ23489	*Punc-17β-LGC-46(M314I)::GFP(juSi282)IV; acr-*	
CZ23753	*Punc-17β-LGC-46(WT)::GFP(juSi295)IV; Pacr-2-RAB-3::mCherry(juEx7053)*	*juEx7053*: *Pacr-2-RAB-3::mCherry(pCZGY1008)* 5ng/µl, *Pmyo-2-mCherry* 1ng/µl
CZ23810	*Punc-17β-LGC-46(M314I)::GFP(juSi282)IV; Pacr-2::RAB-3::mCherry(juEx7053)*	

Information of tm, ok, gk alleles are fromWormbase web site, release WS251, <http://www.wormbase.org> (2015) and Caenorhabditis Genetics Center (CGC), <www.cbs.umn.edu/CGC/> (2015).

Table 2.2. List of constructs used in the study.

Number	Plasmid	Promoter drives expression in:	Construction notes
pCZGY2810	Plgc-46-GFP	Neurons including cholinergic motor neurons (See text)	1.6kb upstream of lgc-46 with first two amino acid coding region was amplified using following primers: YJ11735 CATCGACACCCTCACCCAATC YJ11736 TTGCATTGATGCATCCGTGTC. Promoter was cloned into GFP expressing construct backbone by Gibson assembly.
pCZGY2811	Plgc-46DEST	-	1.6kb upstream of lgc-46 was cloned into Gateway destination vector. pCZGY2810 was used as the template to amplify promoter region with YJ11737 and YJ11738.
pCZGY2812	PCR8-LGC-46(WT)	-	lgc-46 cDNA was amlified using the following primers: YJ11741 ATGCAATATCTGCAATTCCT and YJ11742 TTATATTTATTATCATTCGTTGACTAG. cDNA genrated from N2 wild type was used as the template. The amplified fragment was cloned into Gateway PCR8 vector.
pCZGY2813	PCR8-LGC-46(M314I)	-	lgc-46(M314I) cDNA was amplified using YJ11741 and YJYJ11742. cDNA generated from lgc-46(ju825)III: acr-2(n2420)X was used as the templated. The amplified fragment was cloned into Gateway PCR8 vector.
pCZGY2814	Plgc-4-:LGC-46(WT)	Neurons including cholinergic motor neurons (See text)	LR reaction between pCZGY2811 and pCZGY2812
pCZGY2815	Plgc-46-LGC-46(M314I)	Neurons including cholinergic motor neurons (See text)	LR reaction between pCZGY2811 and pCZGY2813
pCZGY2816	Prgef-1-LGC-46(WT)	Pan-neuron[36]	LR reaction between Prgef-1 destination vector (pCZGY66) and pCZGY2812
pCZGY2817	Prgef-1-LGC-46(M314I)	Pan-neuron[36]	LR reaction between Prgef-1 destination vector (pCZGY66) and pCZGY2813
pCZGY2818	Punc-17β-LGC-46(WT)	Cholinergic motor neuron[37]	LR reaction between Punc-17β destination vector (pCZGY1091) and
pCZGY2819	Punc-17β-LGC-46(M314I)	Cholinergic motor neuron[37]	LR reaction between Punc-17β destination vector (pCZGY1091) and
pCZGY2820	Punc-25-LGC-46(WT)	GABAergic motor neuron[38]	LR reaction between Punc-25 destination vector (pCZGY80) and pCZGY2812
pCZGY2821	Punc-25-LGC-46(M314I)	GABAergic motor neuron[38]	LR reaction between Punc-25 destination vector (pCZGY80) and pCZGY2813
pCZGY2822	Pmyo-3-LGC-46(WT)	Body wall muscle[39]	LR reaction between Pmyo-3 destination vector (pCZGY925) and pCZGY2812
pCZGY2823	Pmyo-3-LGC-46(M314I)	Body wall muscle[39]	LR reaction between Pmyo-3 destination vector (pCZGY925) and pCZGY2813
pCZGY2826	PCR8-LGC-46(WT)::GFP	-	GFP coding sequence was inserted after His396 of pCZGY2812 PCR8-lgc-46(wt) by Gibson assembly.
pCZGY2827	PCR8-LGC-46(M314I)::GFP	-	GFP coding sequence was inserted after His396 of pCZGY2813 PCR8-lgc-46(M314I) by Gibson assembly.
pCZGY2828	Punc-17β-LGC-	Cholinergic motor neuron[37]	LR reaction between Punc-17β destination vector (pCZGY1091) and
pCZGY2829	Punc-17β-LGC-46(M314I)::GFP	Cholinergic motor neuron[37]	LR reaction between Punc-17β destination vector (pCZGY1091) and pCZGY2817
pCZGY2830	Pitr-1-LGC-46(WT)::GFP	DA9 cholinergic motor neuron[40]	LR reaction between Pitr-1 destination vector (pCZGY2259) and pCZGY2816
pCZGY2831	Pitr-1-LGC-46(M314I)::GFP	DA9 cholinergic motor neuron[40]	LR reaction between Pitr-1 destination vector (pCZGY2259) and pCZGY2817
pCZGY2834	Punc-17β-LGC-46(WT)::GFP_attL	Cholinergic motor neuron[37]	attL sites were added to pCZGY2828 by Gibson assembly. For single copy insertion
pCZGY2835	Punc-17β-LGC-46(M314I)::GFP_attL	Cholinergic motor neuron[37]	attL sites were added to pCZGY2829 by Gibson assembly. For single copy insertion
pCZGY2836	ChrIV_Punc-17β-LGC-46(WT)::GFP	Cholinergic motor neuron[37]	LR reaction between pCFJ201[41] with hygromycin resistant gene added, and pCZGY2834
pCZGY2837	ChrIV_Punc-17β-LGC-46(M314I)::GFP	Cholinergic motor neuron[37]	LR reaction between pCFJ201[41] with hygromycin resistant gene added, and pCZGY2835
PCZGY1008	Pacr-2-RAB-3::mCherry	Cholinergic motor neuron[8]	LR reaction between pCZGY410 and pCZGY846
pCZGY2864	PCR8-acc-4cDNA	-	acc-4(cDNA) was amplified using YJ11811 ATGCGACTAATCATATTAGTAATCTCCATTC and YJ11812 CTTAGATAGTTCTAACCAATAGTTTTCCGAG. Cloned into Topo PCR8
pCZGY2865	Punc-17β-acc-4cDNA	Cholinergic motor neuron[37]	LR reaction between Punc-17β destination vector (pCZGY1091) and
pCZGY2866	PCR8-acc-4genomic	-	acc-4 proromoter and genomic region was amplified using YJ11813 TTCTGAGTATGTGGGAAGGATGG and YJ11814 CGTGAAACATGACAAATGCGAG. Cloned into Topo PCR8 vector.
pCZGY3004	PCR8-LGC-46(P301Δ A302E M314I)	-	Site directed mutagenesis kit (NEB) was used to edit amino acid sequences using pCZGY2864 as template.
pCZGY3005	Punc-17β-LGC-46(P301Δ A302E M314I)	Cholinergic motor neuron[37]	LR reaction between Punc-17β destination vector (pCZGY1091) and pCZGY3004

References: [36](Altun-Gultekin et al. 2001) [37](Charlie et al. 2006) [38](Jin et al. 1999) [39](Okkema et al. 1993) [40](Klassen et al. 2007). [41](Frøkjær-Jensen, et al. 2012).

References

Atwood, B. K., Lovinger, D. M., & Mathur, B. N. (2014). Presynaptic long-term depression mediated by Gi/o-coupled receptors. *Trends Neurosci, 37*(11), 663-673.

Belenky, M. A., Sagiv, N., Fritschy, J. M., & Yarom, Y. (2003). Presynaptic and postsynaptic GABAA receptors in rat suprachiasmatic nucleus. *Neuroscience, 118*(4), 909-923.

Cattaert, D., & El Manira, A. (1999). Shunting versus inactivation: analysis of presynaptic inhibitory mechanisms in primary afferents of the crayfish. *J Neurosci, 19*(14), 6079-6089.

Chalifoux, J. R., & Carter, A. G. (2011). GABAB receptor modulation of synaptic function. *Curr Opin Neurobiol, 21*(2), 339-344.

Eccles, J. C., Schmidt, R., & Willis, W. D. (1963). Pharmacological Studies on Presynaptic Inhibition. *J Physiol, 168*, 500-530.

Engelman, H. S., & MacDermott, A. B. (2004). Presynaptic ionotropic receptors and control of transmitter release. *Nat Rev Neurosci, 5*(2), 135-145.

Galzi, J. L., Devillers-Thiéry, A., Hussy, N., Bertrand, S., Changeux, J. P., & Bertrand, D. (1992). Mutations in the channel domain of a neuronal nicotinic receptor convert ion selectivity from cationic to anionic. *Nature, 359*(6395), 500-505.

Giardine, B., Riemer, C., Hardison, R. C., Burhans, R., Elnitski, L., Shah, P., Zhang, Y., Blankenberg, D., Albert, I., Taylor, J., Miller, W., Kent, & W. J., Nekrutenko, A. (2005). Galaxy: a platform for interactive large-scale genome analysis. *Genome Res, 15*(10), 1451-1455.

Hruskova, B., Trojanova, J., Kulik, A., Kralikova, M., Pysanenko, K., Bures, Z., Syka, J., Trussell, L. O., & Turecek, R. (2012). Differential distribution of glycine receptor subtypes at the rat calyx of Held synapse. *J Neurosci, 32*(47), 17012-17024.

Hu, Z., Tong, X. J., & Kaplan, J. M. (2013). UNC-13L, UNC-13S, and Tomosyn form a protein code for fast and slow neurotransmitter release in *Caenorhabditis elegans*. *Elife, 2*, e00967.

Jensen, M. L., Pedersen, L. N., Timmermann, D. B., Schousboe, A., & Ahring, P. K. (2005). Mutational studies using a cation-conducting GABAA receptor reveal the selectivity determinants of the Cys-loop family of ligand-gated ion channels. *J Neurochem, 92*(4), 962-972.

Jensen, M. L., Schousboe, A., & Ahring, P. K. (2005). Charge selectivity of the Cys-loop family of ligand-gated ion channels. *J Neurochem, 92*(2), 217-225.

Jospin, M., Qi, Y. B., Stawicki, T. M., Boulin, T., Schuske, K. R., Horvitz, H. R., Bessereau, J. L., Jorgensen, E. M., & Jin, Y. (2009). A neuronal acetylcholine receptor regulates the balance of muscle excitation and inhibition in *Caenorhabditis elegans*. *PLoS Biol, 7*(12), e1000265.

Kehoe, J. (1972a). Ionic mechanisms of a two-component cholinergic inhibition in Aplysia

neurones. *J Physiol, 225*(1), 85-114.

Kehoe, J. (1972b). The physiological role of three acetylcholine receptors in synaptic transmission in Aplysia. *J Physiol, 225*(1), 147-172.

Kehoe, J., & McIntosh, J. M. (1998). Two distinct nicotinic receptors, one pharmacologically similar to the vertebrate alpha7-containing receptor, mediate Cl currents in aplysia neurons. *J Neurosci, 18*(20), 8198-8213.

Keramidas, A., Moorhouse, A. J., French, C. R., Schofield, P. R., & Barry, P. H. (2000). M2 pore mutations convert the glycine receptor channel from being anion- to cation-selective. *Biophys J, 79*(1), 247-259.

Kullmann, D. M., Ruiz, A., Rusakov, D. M., Scott, R., Semyanov, A., & Walker, M. C. (2005). Presynaptic, extrasynaptic and axonal GABAA receptors in the CNS: where and why? *Prog Biophys Mol Biol, 87*(1), 33-46.

Larkin, M. A., Blackshields, G., Brown, N. P., Chenna, R., McGettigan, P. A., McWilliam, H., Valentin, F., Wallace, I. M., Wilm, A., Lopez, R., Thompson, J. D., Gibson, T. J., & Higgins, D. G. (2007). Clustal W and Clustal X version 2.0. *Bioinformatics, 23*(21), 2947-2948.

Li, Z., Liu, J., Zheng, M., & Xu, X. Z. (2014). Encoding of both analog- and digital-like behavioral outputs by one C. elegans interneuron. *Cell, 159*(4), 751-765.

Mahoney, T. R., Luo, S., & Nonet, & M. L. (2006). Analysis of synaptic transmission in *Caenorhabditis elegans* using an aldicarb-sensitivity assay. *Nat Protoc, 1*(4), 1772-1777.

Pereira, L., Kratsios, P., Serrano-Saiz, E., Sheftel, H., Mayo, A. E., Hall, D. H., Hall, D. H., White, J. G., Leboeuf, B., Garcia, L. R., Alon, U., & Hobert, O. (2015). A cellular and regulatory map of the cholinergic nervous system of C.elegans. *Elife, 4*.

Putrenko, I., Zakikhani, M., & Dent, J. A. (2005). A family of acetylcholine-gated chloride channel subunits in *Caenorhabditis elegans*. *J Biol Chem, 280*(8), 6392-6398.

Qi, Y. B., Po, M. D., Mac, P., Kawano, T., Jorgensen, E. M., Zhen, M., & Jin, Y. (2013). Hyperactivation of B-type motor neurons results in aberrant synchrony of the *Caenorhabditis elegans* motor circuit. *J Neurosci, 33*(12), 5319-5325.

Richmond, J. E., Davis, W. S., & Jorgensen, E. M. (1999). UNC-13 is required for synaptic vesicle fusion in C. elegans. *Nat Neurosci, 2*(11), 959-964.

Ringstad, N., Abe, N., & Horvitz, H. R. (2009). Ligand-gated chloride channels are receptors for biogenic amines in C. elegans. *Science, 325*(5936), 96-100.

Schicker, K. W., Dorostkar, M. M., & Boehm, S. (2008). Modulation of transmitter release via presynaptic ligand-gated ion channels. *Curr Mol Pharmacol, 1*(2), 106-129.

Stawicki, T. M., Takayanagi-Kiya, S., Zhou, K., & Jin, Y. (2013). Neuropeptides function in a homeostatic manner to modulate excitation-inhibition imbalance in C. elegans. *PLoS Genet, 9*(5), e1003472.

Sulston, J. E. (1976). Post-embryonic development in the ventral cord of *Caenorhabditis elegans*. *Philos Trans R Soc Lond B Biol Sci, 275*(938), 287-297.

Van Epps, H., Dai, Y., Qi, Y., Goncharov, A., & Jin, Y. (2010). Nuclear pre-mRNA 3'-end processing regulates synapse and axon development in C. elegans. *Development, 137*(13), 2237-2250.

White, J. G., Albertson, D. G., & Anness, M. A. (1978). Connectivity changes in a class of motoneurone during the development of a nematode. *Nature, 271*(5647), 764-766.

Zhou, K., Stawicki, T. M., Goncharov, A., & Jin, Y. (2013). Position of UNC-13 in the active zone regulates synaptic vesicle release probability and release kinetics. *Elife, 2*, e01180.

Chapter 3

Neuropeptides Function in a Homeostatic Manner to Modulate Excitation-Inhibition Imbalance in *C. elegans*

Abstract

Neuropeptides play crucial roles in modulating neuronal networks, including changing intrinsic properties of neurons and synaptic efficacy. We previously reported a *C. elegans* mutant, *acr-2(gf)* that displays periodic convulsions as the result of a gain-of-function mutation in a neuronal nicotinic acetylcholine receptor subunit. The ACR-2 channel is expressed in the cholinergic motor neurons; and *acr-2(gf)* causes cholinergic overexcitation accompanied with reduced GABAergic inhibition in the locomotor circuit. Here we show that neuropeptides play a homeostatic role that compensates for excitation-inhibition imbalance in the locomotor circuit. Loss of function in genes required for neuropeptide processing or release of dense core vesicles specifically modulate the convulsions of *acr-2(gf)*. The proprotein convertase EGL-3 is required in the cholinergic motor neurons to restrain convulsions. Electrophysiological recordings of neuromuscular junctions show that loss of *egl-3* causes a further reduction of GABAergic inhibition in *acr-2(gf)*. We identify two neuropeptide encoding genes, *flp-1* and *flp-18,* that together counteract the excitation-inhibition imbalance in *acr-2(gf)* mutants. We further find that *acr-2(gf)* causes an increased expression of *flp-18* in the ventral cord cholinergic motor neurons and that overexpression of *flp-18* or *flp-1* can dampen the convulsion of *acr-2(gf)* mutants. The effects of these peptides are in part mediated by two G-protein coupled receptors, NPR-1 and NPR-5. Our data suggest that the chronic overexcitation of the cholinergic motor neurons imposed by *acr-2(gf)* leads to an increased production of FMRFamide neuropeptides, which act to decrease the activity level of the locomotor circuit, thereby homeostatically modulating excitation and inhibition imbalance.

Introduction

Neuropeptides are widespread and diverse modulators of neuronal circuit function, and have long been known to play regulatory roles in complex behaviors, such as learning, feeding, temperature regulation, and pain sensation (Kow & Pfaff, 1988; Krieger, 1983). Additionally, neuropeptide modulation is implicated in a number of neurological diseases including epilepsy and autism (Blake, Badway, & Strowski, 2004; Fetissov et al., 2003; Lerner, Sankar, & Mazarati, 2008; Mitsukawa, Lu, & Bartfai, 2008; Schwarzer, 2009; Wu et al., 2011). In recent years great strides have been made in the recognition of the diverse means by which neuropeptides regulate neuronal circuits (Bargmann, 2012; Chalasani et al., 2010; Davis & Stretton, 1996; Harris-Warrick & Marder, 1991; Hu, Pym, Babu, Vashlishan Murray, & Kaplan, 2011; Marder, 2012; Nässel, 2002; Renn, Park, Rosbash, Hall, & Taghert, 1999). In particular, numerous studies from *C. elegans* have revealed important insights on the precise mechanisms underlying endogenous neuropeptide function in animal behaviors (Bargmann, 2012; Leinwand & Chalasani, 2011; Luedtke, O'Connor, Holden-Dye, & Walker, 2010; Taghert & Nitabach, 2012).

The *C. elegans* genome contains over 100 peptide-encoding genes, which are generally classified as *flp* for FMRFamide-like peptides, *ins* for insulin-like genes, and *nlp* for neuropeptide-like proteins (Li & Kim, 2008). Recent proteomic studies have detected expression of over 150 distinct mature peptides (Husson, Clynen, Baggerman, Janssen, & Schoofs, 2006; Husson et al., 2007; Husson & Schoofs, 2007; Li & Kim, 2008). As in higher vertebrates and other organisms, neuropeptide precursors are packaged into large dense core vesicles, and are further processed into functionally mature neuropeptides through a series of conserved enzymatic reactions (Fuller, Sterne, & Thorner, 1988; Jung & Scheller, 1991). The release of dense core vesicles occurs in response to Ca^{2+} influx, and relies on several unique proteins in addition to those that are also involved in fast neurotransmitter release (Südhof, 2008).

The two best characterized enzymes for neuropeptide processing in *C. elegans* are the proprotein convertase PC2, EGL-3, and the carboxypeptidase E (CPE), EGL-21 (Jacob &

Kaplan, 2003; Kass, Jacob, Kim, & Kaplan, 2001; Li & Kim, 2008). EGL-3/PC2 cleaves the propeptide after the basic residues C-terminus flanking the individual peptides (Li & Kim, 2008). EGL-21/CPE removes the remaining basic residues of the newly cleaved peptides (Li & Kim, 2008). Both genes are expressed primarily in the nervous system (Jacob & Kaplan, 2003; Kass, et al., 2001; Li & Kim, 2008). An early report using an antibody that recognizes fully processed FMRFamide-related peptides showed loss of most staining in *egl-21* mutants, and a dramatic reduction of staining in *egl-3* mutants (Jacob & Kaplan, 2003). Recent peptidomic analyses fail to detect any processed neuropeptides in *egl-3* null mutants (Husson, et al., 2006). In contrast, while *egl-21* mutants show incomplete processing of the majority of FLP and NLP peptides, they also express a number of fully processed peptides (Husson, et al., 2007). Thus, these two enzymes are important for the processing and production of most, but not all, mature neuropeptides. *egl-3* and *egl-21* mutants share similar phenotypes including retention of eggs, sluggish movement, and a reduction in sensitivity to the acetylcholinesterase inhibitor aldicarb (Jacob & Kaplan, 2003; Kass, et al., 2001). However, *egl-3; egl-21* double mutants show increased resistance to aldicarb, compared to either single mutant (Jacob & Kaplan, 2003; Kass, et al., 2001), suggesting that they may not act in a completely linear pathway.

Neuropeptide release in *C. elegans* is well known to influence neural circuit activity and behavior (Bargmann, 2012; Li, 2005; Sieburth et al., 2005). The UNC-31 CAPS (Calcium-dependent Activator Protein for Secretion) protein is essential for peptide-containing dense core vesicle release, and *unc-31* mutants exhibit many sensory deficits and impaired locomotion (Avery, Bargmann, & Horvitz, 1993; Charlie, Schade, Thomure, & Miller, 2006; Lee & Ashrafi, 2008; Liu, Kim, Li, & Barr, 2007; Zhou et al., 2007). Examples of specific neuropeptides regulating locomotor circuit activity include the neuropeptide NLP-12, which has recently been shown to be released by the stretch sensitive neuron DVA and can influence cholinergic motor neuron neurotransmitter release (Hu, et al., 2011). Also, the levels of the FLP-1 FMRFamide peptides can alter locomotor behavior such that *flp-1(lf)* mutants are

hyperactive while overexpression of *flp-1* causes reduced mobility (Nelson, Rosoff, & Li, 1998).

C. elegans sinusoidal locomotion is the result of coordinated muscle contraction due to innervation by the ventral cord excitatory cholinergic motor neurons and inhibitory GABAergic motor neurons (White, Southgate, Thomson, & Brenner, 1976). Neuropeptide signaling has been implicated in modulating the activity of both types of motor neurons as well as the muscles (Chalasani, et al., 2010; Li & Kim, 2008). We have previously reported that the ACR-2 nicotinic acetylcholine receptor is expressed in the cholinergic motor neurons and plays a key role in balancing excitatory and inhibitory neurotransmission in the locomotor circuit (Jospin et al., 2009). Specifically, a gain of function mutation (Val309Met), designated as *acr-2(gf),* in the pore-lining transmembrane domain of the ACR-2 subunit causes an increase in cholinergic excitation, accompanied with a decrease in GABAergic inhibition. This imbalance in excitation and inhibition results in stochastic convulsive behavior due to spontaneous contractions of body muscles. Thus, the frequency of convulsions of the *acr-2(gf)* mutant can be used as an indicator for the imbalanced activity of the locomotor circuit.

In this study we examined the roles of neuropeptides in modulating excitation and inhibition imbalance in the locomotor circuit. We show that neuropeptides processed by EGL-3 and released from the cholinergic motor neurons inhibit the convulsions caused by *acr-2(gf)*. We find that two neuropeptide-encoding genes, *flp-1* and *flp-18,* act together to reduce excitation and inhibition imbalance in the locomotor circuit. *acr-2(gf)* causes a specific up-regulation of *flp-18* expression in the cholinergic motor neurons. Electrophysiological recordings of the neuromuscular junctions indicate that *egl-3* and *flp* genes primarily influence GABAergic synaptic transmission. We also identify two neuropeptide receptors, NPR-1 and NPR-5 that are likely involved in the regulation of convulsions by the FLP-18 neuropeptides. These data suggest that neuropeptide production is regulated by activity, and that in turn neuropeptides function in a homeostatic manner to modulate output of the locomotor circuit. Our findings have implications for our understanding of excitation-inhibition imbalance in disease conditions, and support a

general notion that neuropeptide modulation can provide effective strategies in disease management.

Results

Loss of function in the proprotein convertase EGL-3 enhances the convulsion frequency of *acr-2(gf)*

To specifically test the roles of neuropeptides on *acr-2(gf)* induced convulsions, we first examined a set of mutants that are known to disrupt peptide processing. We found that multiple alleles of *egl-3* caused a significant increase in the convulsion frequency of *acr-2(gf)* (Figure 3.1A). A null mutation in *sbt-1,* a molecular chaperone necessary for EGL-3 function (Husson & Schoofs, 2007), showed a similar enhancement. *egl-3(lf) sbt-1(lf); acr-2(gf)* triple mutants showed a similar level of increased convulsions as *egl-3(lf); acr-2(gf)* and *sbt-1(lf); acr-2(gf)* double mutants, consistent with SBT-1 and EGL-3 acting in the same pathway. The overall locomotion pattern and speed of *sbt-1; acr-2(gf)* was indistinguishable from that of *acr-2(gf),* supporting the specific effects of SBT-1 and EGL-3 on convulsion frequency.

The carboxypeptidase E EGL-21 generally functions together with EGL-3 in producing mature neuropeptides (Li & Kim, 2008). However, we tested three mutations in *egl-21,* including a large deletion *tm5578*, which removes most of the exons 2 and 3 and causes premature stop after 85 amino acids (Table 3.1), and did not observe any effects on *acr-2(gf)* convulsions (Figure 3.1A). A null mutation in *cpd-2,* another carboxypeptidase, also showed no effects. Moreover, *egl-21(lf); egl-3(lf); acr-2(gf)* triple mutants behaved similarly to *egl-3(lf); acr-2(gf)*. These observations suggest that *egl-21* may not be required, or has a partial role, for processing the specific neuropeptides involved in *acr-2(gf)* convulsive behavior. As addressed later and shown in Figure 3.3A, we found the latter interpretation to be true. Overall, these observations indicate that EGL-3-dependent neuropeptides modulate the convulsive behavior of *acr-2(gf)* animals.

The function of neuropeptides is dependent on dense core vesicle release that requires the CAPS protein UNC-31 (Süudhof, 2008). To test further the role of neuropeptides in modulating *acr-2(gf)* convulsions, we introduced a null mutation of *unc-31* into the *acr-2(gf)* background. In contrast to *egl-3(lf); acr-2(gf), unc-31(lf); acr-2(gf)* double mutants showed a significant reduction in the frequency of convulsions as compared to the *acr-2(gf)* mutants alone (Figure 3.1A). Importantly, *unc-31(lf)* blocked the enhancement of *egl-3(lf),* as *egl-3(lf); unc-31(lf); acr-2(gf)* triple mutants convulsed to the same degree as *unc-31(lf); acr-2(gf)* (Figure 3.1A). Dense core vesicles contain complex components that include neuropeptides, whose processing most likely depends on EGL-3, as well as INS-like peptides, whose processing generally does not depend on EGL-3. Upon release, peptides can act in a combinatorial manner to modulate specific pathways. The observed opposite effects on *acr-2(gf)* convulsions by *egl-3(lf)* and *unc-31(lf)* lead us to propose that the effective mature neuropeptides processed by EGL-3 are a subset of dense core vesicle components released via UNC-31.

We further addressed in which cells neuropeptide processing by EGL-3 is required to modulate *acr-2(gf)*. We found that expression of *egl-3(+)*, either pan-neuronally using the *rgef-1* promoter (Altun-Gultekin et al., 2001), or in the cholinergic motor neurons using the *unc-17β* or the *acr-2* promoter (Charlie, et al., 2006), fully rescued the enhanced convulsions in *egl-3(lf); acr-2(gf),* whereas expression of *egl-3(+)* in pre-motor command neurons, driven by the *glr-1* promoter (Brockie, Madsen, Zheng, Mellem, & Maricq, 2001), did not show any effect (Figure 3.1B, Tables 3.1, 3.2). Together, these data reveal that neuropeptides processed in the cholinergic motor neurons modulate convulsion behavior of *acr-2(gf)*, and suggest that the neuropeptide products act to restore the balance of excitation and inhibition in the locomotor circuit.

FMRFamide-like peptides encoded by *flp-1* and *flp-18* act synergistically to decrease locomotor circuit activity in *acr-2(gf)* mutants

We next sought to determine the specific neuropeptides responsible for the inhibition of

acr-2(gf) convulsions. We tested a set of candidate neuropeptide genes that had either been shown to be expressed in the locomotor circuit, or were known to affect locomotion (Li & Kim, 2008). Of 23 neuropeptide mutants tested, none showed significant enhancement of the *acr-2(gf)* convulsion phenotype (Figure 3.2A-C, Table 3.1). We reasoned that the observed inhibitory effects of *egl-3* above could be due to a group of neuropeptides produced by more than one gene. To test this idea, we made selected double mutants among *flp* and *nlp* genes chosen based on similarity in expression patterns or phenotypes. In doing so we found that eliminating both *flp-1* and *flp-18* resulted in a significant enhancement of *acr-2(gf)* convulsions (Figure 3.2D, 3.3A). Two independent *flp-18(lf)* mutants, *flp-18(tm2179)* and *flp-18(db99)*, gave similar effects (Figure 3.3A). None of the other seven neuropeptide gene double mutants affected *acr-2(gf)* convulsion frequency (Figure 3.2D). We note that while *flp-1; flp-18* double mutants cause a significant enhancement of the frequency of the *acr-2(gf)*-induced convulsion, the extent of convulsion is often less obvious than that seen in *egl-3(lf); acr-2(gf)*, suggesting other as yet unidentified neuropeptides may also be influencing *acr-2(gf)* convulsions.

In the recent peptidomic studies of *egl-21(lf)* animals, fully processed FLP-1 peptides are reported to be largely undetectable; however, four of the six fully processed mature peptides from FLP-18 are produced (Husson, et al., 2007). The presence of functional *flp-18*-derived peptides would explain why *egl-21(lf)* single mutants did not show any effects on *acr-2(gf)* (Figure 3.1A). To test this idea, we constructed *egl-21(lf); flp-18(lf) acr-2(gf)* triple mutants, and observed that the convulsion frequency in these animals was comparable to that of *flp-1(lf); flp-18(lf) acr-2(gf)* (Figure 3.3A). Thus, these observations support a role of EGL-21 in the processing of FLP-1 neuropeptides, and imply other unidentified carboxypeptidases in the processing of FLP-18 neuropeptides.

As an independent assay for the effects of *flp-1* and *flp-18* neuropeptides on the locomotor circuit activity associated with *acr-2(gf)* convulsions, we tested the sensitivity of animals to the acetylcholinesterase inhibitor aldicarb (Rand, 2007). *acr-2(gf)* animals show

hypersensitivity to aldicarb, consistent with increased cholinergic transmission and decreased GABAergic transmission (Jospin, et al., 2009) (Figure 3.3B,C). *flp-1(lf)* mutants showed mild resistance to aldicarb (Figure 3.4A), consistent with a previous report (Sieburth, et al., 2005). *flp-18(lf)* showed sensitivity to aldicarb similar to wild type and suppressed the resistance *of flp-1(lf)* (2.4A). The hypersensitivity of *acr-2(gf)* to aldicarb was slightly, but not significantly enhanced by loss of function mutations in either *flp-1* or *flp-18* alone (Figure 3.3B). Notably, triple mutants of *flp-1(lf); flp-18(lf) acr-2(gf)* showed significantly increased sensitivity to aldicarb, compared to *acr-2(gf)* alone (Figure 3.3B). Both the increased convulsion frequency and the increased aldicarb sensitivity of the *flp-1(lf); flp-18(lf) acr-2(gf)* triple mutants were rescued by pan-neuronal expression of *flp-1(+)* (Figure 3.3A, C), indicating FLP genes act in the nervous system to modulate excitation-inhibition imbalance caused by *acr-2(gf)*. Also, transgenic expression of *flp-18(+)* rescued the increased convulsion frequency of *flp-1(lf); flp-(lf)* (Figure 3.3A).

EGL-3 and FLP neuropeptides primarily regulate GABAergic inhibition

To address more precisely how neuropeptides influence locomotor circuit activity in the *acr-2(gf)* background, we performed electrophysiological recordings at the neuromuscular junction. As reported previously (Jospin, et al., 2009; Stawicki, Zhou, Yochem, Chen, & Jin, 2011), when recordings were performed with 2 mM Ca^{2+} in the bath solution, *acr-2(gf)* showed slightly increased frequencies of endogenous acetylcholine release, but a striking reduction of endogenous GABAergic activity (Figure 3.5A). Loss of *egl-3* function in *acr-2(gf)* caused a further reduction in endogenous IPSC rate (Figure 3.5A). We observed a similar, but milder, effect on IPSC rate in *flp-1(lf); flp-18(lf) acr-2(gf)* triple mutants, consistent with the milder enhanced convulsions in these animals. *egl-3(lf); acr-2(gf)* and *flp-1(lf); flp-18(lf); acr-2(gf)* both showed slightly reduced endogenous EPSC rates compared to *acr-2(gf)* single mutant, although the average rate did not significantly differ among the strains (Figure 3.5A). Since the effect of

loss of the neuropeptides on IPSC is larger than that on EPSC, reduced GABAergic transmission is likely to have the stronger effect on the animal, thus causing the increased convulsion phenotype. The amplitudes of endogenous EPSCs and IPSCs were similar in the all four genotypes tested, suggesting that ACh and GABA receptors are expressed and are functional on the muscle membranes of the mutants (Figure 3.5B). Thus, the electrophysiology analysis indicates that neuropeptides processed by EGL-3 compensate for the excitation-inhibition imbalance caused by *acr-2(gf)* primarily by acting on GABAergic transmission, and that FLP-1 and FLP-18 peptides account for most, but not all, of the neuromodulatory effects of EGL-3.

The *acr-2(gf)* mutation increases FLP-18 expression in the cholinergic motor neurons

The specific effect of *flp-1* and *flp-18* on *acr-2(gf)* could be caused by either increased expression or release of these neuropeptides in this mutant background. To address the possibility of increased neuropeptide release, we examined two fluorescent reporters for dense core vesicle release from the cholinergic motor neurons: *Punc-129::NLP-21::venus* and *Punc-129::INS-22::venus* (Sieburth, et al., 2005; Sieburth, Madison, & Kaplan, 2007). Neither reporter showed significant changes in fluorescence intensity or pattern (Figure 3.6), suggesting that the general release machinery is largely normal in *acr-2(gf)*.

We next tested for increased expression of neuropeptides using a bicistronic *flp-18* reporter that contains the entire genomic locus of *flp-18,* including the 3.6 kb upstream promoter, followed by a trans-spliced SL2::GFP (designated as *Pflp-18::flp-18::SL2::gfp*) (Cohen et al., 2009). In the wild type background this reporter was strongly expressed in several head neurons and was detectable at low levels in the ventral nerve cord. In the *acr-2(gf)* background, we found that *Pflp-18::flp-18::SL2::gfp* expression in the ventral cord neurons was strongly enhanced (Figure 3.7A-C), while its expression in the head neurons was not changed (Figure 3.8). We also confirmed that GFP expression pattern in the cholinergic motor neurons under *unc-17* promoter was not affected by *acr-2(gf)* mutation (Figure 3.9). We quantified the number of ventral cord

neuron cell bodies with *Pflp-18::flp-18::SL2::gfp* expression, and found that the fluorescence was consistently visible in more cell bodies in the ventral cord of *acr-2(gf)* animals than in wild type (Figure 3.7D). We were not able to examine *flp-1* expression due to variable expression patterns of different transgenic *flp-1* reporter lines (our unpublished data, and Chris Li, personal communication).

The cells that showed up-regulation of *Pflp-18::flp-18::SL2::gfp* in *acr-2(gf)* were evenly spaced along the ventral nerve cord (Figure 3.7B). To determine in which class of motor neurons *Pflp-18::flp-18::SL2::gfp* expression was affected, we crossed *acr-2(gf); Pflp-18::flp-18::SL2::gfp* with a set of mCherry reporter lines driven by specific motor neuron promoters. We observed consistent co-expression of GFP and mCherry in B-type cholinergic motor neurons, labeled by *Pacr-5*, and occasional expression in A-type cholinergic motor neurons, labeled by *Punc-4*, but no overlapping expression in GABAergic D-type motor neurons, labeled by *Pttr-39* (Figure 3.7 E-H). These data indicate that *acr-2(gf)* primarily up-regulates *flp-18* expression in the cholinergic B-type motor neurons.

Elevated *flp-18* expression correlates with the onset of convulsions and is likely induced by neuronal activity

To further correlate the *acr-2(gf)*-dependent up-regulation of *flp-18* expression, we examined the developmental onset of *Pflp-18::flp-18::SL2::gfp* expression with respect to the onset of convulsions. We have shown earlier that the onset of convulsions in *acr-2(gf)* mutants occurs in mid-larval stage (Jospin, et al., 2009). We found that in *acr-2(gf)* mutants the expression of the *flp-18* reporter also increased sharply in mid-larval stages (Figure 3.10A). The close temporal correlation between the onset of *acr-2(gf)* convulsions and that of *flp-18* up-regulation in cholinergic motor neurons is consistent with *flp-18* up-regulation being caused by increased cholinergic activity. Supporting this idea, we observed increased expression of *Pflp-18::flp-18::SL2::gfp* in wild type animals acutely treated with aldicarb (Figure 3.11). In

contrast, the expression of *Pflp-18::flp-18::SL2::gfp* in *acr-2(gf)* animals was decreased when the animals were grown on plates with the acetylcholine receptor antagonist mecamylamine (Figure 3.11), which as previously reported (Jospin, et al., 2009) suppresses the convulsion behavior.

As FLP-18 functions together with FLP-1 to reduce *acr-2(gf)* convulsions (Figure 3.2D, 3.3A), we hypothesized that the induced expression of *flp-18* could be a homeostatic response to the elevated cholinergic neuronal activity in *acr-2(gf)*. If so, overexpression of *flp-18(+)* or *flp-1(+)* should ameliorate the extent of convulsions. Indeed, overexpressing *flp-18* under the control of its endogenous promoter caused a significant suppression of convulsions (Figure 3.10B). Overexpression of *flp-1,* driven by a pan-neuronal promoter, also resulted in a similar suppression of convulsions (Figure 3.10B). Together, these observations support the conclusion that in the *acr-2(gf)* background where excitation and inhibition balance is impaired, increased expression of *flp-18,* and possibly of *flp-1*, acts as a homeostatic response to dampen imbalanced circuit activity.

npr-1 and _npr-5_ appear to be the major receptors mediating the suppression of convulsions by FLP-1 and FLP-18

Neuropeptides generally act through G-protein coupled receptors (GPCRs). Next we sought to identify which GPCRs are involved in the regulation of convulsions by the *flp* neuropeptides. The CKR-2 receptor can be activated by FLP-1 at high concentration, and is also shown to act as a high-affinity receptor for NLP-12 (Hu, et al., 2011; Janssen et al., 2008). We found that *ckr-2(lf)* or *ckr-2(lf); flp-18(lf)* had no effects on *acr-2(gf)* (Figure 3.12), consistent with the observation that *nlp-12(lf)* did not affect *acr-2(gf)* either alone or in combination with *flp-18* (Figure 2D). Three receptors NPR-1, NPR-4 and NPR-5 can be activated by all six FLP-18 neuropeptides when expressed in *Xenopus* oocytes (Coates & de Bono, 2002; Cohen, et al., 2009; de Bono & Bargmann, 1998; Rogers et al., 2003). NPR-1 is expressed in the VD and

DD GABAergic motor neurons and in multiple head sensory neurons (Coates & de Bono, 2002). NPR-4 is expressed in the AVA, RIV, BDU and PQR neurons as well as in coelomocytes and the intestine (Cohen, et al., 2009). NPR-5 expression is found in amphid and phasmid neurons, interneurons AIA and AUA, as well as in the muscles (Cohen, et al., 2009). We found that loss of function mutation of individual *npr* genes neither suppressed nor enhanced *acr-2(gf)* (Figure 3.13A). We then made selected double mutant combinations among *npr-1, npr-4,* and *npr-5*. Eliminating both *npr-1* and *npr-5* in *acr-2(gf)* largely re-capitulated the effects of *flp-1(lf); flp-18(lf)*, while *npr-4(lf)* showed detectable effects only when both *npr-5* and *flp-1* were eliminated (Figure 3.13B). To further test the roles of these *npr* genes, we examined the suppression effects of *acr-2(gf)* by the overexpression of *flp-18*. We found that the suppression of convulsion by overexpression of *flp-18* were reduced by *npr-1(lf); npr-5(lf)* or *npr-4(lf); npr-5(lf)* double mutation, but not by single mutants of *npr-1(lf)* or *npr-5(lf)* (Figure 3.10B). Based on these observations, we conclude that NPR-1 and NPR-5 likely play a major role in mediating the modulatory action of FLP-18 in *acr-2(gf),* while NPR-4 has a minor role. Interestingly, similar *npr* receptor combination had no effects on the suppression of convulsion by overexpression of *flp-1* (Figure 3.10B). It is possible that this reflects non-physiological effects caused by overexpression of *flp-1* under a pan-neuronal promoter. Alternatively, FLP-1 and FLP-18 are acting through distinct pathways. Supporting the latter idea, we observed a slight but significant difference in aldicarb sensitivity between *npr-5(lf); npr-1(lf) acr-2(gf)* and *flp-1(lf); npr-5(lf); npr-1(lf) acr-2(gf)* (Figure 3.14). Nonetheless, this difference did not result in significant changes in the convulsion frequency of *flp-1(lf); npr-5(lf); npr-1(lf) acr-2(gf)* from that of *npr-5(lf); npr-1(lf) acr-2(gf)* (Figure 3.13A, B).

We next addressed the cell types in which *npr-1* or *npr-5* may act. We found that expression of *npr-5* in muscles by the *Pmyo-3* promoter reduced the convulsion frequency of *npr-5(lf); npr-1(lf) acr-2(gf)* animals to a similar degree as did *npr-5* expression under its endogenous promoter (Figure 3.13C). We also expressed *npr-1* in the GABAergic motor neurons

by the *Punc-25* promoter, and did not detect any significant effect on the convulsion frequency of *npr-5(lf); npr-1(lf) acr-2(gf)*. Overall, our analysis supports a conclusion that NPR-5 acts in the muscle, while NPR-1 expressed in other neurons such as sensory head neurons may be contributing to the locomotor circuit activity in an indirect manner.

Discussion

In this study we have identified two neuropeptide-encoding genes, *flp-1* and *flp-18* that act in a homeostatic manner to dampen the effects of the excitation-inhibition balance of the locomotor circuit caused by the *acr-2(gf)* mutation. The role of *flp-1* and *flp-18* in suppressing overexcitation of the locomotor circuit is dependent on neuropeptide processing by *egl-3* in the cholinergic motor neurons. We provide electrophysiological evidence that this neuropeptide modulation primarily acts on the GABAergic neural transmission at the neuromuscular junctions. Our previous studies have shown that *acr-2(gf)* elevates the activity of the cholinergic motor neurons (Jospin, et al., 2009). Here, we find that *acr-2(gf)* causes up-regulation of *flp-18* expression in the cholinergic motor neurons, and that over-expression of *flp-18* or *flp-1* is able to suppress *acr-2(gf)*. Our analyses of known *flp* neuropeptide receptors suggest that *npr-1* and *npr-5* play a major role in mediating the *flp-18's* function. We show that *npr-5* primarily acts in the muscles. Yet, the combinatorial effects of these receptors on the excitation-inhibition imbalance caused by *acr-2(gf)* likely involve multiple cell types.

The production of mature neuropeptides generally requires sequential enzymatic reactions starting with proprotein convertases followed by carboxypeptidases (Li & Kim, 2008). Neuropeptide mass spectrometry studies indicate that the majority of mature neuropeptides in *C. elegans* require EGL-3/PC2, its chaperone SBT-1, and EGL-21/CPE (Li & Kim, 2008). Previous studies have shown that *egl-3* and *egl-21* generally exhibit similar behavioral defects, although they differ in severities (Jacob & Kaplan, 2003; Kass, et al., 2001). Here we find that loss of function in *egl-3* and *sbt-1*, but not in *egl-21,* enhances the convulsion frequency of *acr-2(gf)*

animals. Proteomic analyses show that several mature peptides of FLP-18 are present in *egl-21* mutants (Husson, et al., 2007). We find that *egl-21(lf); flp-18(lf) acr-2(gf)* triple mutants show an increased convulsion frequency similar to *flp-1(lf); flp-18(lf) acr-2(gf)*. These data provide an explanation for the lack of effect on the *acr-2(gf)* convulsion frequency by the *egl-21* mutation, and also imply the involvement of other carboxypeptidases besides EGL-21 in mature neuropeptide production. Once mature peptides are processed in the dense core vesicles, the release of peptides requires UNC-31/CAPS. Intriguingly, we observed a suppression of *acr-2(gf)* convulsions by *unc-31(lf),* an opposite effect from that of *egl-3(lf)*. However, *egl-3* is necessary for processing primarily NLP and FLP neuropeptides (Husson, et al., 2006; Jacob & Kaplan, 2003), while *unc-31* is required for release of all neuropeptides including INS-like peptides and may also affect fast neurotransmitter release. We find that loss of both *flp-1* and *flp-18* mimicked the effects of *egl-3(lf)*. Importantly, the effects of *egl-3(lf)* are dependent on *unc-31(lf).* These data support a conclusion that EGL-3 is responsible for processing *flp-1* and *flp-18* peptides, which are released via dense core vesicles and in turn act to modulate locomotion circuit in an inhibitory manner. We interpret that the suppression of convulsions of *acr-2(gf)* by *unc-31(lf)* implies the involvement of additional unidentified neuropeptides that may play excitatory roles in modulate locomotion.

Previous studies on *flp-18* have focused on the functions of FLP-18 released from the head interneurons (Cohen, et al., 2009). *flp-18(lf)* mutants show defects in fat accumulation and foraging behavior, and the defects can be rescued by *flp-18* expression in the AIY or RIG neurons (Cohen, et al., 2009). The role of FLP-18 neuropeptides in the locomotor circuit is unknown. In wild type animals, *flp-18* expression, visualized using a reporter that expresses FLP-18 and GFP under the endogenous *flp-18* promoter, is generally low in the cholinergic motor neurons (Cohen, et al., 2009) (Figure 3.7A). We find that the transcriptional expression of *flp-18* is specifically up-regulated in the cholinergic motor neurons at the onset of convulsions induced by *acr-2(gf)* and upon acute upregulation of cholinergic activity by aldicarb treatment.

This result suggests that up-regulation of *flp-18* is a homeostatic response to the overexcitation caused by *acr-2(gf).* We were not able to determine whether *flp-1* expression might be similarly regulated, due to inconsistent expression pattern of different transgenic reporter lines (our unpublished data, and C. Li, personal communication). It is interesting to note that strong up-regulation of *flp-18* is consistently observed in the B type motor neurons, which drive forward locomotion (Chalfie et al., 1985; Wicks, Roehrig, & Rankin, 1996). We have recently found that the AVB neurons, which provide major synaptic input to the B type neurons through gap junctions, are necessary for the onset of convulsions in *acr-2(gf)* (Qi, Garren, Shu, Tsien, & Jin, 2012). Together, these observations support that the AVB-B neuron pathway plays a major role in the excitation-inhibition balance of the locomotor network.

Our analysis of the NPR-1, NPR-4 and NPR-5 receptors, which are known to be activated by FLP-18 (Cohen, et al., 2009; Rogers, et al., 2003), indicates that NPR-1 and NPR-5 have a major, while NPR-4 has a minor, role in mediating the effect of FLP-18 on modulating the convulsion behavior caused by *acr-2(gf)*. These receptors are expressed in multiple cell types. Our data show that muscle-specific expression of NPR-5 can rescue the increased convulsions, suggesting that the FLP-18 neuropeptides can act directly on muscles to inhibit contraction, or to promote relaxation. We previously showed that GABAergic transmission is reduced at the neuromuscular junctions in *acr-2(gf)* animals (Jospin, et al., 2009). Our neuromuscular physiology analysis here shows that the neuropeptide modulation by *flp-1* and *flp-18* primarily acts on GABAergic transmission. Of the three *npr* genes, *npr-1* is expressed in the GABAergic motor neurons (Cohen, et al., 2009; Rogers, et al., 2003). However, our data does not support a direct involvement of *npr-1* in the context of *acr-2(gf)*. *flp-1* is reported to be expressed primarily in the head neurons including AIA, AIY, AVA, AVE, AVK, RIG, RMG, M5 (Nelson, et al., 1998). The effects of *flp-1(lf)* on convulsions appear to be independent of CKR-2, presently the only known receptor for FLP-1 (Figure 3.12).

Interestingly, *npr-1(lf); npr-5(lf)* double mutants cause enhanced convulsions of

acr-2(gf), similar to *flp-1(lf); flp-18(lf)* double mutants, and do not show further enhancement in *flp-1(lf)* background. However, double loss of function in *npr-1* and *npr-5* has little effects on the suppression of convulsions by *flp-1(+)* overexpression under a pan-neuronal promoter. It is possible that *flp-1(+)* overexpression activates other inhibitory pathways that do not require *npr-1* and *npr-5*. NPR-1 and NPR-5 may also be activated by neuropeptides other than FLP-1 or FLP-18, since *npr-5(lf); npr-1(lf) acr-2(gf)* triple mutants show a more severe phenotype than *flp-18(lf); acr-2(gf)* double mutants. As the effect of *flp-1* and *flp-18* double loss of function is milder than the loss of *egl-3* (Figure 3.3), other neuropeptides are likely being involved in inhibiting convulsions. Our method of measurement may not be sensitive enough to detect the effect of losing *flp-1* to further enhance the increased convulsion frequency caused by the *npr-5(lf); npr-1(lf)* double mutants. Enhanced sensitivity to aldicarb of the *flp-1(lf); npr-5(lf); npr-1(lf) acr-2(gf)* animals supports this notion (Figure 3.14). The modest effects of these receptors make it difficult to determine the precise contribution of their signaling in the context of convulsive behavior of *acr-2(gf).* Identification of additional GPCRs that respond to FLP-1 will be necessary for fully understanding the peptidergic transmission pathway that modulates *acr-2(gf)* convulsions. Overall, our results are consistent with a model in which these neuropeptides act on multiple cell types, one of which is body wall muscle, to coordinate the activity state of the locomotion circuit.

The molecular nature and the physiological basis of *C. elegans acr-2(gf)* mutants share similarities with mutations causing epileptic seizures including an imbalance between excitation and inhibition of the nervous system. Examples of neuropeptides acting to inhibit altered neuronal circuit activity, such as in seizures, have also been observed in vertebrates. For example, the neuropeptide galanin has been shown to play a key role in epilepsy (Lerner, et al., 2008; Lundström, Elmquist, Bartfai, & Langel, 2005). Galanin agonists inhibit seizures (Lerner, et al., 2008), and expression of galanin is increased in the mouse brain upon the induction of seizures (Christiansen & Woldbye, 2010). A model for the role of galanin in epilepsy has been proposed

in that increased excitation increases galanin levels in an attempt to normalize the excitation and inhibition balance by reducing glutamatergic transmission (Mitsukawa, et al., 2008). Likewise, our studies have revealed that activity-dependent expression of neuropeptides provides a homeostatic mechanism to modulate neuronal network balance. Together, these findings provide support for manipulations of slow neuropeptide signaling in controlling neuronal circuit activity disruption underlying neurological disorders.

Materials & Methods

Genetics and alleles

All *C. elegans* strains were grown on NGM plates at room temperature (20-22°C) following standard methods. Deletion mutant strains were backcrossed two times against N2 before being used for strain construction. All double mutants were constructed using standard procedures, and genotypes were confirmed by PCR verification of the deletions. Table 3.1 lists the information on the alleles and strains. Specific alleles used in the figures are: *acr-2(gf)* indicates *acr-2(n2420), unc-31(e928)*, *egl-3(n589), egl-3(ok979), egl-3(nr2090), sbt-1(ok901), egl-21(n611), egl-21(n476), egl-21(tm5578), cpd-2(ok3147), flp-1(yn4), flp-9(ok2730), flp-11(tm2706), flp-13(tm2427), flp-18(tm2179), flp-20(ok2964), flp-21(ok889) ,nlp-3(tm3023), nlp-7(tm2984), nlp-9(tm3572), nlp-12(ok335), nlp-14(tm1880), nlp-15(ok1512), ins-3(ok2488), ins-4(ok3534), ins-11(tm1053), ins-18(ok3444), ins-22(ok3616), ins-27(ok2474)*, *ins-28(ok2722), ins-30(ok2343), ins-35(ok3297), npr-1(ok1447), npr-4(tm1782), npr-5(ok1583), ckr-2(tm3082), acr-2(ok1887).*

Molecular biology and transgenes

Molecular biology was performed according to standard methods (Sambrook, Fritsch, & Maniatis, 1989). Expression constructs were generated using Gateway recombination technology (Invitrogen, CA), and Table 3.2 lists the details of the DNA clones generated in this study. An

unc-31 cDNA pDONR construct was provided by Dr. Kaveh Ashrafi (Lee & Ashrafi, 2008), *Punc-17β::unc-31* was provided by Dr. Ken Miller (Charlie, et al., 2006), *Pglr-1::egl-3* , *Pacr-2::egl-3* and *Punc-25::npr-1* were provided by Dr. Josh Kaplan ((Kass, et al., 2001) and personal communication), and *Pflp-18::flp-18::SL2::gfp* and *Pnpr-5::npr-5* were provided by Dr. Merav Cohen and Dr. Mario de Bono (Cohen, et al., 2009).

Quantification of convulsion behavior

Ten to twenty L4 larvae were placed on freshly seeded NGM plates. The following day, young adults were transferred to fresh plates and recorded by video for 90 seconds, five frames per second. Eight animals were recorded for each genotype per trial and at least two trials were performed per genotype. Videos were scored by an observer blind to genotype. A “convulsion” was defined as a visible shortening in the animal’s body length.

Pharmacology analysis

L4 animals were picked the day before an experiment. The day of the experiment ten young adults per genotype were placed on plates containing 150 μM aldicarb, and the effects on animal movement were observed at 30 minute intervals. Animals were scored as paralyzed when no body movements were observed, even in response to touch.

FLP-18 imaging

Confocal images were taken on a Zeiss LSM 510 with 1 μm per section, and processed using ImageJ. Maximum projection images were created from confocal stacks and the average intensity was measured of the ventral cord posterior to the vulva. For cell body counting, L4 animals were picked the day before an experiment, and young adults were observed using a Zeiss Axioplan 2 fluorescence microscope the following day. The number of cell bodies of the ventral nerve cord with visible GFP fluorescence was counted. For identification of the cells

expressing *Pflp-18::flp-18::SL2::gfp* cell bodies with GFP and mCherry fluorescence were observed and counted. For the observation in different stages of animals, animals were synchronized at L1 stage and observed under Zeiss Axioplan 2 Fluorescence microscope at each developmental stage.

Electrophysiology

NMJ dissection methods were adapted from previous studies (Stawicki, et al., 2011). In brief, adult worms were immobilized on Sylgard-coated cover slips with cyanoacrylate glue. A dorsolateral incision was made with a sharp glass pipette and the cuticle flap was folded back and glued down to expose the ventral medial body wall muscles. The preparation was then treated by collagenase type IV (Sigma-Aldrich) for ~ 30 s at a concentration of 0.4 mg/ml. The bath solution contained (in mM): 127 NaCl, 5 KCl, 26 $NaHCO_3$, 1.25 NaH_2PO_4, 2 $CaCl_2$, 4 $MgCl_2$, 10 glucose, and sucrose to 340 mOsm, bubbled with 5% CO_2, 95% O_2 at 20ºC. The pipette solution containing (in mM): 120 CH_3O_3SCs, 4 CsCl, 15 CsF, 4 $MgCl_2$, 5 EGTA, 0.25 $CaCl_2$, 10 HEPES and 4 Na_2ATP, adjusted to pH 7.2 with CsOH. Conventional whole-cell recordings from muscle cells were performed at 20°C with 2-3 MΩ pipettes. An EPC-10 patch-clamp amplifier was used together with the Patchmaster software package (HEKA Electronics, Lambrecht, Germany). Endogenous acetylcholine postsynaptic currents were recorded at -60 mV and GABA postsynaptic currents were recorded at 0 mV. The current traces were imported to IGOR Pro (WaveMetrics, Lake Oswego, OR) for further analysis.

Acknowledgements

This chapter is a reprint in full of Stawicki T.M., Takayanagi-Kiya S., Zhou K.,and Jin, Y. Neuropeptides Function in a Homeostatic Manner to Modulate Excitation-Inhibition Imbalance in *C. elegans*. PloS Genet. with permission of all authors. The disseration author was one of the two primary authors of this paper.

We would like to thank the following people for reagents: Ken Miller and Kaveh Ashrafi for *unc-31* rescue strains and DNA constructs; Josh Kaplan for *egl-3* and *npr-1* DNA constructs, as well as *egl-21* and *egl-3* mutant strains; Mario de Bono and Merav Cohen for *flp-18* and *npr-5* strains and DNA constructs; Yingchuan B. Qi for ventral cord neuron transgenic lines. Additional strains were obtained from the Japan National BioResource Project (NBRP) and the *Caenorhabditis* Genetics Center (CGC), the latter is supported by grants from the NIH. We thank A. D. Chisholm, S. Cherra for comments on the manuscript and our lab members for discussions.

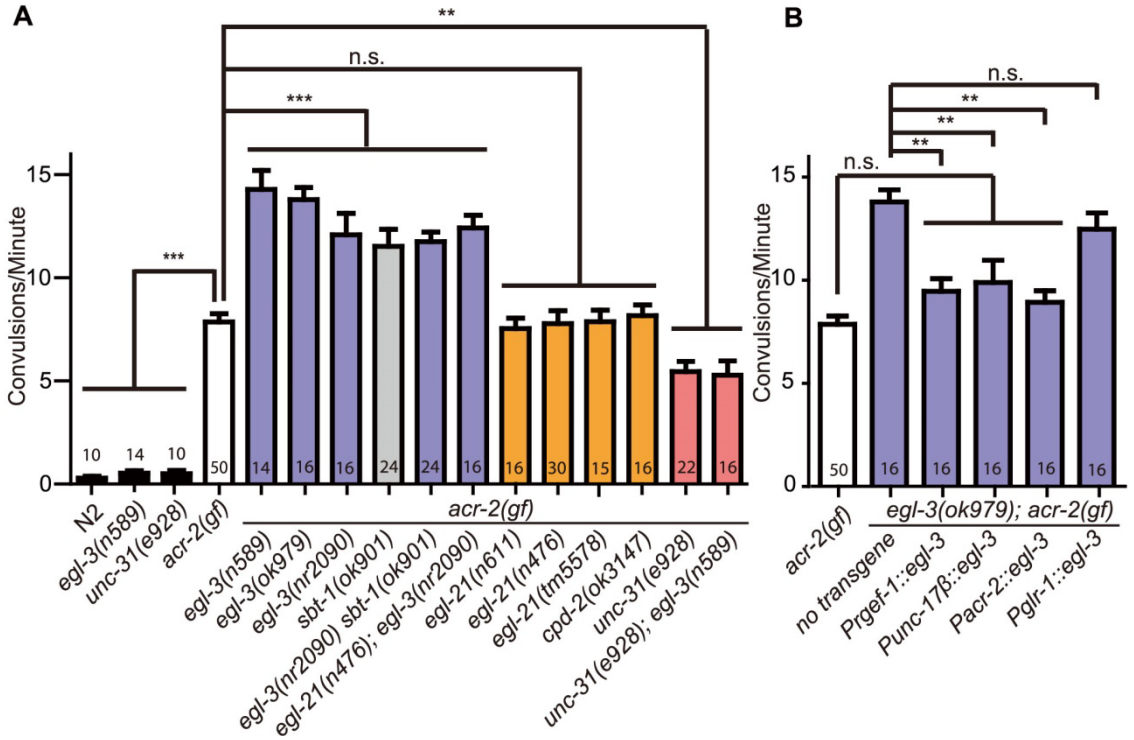

Figure 3.1. Neuropeptide processing and release pathway regulate *acr-2(gf)* convulsions. All mutations are loss of function alleles, except for *acr-2(gf),* which designates *acr-2(n2420).* Mean convulsion frequencies are shown. Error bars indicate SEM. Numbers in the graph indicate sample sizes. Statistics: ***: $p < 0.001$, **: $p < 0.01$, *: $p < 0.05$ by ANOVA and Bonferroni post hoc test. (A) Loss of function in *egl-3* and *sbt-1* significantly enhances *acr-2(gf)* convulsions; and the increased convulsion caused by egl-3(lf) is dependent on *unc-31.* (B) *egl-3* functions in the cholinergic motor neurons to suppress *acr-2(gf)* convulsions. The number of independent transgenic lines tested are the following: *Prgef-1::egl-3*; 4 lines, *Punc-17β::egl-3*; 3 lines, *Pglr-1::egl*-3; 3 lines, *Pacr-2*; 2 lines. Quantification data is shown for one representative line.

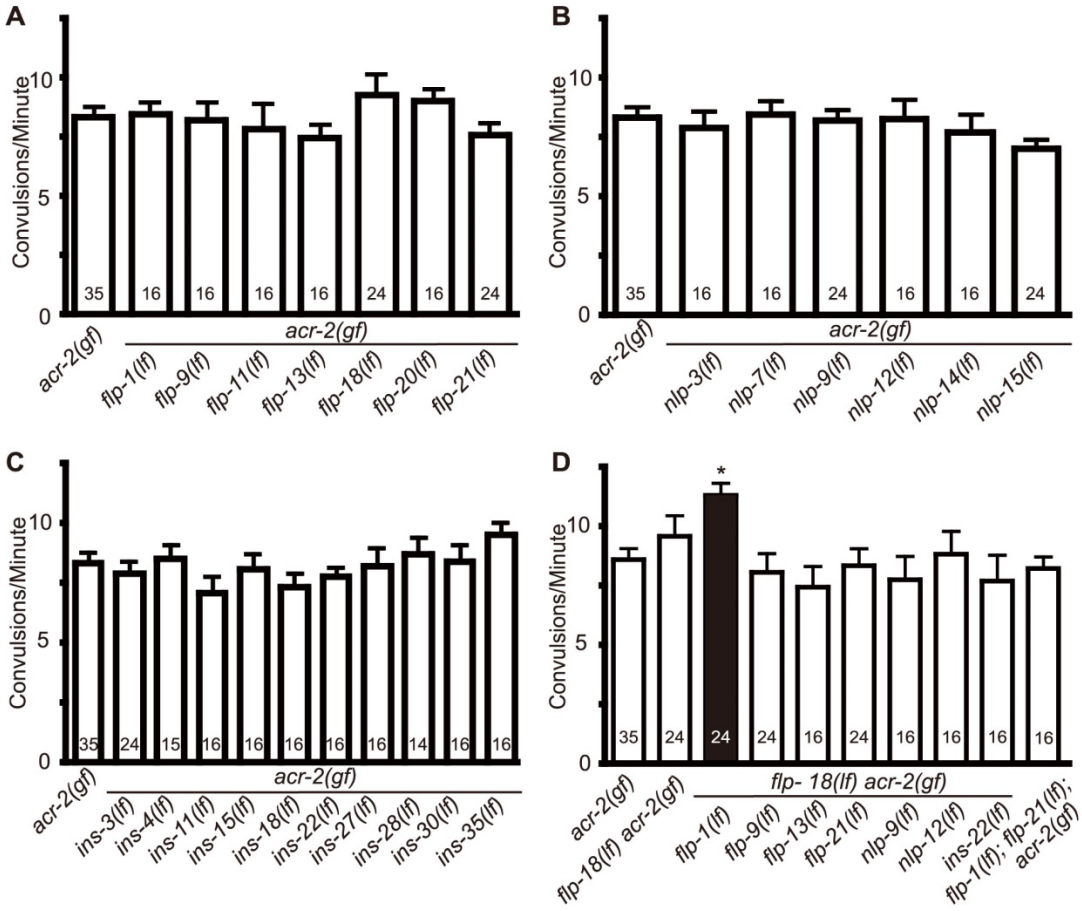

Figure 3.2. Loss of both *flp-1* and *flp-18* enhances *acr-2(gf)* convulsions. Null mutants of candidate neuropeptide genes were tested for effects on *acr-2(gf)* convulsions. *flp-18(lf)* indicates *flp-18(tm2179)*; the allele number for other genes are listed in materials and methods. No significant effects were observed for selected FMRF-amide (*flp)* (A), neuropeptide like proteins (*nls)* (B), or insulins (*ins)* (C). (D) Double mutants of candidate peptide genes with *flp-18*. Loss of both *flp-1* and *flp-18* leads to a significant enhancement of acr-2(gf) convulsions. Numbers in the graph indicate sample sizes. Mean convulsion frequencies are shown. Error bars indicate SEM. Statistics: *: $p < 0.05$ by ANOVA and Dunnett's post hoc test.

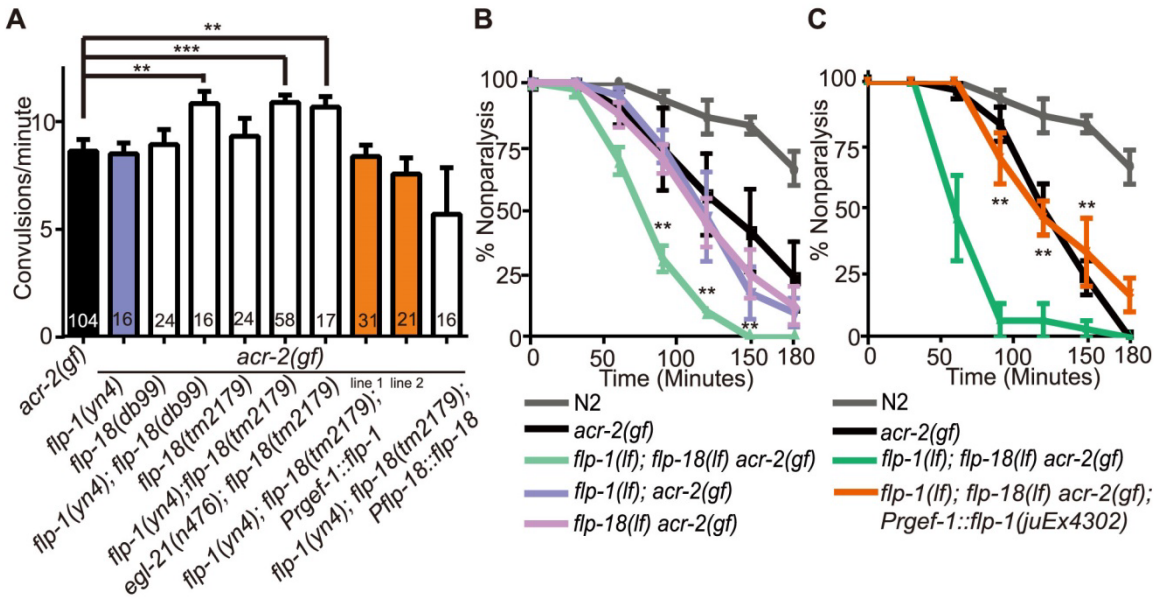

Figure 3.3. *flp-1* and *flp-18* act as inhibitory neuropeptides in the *acr-2(gf)* background. (A) Convulsion frequency of *acr-2(gf)* in combination with loss of function (lf) mutations in *flp-1(yn4)*, *flp-18(tm2179),* or *flp-18(db99)*. The enhanced convulsion frequency of *flp-1(lf); flp-18(lf) acr-2(gf)* animals is rescued with transgenic expression of *flp-1* under the pan-neuronal promoter *Prgef-1* or expression of *flp-18* under *flp-18* promoter. Two independent transgenic lines were tested as indicated by line 1 and 2. Mean convulsion frequencies are shown. Error bars indicate SEM. Numbers in the graph indicate sample sizes. Statistics: ***: $p < 0.001$, **: $p < 0.01$ by ANOVA and Dunnett's post-hoc test. (B, C) Rate of paralysis on 150 µM aldicarb plates in *acr-2(gf)* background. *flp-1(lf); flp-18(lf)* mutants in the *acr-2(gf)* background showed enhanced aldicarb sensitivity compared to *acr-2(gf)* (B). Pan-neuronal expression of *flp-1* rescues the increased aldicarb sensitivity of the *flp-1(lf); flp-18(lf) acr-2(gf)* mutants (C). n=10 for one group per trial; and results of three to five independent trials are shown. Mean rate of paralysis are shown for each time point. Error bars indicate SEM. Two independent transgenic lines were tested, only one is shown in the graph. Statistics in B, C: **: $p < 0.01$, *: $p < 0.05$ by two-way ANOVA and Bonferroni post-hoc test.

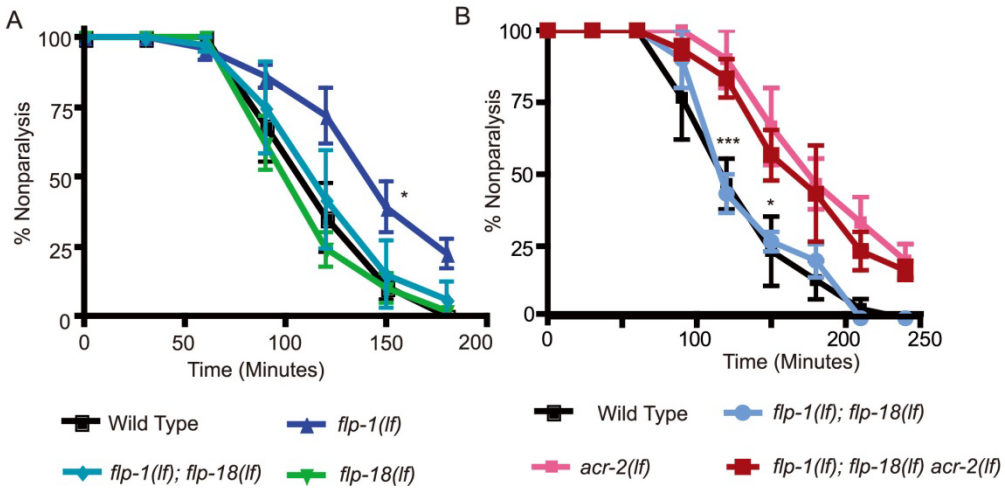

Figure 3.4. Aldicarb sensitivity of *flp-1* and *flp-18* mutants. (A) in wild type and (B) in *acr-2(lf)* background. Animals were placed on an NGM plate with 1mM (A) or 500µM (B) aldicarb and non-paralyzed worms were counted every 30 minutes. (A) *flp-1(lf)* show aldicarb resistance. (B) Loss of *flp-1* and *flp-18* does not significantly affect the aldicarb sensitivity in wild type or *acr-2(lf)* background. Statistics show the comparison of *flp-1(lf); flp-18(lf)* vs *flp-1(lf); flp-18(lf) acr-2(lf)*. ***: $p < 0.001$, **: $p < 0.01$, *: $p < 0.05$ by two-way ANOVA and Bonferroni post-hoc test.

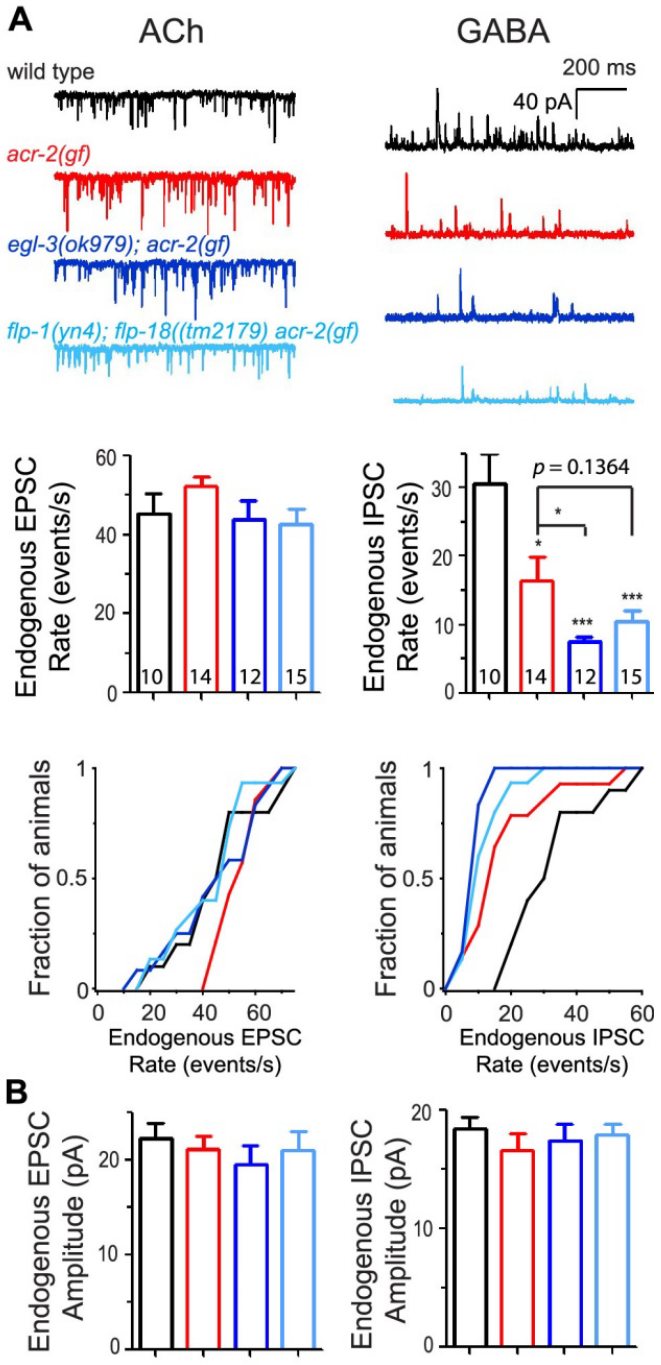

Figure 3.5. Neuropeptide modulation primarily affects GABAergic neuromuscular transmission. (A) Shown are the electrophysiology recording data on the neuromuscular junctions. Top panels are representative traces of genotypes indicated. Middle panels are mean rates of endogenous EPSCs and IPSCs; and bottom panels are cumulative fractions of the animal number with endogenous EPSC rate or IPSC rate less than indicated values in X-axis of genotype indicated. (B) Mean amplitudes of endogenous EPSCs and IPSCs from genotypes shown in A. The number of animals analyzed is indicated for each genotype. Error bars indicate SEM. Statistics, two-tailed t-test, ***, $p < 0.001$; *, $p < 0.05$.

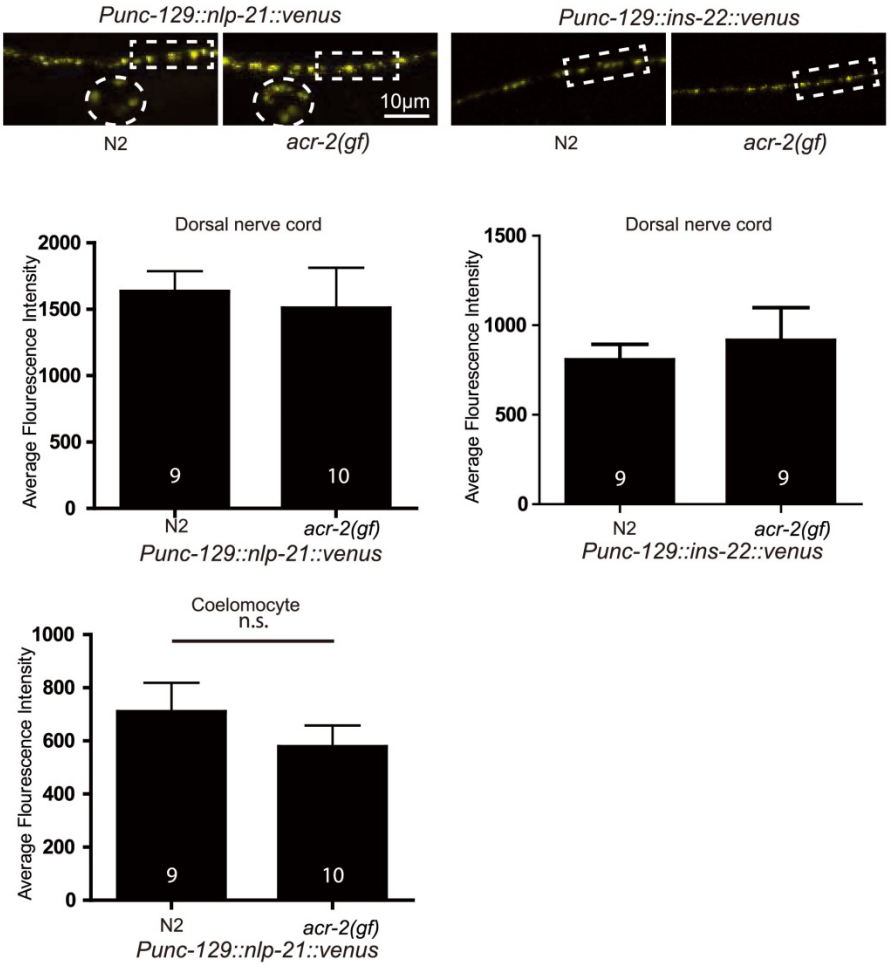

Figure 3.6. Expression of *nlp-21* and *ins-22* is not affected by *acr-2(gf)*. L4 stage animals of *Punc-129::NLP-21::venus* and *Punc-129::INS-22::venus* were subjected to confocal imaging. (Top) Images from *Punc-129::NLP-21::venus* and *Punc-129::INS-22::venus* animals. Dorsal nerve cord near the bend of the gonad was imaged. NLP-21::venus was observed in coelomocyte and in the dorsal nerve cord (DNC). INS::22-venus was observed mainly in the DNC. (Middle, bottom) The fluorescence intensity was measured using ImageJ from three fluorescent patches in the coelomocyte, and the average was used for statistics. Fluorescence intensity of DNC was also examined using ImageJ. The *NLP-21::venus* expression pattern or fluorescence intensity is not affected by *acr-2(gf)*. Dashed circle indicate the position of coelomocytes. Dashed rectangles indicate the DNC region used for the measurement. Student's t-test was performed to compare fluorescence intensities. Error bars indicate SEM. Numbers in the graph indicate sample sizes.

Figure 3.7. FLP-18 expression is selectively increased in the cholinergic motor neurons in the *acr-2(gf)* background. (A-B) Ventral nerve cord expression of *Pflp-18::flp-18::SL2::gfp* in wild type (N2) and *acr-2(gf)* background, respectively. Increased fluorescence intensity and cell body expression is seen in the ventral cord in the *acr-2(gf)* background. Arrows point to the ventral nerve cord posterior to the vulva, and arrowheads point to cell bodies. Scale bar = 25 μm. Two *Pflp-18::flp-18::SL2::gfp* transgenic lines, *juEx4062* and *juEx4073,* were tested. Images from *juEx4073* are shown. (C) Quantification of average fluorescence intensity in the ventral nerve cord posterior to the vulva. Mean fluorescence intensities are shown. N=37 (wild type), =38 (*acr-2(gf)).* ***: p <0.001 by student's t-test. Error bars indicate SEM. (D) Quantification of the number of cell bodies in the ventral cord with visible GFP expression. ***: $p < 0.001$, **: $p < 0.01$ by Student's t-test. Each dot indicates quantification from one animal. Means are indicated by lines. Error bars indicate SEM. Two transgenic lines were tested. (E-H) Identification of the cells showing up-regulation of *Pflp-18::flp-18::SL2::gfp* in the *acr-2(gf)* background. (E) Co-expressing mCherry in GABAergic (*Pttr-39)* motor neurons did not show overlap with *Pflp-18::flp-18::SL2::gfp*. (F) Expression of mCherry in B-type (*Pacr-5)* cholinergic motor neurons overlapped extensively with *Pflp-18::flp-18:SL2::gfp* expression. (G) mCherry expression in A-type (*Punc-4)* cholinergic motor neurons mostly did not overlap with *Pflp-18::flp-18::SL2::gfp* expression. (H) Quantification of the number of cell bodies that showed overlapping expression of *Pflp-18::flp-18::SL2::gfp* and *Pacr-5::mCherry* or *Punc-4::mCherry* in F-G. Each dot indicates quantification from one animal. Means are indicated by lines. Error bars indicate SEM.

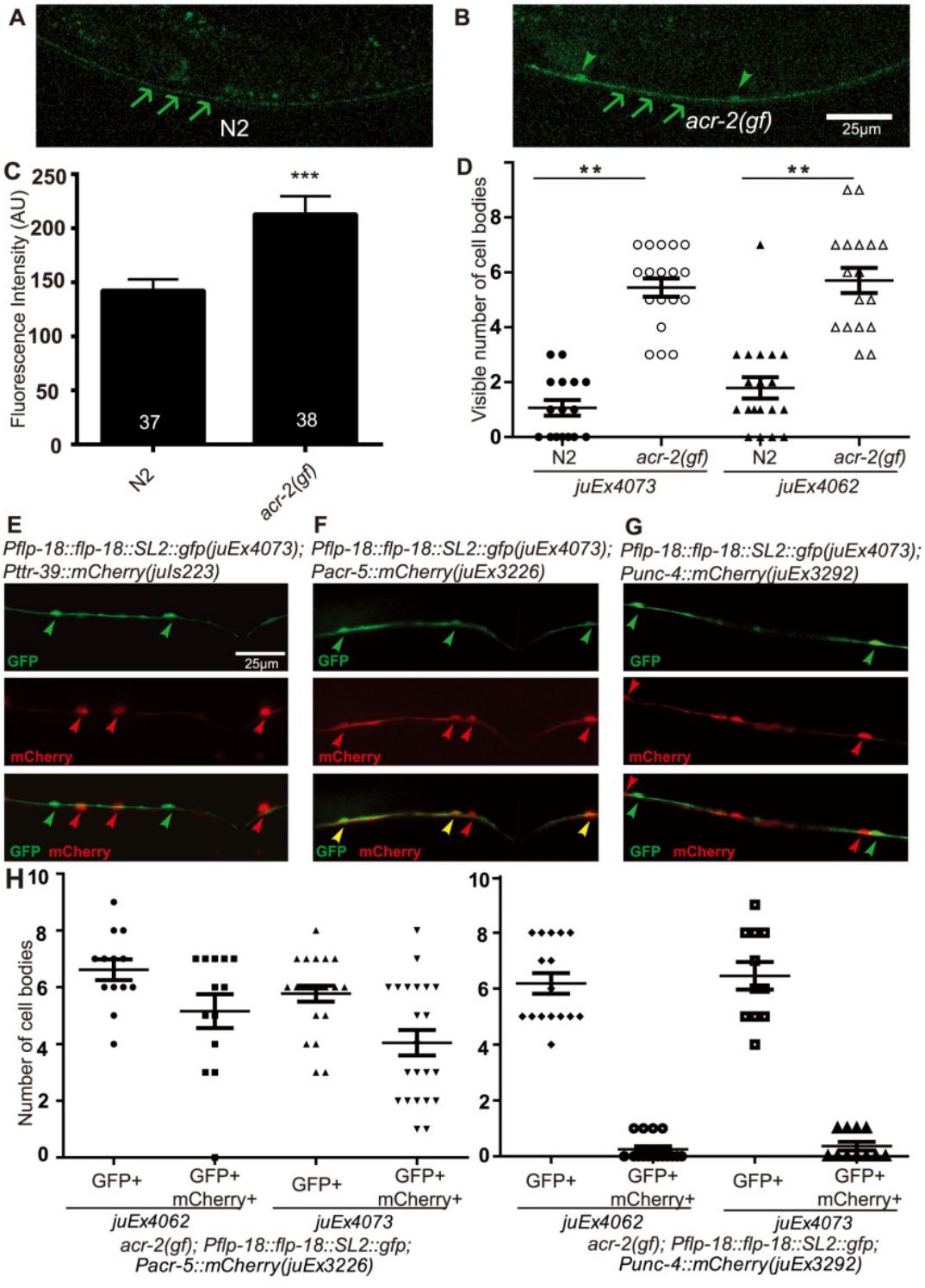
A
N2
B
acr-2(gf)
25µm
C
Fluorescence Intensity (AU)
250
200
150
100
50
0
***
37
38
N2
acr-2(gf)
D
Visible number of cell bodies
**
**
N2
acr-2(gf)
N2
acr-2(gf)
juEx4073
juEx4062
E
Pflp-18::flp-18::SL2::gfp(juEx4073);
Pttr-39::mCherry(juIs223)
GFP
25µm
mCherry
GFP mCherry
F
Pflp-18::flp-18::SL2::gfp(juEx4073);
Pacr-5::mCherry(juEx3226)
GFP
mCherry
GFP mCherry
G
Pflp-18::flp-18::SL2::gfp(juEx4073);
Punc-4::mCherry(juEx3292)
GFP
mCherry
GFP mCherry
H
Number of cell bodies
GFP+
GFP+ mCherry+
GFP+
GFP+ mCherry+
juEx4062
juEx4073
acr-2(gf); Pflp-18::flp-18::SL2::gfp;
Pacr-5::mCherry(juEx3226)
GFP+
GFP+ mCherry+
GFP+
GFP+ mCherry+
juEx4062
juEx4073
acr-2(gf); Pflp-18::flp-18::SL2::gfp;
Punc-4::mCherry(juEx3292)

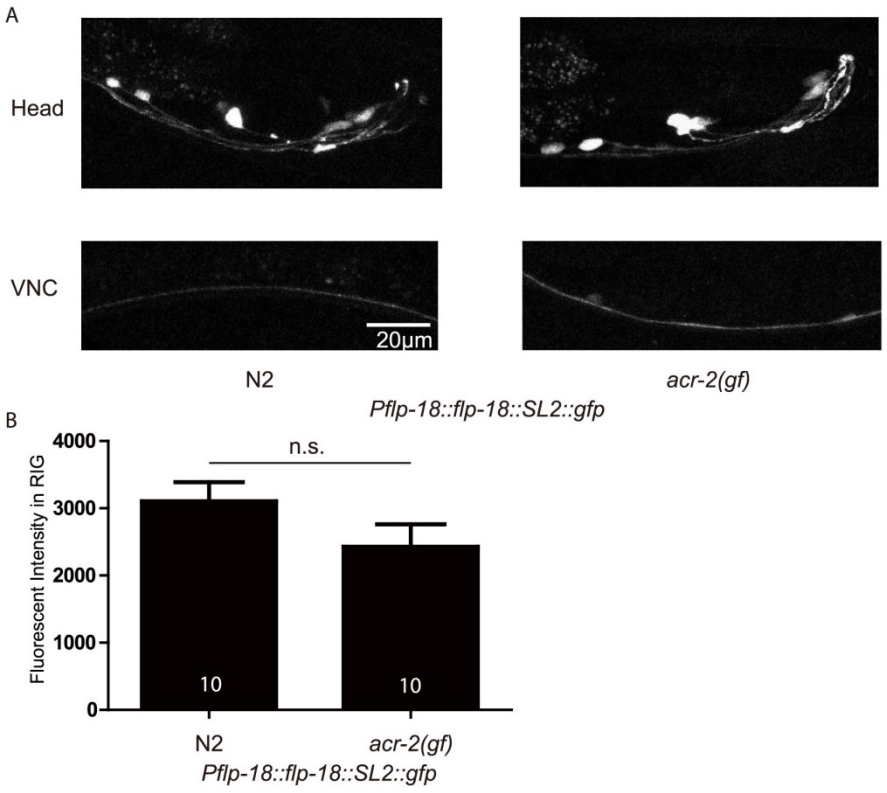

Figure 3.8. Head neuron expression of *Pflp-18::flp-18::SL2::gfp* is not different between wild type and in *acr-2(gf)*. (A) Representative confocal images of the head neurons (top) and the ventral nerve cord (bottom) in L4 animals. (B) Fluorescence intensity in a head neuron RIG is not different between wild type and *acr-2(gf)* animals. Intensity was quantified using ImageJ. Average of fluorescence intensity of the two cell bodies of RIG neuron was taken from each animal. Dashed circle in images indicates the region with two cell bodies of RIG. Numbers in the graph indicate sample sizes. Two transgenic lines (*juEx4062* and *juEx4073*) were examined and no difference was observed between the two. Results from *juEx4073* are shown.

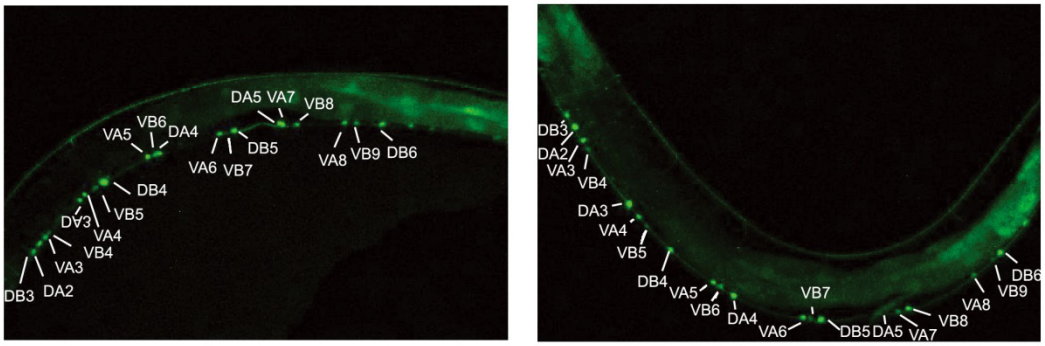

Figure 3.9. Expression pattern of *Punc-17β::gfp.* Images of *Punc-17β::gfp* expression in the wild type (left) and *acr-2(gf)* (right) genetic background. Expression is only seen in the A and B type motor neurons.

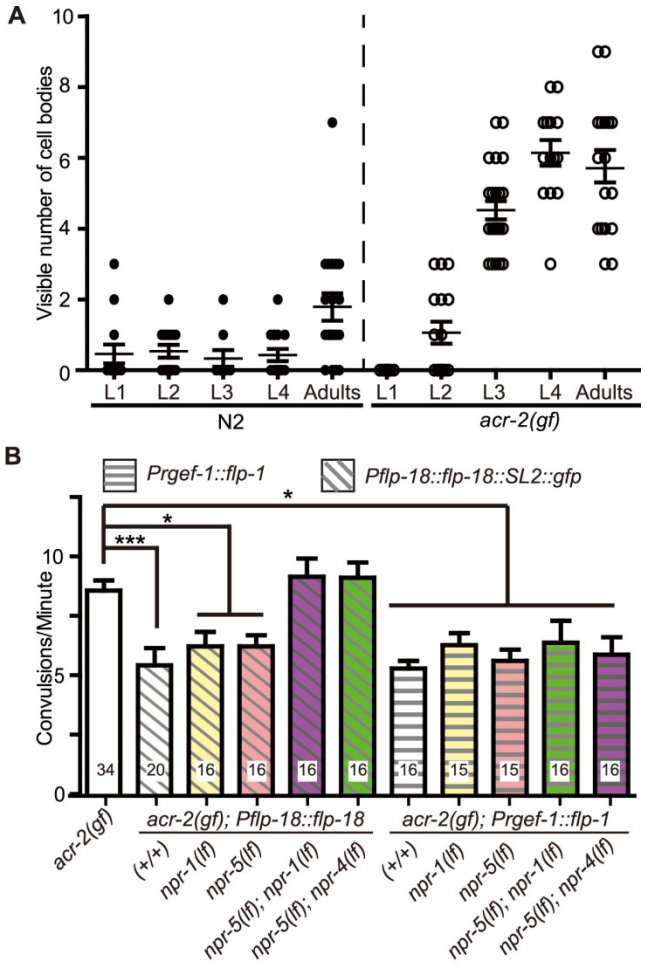

Figure 3.10. Induced expression of FLP-18 in *acr-2(gf)* correlates with the onset of convulsions, and high levels of FLP-18 or FLP-1 suppress convulsions. (A) Quantification of the number of cell bodies in the ventral cord that showed *Pflp-18::flp-18::SL2::gfp* expression in larval and adult stages. Each dot indicates quantification from one animal. Means are indicated by lines. Error bars indicate SEM. Two independent lines *juEx4062* and *juEx4073* were tested. Result from *juEx4073* is shown. (B) Convulsion of *acr-2(gf)* was suppressed by expression of *Pflp-18::flp-18::SL2::gfp* or pan-neuronal expression of *flp-1*. The suppression by *flp-18* overexpression was blocked by loss of both *npr-1* and *npr-5*, or *npr-4* and *npr-5*. The same set of *npr* mutations did not affect the suppression effect of *flp-1* overexpression. Mean convulsion frequencies are shown. Error bars indicate SEM. Statistics: ***: $p < 0.001$, *: $p < 0.05$ by ANOVA and Dunnett's post-hoc test. *(+/+)* indicates strains with no mutations in any of the neuropeptide receptor genes.

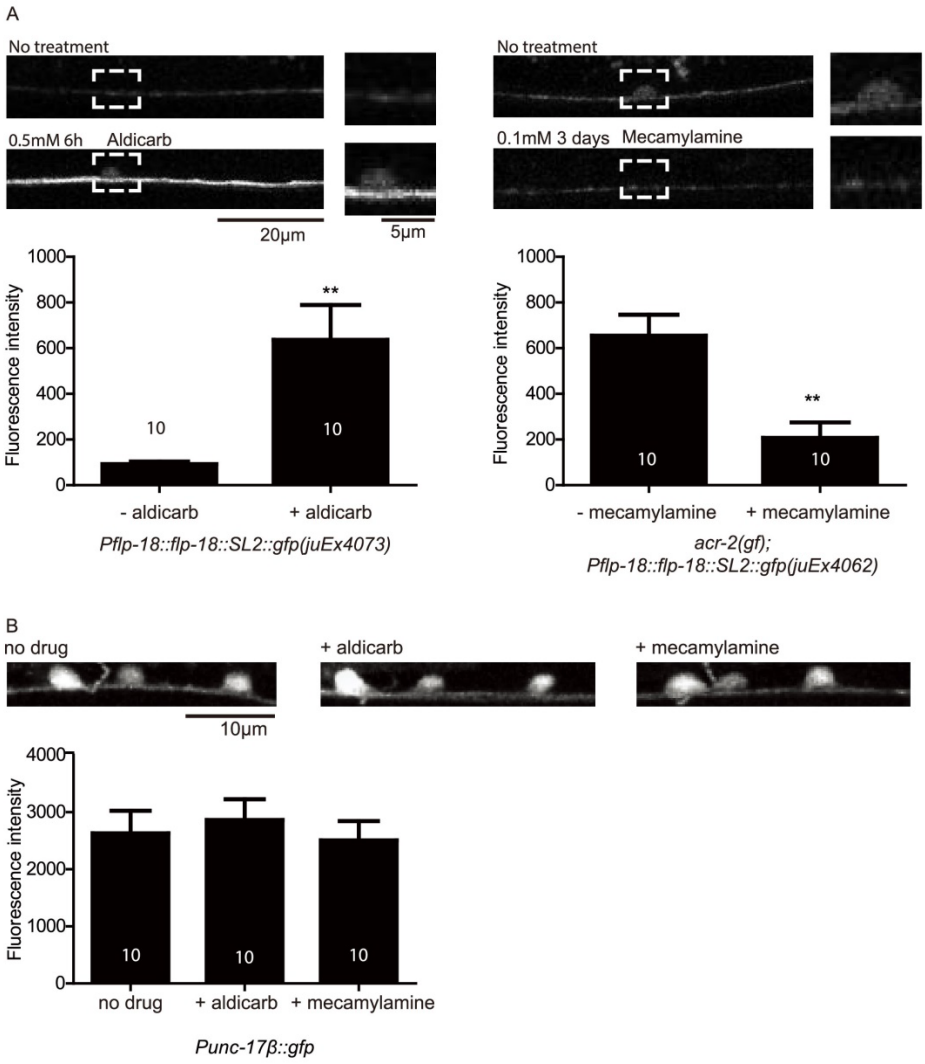

Figure 3.11. Expression of *flp-18* by aldicarb and mecamylamine treatment. (A) *Pflp-18::flp-18::SL2::gfp* expression in the ventral nerve cord is increased by aldicarb and decreased by mecamylamine treatment. (top) Representative images of the ventral nerve cord with and without the drug treatment. White boxes indicate the region of cell body and the enlarged images of the region are shown on right of each image. (bottom) Quantification of GFP fluorescence intensity in cell body. Two transgenic lines (*juEx4062* and *juEx4073*) were examined. Results from *juEx4073* are shown. (B) Expression level of *Punc-17β::gfp* was not affected by drug treatments. GFP fluorescence intensity in cell body was quantified using ImageJ.

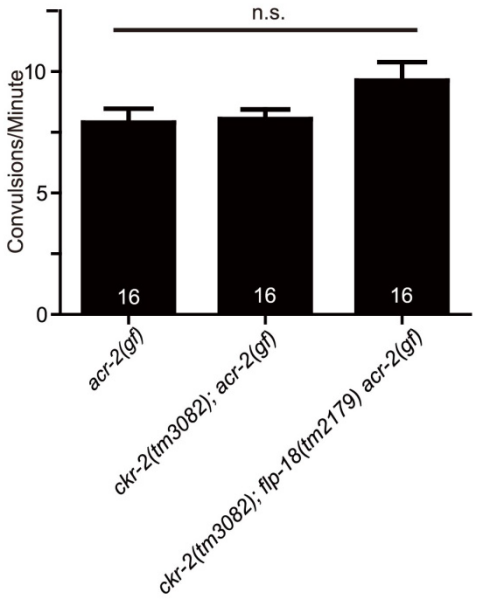

Figure 3.12. *ckr-2* does not affect *acr-2(gf)* convulsions. Loss of *ckr-2* or *ckr-2* in combination with *flp-18* does not affect the convulsion frequency of *acr-2(gf).* Quantification method is the same as in others.

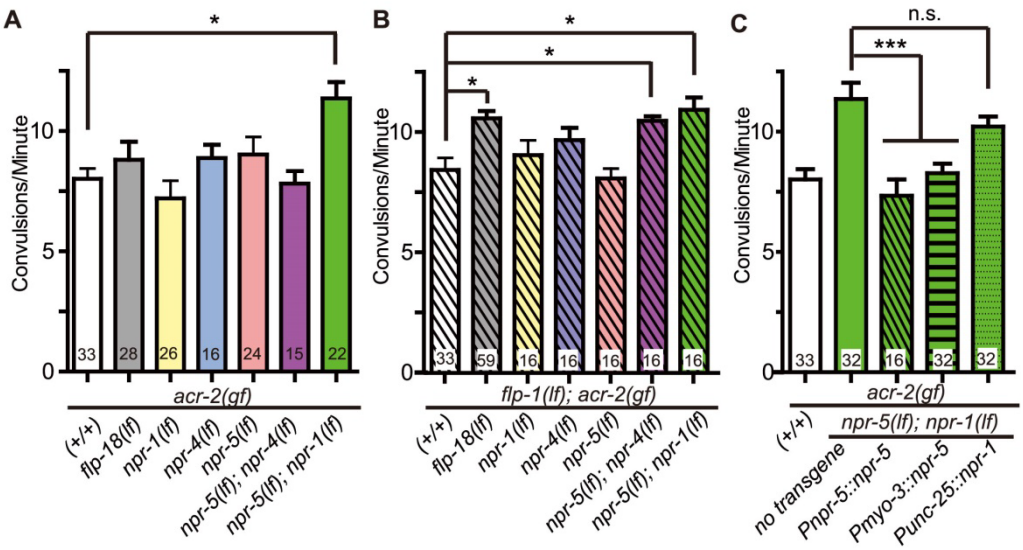

Figure 3.13. NPR-1, NPR-4, NPR-5 act together to mediate the effects of neuropeptides on convulsions. (A-B). Convulsion frequencies of *acr-2(gf)* combined with loss of function mutations in *npr-1(ok1447), npr-4(tm1782), npr-5(ok1583)* (A) and with *flp-1(yn4)* (B). (C) Convulsion frequency of animals with cell type-specific expression of *npr-1* and *npr-5*. *npr-5* expression in the muscle rescued the increased convulsion frequency of *npr-5(lf); npr-1(lf) acr-2(gf)* triple mutant; two independent lines were tested. *npr-1* expression in GABAergic motor neurons did not significantly rescue the increased convulsion frequency; three lines were tested. All strains contain *acr-2(gf)*. Mean convulsion frequencies are shown. Error bars indicate SEM. Statistics: ***: $p < 0.001$, *: $p < 0.05$ by ANOVA and Bonferroni post hoc test. *(+/+)* indicates strain with no mutations in any of the neuropeptide receptor genes.

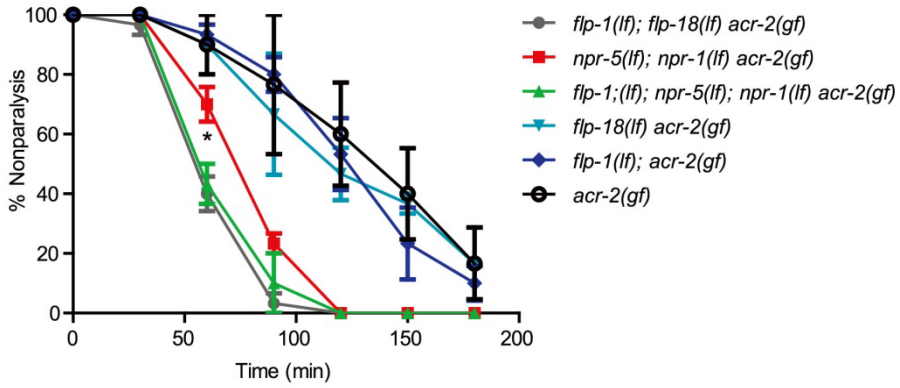

Figure 3.14. Loss of *flp-1* causes increased aldicarb sensitivity in *npr-5: npr-1 acr-2(gf)* background. Animals were placed on an NGM plate with 150μM aldicarb and non-paralyzed worms were counted every 30 minutes. Loss of *flp-1* enhances aldicarb sensitivity of *npr-5; npr-1 acr-2(gf)*. Statistics show the comparison of *flp-1(lf); npr-5(lf); npr-1(lf) acr-2(gf)* vs *npr-5(lf); npr-1(lf) acr-2(gf)*. *: $p < 0.05$ by two-way ANOVA and Bonferroni post-hoc test.

Table 3.1 List of strains and transgenes used in the study.

Strain Number	Genotype	Allele or Transgene Information (reference)
CZ10402	*acr-2(n2420)X*	*n2420:* g925a Val309Met (Jospin, et al., 2009)
CB928	*unc-31(e928)IV*	*e928*: 5.2kb deletion (Livingstone, 1991)
MT6651	*unc-31(e928)IV; acr-2(n2420)X*	
CZ10347	*unc-31(e928)IV; acr-2(n2420)X; Prgef-1::unc-31 (juEx2246)*	*Pregf-1::unc-31cDNA (pCZGY870)* - 35 ng/µl, *Pttx-3::rfp* – 75 ng/µl
CZ10841	*unc-31(e928)IV; acr-2(n2420)X; Punc-17β::unc-31 (juEx2374)*	*Punc-17β:unc-31cDNA (KG126)* - 35 ng/µl *(Charlie, et al., 2006),Pttx-3:rfp* - 75 ng/µl
CZ10302	*unc-31(e928)IV; acr-2(n2420)X; Punc-25::unc-31 (juEx2244)*	*Punc-25::unc-31cDNA (pCZGY868)* – 35 ng/µl, *Pttx-3::rfp* – 75 ng/µl
CZ10791	*unc-31(e928)IV; acr-2(n2420)X; Pnmr-1::unc-31 (juEx2353)*	*Pnmr-1::unc-31cDNA (pCZGY904)* – 35 ng/µl, *Pttx-3::rfp* – 75 ng/µl
CZ11285	*acr-2(n2420)X;Punc-17β:unc-31 (juEx2374)*	
CZ10637	*egl-21(n476)IV; acr-2(n2420)X*	*n476:* 123 bp deletion (Jacob & Kaplan, 2003)
CZ10879	*egl-3(nr2090)V; acr-2(n2420)X*	*nr2090:* 1188 bp deletion (Kass, et al., 2001)
CZ11984	*egl-21(n476)IV; egl-3(nr2090)V; acr-2(n2420)*	
CZ11376	*sbt-1(ok901)V; acr-2(n2420)X*	*ok901:* 1382 bp deletion (Husson & Schoofs, 2007)
CZ10346	*unc-31(e928)IV; egl-3(n589)V; acr-2(n2420)X*	*n589:* G1487a Cys496Tyr (Kass, et al., 2001)
CZ9315	*egl-3(n589)V; acr-2(n2420)X*	
CZ10677	*egl-3(ok979)V; acr-2(n2420)X*	*ok979:* 1579 bp deletion
CZ11977	*egl-3(ok979)V; acr-2(n2420)X; Prgef-1::egl-3(juEx2720)*	*Prgef-1:egl-3 (pCZGY1076)* 20 ng/µl, *Pttx-3::rfp* – 75 ng/µl

Table 3.1. List of strains and transgenes used in the study. (continued)

Strain Number	Genotype	Allele or Transgene Information (reference)
CZ11854	*egl-3(ok979)V; acr-2(n2420)X; Pglr-1::egl-3(juEx2668)*	*Pglr-1:egl-3 (KP509)* – 20 ng/µl (Kass, et al., 2001), *Pttx-3:rfp* – 75 ng/µl
CZ12111	*egl-3(ok979)V; acr-2(n2420)X; Punc-17β::egl-3(juEx2774)*	*Punc-17β::egl-3 (pCZGY1097)* – 20 ng/µl, *Pttx-3:rfp* – 75 ng/µl
CZ11750	*egl-3(ok979)V; acr-2(n2420)X; Pacr-2::egl-3(juEx2640)*	*Pacr-2::egl-3 (KP677)* – 20 ng/µl (Jacob & Kaplan, 2003), *Pttx-3::rfp* – 75 ng/µl
CZ9315	*egl-3(n589)V; acr-2(n2420)X*	
CZ10354	*egl-21(n611)IV; acr-2(n2420)X*	*n611:* g1071a, Trp357Stop
CZ9524	*flp-1(yn4)IV; acr-2(n2420)X*	*yn4:* 2.1kb deletion (Nelson, et al., 1998)
CZ10144	*flp-9(ok2730)IV; acr-2(n2420)X*	*ok2730:* 432 bp deletion + 19 bp insertion
CZ10973	*flp-11(tm2706)X acr-2(n2420)X*	*tm2706:* 154 bp deletion
CZ10927	*flp-13(tm2427)IV; acr-2(n2420)X*	*tm2427:* 380 bp deletion
CZ10676	*flp-18(tm2179)X acr-2(n2420)X*	*tm2179:* 1286 bp deletion
CZ10429	*acr-2(n2420)X flp-20(ok2964)X*	*ok2964:* about 300 bp deletion
CZ11479	*flp-21(ok889)V; acr-2(n2420)X*	*ok889:* 1786 bp deletion
CZ12583	*acr-2(n2420)X nlp-3(tm3023)X*	*tm3023:* 354 bp deletion
CZ14323	*acr-2(n2420)X nlp-7(tm2984)X*	*tm2984:* 1758 bp deletion
CZ12171	*nlp-9(tm3572)V; acr-2(n2420)X*	*tm3572:* 110 bp deletion
CZ10040	*nlp-12(ok335)IV; acr-2(n2420)X*	*ok335:* 1070 bp deletion
CZ12610	*acr-2(n2420)X nlp-14(tm1880)X*	*tm1880:* 661 bp deletion + 12 bp
CZ12286	*nlp-15(ok1512)I; acr-2(n2420)X*	*ok1512:* 889 bp deletion
CZ10948	*ins-3(ok2488)II; acr-2(n2420)X*	*ok2488:* 1449 bp deletion
CZ10857	*ins-4(ok3534)II; acr-2(n2420)X*	*ok3534:* about 400bp deletion
CZ10877	*ins-11(tm1053)II; acr-2(n2420)X*	*tm1053:* 341 bp deletion
CZ11427	*ins-15(ok3444)II; acr-2(n2420)X*	*ok3444:* about 600bp deletion
CZ10774	*ins-18(ok1672)I; acr-2(n2420)X*	*ok1672*: 940 bp

Table 3.1. List of strains and transgenes used in the study. (continued)

Strain Number	Genotype	Allele or Transgene Information (reference)
CZ11414	*ins-22(ok3616)III; acr-2(n2420)X*	*ok3616:* about 700 bp deletion
CZ11768	*ins-27(ok2474)I; acr-2(n2420)X*	*ok2474:* 461 bp deletion
CZ11480	*ins-28(ok2722)I; acr-2(n2420)X*	*ok2722:* 584 bp deletion
CZ11481	*ins-30(ok2343)I; acr-2(n2420)X*	*ok2343:* 1078 bp deletion
CZ11325	*ins-35(ok3297)V; acr-2(n2420)X*	*ok3297:* about 600 bp deletion
CZ11341	*flp-1(yn4)IV; flp-18(tm2179)X acr-2(n2420)X*	
CZ14895	*flp-9(ok2730)IV; flp-18(tm2179)X acr-2(n2420)X*	
CZ14936	*flp-13(tm2427)IV; flp-18(tm2179)X acr-2(n2420)X*	
CZ14915	*flp-21(ok889)V; flp-18(tm2179) acr-2(n2420)X*	
CZ15084	*nlp-9(tm3572)V;flp-18(tm2179) acr-2(n2420)X*	
CZ14680	*nlp-12(ok335)IV; flp-18(tm2179) acr-2(n2420)X*	
CZ14682	*ins-22(ok3616)III; flp-18(tm2179) acr-2(n2420)X*	
CZ14934	*flp-18(db99)X acr-2(n2420)*	*db99:* 2016 bp deletion (Cohen, et al., 2009)
CZ15458	*flp-1(yn4)IV; flp-18(db99)X acr-2(n2420)X*	
NY16	*flp-1(yn4)IV*	
CZ10206	*flp-18(tm2179)X*	
CZ12078	*flp-1(yn4)IV; flp-18(tm2179)X*	
CZ15048	*Pflp-18::flp-18::SL2::gfp (juEx4073)*	*Pflp-18::flp-18::SL2::gfp* – 5 ng/µl (Cohen, et al., 2009), *Pttx-3::rfp* – 75 ng/µl
CZ15032	*Pflp-18::flp-18::SL2::gfp(juEx4062)*	*Pflp-18::flp-18::SL2::gfp* – 5 ng/µl (Cohen, et al., 2009), *Pttx-3::rfp* – 75 ng/µl

Table 3.1. List of strains and transgenes used in the study. (continued)

Strain Number	Genotype	Allele or Transgene Information (reference)
CZ15032	*Pflp-18::flp-18::SL2::gfp(juEx4062)*	*Pflp-18::flp-18::SL2::gfp* – 5 ng/µl (Cohen, et al., 2009), *Pttx-3::rfp* – 75 ng/µl
CZ15164	*acr-2(n2420)X; Pflp-18::flp-18::SL2::gfp (juEx4073)*	
CZ15859	*acr-2(n2420)X; Pflp-18::flp-18::SL2::gfp (juEx4062)*	*Pflp-18::flp-18::SL2::gfp* – 5 ng/µl (Cohen, et al., 2009), *Pttx-3::rfp* – 75 ng/µl
CZ15509	*flp-1(yn4)IV; flp-18(tm2179) acr-2(n2420)X;Pregf-1::flp-1 (juEx4302)*	*Prgef-1::flp-1(pCZGY1692)* -5ng/µl, *Pnmr-1::mCherry*-20ng/µl
CZ15510	*flp-1(yn4)IV; flp-18(tm2179) acr-2(n2420)X;Prgef-1:flp-1 (juEx4303)*	*Prgef-1::flp-1(pCZGY1692)*-5ng/µl, *Pnmr-1::mCherry* - 20ng/µl
CZ16375	*acr-2(n2420)X; Pflp-18:flp-18-SL2-gfp(juEx4073); Pacr-5:mCherry (juEx3226)*	*Pacr-5::mCherry* – 20ng/µl, *Pttx-3::gfp* - 50ng/µl
CZ16377	*acr-2(n2420)X; Pflp-18:flp-18::SL2::gfp(juEx4073); Punc-4:mCherry (juEx3292)*	*Punc-4::mCherry* – 20ng/µl, *Pttx3::gfp* – 50ng/µl
CZ16473	*acr-2(n2420)X; Pttr-39::mCherry(juIs223); Pflp-18::flp-18::SL2-gfp(juEx4073)*	
CZ16466	*egl-3(nr2090)V sbt-1(ok901)V; acr-2(n2420)X*	
CZ10432	*npr-1(ok1447)X acr-2(n2420)X*	*ok1447:* 1263bp deletion
CZ15107	*flp-1(yn4)IV; npr-1(ok1447)X acr-2(n2420)X*	
CZ9713	*npr-5(ok1583)V; acr-2(n2420)X*	*ok1583:* 784bp deletion
CZ14381	*flp-1(yn4)IV; npr-5(ok1583)V; acr-2(n2420)X*	
CZ15511	*acr-2(n2420)X npr-4(tm1782)X*	*tm1782:* 1226bp deletion

Table 3.1. List of strains and transgenes used in the study. (continued)

CZ16964	*flp-1(yn4)IV; acr-2(n2420)X npr-4(tm1782)X*	
CZ17281	*npr-5(ok1583)V; acr-2(n2420)X npr-4(tm1782)X*	
CZ17437	*npr-5(ok1583); npr-1(ok1447)X acr-2(n2420)X*	
CZ17438	*egl-21(tm5578)IV; acr-2(n2420)*	*tm5578:* 839bp deletion
CZ17439	*flp-1(yn4)IV; npr-5(ok1583)V; acr-2(n2420)X npr-4(tm1782)X*	
CZ17215	*egl-21(n476)IV; flp-18(tm2179)X acr-2(n2420)X*	
CZ17214	*acr-2(n2420)X; Pflp-18::flp-18::SL2:gfp*	
AX1444	*Pflp-18:flp-18::SL2::gfp (dbIs1)*	(Cohen, et al., 2009)
CZ18094	*npr-5(ok1583)V; acr-2(n2420)X; Pflp-18::flp-18::SL2::gfp(dbIs1)*	
CZ18095	*npr-1(ok1447)X acr-2(n2420)X; Pflp-18::flp-18::SL2::gfp(dbIs1)*	
CZ18096	*npr-5(ok1583)V; acr-2(n2420)X npr-4(tm1782)X; Pflp-18::flp-18::SL2::gfp(dbIs1)*	
CZ18097	*npr-5(ok1583)V; npr-1(ok1447)X acr-2(n2420)X; Pflp-18::flp-18::SL2::gfp(dbIs1)*	
CZ18098	*flp-1(yn4)IV; flp-18(tm2179)X acr-2(n2420)X; Pflp-18::flp-18::SL2::gfp(dbIs1)*	
CZ18099	*npr-1(ok1447)X acr-2(n2420)X; Prgef-1::flp-1(juEx4303)*	
CZ18100	*npr-5(ok1583)V; npr-1(ok1447)X acr-2(n2420)X; Prgef-1::flp-1(juEx4303)*	
CZ18156	*npr-5(ok1583)V; acr-2(n2420)X npr-4(tm1782)X; Prgef-1::flp-1(juEx4303)*	
CZ18157	*npr-5(ok1583)V; acr-2(n2420)X; Prgef-1::flp-1(juEx4303)*	

Table 3.1. List of strains and transgenes used in the study. (continued)

CZ18304	*npr-5(ok1583)V; npr-1(ok1447)X acr-2(n2420)X; Punc-25::npr-1(juEx5423)*	*Punc-25::npr-1::gfp(KP1856)* – 60ng/µl, *Pmec4::rfp* – 100ng/µl
CZ18305	*npr-5(ok1583)V; npr-1(ok1447)X acr-2(n2420)X; Punc-25::npr-1(juEx5424)*	*Punc-25::npr-1::gfp(KP1856)* – 60ng/µl, *Pmec4::rfp* – 100ng/µl
CZ18306	*npr-5(ok1583)V; npr-1(ok1447)X acr-2(n2420)X; Punc-25::npr-1(juEx5425)*	*Punc-25::npr-1::gfp(KP1856)* – 60ng/µl, *Pmec4::rfp* – 100ng/µl
CZ18303	*npr-5(ok1583)V; npr-1(ok1447)X acr-2(n2420)X; Pnpr-5::npr-5(dbEx2)*	*Pnpr-5::npr-5* (Cohen, et al., 2009)
CZ18313	*npr-5(ok1583)V; npr-1(ok1447)X acr-2(n2420)X; Pmyo-3::npr-5(juEx5468)*	*Pmyo-3::npr-5 (PCZGY2197)* –50ng/µl, *Pmec4::rfp* – 65ng/µl
CZ18314	*npr-5(ok1583)V; npr-1(ok1447)X acr-2(n2420)X; Pmyo-3::npr-5(juEx5469)*	*Pmyo-3::npr-5 (PCZGY2197)* –50ng/µl, *Pmec4::rfp* – 65ng/µ
CZ18183	*ckr-2(tm3082)III; acr-2(n2420)X*	*tm3082*: 569 bp deletion
CZ18184	*ckr-2(tm3082)III; flp-18(tm2179)X acr-2(n2420)X*	
CZ12117	*Punc-17β::gfp(juEx2777)*	*Punc-17β::gfp(PCZGY1098)*
CZ17400	*acr-2(n2420)X; Punc-17β::gfp(juEx2777)*	
CZ18559	*flp-1(yn4)IV;npr-5(ok1588)V;npr-1(ok1447)X acr-2(n2420)X*	
CZ9677	*acr-2(ok1887)X*	ok1887: 2857 bp deletion and 420 bp insertion(Jospin, et al., 2009)
CZ18101	*flp-1(yn4(IV);flp-18(tm2179)X acr-2(ok1887)X*	
CZ9267	*Punc-129::nlp-21::venus(nuIs183)*	(Sieburth, et al., 2007)
CZ9317	*acr-2(n2420)X; Punc-129::nlp-21::venus(nuIs183)*	
CZ9266	*Punc-129::ins-22::venus(nuIs195)*	(Sieburth, et al., 2005)
CZ9318	*acr-2(n2420)X; Punc-129::ins-22::venus(nuIs195)*	

Information on tm and ok alleles came from www.wormbase.org and www.cbs.umn.edu/CGC

Table 3.2. List of constructs used in the study.

Plasmid *	Promoter	Gene
Prgef-1::egl-3 (PCZGY1076)	3.5kb upstream of ATG of *rgef-1*[9]	4.0kb *egl-3* genomic DNA fragment amplified using the following primers :YJ7092 5'-atgaaaaacacacatgtcgacc-3' YJ7093 5'-ttagtggctgcgtttgtggg-3'
Prgef-1::unc-31 (PCZGY870)	3.5kb upstream of ATG of *rgef-1*[9]	*unc-31* cDNA[10]
Punc-25::unc-31 (PCZGY868)	1.3kb upstream of ATG of *unc*-25	*unc-31* cDNA[10]
Pnmr-1::unc-31 (PCZGY904)	1.1kb upstream of ATG of *nmr-1*	*unc-31* cDNA[10]
Punc-17β::egl-3 (PCZGY1097)	0.5kb upstream of ATG of *unc-17β*[3]	*egl-3* genomic DNA, same as *PCXGY1076*
Prgef-1::flp-1 (PCZGY1692)	3.5kb upstream of ATG of *rgef-1*[9]	1.3kb *flp-1* genomic DNA fragment amplified using the following primers: YJ8345 5'- atgactctgctctaccaagtagg-3' YJ8346 5'- ttattttccgaaacgaaggaaatttg-3'
Pmyo-3::npr-5 (PCZGY2197)	2.4kb upstream of ATG of *myo-3*[11]	*npr-5* cDNA[8]
Punc-17β::gfp (PCZGY1098)	0.5kb upstream of ATG of *unc-17β*[3]	GFP cDNA

* DNA constructs were generated using Gateway Cloning Technology (Invitrogen, CA).

References

Altun-Gultekin, Z., Andachi, Y., Tsalik, E. L., Pilgrim, D., Kohara, Y., & Hobert, O. (2001). A regulatory cascade of three homeobox genes, ceh-10, ttx-3 and ceh-23, controls cell fate specification of a defined interneuron class in *C. elegans*. *Development, 128*(11), 1951-1969.

Avery, L., Bargmann, C. I., & Horvitz, H. R. (1993). The *Caenorhabditis elegans* unc-31 gene affects multiple nervous system-controlled functions. *Genetics, 134*(2), 455-464.

Bargmann, C. I. (2012). Beyond the connectome: How neuromodulators shape neural circuits. *Bioessays*.

Blake, A. D., Badway, A. C., & Strowski, M. Z. (2004). Delineating somatostatin's neuronal actions. *Curr Drug Targets CNS Neurol Disord, 3*(2), 153-160.

Brockie, P. J., Madsen, D. M., Zheng, Y., Mellem, J., & Maricq, A. V. (2001). Differential expression of glutamate receptor subunits in the nervous system of *Caenorhabditis elegans* and their regulation by the homeodomain protein UNC-42. *J Neurosci, 21*(5), 1510-1522.

Chalasani, S. H., Kato, S., Albrecht, D. R., Nakagawa, T., Abbott, L. F., & Bargmann, C. I. (2010). Neuropeptide feedback modifies odor-evoked dynamics in *Caenorhabditis elegans* olfactory neurons. *Nat Neurosci, 13*(5), 615-621.

Chalfie, M., Sulston, J. E., White, J. G., Southgate, E., Thomson, J. N., & Brenner, S. (1985). The neural circuit for touch sensitivity in *Caenorhabditis elegans*. *J Neurosci, 5*(4), 956-964.

Charlie, N. K., Schade, M. A., Thomure, A. M., & Miller, K. G. (2006). Presynaptic UNC-31 (CAPS) is required to activate the G alpha(s) pathway of the *Caenorhabditis elegans* synaptic signaling network. *Genetics, 172*(2), 943-961.

Christiansen, S. H., & Woldbye, D. P. (2010). Regulation of the galanin system by repeated electroconvulsive seizures in mice. *J Neurosci Res, 88*(16), 3635-3643.

Coates, J. C., & de Bono, M. (2002). Antagonistic pathways in neurons exposed to body fluid regulate social feeding in *Caenorhabditis elegans*. *Nature, 419*(6910), 925-929.

Cohen, M., Reale, V., Olofsson, B., Knights, A., Evans, P., & de Bono, M. (2009). Coordinated regulation of foraging and metabolism in *C. elegans* by RFamide neuropeptide signaling. *Cell Metab, 9*(4), 375-385.

Davis, R. E., & Stretton, A. O. (1996). The motornervous system of Ascaris: electrophysiology and anatomy of the neurons and their control by neuromodulators. *Parasitology, 113 Suppl*, S97-117.

de Bono, M., & Bargmann, C. I. (1998). Natural variation in a neuropeptide Y receptor homolog modifies social behavior and food response in *C. elegans*. *Cell, 94*(5), 679-689.

Fetissov, S. O., Jacoby, A. S., Brumovsky, P. R., Shine, J., Iismaa, T. P., & Hökfelt, T. (2003). Altered hippocampal expression of neuropeptides in seizure-prone GALR1 knockout

mice. *Epilepsia, 44*(8), 1022-1033.

Fuller, R. S., Sterne, R. E., & Thorner, J. (1988). Enzymes required for yeast prohormone processing. *Annu Rev Physiol, 50*, 345-362.

Harris-Warrick, R. M., & Marder, E. (1991). Modulation of neural networks for behavior. *Annu Rev Neurosci, 14*, 39-57.

Hu, Z., Pym, E. C., Babu, K., Vashlishan Murray, A. B., & Kaplan, J. M. (2011). A neuropeptide-mediated stretch response links muscle contraction to changes in neurotransmitter release. *Neuron, 71*(1), 92-102.

Husson, S. J., Clynen, E., Baggerman, G., Janssen, T., & Schoofs, L. (2006). Defective processing of neuropeptide precursors in *Caenorhabditis elegans* lacking proprotein convertase 2 (KPC-2/EGL-3): mutant analysis by mass spectrometry. *J Neurochem, 98*(6), 1999-2012.

Husson, S. J., Janssen, T., Baggerman, G., Bogert, B., Kahn-Kirby, A. H., Ashrafi, K., & Schoofs, L. (2007). Impaired processing of FLP and NLP peptides in carboxypeptidase E (EGL-21)-deficient *Caenorhabditis elegans* as analyzed by mass spectrometry. *J Neurochem, 102*(1), 246-260.

Husson, S. J., & Schoofs, L. (2007). Altered neuropeptide profile of *Caenorhabditis elegans* lacking the chaperone protein 7B2 as analyzed by mass spectrometry. *FEBS Lett, 581*(22), 4288-4292.

Jacob, T. C., & Kaplan, J. M. (2003). The EGL-21 carboxypeptidase E facilitates acetylcholine release at *Caenorhabditis elegans* neuromuscular junctions. *J Neurosci, 23*(6), 2122-2130.

Janssen, T., Meelkop, E., Lindemans, M., Verstraelen, K., Husson, S. J., Temmerman, L., Nachman, R. J., & Schoofs, L. (2008). Discovery of a cholecystokinin-gastrin-like signaling system in nematodes. *Endocrinology, 149*(6), 2826-2839.

Jospin, M., Qi, Y. B., Stawicki, T. M., Boulin, T., Schuske, K. R., Horvitz, H. R., Bessereau, J. L, Jorgensen, E. M., & Jin, Y. (2009). A neuronal acetylcholine receptor regulates the balance of muscle excitation and inhibition in *Caenorhabditis elegans*. *PLoS Biol, 7*(12), e1000265.

Jung, L. J., & Scheller, R. H. (1991). Peptide processing and targeting in the neuronal secretory pathway. *Science, 251*(4999), 1330-1335.

Kass, J., Jacob, T. C., Kim, P., & Kaplan, J. M. (2001). The EGL-3 proprotein convertase regulates mechanosensory responses of *Caenorhabditis elegans*. *J Neurosci, 21*(23), 9265-9272.

Kow, L. M., & Pfaff, D. W. (1988). Neuromodulatory actions of peptides. *Annu Rev Pharmacol Toxicol, 28*, 163-188.

Krieger, D. T. (1983). Brain peptides: what, where, and why? *Science, 222*(4627), 975-985.

Lee, B. H., & Ashrafi, K. (2008). A TRPV channel modulates *C. elegans* neurosecretion, larval

starvation survival, and adult lifespan. *PLoS Genet, 4*(10), e1000213.

Leinwand, S. G., & Chalasani, S. H. (2011). Olfactory networks: from sensation to perception. *Curr Opin Genet Dev, 21*(6), 806-811.

Lerner, J. T., Sankar, R., & Mazarati, A. M. (2008). Galanin and epilepsy. *Cell Mol Life Sci, 65*(12), 1864-1871.

Li, C. (2005). The ever-expanding neuropeptide gene families in the nematode *Caenorhabditis elegans*. *Parasitology, 131 Suppl*, S109-127.

Li, C., & Kim, K. (2008). Neuropeptides. *WormBook*, 1-36.

Liu, T., Kim, K., Li, C., & Barr, M. M. (2007). FMRFamide-like neuropeptides and mechanosensory touch receptor neurons regulate male sexual turning behavior in *Caenorhabditis elegans*. *J Neurosci, 27*(27), 7174-7182.

Livingstone, D. (1991). *Studies on the unc-31 gene of Caenorhabditis elegans.* University of Cambridge.

Luedtke, S., O'Connor, V., Holden-Dye, L., & Walker, R. J. (2010). The regulation of feeding and metabolism in response to food deprivation in *Caenorhabditis elegans*. *Invert Neurosci, 10*(2), 63-76.

Lundström, L., Elmquist, A., Bartfai, T., & Langel, U. (2005). Galanin and its receptors in neurological disorders. *Neuromolecular Med, 7*(1-2), 157-180.

Marder, E. (2012). Neuromodulation of neuronal circuits: back to the future. *Neuron, 76*(1), 1-11.

Mitsukawa, K., Lu, X., & Bartfai, T. (2008). Galanin, galanin receptors and drug targets. *Cell Mol Life Sci, 65*(12), 1796-1805.

Nässel, D. R. (2002). Neuropeptides in the nervous system of Drosophila and other insects: multiple roles as neuromodulators and neurohormones. *Prog Neurobiol, 68*(1), 1-84.

Nelson, L. S., Rosoff, M. L., & Li, C. (1998). Disruption of a neuropeptide gene, flp-1, causes multiple behavioral defects in *Caenorhabditis elegans*. *Science, 281*(5383), 1686-1690.

Qi, Y. B., Garren, E. J., Shu, X., Tsien, R. Y., & Jin, Y. (2012). Photo-inducible cell ablation in *Caenorhabditis elegans* using the genetically encoded singlet oxygen generating protein miniSOG. *Proc Natl Acad Sci U S A, 109*(19), 7499-7504.

Rand, J. B. (2007). Acetylcholine. *WormBook*, 1-21.

Renn, S. C., Park, J. H., Rosbash, M., Hall, J. C., & Taghert, P. H. (1999). A pdf neuropeptide gene mutation and ablation of PDF neurons each cause severe abnormalities of behavioral circadian rhythms in Drosophila. *Cell, 99*(7), 791-802.

Rogers, C., Reale, V., Kim, K., Chatwin, H., Li, C., Evans, P., & De Bono, M. (2003). Inhibition of *Caenorhabditis elegans* social feeding by FMRFamide-related peptide activation of NPR-1. *Nat Neurosci, 6*(11), 1178-1185.

Süudhof, T. C. (2008). Neurotransmitter release. *Handb Exp Pharmacol*(184), 1-21.

Sambrook, J., Fritsch, E., & Maniatis, T. (1989). *Molecular cloning: a laboratory manual* (2nd ed.). Cold Spring Harbor, New York: Cold Spring Harbor Laboratory Press.

Schwarzer, C. (2009). 30 years of dynorphins--new insights on their functions in neuropsychiatric diseases. *Pharmacol Ther, 123*(3), 353-370.

Sieburth, D., Ch'ng, Q., Dybbs, M., Tavazoie, M., Kennedy, S., Wang, D., Dupuy, D., Rual, J. F., Hill, D. E., Vidal, M., Ruvkun, G., & Kaplan, J. M. (2005). Systematic analysis of genes required for synapse structure and function. *Nature, 436*(7050), 510-517.

Sieburth, D., Madison, J. M., & Kaplan, J. M. (2007). PKC-1 regulates secretion of neuropeptides. *Nat Neurosci, 10*(1), 49-57.

Stawicki, T. M., Zhou, K., Yochem, J., Chen, L., & Jin, Y. (2011). TRPM channels modulate epileptic-like convulsions via systemic ion homeostasis. *Curr Biol, 21*(10), 883-888.

Taghert, P. H., & Nitabach, M. N. (2012). Peptide neuromodulation in invertebrate model systems. *Neuron, 76*(1), 82-97.

White, J. G., Southgate, E., Thomson, J. N., & Brenner, S. (1976). The structure of the ventral nerve cord of *Caenorhabditis elegans*. *Philos Trans R Soc Lond B Biol Sci, 275*(938), 327-348.

Wicks, S. R., Roehrig, C. J., & Rankin, C. H. (1996). A dynamic network simulation of the nematode tap withdrawal circuit: predictions concerning synaptic function using behavioral criteria. *J Neurosci, 16*(12), 4017-4031.

Wu, G., Feder, A., Wegener, G., Bailey, C., Saxena, S., Charney, D., & Mathé, A. A. (2011). Central functions of neuropeptide Y in mood and anxiety disorders. *Expert Opin Ther Targets, 15*(11), 1317-1331.

Zhou, K. M., Dong, Y. M., Ge, Q., Zhu, D., Zhou, W., Lin, X. G., Liang, T., Wu, Z. X., & Xu, T. (2007). PKA activation bypasses the requirement for UNC-31 in the docking of dense core vesicles from *C. elegans* neurons. *Neuron, 56*(4), 657-669.

Chapter 4

Altered function of the DnaJ family co-chaperone DNJ-17 modulates locomotor circuit activity in a *C. elegans* seizure model

Abstract

The highly conserved co-chaperone DnaJ/Hsp40 family proteins are known to interact with molecular chaperone Hsp70, and can regulate many cellular processes including protein folding, translocation and degradation. In studies of *C. elegans* locomotion mutants, we identified a gain-of-function (gf) mutation in *dnj-17* closely linked to the widely used *e156* null allele of *C. elegans* GAD (glutamic acid decarboxylase) *unc-25*. *dnj-17* encodes a DnaJ protein orthologous to human DNAJA5. In *C. elegans* DNJ-17 is a cytosolic protein and is broadly expressed in many tissues. *dnj-17(gf)* causes a single amino acid substitution in a conserved domain, and behaves as a hypermorphic mutation. The effect of this *dnj-17(gf)* is most prominent in mutants lacking GABA synaptic transmission. In a seizure model caused by a mutation in the ionotropic aceytylcholine receptor *acr-2(gf)*, *dnj-17(gf)* exacerbates the convulsion phenotype in conjunction with absence of GABA. Null mutants of *dnj-17* show mild resistance to aldicarb, while *dnj-17(gf)* is hypersensitive. These results highlight the importance of DnaJ proteins in regulation of locomotor circuit, and provide insights to the possible roles of DnaJ proteins in human disease.

Introduction

Cells have molecular mechanisms to protect themselves from the stress caused by misfolded or aggregated proteins. DnaJ/Hsp40 family proteins are highly conserved through evolution and act as co-chaperones by interacting with and activating the ATPase activity of Hsp70 chaperone proteins (Ohtsuka and Suzuki 2000; Qiu *et al.* 2006). Together, Hsp40 and

Hsp70 help folding of nascent proteins and refolding and degradation of misfolded proteins.

Accumulation of protein aggregation underlies various human diseases including neurodegenerative diseases such as Parkinson's disease and Huntington's disease (Muchowski and Wacker 2005; Sherman and Goldberg 2001). Mutations in DnaJ/Hsp40 proteins have been associated with such diseases, suggesting the importance of co-chaperones in cellular protein homeostasis (Blumen *et al.* 2012; Borrell-Pagès *et al*. 2006; Trinh and Farrer 2013). In *C. elegans*, overexpression of polyglutamine repeats in muscles or neurons causes formation of protein aggregation in age-dependent manner (Brignull *et al.* 2006a; Brignull *et al.* 2006b), similar to that observed in human polyglutamine diseases (Sakahira *et al.*2002). In addition, excess excitatory neuronal signaling at the neuromuscular junction causes locomotion defects and increased protein aggregation in muscles in a *C. elegans* polyglutamine disease model, suggesting that neuronal activity can affect protein homeostasis in other tissues (Garcia *et al.* 2007).

Functions of neural circuits depend critically on balanced activity between excitatory and inhibitory transmission. In *C. elegans*, locomotion is controlled by the coordinated activities of excitatory cholinergic and inhibitory GABAergic motor neurons (Von Stetina *et al*. 2006). GABA plays crucial roles in the nervous system of both vertebrates and invertebrates. In *C. elegans,* mutants affecting GABA transmission were isolated from forward genetic screens for locomotor defects (Brenner 1974; Jin *et al*. 1999; McIntire *et al*. 1993). The *C. elegans* genes required for GABA neurotransmission including *unc-25/GAD* (Jin *et al.* 1999), *unc-47/VGAT* (McIntire *et al.* 1997) and *unc-49/GABA$_A$R* (Bamber *et al.*1999; Richmond and Jorgensen 1999) are highly conserved among animals. Analysis of unc-25/GAD mutants has revealed that the canonical reference allele *unc-25(e156)* causes a premature termination codon (Trp383amber) in the enzymatic domain; *e156* mutants completely lack GABA immunoreactivity and have been widely used as representative of complete loss of GABA function.

The nicotinic acetylcholine receptor subunit *acr-2* is expressed in the cholinergic motor

neurons. A gain-of-function mutation of *acr-2* causes increased cholinergic motor neuron activity accompanied by decreased GABAergic motor neuron activity, generating excitation-inhibition (E/I) imbalance in locomotor circuit. *acr-2(gf)* animals exhibit a characteristic repetitive convulsion behavior, whose frequency provides a quantitative measure of E/I imbalance (Jospin *et al*. 2009; Stawicki *et al*. 2013).

Through studying the effects of defective GABAergic transmission on *acr-2(gf)* animals, we unexpectedly found a gain-of-function mutation in a co-chaperone protein *dnj-17* to be present in the widely used strain CB156 *unc-25(e156).* We show that the DNJ-17 gain-of-function mutation behaves in a hypermorphic manner, and exacerbates excitation-inhibition imbalance in *acr-2(gf)*. Null mutations of *dnj-17* exhibit mild resistance to aldicarb, suggesting a role in modulating neurotransmission. Homologs of DNJ-17 include human DNAJA5, which is expressed in the brain and other tissues. Our findings provide insights to the *in vivo* function of these co-chaperone proteins.

Materials and Methods

Strains

C. elegans strains were kept at 22.5°C according to standard procedures. Table 4.1 lists strain information with alleles and transgenes. Galaxy platform (Giardine *et al*. 2005) and CloudMap workflows (Minevich *et al.* 2012) were used to analyze the whole-genome sequence data of MT6648 *unc-25(e156) dnj-17(ju1162)III; acr-2(n2420)X* and CZ19995 *unc-25(e156) dnj-17(ju1162)III; acr-2(n2420)X,* obtained by Beijing Genomics Institute (Shenzhen, China). Subsequent analyses based on chromosomal linkage and recombination mapping identified the *ju1162* missense mutation in *dnj-17*. We verified the presence of *dnj-17(ju1162)* in CB156, and generated CZ22168 *unc-25(e156)* that lacks *dnj-17(ju1162)* through multi-step recombination as follows: We verified that the CGC strain SP1104 *unc-25(e156) bli-5(e518)III* is wild type for *dnj-17*. We outcrossed SP1104 to N2, and isolated recombinant animals that showed *unc-25(0)*

shrinker phenotype without blister phenotype. We performed genotyping on isogenic strains of the recombinants, and confirmed the presence of *unc-25(e156)* and the loss of *bli-5(e518)*. In this process, we also found SP1104 has another mutation linked to chromosome III that caused egg-laying defects. Through further outcrossing to N2, we re-isolated *unc-25(e156)* based on behavior and genotyping and established strain CZ22168. Primers used for PCR and genotyping were as follows: YJ10801 CCGTAGAAACCATTCACAGTTTGC and YJ10802 CTATGAAATGCCATTACGAAGTGCTC for *dnj-17(ju1162)*, YJ11985 CATTGGCGCAGACTATTGCTTC and YJ11986 AATTGCTCACCGAAACTCACATTCT for *unc-25(e156*), YJ10799 TACTTGGTATCCAGCTCCTTCC and YJ10800 ATTATTTGGACAGTTTAGCCCACC for *bli-5(e518)*. The information on the alleles and CB156 is deposited in CGC and Wormbase.

Several researchers have observed that *unc-25(e156)* behaved differently from other *unc-25* alleles or GABA mutants, in a number of behavioral and pharmacological assays (C. Bargmann, E. Jorgensen, S. Chalasani, J. Kaplan, personal communications). For future experiments on *unc-25* mutants, we recommend CZ22168, as well as other *unc-25* alleles.

Molecular biology and transgenes

Molecular biology was performed following standard methods. Gateway recombination technology (Invitrogen, CA) was used for expression vectors. Table 4.2 describes the details of constructs generated in this study. We amplified 3.5 kb genomic sequences of *dnj-17* with 0.9 kb 5' upstream sequences to 0.1 kb 3' downstream region using following primers: YJ11121 AAACTCCATCAACCTGACTTCCCTG and YJ11122 TTGCCCATTATTCTTCCCGAAAC. To determine the gene structure of *dnj-17,* we isolated mRNAs from mixed-stage animals of N2 wild type and CB156 *unc-25(e156) dnj-17(ju1162)* using Trizol (ThermoFisher Scientific). cDNA synthesis was performed using SuperScript III (ThermoFisher Scientific), with random primers according to the manufacturers' instructions.

We performed RT-PCR using SL1 primer GTTTAATTACCCAAGTTTGAG and a reverse primer p3 GCGACCAGATTCCTAATTTGCTCGTTC designed on the junction of exon 3 and exon 4 to determine the 1st exon of *dnj-17* mRNA, and p2 ATGAAATGCCATTACGAAGTGCTC and p4 AATGTTTCACCAATCCTCATCATCC primers designed on the 1st and 6th exon to verify the coding sequence. Sequences of all clones were verified by Sanger sequencing. Protein domain analysis was performed using NCBI domain database (Marchler-Bauer *et al.* 2015) and Treefam (Li *et al.* 2006).

Generation of deletion alleles of *dnj-17* by CRISPR-Cas9 editing

*dnj-17(ju1239)*and *dnj-17(ju1276)* deletion alleles were generated by CRISPR-Cas9 editing in the germline, using modifications of previously described methods (Dickinson, Ward, Reiner, & Goldstein, 2013) (Z. Wang and Y.J., unpublished data). Briefly, adult animals were injected with the Cas9-sgRNA expression constructs (pCZGY2647 and pCZGY2646, made from pDD162 with sgRNA) and *Pmyo-2-mCherry* as a coinjection marker. F1 animals expressing mCherry in pharynx were isolated, allowed to lay eggs and then genotyped for *dnj-17* to detect deletions. The F2 progeny of F1 animals with deletions were isolated to establish strains containing *dnj-17* deletion. sgRNA sequences used to target *dnj-17* are the following: ACAGAAAACTAGCGCTCAAA and GAGTTTGGCGACAAGGATAC. *ju1239* was generated following microinjection into CB156 *unc-25(e156)* animals. *ju1276* was generated following microinjection into N2 animals.

To analyze the temperature effects on *dnj-17(ju1239)*, we examined the growth and locomotion of N2 and CZ21429 *dnj-17(ju1239)* under different temperature conditions. Briefly, 10 gravid adults of each strain were allowed to lay eggs for 6 hours at 22.5C. Then, adult animals were removed, and the plates with embryos were kept under 15°C, 22.5°C or 25°C. Hatched progeny were kept under the same temperature, and their growth and general locomotion were visually scored once within 16-24 hours.

When the progeny reached L4 stage, animals from each condition were placed onto individual plates. Number of eggs laid by each animal was scored to compare the brood size. The experiment was repeated twice.

Generation of single-copy inserted strains

Single-copy insertion transgenes of *Pdnj-17-dnj-17(+)* and *Pdnj-17-dnj-17(ju1162)* were generated at Chromosome II site ttTi5605 using modified vectors (Z. Wang and Y.J., unpublished data). Briefly, N2 young adult animals were injected with the following constructs: a construct (pCZGY3031 or pCZGY3032) containing *dnj-17* sequence with ttTi5605 homology arms and a copy of hygromycin resistance gene, a construct (pDD122) which drives expression of Cas9 and sgRNA targeting ttTi5605 in the germline, and a Pmyo-2-mCherry fluorescent coinjection marker. F2 animals were selected for the resistance to hygromycin. Single-copy insertion lines were confirmed by PCR using primers designed outside of the homology arms. Loss of extrachromosomal array was confirmed by PCR and the loss of co-injection marker. Each insertion line was outcrossed twice before used in experiments.

Quantification of convulsion behavior

Scoring of convulsions was performed as previously described (Stawicki *et al*. 2013). Briefly, L4 larvae were transferred to NGM plates seeded with *E. coli* OP50. On the following day, young adults were transferred to fresh plates with OP50 and visually scored for convulsion behavior under a dissecting scope. The observer was blinded to the genotype of the animals tested. A convulsion event was defined as a shortening of the animals body length. The assay was repeated at least twice per genotype in two different generations. Two independent transgenic lines were used for each construct.

Aldicarb assay

One day before experiment, L4 animals were transferred to fresh plates seeded with OP50. On the next day, 10 animals were transferred to a NGM plate with 500 μM aldicarb. Animal behavior was scored every 30 min. Animals were scored paralyzed when they did not move for more than 5 seconds in response to touch stimulus.

Confocal microscopy

L4 animals were imaged using a Zeiss LSM 710 confocal microscope (63x objective). Animals were immobilized by 1 mM levamisole and placed on 4% agar pads. Images are maximum-intensity projections of z stacks obtained at 1 μm intervals. ImageJ was used to process the images obtained.

Results and Discussion

Identification of a missense mutation in *dnj-17* in *unc-25(e156)* strains

acr-2(n2420gf) animals show spontaneous convulsion behavior, due to increased cholinergic excitation and reduced GABAergic inhibition (Jospin *et al.* 2009). We wanted to further examine the effects of GABAergic transmission on the convulsive behavior of *acr-2(gf)* animals. We generated double mutants of *acr-2(gf)* with genes essential for GABA signaling, using canonical or null alleles of *unc-25/GAD, unc-47/VGAT, unc-49/GABAR*. We used three null mutations of *unc-25: e156, n2324,* and *n2328*, which cause amber stop codons at Trp383, Trp291 and Glu486, respectively, and which are all predicted to encode truncated proteins that lack the cofactor binding site and enzymatic activity site at the C-terminus. All double mutants showed increased convulsion frequency compared to *acr-2(gf)* single mutants (Figure 4.1A). While *unc-25(n2324)* and *unc-25(n2328)* enhanced *acr-2(gf)* behavioral defects to similar degrees as *unc-47(gk192)* and *unc-49(e382), unc-25(e156)* increased the convulsion frequency significantly more than these four mutations. Further outcrossing of *unc-25(e156); acr-2(gf)* (MT6648) did not eliminate this enhancement. We thus hypothesized that the ancestral CB156

strain may contain additional modifier mutation(s) linked to *unc-25(e156)*.

We performed whole-genome sequencing analysis of MT6648 and of an outcrossed strain CZ19995 *unc-25(e156); acr-2(gf).* Following chromosomal linkage mapping, we identified a single nucleotide transversion from thymine to adenine in the coding sequence of the gene *dnj-17*, approximately 0.5 map units right of *unc-25* on chromosome III (Figure 4.1B), and hereafter referred to as *dnj-17(ju1162).* The *ju1162* mutation was present in the CGC strain CB156 *unc-25(e156)*, but not in SP1104 *unc-25(e156) bli-5(e518) III*, which was generated about 1987 through recombination from trans-heterozygous animals of *unc-25(e156)* with a chromosome containing *bli-5(e518)* (R. Herman, personal communication). *dnj-17(ju1162)* was also not present in MT5957 *unc-25(n2324) III* and MT5969 *unc-25(n2328) III*. Therefore, *dnj-17(ju1162)* did not arise as a spontaneous mutation in strain passage in our laboratory, but was inherited from the original CB156 stock.

dnj-17 encodes a homolog of human DNAJA5

Gene structure predictions (Wormbase WS251) indicate *dnj-17* contains seven exons, generating a mature mRNA predicted to encode a protein of 510 amino acids. To verify the *dnj-17* gene structure we used cDNA analyses using mRNA isolated from N2 and CB156 *unc-25(e156) dnj-17(ju1162).* RT-PCR analyses using SL1 and gene-specific primers revealed that the 5' end of *dnj-17* mRNA contained an SL1 leader, but predicted exon 1 was not present in the mature mRNA. We obtained full-length *dnj-17* cDNA and found that DNJ-17 protein consists of 485 amino acids (Figure 4.1B, C). From NCBI protein domain analysis, the N-terminus of DNJ-17 has a highly conserved DnaJ domain, known to interact with Hsp70 family proteins, and the C-terminal half contains two C2H2-type zinc finger motifs that have been implicated to be important for polypeptide binding (Banecki *et al.* 1996; Lu and Cyr, 1998; Szabo *et al*. 1996). Relatives of DNJ-17 are found widely in eukaryotes, with orthologs named as JJJ1 in yeast, DNAJA5/DNAJC21 in human, DNAJC21 in mouse, and

CG2790 in Drosophila (Fig 1D). The J domain of DNJ-17 also has a highly conserved HPD motif that is crucial for interaction with Hsp70 proteins (Tsai and Douglas, 1996). Yeast JJJ1 activates ATPase activity of Hsp70, and lack of JJJ1 results in cold sensitivity (Meyer *et al*. 2007). On the other hand, functions of the DNJ-17 family proteins in animals remain mostly unknown, though human *DNAJA5* is expressed in several tissues including the brain (Chen *et al.* 2004). We confirmed that cDNAs from CB156 *unc-25(e156) dnj-17(ju1162)* contained a single nucleotide change, which causes Asp77 to Lys amino acid substitution (N77K) in the region immediately adjacent to the DnaJ domain (Figure 4.1B, D).

***dnj-17(ju1162)* is a gain-of-function mutation**

Several lines of evidence support that *ju1162* is a gain-of-function mutation of *dnj-17*. First, we examined the effect of a *dnj-17* deletion allele *dnj-17(tm570)*, which removes the C-terminal half of the protein (Figure 4.1B). *dnj-17(tm570)* homozygous animals showed normal growth rate, wild-type locomotion, and did not affect convulsion frequency of *acr-2(gf)* (Figure 4.2A). We also generated *unc-47(gk192) dnj-17(tm570); acr-2(n2420)* triple mutants and found that they resembled *unc-47(gk192); acr-2(n2420)* double mutants in their convulsion frequency. As *dnj-17(tm570)* mutants potentially produce mRNAs encoding a truncated protein with intact DnaJ domain, we next generated a deletion allele targeting the DnaJ domain using CRISPR-Cas9-mediated genome editing technology (Dickinson *et al*. 2013; Friedland *et al*. 2013)(Z. Wang and Y. Jin, unpublished results). *dnj-17(ju1239)* removes a large portion of the DnaJ domain and is predicted to cause a frameshift and premature stop after amino acid 34 (Figure 4.1B). Since the null mutation of a yeast protein with J domain, *Jjj1*, was previously reported to cause cold sensitivity in yeast (Meyer *et al*. 2007), we examined the viability and locomotion of *dnj-17(ju1239)* mutants. The mutant animals had similar brood size as wild type under three temperature conditions (Fig. 4.2B). Their growth rate,

body shape and movement were also indistinguishable from wild type. Finally, *dnj-17(ju1239)* did not affect the convulsion frequency of *acr-2(n2420)* (Fig. 4.2A). These observations show that *dnj-17* is a non-essential gene for *C. elegans* development and behavior, and that *dnj-17* loss-of-function does not affect convulsion of *acr-2(gf)* by itself or when GABA transmission is eliminated in *unc-47(null)* animals.

We further examined if removing *dnj-17(ju1162)* from *unc-25(e156)* background would eliminate the increased convulsion frequency phenotype of *acr-2(gf)*. As *dnj-17* is located 0.5 map unit apart from *unc-25* it is challenging to separate *unc-25(e156)* and *dnj-17(ju1239)* by genetic recombination. We therefore generated another deletion allele in the *unc-25(e156) dnj-17(ju1162)* background using CRISPR editing (Figure 4.1B). *dnj-17(ju1276)* removes the DnaJ domain and the region including *ju1162(N77K).* Furthermore, through isolation of *unc-25(e156)* recombinants after outcrossing SP1104 *unc-25(e156) dnj-17(+) bli-5(e518)*, we obtained CZ22169 *unc-25(e156) dnj-17(+); acr-2(n2420).* Animals of genotype *unc-25(e156) dnj-17(ju1276); acr-2(gf)* and *unc-25(e156) dnj-17(+); acr-2(gf)* showed convulsion frequencies lower than *unc-25(e156) dnj-17(ju1162); acr-2(gf),* and instead resembled *acr-2(gf)* double mutants with *unc-25(n2324)* or with other GABA mutants (Figure 4.2C). Finally, we also observed that *dnj-17(ju1162)* showed semi-dominant effects on convulsion frequency in the *acr-2(gf); unc-25(0)* background (Figure 4.2D). Thus, we conclude that *dnj-17(ju1162)* is a semi-dominant gain-of-function mutation, designated as *dnj-17(ju1162gf)*.

DNJ-17 is a cytosolic protein expressed in multiple tissues

We next analyzed the expression pattern of *dnj-17.* We first generated an extrachromosomal transcriptional GFP reporter using 0.9 kb promoter region of *dnj-17.* GFP was seen throughout the body with enrichment in the intestine and several cells around the pharynx, and the expression pattern was similar in both wild type and *acr-2(gf)* background (Fig. 4.3A). We then made GFP-fused translational DNJ-17

reporters. GFP signals from *Pdnj-17-dnj-17::gfp* localized to the cytosol of head neurons, and in other unidentified cells at lower levels throughout the body (Figure 3B). A weaker but similar pattern was observed in an integrated fosmid expression line which expresses DNJ-17 tagged with C-terminal TY1::EGFP:3xFLAG (not shown) (Zhong *et al*. 2010). Moreover, DNJ-17(N77K)::GFP showed similarly diffused expression. Both DNJ-17(+)::GFP and DNJ-17(N77K) expression patterns were similar in wild type and in *acr-2(gf)* background, suggesting that the presence of *acr-2(gf)* does not largely affect the localization of DNJ-17.

DNJ-17(N77K) behaves as a hypermorph

We next examined the nature of DNJ-17(N77K) using transgenic overexpression. Overexpression of wild type *dnj-17* by genomic sequence of *dnj-17* including 0.9 kb upstream promoter region caused increase of *acr-2(gf)* convulsion frequency (Figure 4.4A). This transgene also enhanced convulsion frequency in *unc-47(0)* mutant background, suggesting that the increase in convulsion by overexpression of *dnj-17* is independent of the effect caused by defects in GABAergic transmission. Interestingly, this enhanced effect was also observed by overexpression of *dnj-17(ju1162gf)*. ACR-2 is expressed specifically in neurons (Jospin *et al*. 2009). However, overexpression of *dnj-17* using a pan-neuronal promoter did not affect convulsion frequency of *acr-2(gf)* (Figure 4.4B), suggesting that the effect of *dnj-17* on convulsion frequency may require expression in a non-neuronal tissue or in multiple tissues.

To precisely compare the effect of *dnj-17(ju1162gf)* to wild type *dnj-17,* we generated single-copy insertion transgene expressing full-length genomic *dnj-17(ju1162gf)* or *dnj-17(+)* on chromosome II. Animals with *Pdnj-17-dnj-17(ju1162gf)* expressed from a single-copy transgene showed overall normal locomotion, growth speed and brood size. We found that *Pdnj-17-dnj-17(ju1162gf);acr-2(gf)* increased convulsion compared to *acr-2(gf)* single mutants, whereas *Pdnj-17-dnj-17(+)* single copy expression did not (Figure 4.4C), consistent with

dnj-17(ju1162gf) acting semi-dominantly in *unc-25(e156)* background (Figure 4.2C). These results suggest that the DNJ-17(N77K) mutation has higher activity than wild type DNJ-17, implying that the increase in convulsion by overexpression of wild-type *dnj-17* is caused by excess levels of the protein.

***dnj-17* activity affects the response to aldicarb**

To further assess the effect of *dnj-17* mutations on neurotransmission at the neuromuscular junction, we examined the sensitivity of the mutant animals to an acetylcholine esterase inhibitor aldicarb. *dnj-17(ju1239)* null animals showed mild resistance to aldicarb, which was rescued by single-copy insertion of *dnj-17(+)*, implying that *dnj-17* affects cholinergic transmission at the neuromuscular junction (Figure 4.2C). Expression of *dnj-17(ju1162gf)* caused increased sensitivity to aldicarb, consistent with the allele being a hypermorph mutation. These results raise a possibility that the function of *dnj-17* is required for folding and/or function of proteins involved in cholinergic transmission. Overexpression of wild type DNJ-17 may also lead to high level of cholinergic transmission by contributing to folding of the proteins in the pathway.

Other mechanisms might account for the effects of *dnj-17(ju1162).* The N77K mutation may make DNJ-17 protein prone to form aggregates. DnaJ/Hsp40 proteins bind to misfolded proteins and bring them to Hsp70 (Cheetham and Caplan, 1998). The N77K mutation could alter the kinetics for DNJ-17 to detach from the protein(s) it binds to, and prevent the misfolded protein from being degraded, resulting in accumulation of misfolded proteins that cause cellular stress. Such cellular stress could alter neuronal and muscular functions. Another possibility is that the mutation disrupts certain cellular functions. Recently it was reported that an Asn to Ser mutation in the DnaJ domain of human DNAJC13 is found in a family with Parkinson disease, where the diseases is transmitted in an autosomal-dominant manner (Vilariño-Güell *et al*. 2014). The mutant

protein exhibited a toxic gain-of-function characteristic affecting endosomal transport. The N77K mutation in *C. elegans* DNJ-17 may affect similar cellular functions such as endocytosis and subcellular trafficking, thus disrupting the coordination of the motor neuron circuit.

E. coli has only one gene coding DnaJ/Hsp40, whereas animals typically express multiple DnaJ family members. The DnaJ protein in *E. coli* has been well-characterized, but functions of individual DnaJ/Hsp40 family proteins in animals remain largely unknown. DNAJA5, the closest human homolog of DNJ-17, shows enhanced expression in the brain (Chen *et al*. 2004) which suggests neuron-specific roles, but its substrates and functions are yet to be characterized. Studies of DnaJ/Hsp40 in animals may lead to further understanding of the physiological mechanisms of protein homeostasis in neurodegenerative diseases.

Acknowledgements

This chapter is a reprint in full of Takayanagi-Kiya, S. and Jin, Y. Altered function of the DnaJ family co-chaperone DNJ-17 modulates locomotor circuit activity in a *C. elegans* seizure model (in press) with permission of all authors.

We thank Tamara Stawicki for first noticing the difference between *unc-25(e156)* and other alleles of *unc-25* and GABA pathway mutants. We thank A. Chisholm, K. Noma and K. Mcculloch for comments and our lab members for discussion. Some strains were obtained from the Japan National BioResource Project (NBRP) and the Caenorhabditis Genetics Center (CGC). This work is supported by NIH R01 NS 035546 to YJ and Nakajima Foundation Fellowship to ST-K.

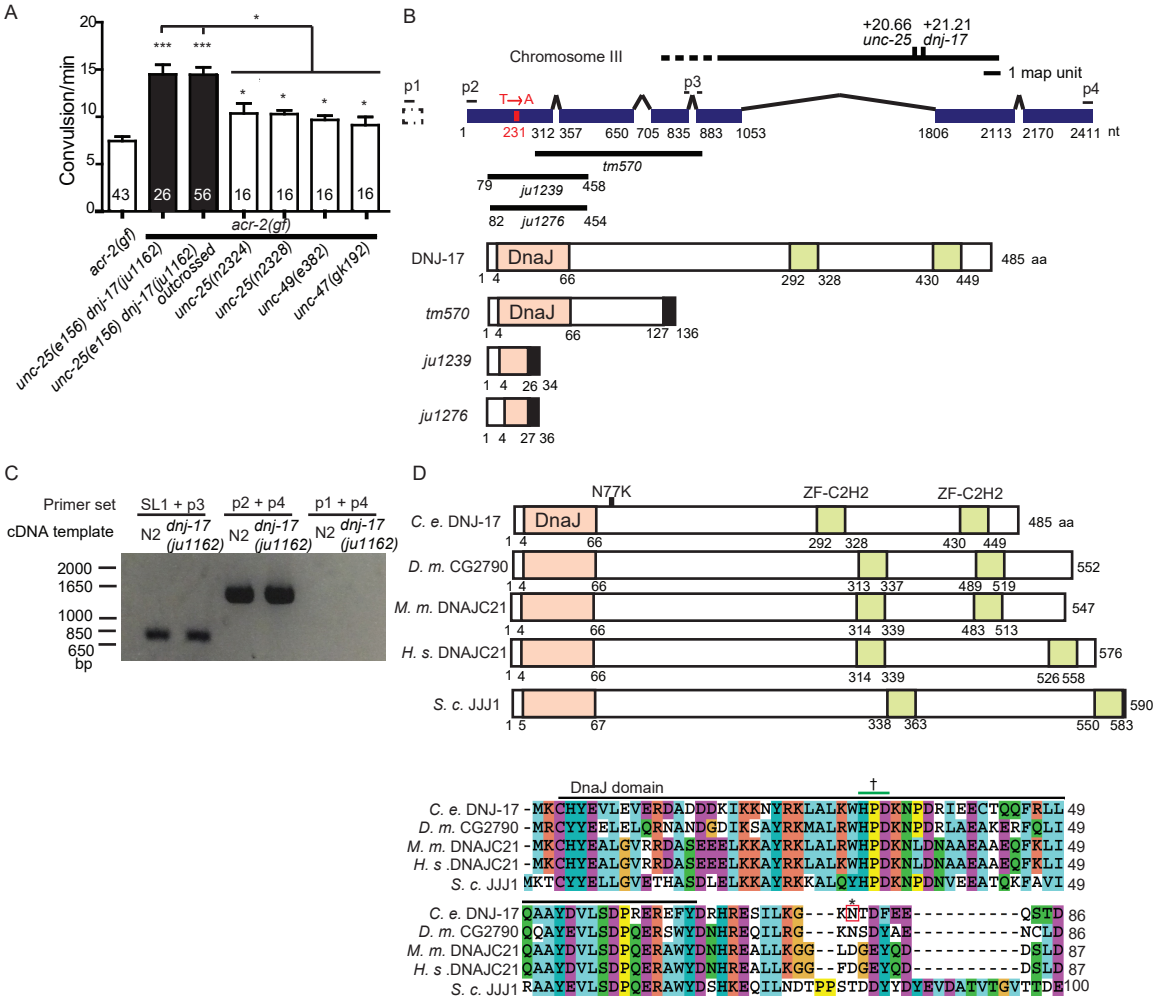

Figure 4.1. Single amino acid substitution in DNJ-17 in the background of *unc-25(e156)* causes increase of *acr-2(gf)* convulsions. (A) Quantification of convulsion frequency of strains with mutations in genes required for GABA transmission. Note the higher convulsion frequency of the animals with *unc-25(e156) dnj-17(ju1162)*. Statistics, one way ANOVA followed by Bonferroni's post hoc test. * $p < 0.05$, *** $p < 0.001$. Error bars indicate SEM. Numbers in the column indicate sample sizes. (B) Upper panel shows *dnj-17* gene structure, with the location of the *ju1162* T to A nucleotide change, deletion mutations, and primers (p1, p2: forward primer, p3, p4: reverse primer) designed for cDNA amplification. Lower panel shows predicted DNJ-17 protein in wild type and in deletion mutants. All three mutations cause frameshift and produce premature stop codons. Note that *ju1239* and *ju1276* remove the highly conserved DnaJ domain. Black fills designate frame-shifted regions. (C) Gel electrophoresis of the cDNA fragments amplified by PCR using the designated primers (shown in B). SL1 with p3 primer amplified cDNA fragment including the start codon. (D) Upper panel shows DNJ-17 family protein structure. D. m.: Drosophila melanogaster, *M. m.*: *Mus musculus*, H.s.: *Homo sapiens*. *S.c.*: *Saccharomyces cerevisiae*. Lower panel shows amino acid sequence alignment around the DnaJ domain. * marks the position of N to K mutation in *ju1162*. † marks the HPD motif, highly conserved among the J domain and required for the activation of Hsp70 (Tsai and Douglas 1996, Meyer et al. 2007).

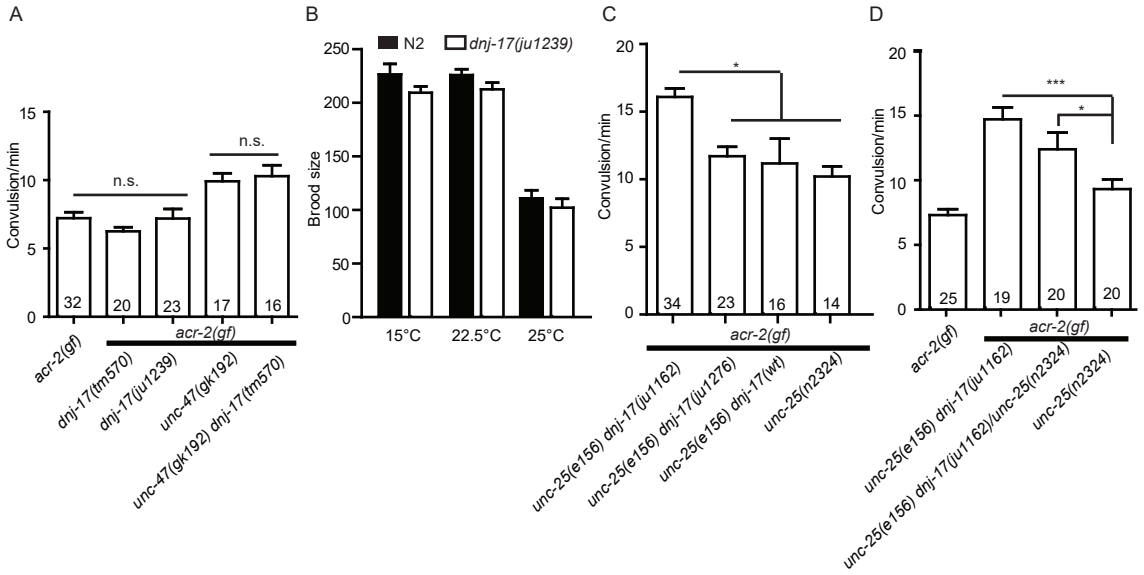

Figure 4.2. *dnj-17(ju1162)* acts as a gain-of-function mutation. (A,C,D) Quantification of convulsion frequency. (A) Loss-of-function deletion alleles of *dnj-17* do not affect *acr-2(gf)* convulsion frequency. (C) Removal of *dnj-17(ju1162gf)* reduces the convulsion frequency. (D) *dnj-17(ju1162gf)* shows semi-dominant effects on convulsion frequency. Statistics, one way ANOVA followed by Bonferroni's post hoc test. * $p < 0.05$. Numbers in the column indicate sample sizes. (B) Brood size is not affected by deletion of *dnj-17.* n=6 for each condition. Error bars indicate SEM.

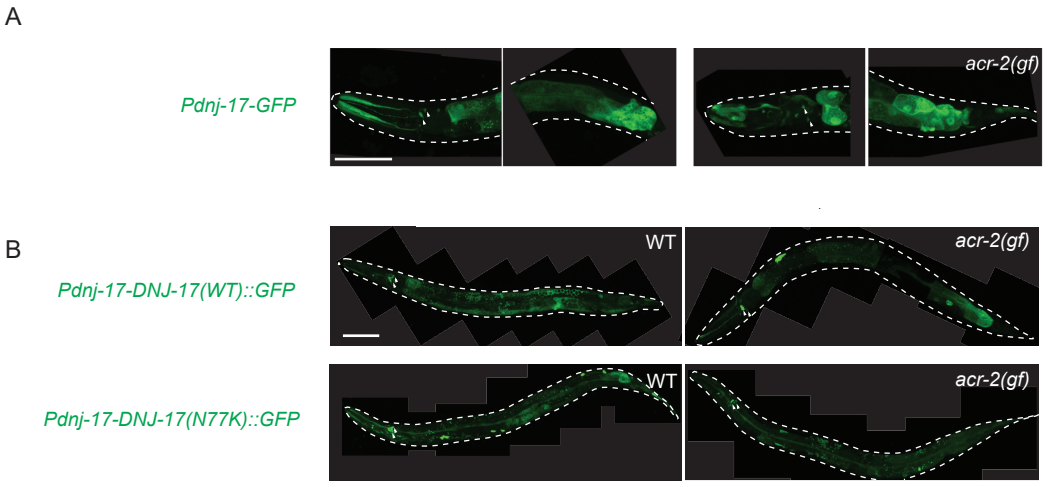

Figure 4.3. Expression pattern of DNJ-17 is not affected the N77K mutation or by *acr-2(gf)*. (A) Confocal images of animals expressing *dnj-17* transcriptional reporter. (B) Confocal images of animals expressing DNJ-17 translational reporter. Scale bar: 50µm. Arrowheads point expression in cell bodies of the head neurons.

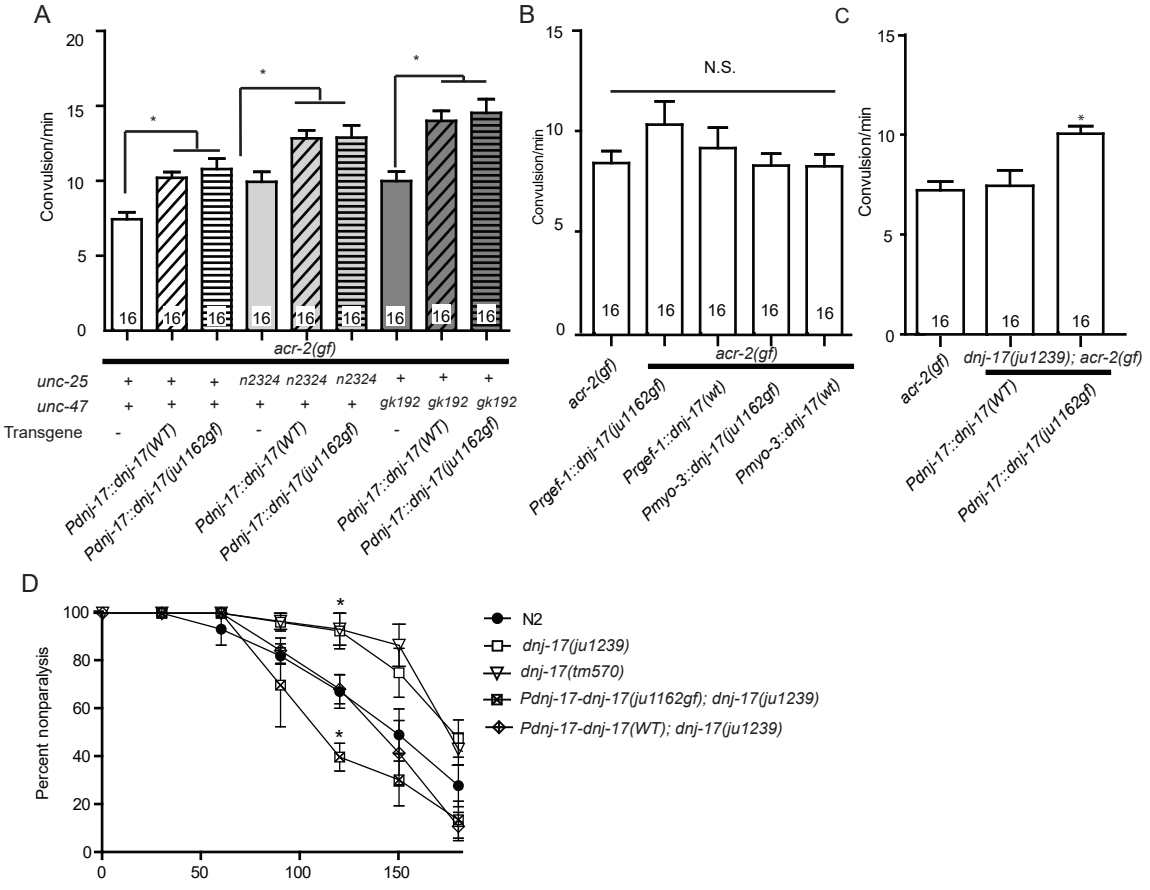

Figure 4.4. Single-copy expression of *dnj-17(ju1162gf)* is sufficient to cause increase in convulsion frequency. (A-C) Quantification of convulsion frequency. (A) Overexpression of *dnj-17(+)* or *dnj-17(ju1162gf)* by high-copy extrachromosomal arrays cause increase of *acr-2(gf)* convulsion frequency. (B) Single-copy expression of *dnj-17(ju1162gf)*, but not *dnj-17(+),* causes increase in convulsion frequency. Statistics, one way ANOVA followed by Bonferroni's post hoc test. *: $p < 0.05$. Error bars indicate SEM. Numbers in the column indicate sample sizes. (D) Aldicarb resistance of *dnj-17(ju1239)* null is suppressed by expression of wild type *dnj-17.* Expression of *dnj-17(ju1162gf)* causes increased sensitivity to aldicarb. Statistics, two way ANOVA. *: $p < 0.05$ compared to N2 at the given time point.

Table 4.1. List of strains and genotypes used in the study.

Strain number	Genotype	Notes
MT6241	*acr-2(n2420)X*	
CZ20444	*dnj-17(tm570)III*	
CZ21429	*dnj-17(ju1239)III*	
CB156	*unc-25(e156) dnj-17(ju1162 N77K)III*	
MT6648	*unc-25(e156) dnj-17(ju1162 N77K)III; acr-2(n2420)X*	
CZ19995	*unc-25(e156) dnj-17(ju1162 N77K)III; acr-2(n2420)X*	2x outcrossed MT6648
SP1104	*unc-25(e156) bli-5(e518)III*	*dnj-17(wt)*
CZ22168	*unc-25(e156)III*	*dnj-17(wt)* Obtained from outcrossing SP1104
MT5957	*unc-25(n2324)III*	*dnj-17(wt)*
MT5969	*unc-25(n2328)III*	*dnj-17(wt)*
CZ20874	*unc-25(n2324)III; acr-2(n2420)X*	*dnj-17(wt)*
CZ9381	*unc-25(n2328)III; acr-2(n2420)X*	*dnj-17(wt)*
CZ9307	*unc-49(e382); acr-2(n2420)X*	*dnj-17(wt)*
CZ9304	*unc-47(gk192); acr-2(n2420)X*	*dnj-17(wt)*
CZ21261	*Pdnj-17-GFP(juEx6433)*	
CZ22374	*acr-2(n2420)X; Pdnj-17-GFP(juEx6433)*	
CZ21262	*Pdnj-17-dnj-17(wt)::GFP(juEx6434)*	
CZ21263	*Pdnj-17-dnj-17(ju1162 N77K)::GFP(juEx6435)*	
CZ22170	*dnj-17(tm570)III; acr-2(n2420)X*	
CZ21431	*dnj-17(ju1239)III; acr-2(n2420)X*	
CZ20873	*unc-47(gk192)III dnj-17(tm570)III; acr-2(n2420)X*	
CZ22173	*unc-25(e156)III dnj-17(ju1276)III; acr-2(n2420)X*	
CZ22169	*unc-25(e156)III dnj-17(wt)III; acr-2(n2420)X*	
CZ21065	*acr-2(n2420)X; Pdnj-17-dnj-17(wt)(juEx6328)*	
CZ20975	*acr-2(n2420)X; Pdnj-17-dnj-17(ju1162 N77K)(juEx6324)*	
CZ22175	*acr-2(n2420)X; Prgef-1-dnj-17(ju1162 N77K)(juEx6710)*	
CZ22177	*acr-2(n2420)X; Prgef-1-dnj-17(wt)(juEx6712)*	
CZ24592	*acr-2(n2420)X; Pmyo-3-dnj-17(ju1162 N77K)(juEx7546)*	
CZ24595	*acr-2(n2420)X; Pmyo-3-dnj-17(wt)(juEx7549)*	
CZ21071	*unc-25(n2324)III; acr-2(n2420)X; Pdnj-17-dnj-17(wt)(juEx6328)*	
CZ21070	*unc-25(n2324)III; acr-2(n2420)X; Pdnj-17-dnj-17(ju1162 N77K))(juEx6324)*	
CZ21068	*unc-47(gk192)III; acr-2(n2420)X; Pdnj-17-dnj-17(ju1162 N77K)(juEx6328)*	
CZ21258	*unc-47(gk192)III; acr-2(n2420)X; Pdnj-17-dnj-17(WT)(juEx6324)*	
CZ24445	*Pdnj-17-dnj-17(wt)(juSi276)II; dnj-17(ju1239)III*	
CZ24225	*Pdnj-17-dnj-17(ju1162 N77K)(juSi278)II; dnj-17(ju1239)III*	
CZ23083	*Pdnj-17-dnj-17(wt)(juSi276)II; dnj-17(ju1239)III; acr-2(n2420)X*	
CZ23084	*Pdnj-17-dnj-17(ju1162 N77K)(juSi278)II; dnj-17(ju1239)III; acr-2(n2420)X*	
OP492	*unc-119(tm4063)III; [dnj-17::TY1::EGFP::3xFLAG(92C12) + unc-119(+)](wgIs492)*	Fosmid integrated line (Zhong *et al.*, 2010)

Allele	Description
juEx6433	Injection into N2. pCZGY2641 Pdnj-17-gfp 25ng/ul Coelomocyte::RFP 60ng/u
juEx6434	Injection into N2. pCZGY2642 Pdnj-17-dnj-17(wt)::gfp 45ng/u Coelomocyte::RFP 60ng/ul
juEx6435	Injection into N2. pCZGY2643 Pdnj-17-dnj-17(ju1162 N77K)::gfp 45ng/u Coelomocyte-RFP 60ng/ul
juEx6324	Injection into MT6241 acr-2(n2420)X. pCZGY2636 Pdnj-17-dnj-17(ju1162) 50ng/ul
juEx6328	Injection into MT6241 acr-2(n2420)X. pCZGY2635 Pdnj-17-dnj-17(wt) 50ng/u Coelomocyte-rfp 60ng/ul
juEx6710	Injection into MT6241 acr-2(n2420)X. pCZGY2639 Prgef-1-dnj-17(wt) 5ng/u Coelomocyte-rfp 60ng/ul
juEx6712	Injection into MT6241 acr-2(n2420)X. pCZGY2640 Prgef-1-dnj-17(ju1162 N77K) 5ng/ul Coelomocyte-rfp 60ng/ul
juEx7546	Injection into MT6241 acr-2(n2420)X. pCZGY2 Pmyo-3-dnj-17(wt) 5ng/u Pmyo-2-mCherry 1ng/ul
juEx7549	Injection into MT6241 acr-2(n2420)X. pCZGY2635 Pmyo-3-dnj-17(ju1162 N77K) 5ng/ul Pmyo-2-mCherry 1ng/ul
juSi276	Single copy insertion of Pdnj-17-dnj-17(wt) on ChrII.
juSi278	Single copy insertion of Pdnj-17-dnj-17(ju1162 N77K) on ChrII
ju1162	*dnj-17* t to a mutation at 231th nucleotide in the first exon. N77K mutation ir dnj-17. CB156 has this allele.
ju1239	*dnj-17* 378 bp deletion. Expected truncated protein product in this allele is 26 amino acids from 1st exon + 8 amino acids after frame shift and then stop codon. Removes most of the DnaJ domain.
ju1276	*dnj-17* 372 bp deletion. Expected truncated protein product in this allele is 27 amino acids from 1st exon + 9 amino acids after frame shift and then stop codon. Removes most of the DnaJ domain.

Table 4.2. List of constructs used in the study.

pCZGY number	Plasmid	Construction notes
pCZGY2635	Pdnj-17-dnj-17(wt)	N2 dnj-17 Genomic DNA amplification by primer YJ11121 Forward AAACTCCATCAACCTGACTTCCCTG and and YJ11122 Reverse TTGCCCATTATTCTTCCCGAAAC. Fragment was inserted to Topo pcr8 vector backbone by TA cloning.
pCZGY2636	Pdnj-17-dnj-17(ju1162 N77K)	CZ19995 dnj-17 genomic DNA amplification by primer YJ11121 Forward AAACTCCATCAACCTGACTTCCCTG and and YJ11122 Reverse TTGCCCATTATTCTTCCCGAAAC. Fragment was inserted to Topo pcr8 vector backbone by TA cloning. Has dnj-17 (ju1162 N77K) sequence.
pCZGY2637	TopoPCR8 dnj-17(wt)	N2 Genomic DNA amplification by primer YJ11123 Forward ATGAAATGCCATTACGAAGTGCTCG and and YJ11122 Reverse TCACCAATCCTCATCATCCCCCTTA Fragment was inserted to Topo pcr8 vector backbone by TA cloning. Has dnj-17 wt sequence.
pCZGY2638	TopoPCR8 dnj-17(ju1162 N77K)	CZ19995 Genomic DNA amplification by primer YJ11123 Forward ATGAAATGCCATTACGAAGTGCTCG and and YJ11122 Reverse TCACCAATCCTCATCATCCCCCTTA Fragment was inserted to Topo pcr8 vector backbone by TA cloning. Has dnj-17 ju1162 sequence.
pCZGY2639	Prgef-1-dnj-17(WT)	LR reaction between pCZGY2637 dnj-17(wt) TopoPCR8 and pCZGY66 Prgef-1
pCZGY2640	Prgef-1-dnj-17(ju1162 N77K)	LR reaction between pCZGY2638 dnj-17(ju1162 N77K) TopoPCR8 and pCZGY66 Prgef-1 DEST
pCZGY	Pmyo-3-dnj-17(WT)	LR reaction between pCZGY2637 TopoPCR8 dnj-17(wt) and pCZGY925 Pmyo-
pCZGY	Pmyo-3-dnj-17(ju1162 N77K)	LR reaction between pCZGY2638 TopoPCR8 dnj-17(ju1162 N77K) and pCZGY925 Pmyo-3 DEST
pCZGY2642	Pdnj-17-dnj-17(wt)::gfp	Promoter and the coding sequence of dnj-17 was amplified by YJ11129 and YJ11130 using pCZGY2635 as template. The last codon (the termination codon) was removed. GFP and backbone was amplified using PKK74 (Pcebp-1::cebp-1::gfp) as template with primers YJ11131 and YJ11132. Two fragments were assembled using Gibson assembly method.
pCZGY2643	Pdnj-17-dnj-17(ju1162 N77K)::gfp	Promoter and the coding sequence of dnj-17 was amplified by YJ11129 and YJ11130 using pCZGY2636 as template. The last codon (the termination codon) was removed. GFP and backbone was amplified using PKK74 (Pcebp-cebp-1::gfp) as template with primers YJ11131 and YJ11132. Two fragments were assembled using Gibson assembly method.
pCZGY2641	Pdnj-17-gfp	Promoter and the first 7 amino acid sequence of dnj-17 was amplified by YJ11125 GCTTGCATGCAAACTCCATCAACCTGACTT and YJ11126 CTCCTTTACTCACTTCGTAATGGCATTTCATAGC. GFP coding sequence and backbone was amplified using pczgy51 (Prgef-1-gfp) as template with YJ11127 CGAAGTGAGTAAAGGAGAAGAACTTTTCACTGG and YJ11128 GGAGTTTGCATGCAAGCTTGGCGTAATCA. Two PCR fragements were assembled by Gibson assembly protocol. Gfp is expressed in-frame with the first 7 amino acid of dnj-17. Designed as transcriptional reporter.
pCZGY3031	Pdnj-17-dnj-17(wt) with ttTi5605 homology arms on Chr II	LR reaction between pDEST5605 and pCZGY2635
pCZGY3032	Pdnj-17-dnj-17(ju1162 N77K)with ttTi5605 homology arms on Chr II	LR reaction between pDEST5605 and pCZGY2636
pCZGY2646	Peft-3-Cas9+sgRNA1	sgRNA sequence ACAGAAAACTAGCGCTCAAA was added to pDD162 (Pefit-3-Cas9 + empty sgRNA) by PCR site-directed mutagenesis.
pCZGY2647	Peft-3-Cas9+sgRNA2	sgRNA sequence ACTCATATCTGAACGACAAA was added to pDD162 (Pefit-3-Cas9 + empty sgRNA) by PCR site-directed mutagenesis.

References

Bamber, B. A., Beg, A. A., Twyman, R. E., & Jorgensen, E. M. (1999). The *Caenorhabditis elegans* unc-49 locus encodes multiple subunits of a heteromultimeric GABA receptor. *J Neurosci, 19*(13), 5348-5359.

Banecki, B., Liberek, K., Wall, D., Wawrzynów, A., Georgopoulos, C., Bertoli, E., Tanfani, F., & Zylicz, M. (1996). Structure-function analysis of the zinc finger region of the DnaJ molecular chaperone. *J Biol Chem, 271*(25), 14840-14848.

Blumen, S. C., Astord, S., Robin, V., Vignaud, L., Toumi, N., Cieslik, A., Achiron, A., Carasso, R. L., Gurevich, M., Braverman, I., Blumen, N., Munich, A., Barkats, M., & Viollet, L. (2012). A rare recessive distal hereditary motor neuropathy with HSJ1 chaperone mutation. *Ann Neurol, 71*(4), 509-519.

Borrell-Pagès, M., Canals, J. M., Cordelières, F. P., Parker, J. A., Pineda, J. R., Grange, G., Bryson, E. A., Guillermier, M., Hirsch, E., Hantraye, P., Cheetham, M. E., Néri, C., Alberch, J., Brouillet, E., Saudou, F., & Humbert, S. (2006). Cystamine and cysteamine increase brain levels of BDNF in Huntington disease via HSJ1b and transglutaminase. *J Clin Invest, 116*(5), 1410-1424.

Brenner, S. (1974). The genetics of *Caenorhabditis elegans*. *Genetics, 77*(1), 71-94.

Brignull, H. R., Moore, F. E., Tang, S. J., & Morimoto, R. I. (2006a). Polyglutamine proteins at the pathogenic threshold display neuron-specific aggregation in a pan-neuronal *Caenorhabditis elegans* model. *J Neurosci, 26*(29), 7597-7606.

Brignull, H. R., Morley, J. F., Garcia, S. M., & Morimoto, R. I. (2006b). Modeling polyglutamine pathogenesis in *C. elegans*. *Methods Enzymol, 412*, 256-282.

Cheetham, M. E., & Caplan, A. J. (1998). Structure, function and evolution of DnaJ: conservation and adaptation of chaperone function. *Cell Stress Chaperones, 3*(1), 28-36.

Chen, J., Yin, G., Lu, Y., Lou, M., Cheng, H., Ni, X., hu, G., Luo, C., Ying, K., Xie, Y., & Mao, Y. (2004). Cloning and characterization of a novel human cDNA encoding a J-domain protein (DNAJA5) from the fetal brain. *Int J Mol Med, 13*(5), 735-740.

Dickinson, D. J., Ward, J. D., Reiner, D. J., & Goldstein, B. (2013). Engineering the *Caenorhabditis elegans* genome using Cas9-triggered homologous recombination. *Nat Methods, 10*(10), 1028-1034.

Friedland, A. E., Tzur, Y. B., Esvelt, K. M., Colaiácovo, M. P., Church, G. M., & Calarco, J. A. (2013). Heritable genome editing in *C. elegans* via a CRISPR-Cas9 system. *Nat Methods, 10*(8), 741-743.

Garcia, S. M., Casanueva, M. O., Silva, M. C., Amaral, M. D., & Morimoto, R. I. (2007). Neuronal signaling modulates protein homeostasis in *Caenorhabditis elegans* post-synaptic muscle cells. *Genes Dev, 21*(22), 3006-3016.

Giardine, B., Riemer, C., Hardison, R. C., Burhans, R., Elnitski, L., Shah, P., Zhang, Y, Blankenberg, D., Albert, I., Taylor, J., Miller, W., Kent, W. J., & Nekrutenko, A. (2005). Galaxy: a platform for interactive large-scale genome analysis. *Genome Res, 15*(10),

1451-1455.

Jin, Y., Jorgensen, E., Hartwieg, E., & Horvitz, H. R. (1999). The *Caenorhabditis elegans* gene *unc-25* encodes glutamic acid decarboxylase and is required for synaptic transmission but not synaptic development. *J Neurosci, 19*(2), 539-548.

Jospin, M., Qi, Y. B., Stawicki, T. M., Boulin, T., Schuske, K. R., Horvitz, H. R., Bessereau, J. L., Jorgensen, E. M., & Jin, Y. (2009). A neuronal acetylcholine receptor regulates the balance of muscle excitation and inhibition in *Caenorhabditis elegans*. *PLoS Biol, 7*(12), e1000265.

Li, H., Coghlan, A., Ruan, J., Coin, L. J., Hériché, J. K., Osmotherly, L., Li, R., Liu, T., Zhang, Z., Bolund, L., Wong, G. K., Zheng, W., Dehal, P., Wang, J. & Durbin, R. (2006). TreeFam: a curated database of phylogenetic trees of animal gene families. *Nucleic Acids Res, 34*(Database issue), D572-580.

Lu, Z., & Cyr, D. M. (1998). The conserved carboxyl terminus and zinc finger-like domain of the co-chaperone Ydj1 assist Hsp70 in protein folding. *J Biol Chem, 273*(10), 5970-5978.

Marchler-Bauer, A., Derbyshire, M. K., Gonzales, N. R., Lu, S., Chitsaz, F., Geer, L. Y., Geer, R. C., He, J., Gwadz, M., Hurwitz, D. I., Lanczycki, C. J., Lu, F., Marchler, G. H., Song, J. S., Thanki, N., Wang, Z., Yamashita, R. A., Zhang, D., Zheng, C., & Bryant, S. H. (2015). CDD: NCBI's conserved domain database. *Nucleic Acids Res, 43*(Database issue), D222-226.

McIntire, S. L., Jorgensen, E., & Horvitz, H. R. (1993). Genes required for GABA function in *Caenorhabditis elegans*. *Nature, 364*(6435), 334-337.

McIntire, S. L., Reimer, R. J., Schuske, K., Edwards, R. H., & Jorgensen, E. M. (1997). Identification and characterization of the vesicular GABA transporter. *Nature, 389*(6653), 870-876.

Meyer, A. E., N. Hung, P. Yang, A. W. Johnson, & E. A. Craig. (2007) The specialized cytosolic J-protein, Jjj1, functions in 60S ribosomal subunit biogenesis. *Proc. Natl. Acad. Sci. USA*, 104: 1558-1563.

Muchowski, P. J., & Wacker, J. L. (2005). Modulation of neurodegeneration by molecular chaperones. *Nat Rev Neurosci, 6*(1), 11-22.

Ohtsuka, K., & Suzuki, T. (2000). Roles of molecular chaperones in the nervous system. *Brain Res Bull, 53*(2), 141-146.

Qiu, X. B., Shao, Y. M., Miao, S., & Wang, L. (2006). The diversity of the DnaJ/Hsp40 family, the crucial partners for Hsp70 chaperones. *Cell Mol Life Sci, 63*(22), 2560-2570.

Richmond, J. E., & Jorgensen, E. M. (1999). One GABA and two acetylcholine receptors function at the *C. elegans* neuromuscular junction. *Nat Neurosci, 2*(9), 791-797.

Sakahira, H., Breuer, P., Hayer-Hartl, M. K., & Hartl, F. U. (2002). Molecular chaperones as modulators of polyglutamine protein aggregation and toxicity. *Proc Natl Acad Sci U S A, 99 Suppl 4*, 16412-16418.

Sherman, M. Y., & Goldberg, A. L. (2001). Cellular defenses against unfolded proteins: a cell biologist thinks about neurodegenerative diseases. *Neuron, 29*(1), 15-32.

Stawicki, T. M., Takayanagi-Kiya, S., Zhou, K., & Jin, Y. (2013). Neuropeptides function in a homeostatic manner to modulate excitation-inhibition imbalance in *C. elegans*. *PLoS Genet, 9*(5), e1003472.

Szabo, A., Korszun, R., Hartl, F. U., & Flanagan, J. (1996). A zinc finger-like domain of the molecular chaperone DnaJ is involved in binding to denatured protein substrates. *EMBO J, 15*(2), 408-417.

Trinh, J., & Farrer, M. (2013). Advances in the genetics of Parkinson disease. *Nat Rev Neurol, 9*(8), 445-454.

Tsai, J., & Douglas, M. G. (1996). A conserved HPD sequence of the J-domain is necessary for YDJ1 stimulation of Hsp70 ATPase activity at a site distinct from substrate binding. *J Biol Chem, 271*(16), 9347-9354.

Vilariño-Güell, C., Rajput, A., Milnerwood, A. J., Shah, B., Szu-Tu, C., Trinh, J., Yu, I., Encarnacion, M., Munsie, L. N., Tapia, L., Gustavsson, E. K., Chou, P., Tatarnikov, I., Evans, D. M., Pishotta, F. T., Volta, M., Beccano-Kelly, D., Thompson, C., Lin, M. K., Sherman, H. E., Han, H. J., Guenther, B. L., Wasserman, W. W., Bernard, V., Ross, C. J., Appel-Cresswell, S., Stoessl, A. J., Robinson, C. A., Dickson, D. W., Ross, O. A., Wszolek, Z. K., Aasly, J. O., Wu, R. M., Hentati, F., Gibson, R. A., McPherson, P. S., Girard, M., Rajput, M., Rajput, A. H., & Farrer, M. J. (2014). DNAJC13 mutations in Parkinson disease. *Hum Mol Genet, 23*(7), 1794-1801.

Von Stetina, S. E., Treinin, M., & Miller, D. M. (2006). The motor circuit. *Int Rev Neurobiol, 69*, 125-167.

Zhong, M., W. Niu, Z. J. Lu, M. Sarov, J. I Murray, Janette, J., Raha, D., Sheaffer, K. L., Lam, H. Y., Preston, E., Slightham, C., Hillier, L. W., Brock, T., Agarwal, A., Auerbach, R., Hyman, A. A., Gerstein, M., Mango, S. E., Kim, S. K., Waterston, R. H., Reinke, V., & Snyder, M. (2010). Genome-Wide Identification of Binding Sites Defines Distinct Functions for *Caenorhabditis elegans* PHA-4/FOXA in Development and Environmental Response. *PLoS Genet.* 6:e1000848.

Chapter 5

A single amino acid substitution in a highly conserved eIF3 subunit EIF-3.G affects E/I balance

Abstract

Eukaryotic initiation factor 3 (eIF3) are involved in various steps of translation initiation and several eIF3 subunit proteins are highly conserved through evolution. However, their molecular roles in animals remain largely unknown. Here, from a forward genetic suppressor screen for *acr-2(gf) C. elegans* seizure model, we isolated a viable single amino acid substitution mutation *eif-3.g(ju807)* in the gene encoding eIF3 subunit g EIF-3.G/EIF3G. The mutation affects a conserved cysteine in a zinc-finger motif of the protein. We generated an *eif-3.g* null allele which causes homozygous larval arrest phenotype, which could be rescued by expression of GFP-tagged EIF-3.G. EIF-3.G protein showed ubiquitous expression pattern. Importantly, expression of wild type *eif-3.g* specifically in cholinergic motor neurons could affect excitation-inhibition (E/I) imbalance of the *acr-2(gf)* animals. In addition, the conserved RNA recognition motif in EIF-3.G was required for its effect on E/I balance. Using tissue-specific knockout techniques, we generated a transgenic strain that causes loss of EIF-3.G specifically in cholinergic motor neurons for further analysis. Overall, our results demonstrate that EIF-3.G in cholinergic motor neurons affect pathways that regulate E/I balance.

Introduction

Initiation of translation in eukaryotes involves a number of eukaryotic initiation factors (eIFs). eIF3 is known to have many functions in initiation of protein translation. It interacts with other eIF complexes (eIF1, eIF5, eIF4B and eEIF4G), and also stabilizes the interaction between tRNA-bound eIF2 complex to the ribosome 40S subunit (Chaudhuri, Chowdhury, & Maitra,

1999; Erzberger et al., 2014; Hershey & Merrick, 2000). eIF3 is composed of 10 to 13 different subunit proteins (eIF3a to eIF2m) in mammalian cells. All 13 proteins have orthologs in *C. elegans* (Rezende et al., 2014). Budding yeast has 5 orthologs of mammalian eIF3 subunits (eIF3a, eIf3b, eIF3c, eIF3g and eIF3i) that are all essential for translation initiation *in vivo* (Asano, Phan, Anderson, & Hinnebusch, 1998; Cuchalová et al., 2010; Naranda, Kainuma, MacMillan, & Hershey, 1997; Verlhac, Chen, Hanachi, Hershey, & Derynck, 1997; Vornlocher, Hanachi, Ribeiro, & Hershey, 1999). On the other hand, *in vitro* analyses suggest that mammalian eIF3 does not require eIF3g or eIF3i for initiation of translation, and lack of the two subunits do not largely affect protein synthesis (Masutani, Sonenberg, Yokoyama, & Imataka, 2007). Both yeast and mammalian eIF3g and eIF3i are known to bind to each other (Asano, et al., 1998; Verlhac, et al., 1997).

Molecular functions of eIF3 in animals *in vivo* remain mostly unknown, partly due to the lack of genetic models available. Knockdown of the highly conserved eiF3 subunits at early developmental stage result in severe developmental defects in *C. elegans* and in zebrafish (Choudhuri, Evans, & Maitra, 2010; Choudhuri, Maitra, & Evans, 2013; Kamath et al., 2003; Sönnichsen et al., 2005). Interestingly, in *C. elegans*, knockdown of eIF3 subunit proteins at late larval stage extends lifespan, suggesting that eIF3 may not be essential for survival after development(Curran & Ruvkun, 2007).

Though initial studies focused on general role of eIF3 in translation, recent evidence suggests that it can have more specific roles on certain mRNAs. In human cell culture, PAR-CLIP analysis show that eIF3 binds to only a subset of mRNAs, suggesting that there can be specific regulation of translation by eIF3 on those mRNAs (Lee, Kranzusch, & Cate, 2015). Binding of eIF3 is mainly detected in 5' UTR, consistent with the 5' UTR being the major site of translational regulation (Jackson, Hellen, & Pestova, 2010; Lee, et al., 2015). The binding of eIF3 to the 5'UTR is dependent on secondary structures of the 5'UTR, further supporting roles of eIF3 on specific mRNAs. In addition, knockdown of eIF3 subunit h in zebrafish leads to

decreased levels of polysome-associated mRNAs suggesting decreased level of translation (Choudhuri, et al., 2013). The mRNAs targeted by eIF3h are predominantly from neural-associated genes, implying that there is tissue-specific regulation of mRNA translation mediated by eIF3.

Coordinated locomotion of *C. elegans* requires the balanced activity of excitatory and inhibitory motor neurons that synapse onto the body wall muscle (Jorgensen, 2005). Previously, we characterized a mutant *acr-2(gf)* that exhibits over-excitation of cholinergic motor neurons accompanied by decreased activity of GABAergic motor neurons(Jospin et al., 2009). The behavioral outcome of this excitation-inhibition (E/I) imbalance is that the animals have locomotion defects and show spontaneous whole-body muscle contraction termed convulsion, providing a behavioral readout of the E/I imbalance in the locomotor circuit (Jospin, et al., 2009; Qi et al., 2013; Stawicki, Takayanagi-Kiya, Zhou, & Jin, 2013). We reasoned that characterization of genetic modifiers of the convulsion phenotype can lead to previously unknown pathways that regulate E/I balance.

Here we report a single amino acid substitution mutation in a highly conserved translation initiation factor subunit *eif-3.g*, identified from a forward genetic suppressor screen of *acr-2(gf)*. We find that wild type *eif-3.g* functions in cholinergic motor neurons and affects the E/I balance.

Methods

C. elegans genetics and strains

All *C. elegans* strains were kept at 22.5°C and maintained following the standard procedures. The suppressor screen for *acr-2(gf)* convulsion was performed as previously described (Jospin, et al., 2009) (Y. B. Qi and Y. J., unpublished data). The obtained CZ21291 *eif-3.g(ju807); acr-2(gf)* double mutant was subjected to whole-genome sequencing (Beijing Genomics Institute), and the data were analyzed on Galaxy platform (Giardine et al., 2005;

Goecks, Nekrutenko, Taylor, & Team, 2010). Genetic mapping using outcrossed strains lead to the identification of the missense *ju807* mutation in *eif-3.g*. Strains used in this chapter are listed on Table 5..

Molecular biology and cloning

Molecular biology was performed according to standard procedures. Gateway cloning techniques (Invitrogen, CA) were used to generate expression vectors. cDNA clones were generated using mRNA isolated from wild-type and CZ21291 *eif-3.g(ju807); acr-2(n2420)* mixed-stage animals using Trizol and Superscript III (ThermoFisher Scientific), according to manufacturer's instructions. PCR using SL1 GTTTAATTACCCAAGTTTGAG and a reverse primer designed at the predicted 3'UTR OST597 AACTATGATATTTTACATTGGACAG amplified the cDNA fragment corresponding to *eif-3.g* coding sequence ("Wormbase web site, release WS251," 2015). Constructs used in this chapter are listed on Table 5.2. Generation of Single-copy insertion of *Peif-3.g-loxp-GFP::EIF-3.G(WT)-loxp* was made at ChrIV site cxTi10882 (pCFJ201) by microinjections of modified vectors (Wang and Jin, unpublished data), essentially as described in Chapter II. Briefly, a construct expressing Cas9 in the germline along with sgRNA targeted to cxTi10882 and *Peif-3.g-loxp-GFP::EIF-3.G(WT)-loxp* with homology arms for cxTi10882 were injected to N2 animals. F2 animals were screened for hygromycin drug resistance. Single copy insertion was confirmed by PCR using primers designed outside of the homology arms. The obtained strain was outcrossed twice before being used in experiments.

Generation of deletion allele was performed essentially as described in Chapter IV. Following sgRNA sequence was used for sgRNA targeting *eif-3.g* gene: CAATTCACAAGAAATCGCGC.

Quantification of convulsion frequency

Convulsion frequencies of *acr-2(gf)* strains were quantified as previously described (Stawicki, et al., 2013). The quantification was repeated at least twice per genotype on different days. At least two independent lines were used to score the phenotype of animals with extrachromosomal arrays.

Confocal microscopy

Animals at L4 stage were imaged using Zeiss LSM 710 confocal microscope (63x objective). Animals were placed on 4% agar pads and immobilized by 1mM Levamisole. Maximum-intensity z stack images were obtained at 0.5μm intervals. Obtained images were processed using ImageJ.

Results

A single amino acid substitution in EIF-3.G suppresses *acr-2(gf)* convulsion

We isolated *ju807* from an EMS forward genetic screen for suppressors of *acr-2(gf)* convulsion phenotype. *ju807* strongly suppressed the convulsion of *acr-2(gf)* (Figure 5.1A). From whole-genome sequencing analysis of the double mutant, we identified a missense mutation in *eif-3.g*, which encodes *C. elegans* homolog of eukaryotic translation initiation factor subunit g (EIF3G) (Figure 1B). *ju807* substitutes a highly conserved cysteine to tyrosine (C130Y) in the zinc finger motif in EIF3G domain (Figure 5.1B, 5.2). Since EIF3G protein is known to be involved in protein translation, we first examined if the suppression effect is due to the decreased level of ACR-2 protein. Translational reporter of ACR-2 did not show a large difference in the expression level of ACR-2::GFP in the *eif-3.g(ju807)* mutant background (Figure 5.3), suggesting that *ju807* mutants retain the ability to translate ACR-2 protein.

Overexpression of wild-type *eif-3.g* driven by 1.5 kb upstream promoter reversed the suppression effect in the double mutant, confirming that *eif-3.g(ju807)* is the causative mutation (Fig. 5.1A). Interestingly, overexpression of the mutant *eif-3.g(ju807)* caused mild suppression of *acr-2(gf)* convulsions. In addition, *eif-3.g(ju807)* behaved as a semi-dominant allele, as *eif-3.g(+/ju807)* heterozygous animals reduced *acr-2(gf)* convulsion frequency, but not to the extent of *eif-3.g(ju807)* homozygous mutant (Figure 5.1C).

***eif-3.g(ju807)* is not a null allele**

In order to further examine the function of *eif-3.g,* we generated a deletion allele of *eif-3.g* by CRISPR-mediated genome-editing (Dickinson, Ward, Reiner, & Goldstein, 2013; Friedland et al., 2013)(Wang and Jin, unpublished data). The obtained 19bp deletion allele *eif-3.g(ju1327)* causes a frameshift in the conserved EIF3G domain, presumably resulting in a null allele, hereafter *eif-3.g(0)*. We found that animals with homozygous *eif-3.g(0)* show early larval arrest phenotype, consistent with previously reported RNAi results (Kamath, et al., 2003; Sönnichsen, et al., 2005). Heterozygous *eif-3.g(+/0)* did not have significant effect on *acr-2(gf)* convulsions, suggesting that *ju807* is not a null allele (Figure 5.1C). Collectively, these results indicate that the *eif-3.g(ju807)* allele is a gain-of-function mutation. The mutant protein may act as a weak dominant negative or a neomorph with novel functions, which leads to suppression of *acr-2(gf)* convulsion.

***eif-3.g* functions in cholinergic motor neurons and it requires the RRM motif**

Transcriptional reporter of *eif-3.g* showed ubiquitous expression pattern (Figure 5.4A). In order to examine in which tissue *eif-3.g* functions to regulate convulsions, we analyzed transgenic animals that express *eif-3.g* in tissue-specific manner in the *eif-3.g(ju807); acr-2(n2420)* double mutant background. Neuron-specific overexpression of wild type *eif-3.g* was sufficient to reverse the suppression effect whereas expression in the muscle did not affect

convulsion (Figure 5.1D). Further, expression of *eif-3.g(wt)* only in the cholinergic motor neurons caused convulsion phenotype, suggesting that *eif-3.g* functions in cholinergic motor neurons and affects E/I balance. Importantly, animals expressing a truncated version of EIF-3.G that lacks the highly conserved RNA recognition motif (RRM) did not show increase in convulsion (Figure 5.1D, 2), suggesting that RRM is necessary for the function of EIF-3.G.

Animals expressing EIF-3.G tagged with GFP at the N-terminus were analyzed In order to examine the localization of EIF-3.G. In order to generate a translational reporter of EIF-3.G, we tagged GFP to the N-terminus EIF-3.G cDNA construct (Figure 5.4B) The GFP-tagged EIF-3.G was functional since it could increase the convulsion frequency when expressed pan-neuronally in *eif-3.g(ju807); acr-2(gf)* double mutant.

Generation of cholinergic motor neuron-specific knockout of *eif-3.g*

What can be the mechanism of suppression by *eif-3.g(ju807)*? The larval arrest phenotype in *eif-3.g(0)* and the broad expression pattern of the gene suggested that the protein has functions in various tissues. However, cholinergic motor neuron-specific expression of wild type EIF-3.G was sufficient to cause the convulsion in *eif-3.g(ju807); acr-2(gf)* double mutant background (Figure 5.1D). One possible explanation is that EIF-3.G is involved in different molecular pathways in different tissues, but its function specifically in cholinergic motor neurons is required for the convulsion phenotype of *acr-2(gf)*. If *eif-3.g(ju807)* suppresses convulsion by acting as a weak dominant-negative in cholinergic motor neurons, it is possible that the loss of EIF-3.G only in those neurons leads to a similar suppression effect.

To examine this hypothesis, I planned to assess the effect of tissue-specific knockout of *eif-3.g.* To this end, I generated a single copy insertion of loxp-flanked *Peif-3.g-GFP::EIF-3.G*

(Figure 5.4B). The allele was functional, as it could rescue the larval arrest phenotype in the *eif-3.g(0)* mutant background and the animals reached the adult stage. However, it is noteworthy that GFP::EIF-3.G did not rescue the sterility of animals with *eif-3.g(0),* possibly

because of lack of transgene expression in the germline or cells required for germline maturation, or incomplete function of GFP::EIF-3.G. As animals expressing *Peif-3.g-loxp-GFP::EIF-3.G-loxp* in the *eif-3.g(0); acr-2(gf)* background exhibited convulsion, I considered that the functions of EIF-3.G required in the neurons to generate *acr-2(gf)* convulsion is retained in the GFP-tagged protein.

The GFP::EIF-3.G signals were found ubiquitously in the animal (Figure 5.4C). Importantly, the EIF-3.G::GFP signal was higher in the *acr-2(gf)* background. I confirmed that expression of nuclear Cre recombinase (nCre) under cholinergic motor neuron-specific promoter could excise the targeted region (Fig. 5.4D, E). This strain will be useful to study the roles of EIF-3.G in cholinergic motor neurons.

Discussion

Here I characterized a single amino acid substitution mutation of a highly conserved eIF3 subunit g protein EIF-3.G. I found that EIF-3.G expression in cholinergic motor neurons is important for the convulsion phenotype of *acr-2(gf).* Also I found that *eif-3.g(0)* animals show larval arrest phenotype. One possible mechanism of suppression by *eif-3.g(ju807)* is that EIF-3.G(C130Y) behaves as a weak dominant-negative but still retains some function of the wild type EIF-3.G. In this case, the reduced function of EIF-3.G in cholinergic motor neurons may cause the suppression in *eif-3.g(ju807); acr-2(gf)* double mutants. Since the protein retains functions required for growth of the animal, the homozygous mutants are viable. Another mechanism can account for the suppression by *eif-3.g(ju807)*. *eif-3.g(ju807)* may have gain-of-function mechanisms different from interfering with only the function of EIF-3.G protein. For example, it may activate pathways that are not activated by the wild type protein. In future experiments, it will be important to compare the synaptic morphology and neural activities in the motor neurons to distinguish these possibilities.

Is EIF-3.G, and possibly the eIF3 complex, required for translation of a specific set of proteins in the cholinergic motor neurons, or functions as a general translation initiation factor involved in translation of all mRNAs? As I found that the RRM motif is required for the function of the protein, analyzing the interaction of EIF-3.G and mRNA in cholinergic motor neurons will provide further insight of how the protein contributes to the regulation of the function of cholinergic motor neurons and thus the regulation of E/I balance in the entire locomotion circuit.

Acknowledgements

I thank Qi Y.B, for first isolating the *ju807* allele from forward genetic suppressor screen using *acr-2(gf)*.

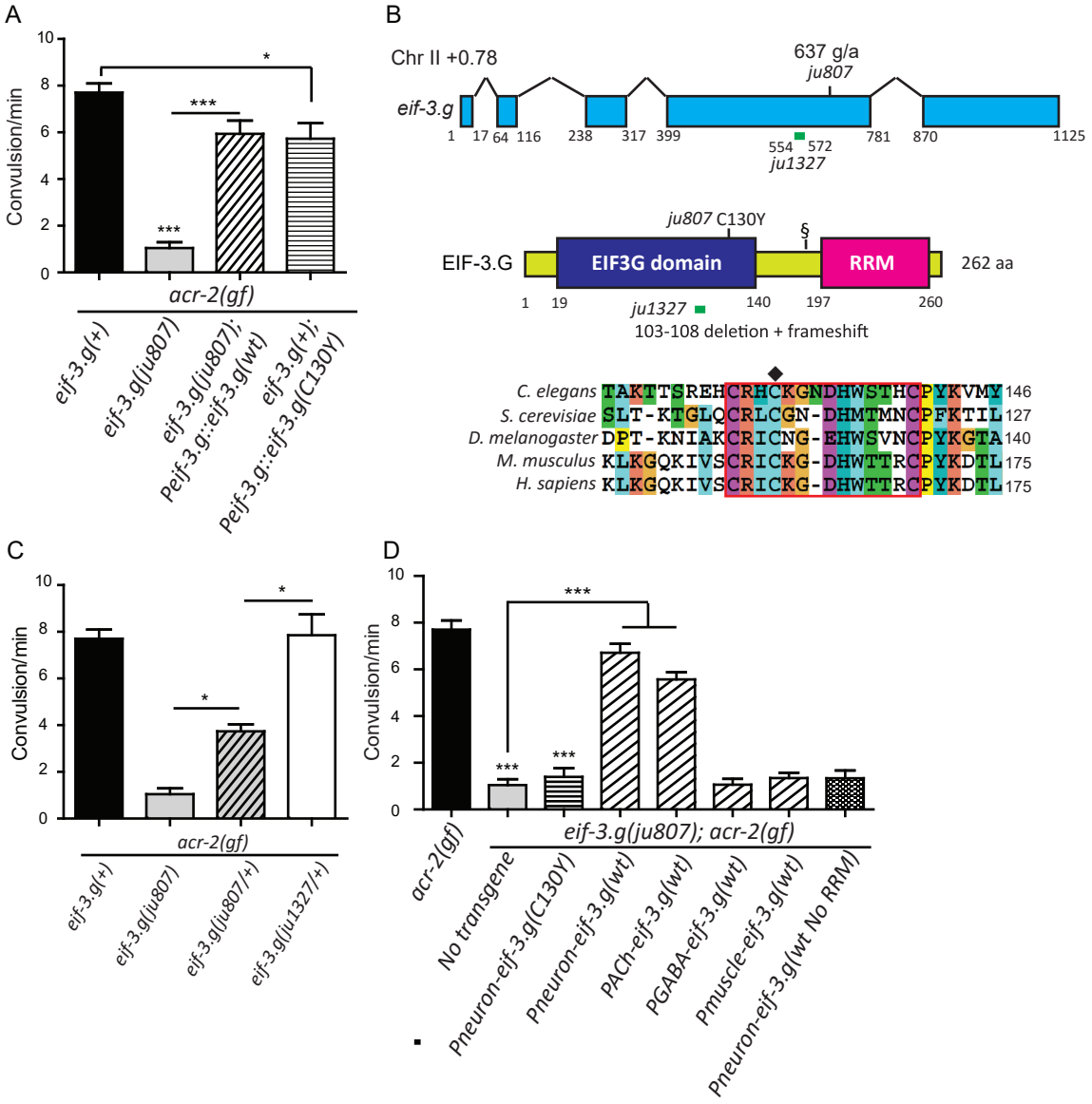

Figure 5.1. *eif-3.g* functions in cholinergic motor neurons and affects E/I balance. (A) Quantification of convulsion frequencies. *eif-3.g(ju807)* suppresses convulsion. Expression of *eif-3.g(wt)* in the double mutant background reverses the suppression effect. Expression of *eifj-3.g(C130Y)* in the *acr-2(gf)* single mutant caused slight suppression of convulsion. (B) Gene and protein structure of *C. elegans eif-3.g.* middle panel shows the positions of mutations addressed in the text. § marks the position of stop-codon insertion for expression of truncated protein. Lower panel shows alignment of the protein sequence near the C to Y mutation in *eif-3.g(ju807)*, marked by ◆. Red box marks the conserved zinc finger motif. (C) *eif-3.g(ju807)* behaves as a semi-dominant suppressor on *acr-2(gf)* convulsion phenotype, different from the *eif-3.g(ju1327)* null allele. (D) Pan-neuronal- or cholinergic motor neuron-specific expression of *eif-3.g(wt)* is sufficient for causing the convulsion phenotype in *eif-3.g(ju807); acr-2(gf)* double mutants. The function requires the RRM domain. (A,C,D) Statistics: One way ANOVA followed by Bonferroni's post-hoc test. *: $p < 0.05$, ***: $p < 0.001$. $n > 16$ for all strains.

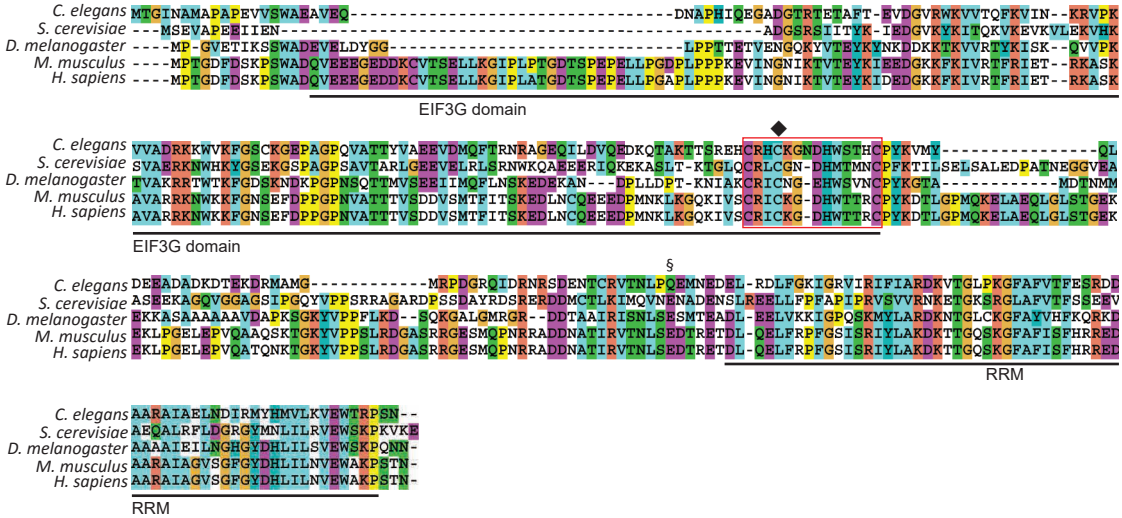

Figure 5.2. Alignment of full-length EIF-3.G proteins. § marks the location of STOP codon insertion in "no RRM" expression experiments. EIF3G and RRM domains are marked by black lines. Red box marks the C2HC-type zinc finger motif.

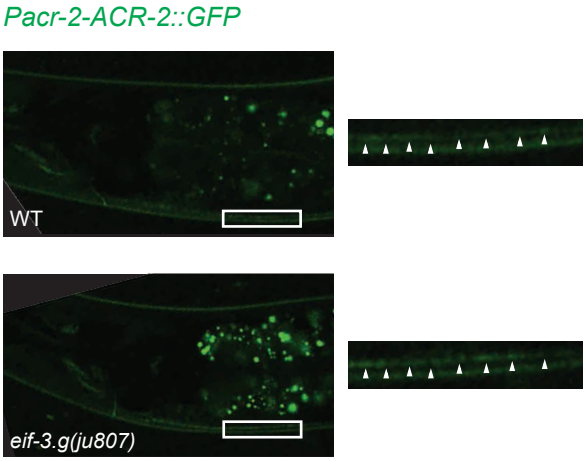

Figure 5.3. ACR-2::GFP signals are not affected by *eif-3.g(ju807)*. Confocal images from animals expressing ACR-2::GFP in *eif-3.g(wt)* (top) or *eif-3.g(ju807)* background.

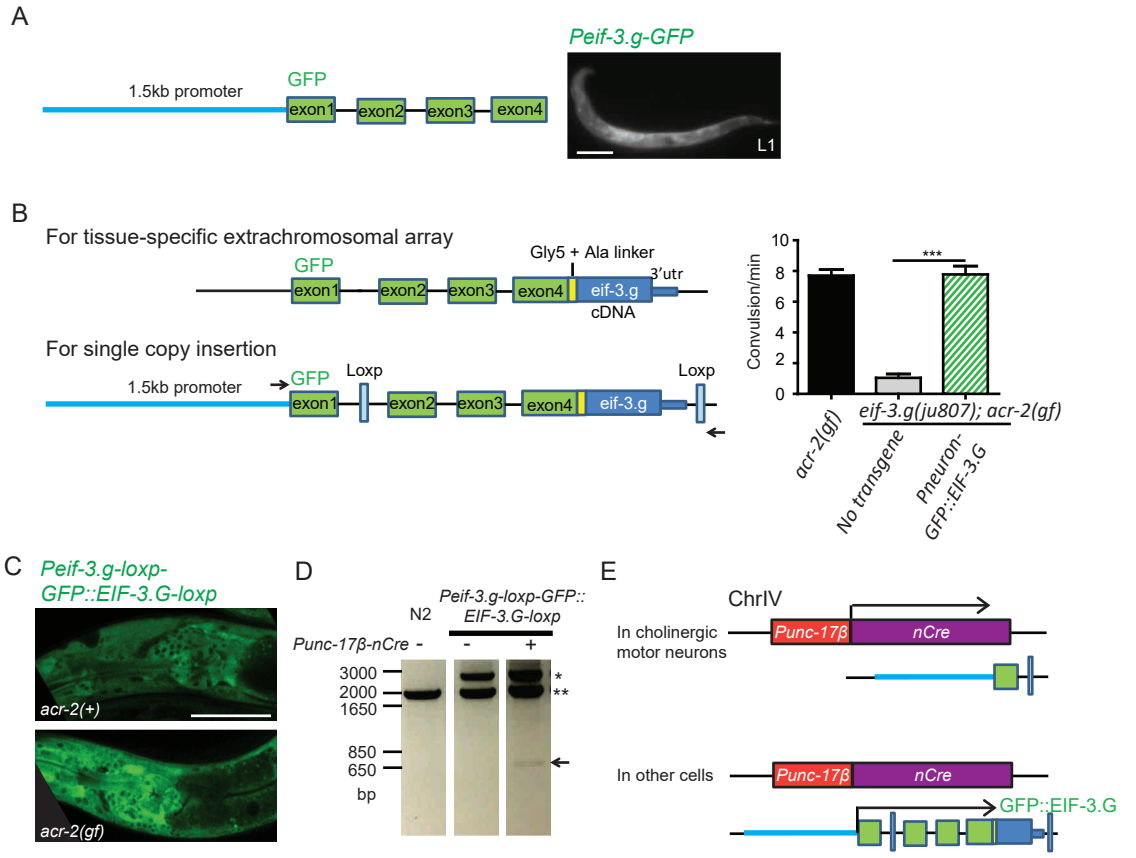

Figure 5.4. Generation of cholinergic neuron-specific knockout of *eif-3.g* using a functional GFP-tagged protein. (A) (Left) Structure of transcriptional reporter of *eif-3.g*. (Right) An animal expressing the transcriptional reporter, exhibiting diffused expression throughout the body. Scale bar: 20µm. (B) (Left) Structures of constructs for GFP-tagged EIF-3.G. (Right) Quantification of convulsion frequency. Expression of GFP-tagged EIF-3.G in neurons can reverse the suppression. n > 16. Statistics: one-way ANOVA followed by Bonferroni's post-hoc test. ***: $p < 0.01$. (C) Confocal images showing GFP::EIF-3.G signals expressed from single-copy inserted allele. The GFP::EIF-3.G signal is stronger in the *acr-2(gf)* background. (Top) *eif-3.g(0); Peif-3.g-loxp-GFP::EIF-3.G-loxp* (Bottom) *eif-3.g(0); Peif-3.g-loxp-GFP::EIF-3.G-loxp; acr-2(gf)* (D) Agarose/EtBR image of PCR products using primers ost451 and ost812 to detect the excision of floxed region. Cre expression in cholinergic motor neurons caused excision resulted in a smaller fragment (marked by arrow). * marks PCR product from unexcised transgene. ** marks PCR product from endogenous copy of *eif-3.g* on ChrII. (E) Excision of *GFP::EIF-3.G* sequence only occurs in cholinergic motor neurons which express nCre.

Table 5.1. Strains used in this study.

Strain number	genotype
MT6242	*acr-2(n2420)X*
CZ21291	*eif-3.g(ju807)II; acr-2(n2420)X*
CZ22197	*eif-3.g(ju807)II*
CZ22974	*eif-3.g(ju1327)/mnC1 II*
CZ22976	*acr-2(n2420)X; Peif-3.g::eif-3.g(ju807)(juEx7015)*
CZ22978	*eif-3.g(ju807)II; acr-2(n2420)X; Prgef-1-eif-3.g(wt)(juEx7017)*
CZ22980	*eif-3.g(ju807)II; acr-2(n2420)X; Pmyo-3-eif-3.g(wt)(juEx7019)*
CZ22982	*eif-3.g(ju807)II; acr-2(n2420)X; Punc-17b-eif-3.g(wt)(juEx7021)*
CZ23791	*eif-3.g(ju807)II; acr-2(n2420)X; Punc-25-eif-3.g(wt)(juEx7439)*
CZ23310	*eif-3.g(ju1327)/mnC1 II; acr-2(n2420)*
CZ24079	*eif-3.g(ju1327)/mnC1 II; Peif-3.g-GFP::EIF-3.G(juSi320)*
CZ24080	*eif-3.g(ju1327)/mnC1 II; Peif-3.g-GFP::EIF-3.G(juSi320); acr-2(n2420*
CZ23209	*eif-3.g(+)/mnC1 II; acr-2(n2420)*
CZ24064	*eif-3.g(+)/mnC1 II; Peif-3.g-GFP::EIF-3.G(juSi320); acr-2(n2420)*
CZ12338	*Pacr-2-ACR-2::GFP(oxSi39)*
CZ23854	*eif-3.g(ju807); Pacr-2-ACR-2::GFP(oxSi39)*

Table 5.2. Constructs used in this study.

pCZGY number	Plasmid	Construction notes
pCZGY3006	eif-3.G wt genomic pcr8	PCR amplification of eif-3.g with its promoter region using ost 450 and 451 with N2 lysate as template. Cloned into TopoPCR8 vector.
pCZGY3007	eif-3.G C130Y genomic pcr8	PCR amplification of eif-3.g with its promoter region using ost 450 and 451 with CZ21291 lysate as template. Cloned into TopoPCR8 vector.
pCZGY3008	eif3g_cDNA_pcr8_isoforma	PCR8 clone from N2 cDNA using SL1 and ost597.
pCZGY3009	eif3gC130Y_cDNA_pcr8_isoforma	PCR8 clone from cz21291 cDNA using SL1 and ost597.
pCZGY3010	Prgef-1::eif3-g(wt)	LR reaction between pCZGY66 and pSK142
pCZGY3012	Pmyo-3::eif-3.g(wt)	LR reaction between pCZGY925 and pSK142
pCZGY3014	Punc-17b::eif-3.g(wt)	LR reaction between pczgy1091 and pSk142
pCZGY3015	Punc-17b::eif-3.g(C130Y)	LR reaction between pczgy1091 and psk143
pCZGY3016	Punc-25::eif-3.g(wt)	LR reaction between pczgy80 and psk142
pCZGY3018	PCR8 eif-3.g::GFP(N-terminal tag)	Gibson assembly oST659+oST653 for GFP Ost660+661 for backbone (pSK142)
pCZGY3019	PCR8 eif-3.g(C130Y)::GFP(N-terminal	Gibson assembly oST659+oST653 for GFP Ost660+661 for backbone (pSK143)
pCZGY3020	Prgef-1::GFP-EIF-3.G(WT) N	LR reaction between PCZGY66 and pSK160
pCZGY3021	Prgef-1::GFP-EIF-3.G(C13oY) N	LR reaction between pCZGY66 and pSK163
pCZGY2721	PCR8 eif-3.g(wt) without RRM	PCR site directed mutagenesis on pSK169
pCZGY2722	PCR8 eif-3.g(C130Y) without RRM	PCR site directed mutagenesis on pSK170
pCZGY3022	Prgef-1::eif-3.g(wt) without RRM	LR reaction between pCZGY66xpSK171
pCZGY3023	Prgef-1::eif-3.g(C130Y) without RRM	LR reaction between pCZGY66xpSK172
pCZGY3024	PCR8 gfp::eif-3.g(wt) without RRM	PCR site directed mutagenesis using ost675 and 676 on pSK160
pCZGY3025	PCR8 GFP::eif-3.g(C130Y) without RRM	PCR site directed mutagenesis using ost675 and 676 on pSK163
pCZGY3026	Prgef-1::gfp::eif-3.g(wt) without RRM	LR reaction pCZGY66 x pSK179
pCZGY3027	Prgef-1::gfp::eif-3.g(C130Y) without RRM	LR reaction pczgy66 x pSk180
pCZGY3028	loxp flanked eif-3.g_GFP_cDNA	PCR site directed mutagenesis followed by KDL reaction (NEB)
pCZGY3030	ChrIV gfp-eif-3.g	LR reaction between pCFJ201 x pSK246

References

Asano, K., Phan, L., Anderson, J., & Hinnebusch, A. G. (1998). Complex formation by all five homologues of mammalian translation initiation factor 3 subunits from yeast Saccharomyces cerevisiae. *J Biol Chem, 273*(29), 18573-18585.

Chaudhuri, J., Chowdhury, D., & Maitra, U. (1999). Distinct functions of eukaryotic translation initiation factors eIF1A and eIF3 in the formation of the 40 S ribosomal preinitiation complex. *J Biol Chem, 274*(25), 17975-17980.

Choudhuri, A., Evans, T., & Maitra, U. (2010). Non-core subunit eIF3h of translation initiation factor eIF3 regulates zebrafish embryonic development. *Dev Dyn, 239*(6), 1632-1644.

Choudhuri, A., Maitra, U., & Evans, T. (2013). Translation initiation factor eIF3h targets specific transcripts to polysomes during embryogenesis. *Proc Natl Acad Sci U S A, 110*(24), 9818-9823.

Cuchalová, L., Kouba, T., Herrmannová, A., Dányi, I., Chiu, W. L., & Valásek, L. (2010). The RNA recognition motif of eukaryotic translation initiation factor 3g (eIF3g) is required for resumption of scanning of postermination ribosomes for reinitiation on GCN4 and together with eIF3i stimulates linear scanning. *Mol Cell Biol, 30*(19), 4671-4686.

Curran, S. P., & Ruvkun, G. (2007). Lifespan regulation by evolutionarily conserved genes essential for viability. *PLoS Genet, 3*(4), e56.

Dickinson, D. J., Ward, J. D., Reiner, D. J., & Goldstein, B. (2013). Engineering the *Caenorhabditis elegans* genome using Cas9-triggered homologous recombination. *Nat Methods, 10*(10), 1028-1034.

Erzberger, J. P., Stengel, F., Pellarin, R., Zhang, S., Schaefer, T., Aylett, C. H., Cimermančič, P., Boehringer, D., Sali, A., Aebersold, R., & Ban, N. (2014). Molecular architecture of the 40S·eIF1·eIF3 translation initiation complex. *Cell, 158*(5), 1123-1135.

Friedland, A. E., Tzur, Y. B., Esvelt, K. M., Colaiácovo, M. P., Church, G. M., & Calarco, J. A. (2013). Heritable genome editing in *C. elegans* via a CRISPR-Cas9 system. *Nat Methods, 10*(8), 741-743.

Giardine, B., Riemer, C., Hardison, R. C., Burhans, R., Elnitski, L., Shah, P., Zhang, Y, Blankenberg, D., Albert, I., Taylor, J., Miller, W., Kent, W. J., & Nekrutenko, A. (2005). Galaxy: a platform for interactive large-scale genome analysis. *Genome Res, 15*(10), 1451-1455.

Goecks, J., Nekrutenko, A., Taylor, J., & Team, G. (2010). Galaxy: a comprehensive approach for supporting accessible, reproducible, and transparent computational research in the life sciences. *Genome Biol, 11*(8), R86.

Hershey, J. W. B., & Merrick, W. C. (2000). The pathway and mechanism of initiation of protein synthesis. In N. Sonenberg, J. W. B. Hershey & M. B. Mathews (Eds.), *Translational Control of Gene Expression* (pp. 33-88). Cold Spring Harbor: Cold Spring Harbor Laboratory.

Jackson, R. J., Hellen, C. U., & Pestova, T. V. (2010). The mechanism of eukaryotic translation initiation and principles of its regulation. *Nat Rev Mol Cell Biol, 11*(2), 113-127.

Jorgensen, E. M. (2005). GABA. *WormBook*, 1-13.

Jospin, M., Qi, Y. B., Stawicki, T. M., Boulin, T., Schuske, K. R., Horvitz, H. R., Bessereau, J. L., Jorgensen, E. M., & Jin, Y. (2009). A neuronal acetylcholine receptor regulates the balance of muscle excitation and inhibition in *Caenorhabditis elegans*. *PLoS Biol, 7*(12), e1000265.

Kamath, R. S., Fraser, A. G., Dong, Y., Poulin, G., Durbin, R., Gotta, M., Kanapin, A., Le Bot, N., Moreno, S., Sohrmann, M., Welchman, D. P., Zipperlen, P., & Ahringer, J. (2003). Systematic functional analysis of the *Caenorhabditis elegans* genome using RNAi. *Nature, 421*(6920), 231-237.

Lee, A. S., Kranzusch, P. J., & Cate, J. H. (2015). eIF3 targets cell-proliferation messenger RNAs for translational activation or repression. *Nature, 522*(7554), 111-114.

Masutani, M., Sonenberg, N., Yokoyama, S., & Imataka, H. (2007). Reconstitution reveals the functional core of mammalian eIF3. *EMBO J, 26*(14), 3373-3383.

Naranda, T., Kainuma, M., MacMillan, S. E., & Hershey, J. W. (1997). The 39-kilodalton subunit of eukaryotic translation initiation factor 3 is essential for the complex's integrity and for cell viability in Saccharomyces cerevisiae. *Mol Cell Biol, 17*(1), 145-153.

Qi, Y. B., Po, M. D., Mac, P., Kawano, T., Jorgensen, E. M., Zhen, M., & Jin, Y. (2013). Hyperactivation of B-type motor neurons results in aberrant synchrony of the *Caenorhabditis elegans* motor circuit. *J Neurosci, 33*(12), 5319-5325.

Rezende, A. M., Assis, L. A., Nunes, E. C., da Costa Lima, T. D., Marchini, F. K., Freire, E. R., Reis, C. R., & de Melo Neto, O. P. (2014). The translation initiation complex eIF3 in trypanosomatids and other pathogenic excavates--identification of conserved and divergent features based on orthologue analysis. *BMC Genomics, 15*, 1175.

Sönnichsen, B., Koski, L. B., Walsh, A., Marschall, P., Neumann, B., Brehm, M., et al. (2005). Full-genome RNAi profiling of early embryogenesis in *Caenorhabditis elegans*. *Nature, 434*(7032), 462-469.

Stawicki, T. M., Takayanagi-Kiya, S., Zhou, K., & Jin, Y. (2013). Neuropeptides function in a homeostatic manner to modulate excitation-inhibition imbalance in C. elegans. *PLoS Genet, 9*(5), e1003472.

Verlhac, M. H., Chen, R. H., Hanachi, P., Hershey, J. W., & Derynck, R. (1997). Identification of partners of TIF34, a component of the yeast eIF3 complex, required for cell proliferation and translation initiation. *EMBO J, 16*(22), 6812-6822.

Vornlocher, H. P., Hanachi, P., Ribeiro, S., & Hershey, J. W. (1999). A 110-kilodalton subunit of translation initiation factor eIF3 and an associated 135-kilodalton protein are encoded by the Saccharomyces cerevisiae TIF32 and TIF31 genes. *J Biol Chem, 274*(24), 16802-16812.

Wormbase web site, release WS251. (2015). from http://www.wormbase.org.

Chapter 6

Conclusion and Discussion

In my dissertation, I have identified multiple genes and pathways involved in regulation of excitation-inhibition (E/I) balance in *C. elegans* locomotion circuit. In Chapter I, I discussed conservation of genes involved in regulation of neural activity, and introduced several seizure models of *C. elegans*. Throughout the dissertation, I used a genetic seizure model *acr-2(gf)* established previously in the lab to examine the genetic and molecular pathways involved in regulation of circuit activity. *acr-2(gf)*carries an activating mutation in the pore-lining transmembrane domain of an ionotropic acetylcholine receptor subunit ACR-2, that causes E/I imbalance in the motor neuron circuit and aberrant synchronous activity of motor neurons (Jospin et al., 2009; Qi et al., 2013). Strengths of this model include the robustness of the phenotype and the unnecessity of drug treatments to cause the seizure events. The behavioral convulsion phenotype of *acr-2(gf)* is easily detectable under dissecting microscope and provide consistent readout of the E/I imbalance.

An advantage of using *C. elegans* as a seizure model is that genetic screens can be performed relatively easily (Brenner, 1974). Chapters II to V described genetic modifiers of *acr-2(gf)* convulsion, identified from a forward genetic screen or from candidate gene approach.

In Chapter II, I characterized an ionotropic receptor isolated from a forward genetic screen for *acr-2(gf)* suppressors. A gain-of-function mutation of an acetylcholine-gated chloride channel group protein LGC-46 strongly suppressed the *acr-2(gf)* convulsions. Strikingly, I found that LGC-46 localizes presynaptically to the axons of cholinergic motor neurons and forms puncta which co-localize with presynaptic proteins. Presynaptic chloride channels were previously found in other animals including mammals (Ruiz, Campanac, Scott, Rusakov, & Kullmann, 2010; Trojanova et al., 2014; Turecek & Trussell, 2001; Xiong et al., 2014), but their

localization and precise functions remain mostly unknown partly due to lack of genetic models to decipher pre- and post-synaptic effects. LGC-46 was the first ligand-gated ionotropic receptor in *C. elegans* to show presynaptic localization. From electrophysiological analyses using *lgc-46* null alleles and genetic rescue experiments, LGC-46 was found to be required to suppress synaptic vesicle (SV) release after the activation of neurons. The gain-of-function mutant LGC-46 showed higher efficiency on the suppression of SV release. Based on these results, I proposed a model where LGC-46 mediates presynaptic inhibition by acting as an autoreceptor. Although acetylcholine-gated chloride channels are not identified in mammals, similar mechanisms to fine-tune neural activities with presynaptic ligand-gated ion channels may exist broadly among animals.

Interestingly, the *lgc-46(0)* animals showed overall normal locomotion. Considering *lgc-46(gf)* showed slow locomotion and curly body posture, one possible defect of the *lgc-46(0)* animals is subtle change in body posture. In addition, as LGC-46 was required for neural suppression upon activation of the neurons, it is possible that in an event of increased neural activity, the importance of LGC-46 functions becomes higher. For example, when there is frequent mechanical stimulus that forces the animal to move forward, the performance of *lgc-46(0)* animals may become lower compared to wild type. It could be of interest for future studies to examine possible locomotion phenotype of *lgc-46(0).*

Another question remaining is the channel composition of LGC-46. Up to this point, there is no evidence suggesting that LGC-46 forms homomeric channel (Ringstad, Abe, & Horvitz, 2009), and I found that another ligand-gated ion channel subunit ACC-4 is required for the function of LGC-46. It is possible that there still are other channel subunit proteins or accessory proteins required for function of the channel. Channel reconstitution analyses using heterologous system such as cell culture or Xenopus oocyte will be desired to further characterize LGC-46. A possible approach to address this question is to perform a forward genetic screen on *lgc-46(gf)* animals, which show strong locomotion phenotype.

In Chapter III, the roles of neuropeptides in regulation of E/I imbalance in *C. elegans* were examined. In addition to classical neurotransmitters, neuropeptides released from dense core vesicles contribute to the coordination of neural circuit activity. Though neuropeptides were previously reported to have anti-seizure effect in mammalian seizure models (Kovac & Walker, 2013; Lerner, Sankar, & Mazarati, 2008), it was unknown whether a similar mechanism is conserved in *C. elegans.* The *acr-2(gf)* convulsion phenotype was exacerbated when neuropeptide processing was blocked, suggesting that neuropeptides have inhibitory effects on convulsion. Candidate gene approach identified specific neuropeptide-encoding genes *flp-1* and *flp-18* which function to suppress the E/I imbalance and *acr-2(gf)* convulsion (Stawicki, Takayanagi-Kiya, Zhou, & Jin, 2013). *flp-1* and *flp-18* encode FMRF neuropeptides which have similarity to mammalian neuropeptide Y (Cohen et al., 2009; Nelson, Rosoff, & Li, 1998). I further identified the G-protein coupled receptors required for the effect by *flp-1* and *flp-18*. Importantly, overexcitation of neurons either by *acr-2(gf)* or by drug treatment caused upregulation of *flp-18* expression, suggesting that *flp-18* functions in a homeostatic manner to suppress E/I imbalance. Mechanisms regulating the expression of neuropeptides upon neural activity will be the next step to address.

In Chapter IV, I described that a co-chaperone gene with a highly conserved DnaJ/Hsp40 domain affects E/I balance. DnaJ/Hsp40 proteins interact with and activate Hsp70s, and are involved in many cellular processes (Cheetham & Caplan, 1998; Qiu, Shao, Miao, & Wang, 2006). Mutations in DnaJ/Hsp40 proteins have been implicated in human diseases including neurodegenerative diseases (Trinh & Farrer, 2013; Vilariño-Güell et al., 2014), emphasizing the importance of the protein family. I identified a gain-of-function mutation in a DnaJ protein DNJ-17 in the background of a null allele of gene encoding glutamic acid decarboxylase, *unc-25(e156).* Examination of *acr-2(gf)* convulsion phenotype and drug sensitivity analyses suggested that *dnj-17(gf)* worsens the E/I balance in the locomotor circuit. I observed broad expression of *dnj-17* and also found that neural expression of *dnj-17(gf)* is insufficient to

exacerbate the E/I imbalance phenotype in *acr-2(gf)*. These results suggested that *dnj-17* functions in multiple tissues to regulate the locomotor circuit. The drug sensitivity analysis also implied that *dnj-17* null allele causes decrease in cholinergic transmission at the neuromuscular junction. One speculative mechanism underlying this is that *dnj-17* is necessary for folding or translation of proteins which contribute to cholinergic transmission. In this case, *dnj-17(gf)* phenotypes may be caused by increased level of those proteins.

In Chapter V, I examined another suppressor mutation of *acr-2(gf)* which affects a highly conserved eukaryotic initiation factor (eIF) subunit protein. Protein translation in eukaryotic cells involve many eIFs, and eIF3 is known to be necessary for translation initiation (Naranda, Kainuma, MacMillan, & Hershey, 1997). eIF3 has 10 to 13 subunits in mammals, of which 5 subunits are conserved from yeast (Asano, Phan, Anderson, & Hinnebusch, 1998; Masutani, Sonenberg, Yokoyama, & Imataka, 2007). Many studies have focused on eIF3 proteins in yeast (Vornlocher, Hanachi, Ribeiro, & Hershey, 1999), but *in vivo* functions of the protein complex in animals remain mostly unknown. A suppressor isolated from a forward genetic screen on *acr-2(gf)* carried a single amino acid substitution in the gene encoding *C. elegans* eIF3 subunit g (EIF3G), *eif-3.g*. EIF3G is one of the five subunits conserved from yeast to mammals, and the mutation causes substitution of a conserved cysteine to tyrosine (C130Y) in the zinc-finger motif of the protein. I generated a null allele of *eif-3.g* and found that it causes larval arrest phenotype, different from the C130Y mutant which is viable and show normal growth rate. Also, *eif-3.g(0/+)* heterozygous did not have an effect on *acr-2(gf)* convulsion whereas the C130Y mutation behaved as a semi-dominant allele. This indicated that C130Y mutation causes a gain-of-function of the protein. It possibly acts as a weak dominant negative or a neomorph. Furthermore, I found that although *eif-3.g* shows ubiquitous expression, wild type *eif-3.g* expression only in cholinergic motor neurons is required for the *acr-2(gf)* convulsion in the double mutant background, suggesting that the phenotype caused by *eif-3.g* is not the result of a general effect on overall reduced protein translation in the body, but rather a specific

effect in limited number of cells. Interestingly, EIF-3.G translational reporter showed an overall upregulation of protein level in *acr-2(gf)* background, possibly caused by an activity-dependent mechanism which regulates the level of the protein. I generated a tissue-specific knockout system which will be useful for examining the function of *eif-3.g* in cholinergic motor neuron more precisely. Recent studies suggested the effects of eIF3 proteins on specific set of mRNAs (Choudhuri, Evans, & Maitra, 2010; Choudhuri, Maitra, & Evans, 2013; Lee, Kranzusch, & Cate, 2015). Human EIF3G was shown to directly interact with mRNAs (Lee, et al., 2015) and *C. elegans* EIF-3.G contains a RNA recognition motif, which I observed was necessary for the protein to affect *acr-2(gf)* convulsion. Analyzing targets of EIF-3.G by RNA cross-linking and immunoprecipitation will provide further insight to the *in vivo* function of the protein.

Through my dissertation, I presented that genes involved in various pathways contribute to the regulation of E/I balance. A forward genetic suppressor screen identified gain-of-function mutations of proteins which have not been previously characterized from the perspective of regulation of neural activity. This stresses the advantage of forward genetic screens, where one can identify genes involved in the phenotype of interest which may not be achieved from examination of loss-of-function mutants and gene knockdowns.

References

Asano, K., Phan, L., Anderson, J., & Hinnebusch, A. G. (1998). Complex formation by all five homologues of mammalian translation initiation factor 3 subunits from yeast Saccharomyces cerevisiae. *J Biol Chem, 273*(29), 18573-18585.

Brenner, S. (1974). The genetics of *Caenorhabditis elegans*. *Genetics, 77*(1), 71-94.

Cheetham, M. E., & Caplan, A. J. (1998). Structure, function and evolution of DnaJ: conservation and adaptation of chaperone function. *Cell Stress Chaperones, 3*(1), 28-36.

Choudhuri, A., Evans, T., & Maitra, U. (2010). Non-core subunit eIF3h of translation initiation factor eIF3 regulates zebrafish embryonic development. *Dev Dyn, 239*(6), 1632-1644.

Choudhuri, A., Maitra, U., & Evans, T. (2013). Translation initiation factor eIF3h targets specific transcripts to polysomes during embryogenesis. *Proc Natl Acad Sci U S A, 110*(24), 9818-9823.

Cohen, M., Reale, V., Olofsson, B., Knights, A., Evans, P., & de Bono, M. (2009). Coordinated regulation of foraging and metabolism in *C. elegans* by RFamide neuropeptide signaling. *Cell Metab, 9*(4), 375-385.

Jospin, M., Qi, Y. B., Stawicki, T. M., Boulin, T., Schuske, K. R., Horvitz, H. R., Bessereau, J. L., Jorgensen, E. M., & Jin, Y. (2009). A neuronal acetylcholine receptor regulates the balance of muscle excitation and inhibition in *Caenorhabditis elegans*. *PLoS Biol, 7*(12), e1000265.

Kovac, S., & Walker, M. C. (2013). Neuropeptides in epilepsy. *Neuropeptides, 47*(6), 467-475.

Lee, A. S., Kranzusch, P. J., & Cate, J. H. (2015). eIF3 targets cell-proliferation messenger RNAs for translational activation or repression. *Nature, 522*(7554), 111-114.

Lerner, J. T., Sankar, R., & Mazarati, A. M. (2008). Galanin and epilepsy. *Cell Mol Life Sci, 65*(12), 1864-1871.

Masutani, M., Sonenberg, N., Yokoyama, S., & Imataka, H. (2007). Reconstitution reveals the functional core of mammalian eIF3. *EMBO J, 26*(14), 3373-3383.

Naranda, T., Kainuma, M., MacMillan, S. E., & Hershey, J. W. (1997). The 39-kilodalton subunit of eukaryotic translation initiation factor 3 is essential for the complex's integrity and for cell viability in Saccharomyces cerevisiae. *Mol Cell Biol, 17*(1), 145-153.

Nelson, L. S., Rosoff, M. L., & Li, C. (1998). Disruption of a neuropeptide gene, flp-1, causes multiple behavioral defects in *Caenorhabditis elegans*. *Science, 281*(5383), 1686-1690.

Qi, Y. B., Po, M. D., Mac, P., Kawano, T., Jorgensen, E. M., Zhen, M., & Jin, Y. (2013). Hyperactivation of B-type motor neurons results in aberrant synchrony of the *Caenorhabditis elegans* motor circuit. *J Neurosci, 33*(12), 5319-5325.

Qiu, X. B., Shao, Y. M., Miao, S., & Wang, L. (2006). The diversity of the DnaJ/Hsp40 family, the crucial partners for Hsp70 chaperones. *Cell Mol Life Sci, 63*(22), 2560-2570.

Ringstad, N., Abe, N., & Horvitz, H. R. (2009). Ligand-gated chloride channels are receptors for biogenic amines in *C. elegans*. *Science, 325*(5936), 96-100.

Ruiz, A., Campanac, E., Scott, R. S., Rusakov, D. A., & Kullmann, D. M. (2010). Presynaptic GABAA receptors enhance transmission and LTP induction at hippocampal mossy fiber synapses. *Nat Neurosci, 13*(4), 431-438.

Stawicki, T. M., Takayanagi-Kiya, S., Zhou, K., & Jin, Y. (2013). Neuropeptides function in a homeostatic manner to modulate excitation-inhibition imbalance in *C. elegans*. *PLoS Genet, 9*(5), e1003472.

Trinh, J., & Farrer, M. (2013). Advances in the genetics of Parkinson disease. *Nat Rev Neurol, 9*(8), 445-454.

Trojanova, J., Kulik, A., Janacek, J., Kralikova, M., Syka, J., & Turecek, R. (2014). Distribution of glycine receptors on the surface of the mature calyx of Held nerve terminal. *Front Neural Circuits, 8*, 120.

Turecek, R., & Trussell, L. O. (2001). Presynaptic glycine receptors enhance transmitter release at a mammalian central synapse. *Nature, 411*(6837), 587-590.

Vilariño-Güell, C., Rajput, A., Milnerwood, A. J., Shah, B., Szu-Tu, C., Trinh, J., Yu, I., Encarnacion, M., Munsie, L. N., Tapia, L., Gustavsson, E. K., Chou, P., Tatarnikov, I., Evans, D. M., Pishotta, F. T., Volta, M., Beccano-Kelly, D., Thompson, C., Lin, M. K., Sherman, H. E., Han, H. J., Guenther, B. L., Wasserman, W. W., Bernard, V., Ross, C. J., Appel-Cresswell, S., Stoessl, A. J., Robinson, C. A., Dickson, D. W., Ross, O. A., Wszolek, Z. K., Aasly, J. O., Wu, R. M., Hentati, F., Gibson, R. A., McPherson, P. S., Girard, M., Rajput, M., Rajput, A. H., & Farrer, M. J. (2014). DNAJC13 mutations in Parkinson disease. *Hum Mol Genet, 23*(7), 1794-1801.

Vornlocher, H. P., Hanachi, P., Ribeiro, S., & Hershey, J. W. (1999). A 110-kilodalton subunit of translation initiation factor eIF3 and an associated 135-kilodalton protein are encoded by the Saccharomyces cerevisiae TIF32 and TIF31 genes. *J Biol Chem, 274*(24), 16802-16812.

Xiong, W., Chen, S. R., He, L., Cheng, K., Zhao, Y. L., Chen, H., Li, D. P., Homanics, G. E., Peever, J., Rice, K. C., Wu, L. G., Pan, H. L, & Zhang, L. (2014). Presynaptic glycine receptors as a potential therapeutic target for hyperekplexia disease. *Nat Neurosci, 17*(2), 232-239.